FOSSIL ENERGY

DOE/ET/12056-26
(DE82019075)

ANALYSIS OF FUEL OXIDATION IN IN-SITU COMBUSTION OIL RECOVERY

Topical Report

By
Mohammad R. Fassihi
William E. Brigham

August 1982
Date Published

Work Performed Under Contract No. AC03-76ET12056

Stanford University Petroleum Research Institute
Stanford, California

Bartlesville Project Office
U. S. DEPARTMENT OF ENERGY
Bartlesville, Oklahoma

DISCLAIMER

"This report was prepared as an account of work sponsored by an agency of the United States Government. Neither the United States Government nor any agency thereof, nor any of their employees, makes any warranty, express or implied, or assumes any legal liability or responsibility for the accuracy, completeness, or usefulness of any information, apparatus, product, or process disclosed, or represents that its use would not infringe privately owned rights. Reference herein to any specific commercial product, process, or service by trade name, trademark, manufacturer, or otherwise, does not necessarily constitute or imply its endorsement, recommendation, or favoring by the United States Government or any agency thereof. The views and opinions of authors expressed herein do not necessarily state or reflect those of the United States Government or any agency thereof."

This report has been reproduced directly from the best available copy.

Available from the National Technical Information Service, U. S. Department of Commerce, Springfield, Virginia 22161.

Price: Printed Copy A13
Microfiche A01

Codes are used for pricing all publications. The code is determined by the number of pages in the publication. Information pertaining to the pricing codes can be found in the current issues of the following publications, which are generally available in most libraries: *Energy Research Abstracts, (ERA); Government Reports Announcements* and Index (*GRA* and I); *Scientific and Technical Abstract Reports (STAR);* and publication, NTIS-PR-360 available from (NTIS) at the above address.

DOE/ET/12056-26
(DE82019075)
Distribution Category UC-92a

ANALYSIS OF FUEL OXIDATION IN IN-SITU COMBUSTION OIL RECOVERY

Topical Report

SUPRI TR-26

By

Mohammad R. Fassihi
and
William E. Brigham, *Principal Investigator*
Stanford University Petroleum Research Institute
Stanford, California 94305

H. J. Lechtenberg, *Technical Project Officer*
San Francisco Operations Office
Fossil Energy Division
1333 Broadway
Oakland, California 94612

Work Performed for the Department of Energy
Under Contract No. DE-AC03-76ET12056

Date Published—August 1982

UNITED STATES DEPARTMENT OF ENERGY

TABLE OF CONTENTS

	Page
ACKNOWLEDGEMENTS	xii
ABSTRACT	xiii
1. INTRODUCTION	1
1.1 Thermal and Hydrodynamic Aspects	2
1.2 Kinetics Aspects	5
2. LITERATURE REVIEW	8
2.1 Fuel Deposition	10
2.2 Fuel Combustion	13
2.3 Low-Temperature Oxidation	17
3. STATEMENT OF THE PROBLEM	21
4. EXPERIMENTAL EQUIPMENT	23
4.1 Combustion Tube Apparatus	23
4.2 Reaction Kinetics Apparatus	29
4.2-1 Temperature Control	34
4.2-2 Gas Separation	34
4.2-3 Gas Sampling	38
4.2-4 Flow Metering	38
4.2-5 Pressure Regulation	40
5. PROCEDURE	41
5.1 Properties of the Crude Oils	41
5.2 Properties of the Sand Pack	48

5. PROCEDURE (continued) Page

5.3 Preparation of the Combustion Tube 48

5.3-1 Volume Measurement and Analysis of the Produced Liquids in Combustion Tube Runs . . . 52

5.4 Preparation of the Kinetic Cell 52

5.4-1 Constant-Temperature Runs 53

5.4-2 Variable-Temperature Runs 53

6. OPERATION 55

6.1 Operation of the Combustion Tube 55

6.2 Operation of the Reaction Kinetic Apparatus 58

6.3 Accuracy of Measurements 66

7. ANALYSIS OF PRODUCTS AND RESULTS OF COMBUSTION RUNS 68

7.1 Properties of Produced Oils 68

7.2 Oil Production-Burned Volume Correlation 68

7.3 Effect of Air Flux on Frontal Velocity 76

7.4 Effect of Clay on Frontal Temperature 82

7.5 Measurement of the Burning Front Thickness 82

7.6 Fuel Content of the Bed 92

7.6-1 Measurement of the Fuel Saturation 98

7.6-2 Effect of Pressure on Fuel Deposition 98

7.7 Discussion of Results of Combustion Tube Runs 101

7.8 Conclusions from the Combustion Tube Runs 101

8. ANALYSIS OF THE RESULTS OF KINETICS RUNS 105

8.1 Isothermal Runs 105

8.2 Variable Temperature Runs 111

8.3 Molar CO_2/Co Ratio 117

8.3-1 Effect of Temperature on λ 117

8.3-2 Effect of Pressure on λ 122

8. ANALYSIS OF RESULTS OF KINETICS RUNS (continued) Page

8.4 The Apparent H/C Ratio, η 125

8.4-1 Effect of Distillation on η 126

8.4-2 Effect of Pyrolysis on η 126

8.5 Modelling of the Reactions 130

8.6 Repeatability and Accuracy of Experiments 139

8.7 Evaluation of Arrhenius Constant 146

8.8 Diffusion Effects 156

8.9 Effect of Lithology on the Reactions 156

8.9-1 Effect of Matrix 164

8.9-2 Effect of Clay 177

8.9-3 Effect of Metallic Additives 179

9. SUMMARY AND CONCLUSIONS 180

9.1 Summary 180

9.2 Conclusions 182

9.3 Suggestions for Future Work 183

REFERENCES 185

NOMENCLATURE 189

APPENDIX A: Discussion of the Temperature Distribution in the Heated Porous Medium 191

APPENDIX B: Combustion Tube Runs Data 196

APPENDIX C: Derivation of Equations Used in the Analysis of Reaction Rate Data 209

APPENDIX D: Calculation of the True $\Delta\gamma$ 214

APPENDIX E: Calculations of the Area Under the Relative Reaction Rate Curve vs Time 216

APPENDIX F: Evaluation of Effect of Diffusion 218

APPENDIX G: Experimental Data 222

LIST OF FIGURES

Figure		Page
1.1	Temperature Profile of an In-Situ Combustion Process	3
2.1	Thermograms of the Original Oil and the Samples Taken Along the Combustion Tube (Berry, 1968)	9
4.1	Schematic Diagram of the Combustion Tube Apparatus	24
4.2	Combustion Tube Assembly	27
4.3	Schematic Diagram of Apparatus for Kinetics Studies of In-Situ Combustion	30
4.4	Combustion Cell	32
4.5	The Bottom Flange	35
4.6	Gas Analysis Setup	39
5.1	Oil Viscosity vs 1/T	42
5.2	Distillation Analysis of the San Ardo Crude Oil	44
5.3	Distillation Analysis of the Huntington Beach Crude Oil	45
5.4	Distillation Analysis of San Ardo Oil	46
5.5	Distillation Analysis of Huntington Beach Oil	47
5.6	The X-Ray Diffraction Pattern of the Clay Used in the Experiments	50
6.1	Pressure Buildup Observed in Run No. 78-6	56
6.2	Pressure Buildup Observed in Run No. 78-7	57
6.3	Temperature Profiles Along the Sand Pack	64
6.4	Gas Composition and Temperature for Run No. 130	65
7.1	Produced Oil Viscosity in Run No. 78-6	69
7.2	Produced Oil Viscosity in Run No. 78-7	70
7.3	Produced Oil Viscosity in Run No. 79-6	71

Figure		Page
7.4	Percent Recovery vs Percent Volume Burned for Run No. 78-7	73
7.5	Percent Recovery vs Percent Volume Burned for Run No. 79-7	74
7.6	Oil Produced vs Volume Burned	75
7.7	Volume Burned vs Gas Saturation	77
7.8	Effect of Gas Flux on Front Velocity	78
7.9	Effect of Gas Flux on Front Velocity	80
7.10	Effect of Gas Flux on Front Velocity	81
7.11	Temperature Profile for Run No. 78-3	83
7.12	Temperature Profiles for Run No. 80-1	84
7.13	Produced Gas Composition vs Time for Run No. 80-1 (from the tube)	85
7.14	Produced Gas Composition vs Time for Run No. 80-1 (from the top gas probe)	86
7.15	Produced Gas Composition vs Time for Run No. 80-1	87
7.16	Produced Gas Composition vs Time for Run No. 80-1 (from the bottom probe)	88
7.17	Temperature Profiles at Gas Sampling Points vs Time	89
7.18	Gases Produced Within the Middle Section of the Combustion Tube	94
7.19	Operating Conditions for Run No. 79-2	95
7.20	Operating Conditions for Run No. 79-4	96
7.21	Operating Conditions for Run No. 79-6	97
7.22	Saturation Distribution	99
7.23	Effluent Gas Composition vs Time	100
7.24	Production vs Volume Burned for Run No. 79-6	102
8.1	Gas Composition and Temperature vs Time for Isothermal Run No. 107	106

Figure		Page
8.2a	Data for Isothermal Run No. 111	107
8.2b	Data for Isothermal Run No. 111	108
8.2c	Data for Isothermal Run No. 111	109
8.3	Gas Composition and Temperature vs Time for Huntington Beach Oil	112
8.4	Gas Composition and Temperature for Venezuelan Oil	113
8.5	Gas Composition and Temperature for San Ardo Oil	114
8.6	Gas Composition and Temperature for French Oil	115
8.7	Molar CO_2/CO Ratio and Apparent H/C Ratio vs Temperature for Huntington Beach Oil	118
8.8	Molar CO_2/CO Ratio and Apparent H/C Ratio for Venezuelan Oil	119
8.9	Molar CO_2/CO Ratio and Apparent H/C Ratio for San Ardo Oil	120
8.10	Molar CO_2/CO Ratio and Apparent H/C Ratio for French Oil	121
8.11	Molar CO_2/CO Ratio vs Pressure	123
8.12	Atomic H/C Ratio of the Fractions of Huntington Beach Crude Distilled	128
8.13	Alteration of Residual Oil in the Presence of Nitrogen During Heating to a Maximum Temperature, T_{max}, of a Mixture of Crushed Silica and Oil; Heating Rate 500 °C/hr	129
8.14	Relative Reaction Rate vs Inverse Temperature for Run No. 110	131
8.15a	Arrhenius Plot for Combustion Reaction Rate (Run No. 110)	133
8.15b	Arrhenius Plot for Fuel Combustion and Deposition Reaction Rates (Run No. 110)	134
8.15c	Arrhenius Plot for Run No. 110	135
8.16a	Decomposition of the Consumed Oxygen in Fuel Combustion Reaction	136

Figure		Page
8.16b	Decomposition of the Consumed Oxygen in Middle-Temperature Reaction	137
8.16c	Decomposition of the Consumed Oxygen in LTO Reaction	138
8.17	Arrhenius Plot for French Oil	140
8.18	Decomposition of the Produced Gases Graphed in Fig. 8.6	141
8.19	Arrhenius Plot for Venezuelan Oil	142
8.20	Decomposition of Gases Produced in Run No. 112	143
8.21	Match Between Experimental Data and the Proposed Kinetic Model (Run No. 110)	144
8.22	Match Between Experimental Data and the Kinetic Model (French Oil)	145
8.23	Arrhenius Plot for Fuel Combustion Reaction (Huntington Beach Oil)	148
8.24	Arrhenius Plot for Fuel Deposition Reaction (Huntington Beach Oil)	149
8.25	Arrhenius Plot for LTO Reaction (Huntington Beach Oil)	150
8.26	Plot of Intercept vs Pressure for Combustion Reaction (Huntington Beach Oil)	153
8.27	Plot of Intercept vs Pressure for Fuel Deposition Reaction (Huntington Beach Oil)	154
8.28	Plot of Intercept vs Pressure for LTO Reaction (Huntington Beach Oil)	155
8.29	Arrhenius Plot for Different Reactions (San Ardo Oil)	157
8.30	Arrhenius Plot for Combustion Reaction (Venezuelan Oil)	158
8.31	Arrhenius Plot for Different Reactions (Venezuelan Oil)	159
8.32	Plot of Intercept vs Pressure (San Ardo Oil)	160
8.33	Plot of Intercept vs Pressure (Venezuelan Oil)	161
8.34	Gas Composition and Temperature vs Time for Venezuelan Oil in Original Core	165
8.35	Gas Composition and Temperature vs Time for Lynch Canyon Oil in Original Core	166

Figure		Page
8.36	Molar CO_2/CO Ratio and Apparent H/C Ratio vs Temperature for Venezuelan Oil in Original Core	167
8.37	Molar CO_2/CO Ratio and Apparent H/C Ratio vs Temperature for Lynch Canyon Oil in Original Core	168
8.38	Arrhenius Plot for Run No. 126 (Original Core)	169
8.39	Arrhenius Plot for Lynch Canyon Oil	170
8.40	Arrhenius Plot for Combustion Reaction (French Oil)	174
8.41	Arrhenius Plot for Fuel Deposition Reaction (French Oil)	175
8.42	Arrhenius Plot for LTO Reaction (French Oil)	176
8.43	Gas Composition and Temperature vs Time for San Ardo Oil with Clay	178

LIST OF TABLES

Table		Page
2.1	Fuel Deposition Rate	14
2.2	Combustion Reaction Rate	18
2.3	LTO Reaction Rates	20
4.1	Combustion Tube Apparatus	26
4.2	Reactor Data	33
4.3	Equipment in the Circuit	36
5.1	Crude Oil Properties	43
5.2	Initial Pack Conditions for Tube Runs	49
6.1a	Gross Recovery and Pack Data for Combustion Runs	59
6.1b	Recovery of Tube Runs	60
6.2a	Initial Pack Conditions for Tube Runs: Homogeneous Runs	61
6.2b	Initial Pack Conditions for Tube Runs: Heterogeneous Runs	62
6.3	Initial Conditions for Kinetics Runs	67
7.1	Produced Oil Characteristics	72
7.2	Burning Front Thickness Calculations for Run No. 80-1	91
7.3	Probe Temperatures and Produced Gases within the Middle Sector of the Tube in Run No. 80-1	93
7.4	Summary of Combustion Tube Run Results	103
8.1	Constants of the Correlation, $\ln \eta = a + bT$	127
8.2	Fuel Combustion Reaction Rate (Huntington Beach Crude Oil)	147
8.3	Fuel Deposition Reaction Rate (Huntington Beach Crude Oil)	151
8.4	Low-Temperature Oxidation Rate (Huntington Beach Crude Oil)	152

Table		Page
8.5	Kinetic Data for San Ardo Crude Oil	162
8.6	Kinetic Data for Venezuelan Oil	163
8.7	Kinetic Data for Lynch Canyon Oil (Run No. 131)	171
8.8	The Properties of the French Crude Oil Used by Bardon and Gadelle (1977)	171
8.9	Initial Pack Conditions for Runs Conducted by Bardon and Gadelle (1977)	172
8.10	Analysis of Data of Bardon and Gadelle	173
8.11	Kinetic Data for Combustion of San Ardo Oil (sand with clay)	179
9.1	Summary of Kinetic Data	181

ACKNOWLEDGEMENTS

The authors would like to gratefully acknowledge the financial support of the United States Department of Energy (Contract Number DE-AC03-76ET-12056) which made this research possible, and to Harold Lechtenberg of the DOE San Francisco Operations Office for his help over the years.

Gratitude is also extended to Prof. Henry J. Ramey, Jr., under whose guidance this work was originally started, and to Professors Frank G. Miller, Sullivan S. Marsden, Jr., and Subir K. Sanyal, former manager of the Stanford University Petroleum Research Institute, who provided valuable insights and advice. The authors are especially grateful to Paul Pettit and John Grim for helping to build the laboratory apparatus and to run the experiments.

ABSTRACT

In-situ combustion is a thermal method of enhanced oil recovery whereby oil is ignited underground, creating a combustion front which is propagated through the reservoir by continuous air injection.

In recent years, results of laboratory and field experiments have been reported in literature describing the forward combustion process, but as yet, only limited qualitative or quantitative studies of the kinetics of fuel combustion involved in this process have been reported. The main purpose of this work was to study the oxidation reaction kinetics in the forward combustion oil recovery process. To accomplish this, an apparatus was designed. A total of 31 runs were made wherein a thin, stationary layer of oil sand was oxidized isothermally in a combustion cell. Individual runs were made at various temperatures, pressures, and flow rates to permit determination of the effects of these variables upon the reaction. In addition, regular combustion tube experiments were run to assess the importance of process variables on frontal behavior.

By continuous analysis of the produced gases from the reactor, at both isothermal and linearly-increasing temperatures, it was found that combustion of crude oil in porous media follows a complex series of reactions. These reactions can be divided into three sequences: (1) low-temperature oxidation, (2) fuel deposition, and (3) fuel combustion.

A model is proposed to analyze and differentiate among these reactions. The method developed is reasonably fast and can be used to measure the oxidation and deposition of fuel for a given crude oil and porous medium.

The conclusions are:

1. The amount of fuel deposited on sand decreases as reaction temperature is increased;
2. Larger amounts of fuel are deposited on the system containing clays and finer sands;
3. The atomic hydrogen-carbon ratio for the deposited fuel decreases when temperature increases;
4. A higher weight percentage of hydrogen than weight percentage of carbon is burned at the beginning of the combustion run; and
5. Increasing the partial pressure of oxygen increases the molar carbon dioxide-carbon monoxide ratio.

Expressions were obtained for the low-temperature oxidation rate of oil, the fuel deposition rate and the burning rate of fuel as functions of fuel concentration, reaction temperature, and oxygen partial pressure. The results show that the reaction rate constants match the Arrhenius equation. The reaction rates for four types of crude oil indicated a reaction order of one with respect to fuel concentration, but less than one with respect to oxygen partial pressure. The activation energy of each reaction was different for the few crude oils examined. It decreased for a porous medium containing metallic additives or clays. This is attributable to the catalytic effects of these additives on the reactions. Due to the importance of these effects, it was finally concluded that any laboratory study of in-situ combustion should be made on the native core material to evaluate the feasibility of this process in the field.

1. INTRODUCTION

In many heavy oil reservoirs, the most effective way and sometimes the only way to stimulate production is the application of heat. The thermal energy may be introduced from the surface in the form of either hot water, oil, or gases, or by steam injection. It may also be generated in situ by burning part of the oil in the underground reservoirs, a process known as "in-situ combustion."

In-situ combustion is basically the process of injecting air into an oil reservoir through selected injection wells to create an air sweep within the reservoir, then igniting the crude oil and propagating a combustion front through the reservoir with continued air injection. This idea dates back to 1923 when a patent was granted on a process similar to in-situ combustion. However, it was not until 1952 that two modern field tests were conducted in the state of Oklahoma (Kuhn and Koch, 1953; Grant and Szasz, 1954). In-situ combustion has been tested in over a hundred field applications, many of which have been reviewed and compared in the literature (Farouq Ali, 1972; Brigham *et al.*, 1980).

There have been significant variations of this method devised for the purpose of handling reservoir situations apparently not dealt with by ordinary in-situ combustion. For example, in the reverse combustion method, the injected air and the burning front move countercurrently. The objective of this process was recovery of heavy tars which have little or no native mobility. After the reverse process was discovered,

the adjective "forward" was applied to the older in-situ combustion process. Water injection into the well either concurrently or alternatively with air injection is used in order to get a more efficient heat utilization. The adjective "wet" describes this process. In this paper we will be concerned primarily with dry forward combustion.

1.1 Thermal and Hydrodynamic Aspects

Figure 1.1 presents a schematic drawing of the dry, forward in-situ combustion process. The events occurring as a high-temperature combustion front approaches a volume element in the porous bed may be visualized as follows: (Martin *et al.*, 1958; Wilson *et al.*, 1958; Tadema, 1959; Ramey, 1971; Wu and Fulton, 1971; Burger and Sahuquet, 1977). When the temperature of the volume element starts rising, water and some light hydrocarbons are vaporized and carried ahead in the gas stream. Because the vapors move faster than the combustion front, they soon hit the colder areas where they condense. Then, after the leading edge of zone E passes through the element, the original oil is subjected not only to hot water drive, vaporization, steam and gas drive, but also to miscible displacement by the recondensed light hydrocarbons.

After all the water has been vaporized, the temperature increases more rapidly causing a marked reduction in the oil viscosity and an increase in both oil and gas volumes by thermal expansion. These effects result in additional flow of liquid oil. In addition, more components of the oil will vaporize as their vapor pressures exceed their partial pressures in the gas phase.

As the combustion front moves closer to the volume element and when the temperature exceeds about 600°F, the residual oil in the

FIG. 1.1

TEMPERATURE PROFILE OF AN IN-SITU COMBUSTION PROCESS

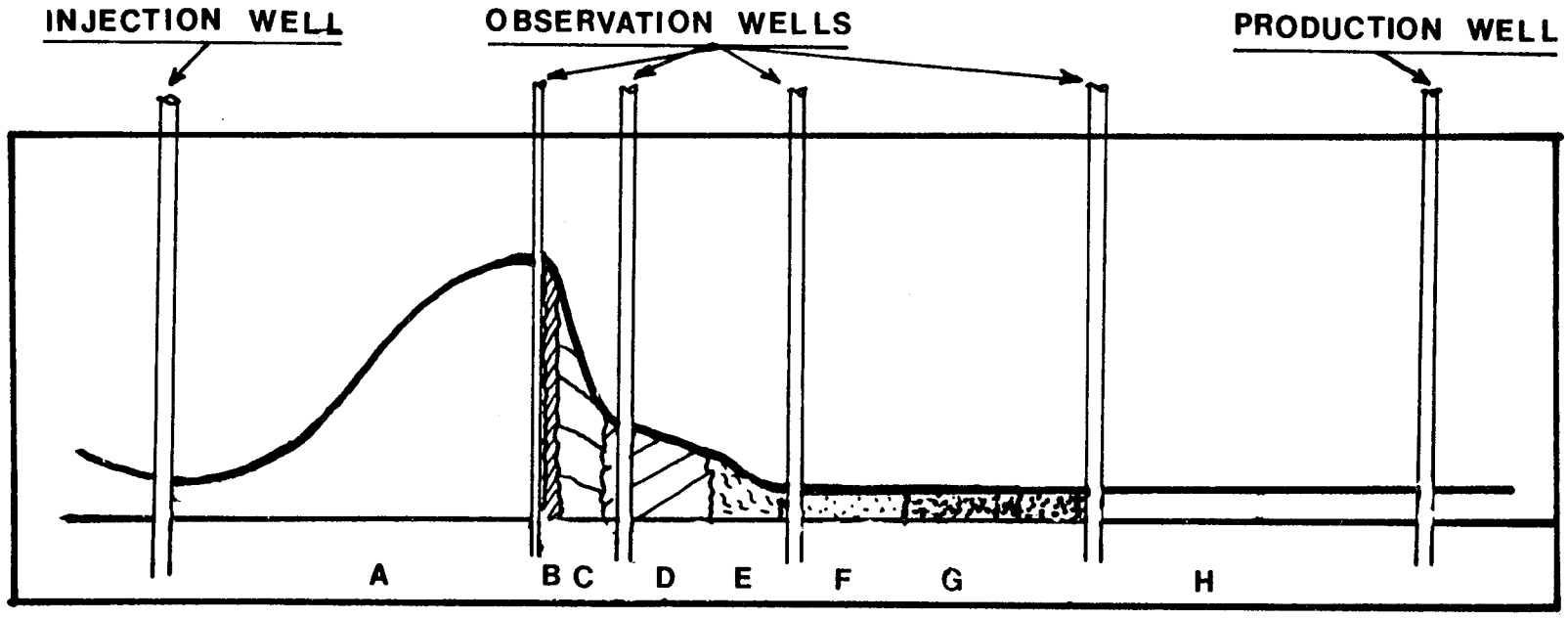

A BURNED ZONE
B COKE
C CRACKING ZONE
D STEAM PLATEAU
E LIGHT HYDROCARBON
F WATER BANK
G OIL BANK
H INITIAL ZONE

element cracks into a volatile fraction and a non-volatile heavy residue. Part of the volatile fraction recondenses in the cooler zones downstream, and the rest remains in the gas phase. The non-volatile, non-distillable residuum consisting of coke, tar, and pitch constitutes the primary fuel for combustion. The cracking zone is followed by the combustion zone (B), where the fuel for combustion generates the thermal heat energy for the process. The burning front is a narrow region only inches thick. This front temperature may range between 600-1200°F. The movement of the front is a result of combustion of all fuel which can be consumed at existing conditions. If air is used as the injection medium, the convection wave formed by heat recovery will move at about one-quarter the velocity of the combustion front (Martin et al., 1959; Ramey, 1971). After all the fuel has been burned, a zone of clean sand (A), will be left behind where only air is flowing.

The most important factors in any in-situ combustion project are: (1) the amount of fuel consumed per unit of reservoir volume swept by the combustion zone, (2) the composition of the fuel consued, (3) the amount of air required to consume this fuel, (4) the portion of the reservoir swept by the combustion zone, (5) the appropriate air-injection rates and pressures, (6) the amount of oil that will be recoveredy, (7) the rate of oil production and (8) the operating costs (Alexander et al., 1962).

Nelson and McNiel (1961) described a procedure which utilized laboratory combustion-tube data as a basis for the calculation of some of these design factors (see Appendix B). They used the following stoichiometric equation as a basis for their calculations:

$$CH_\eta + \left(\frac{2\lambda + 1}{2\lambda + 2} + \frac{\eta}{4}\right)O_2 \rightarrow \frac{\lambda}{1 + \lambda}CO_2 + \frac{1}{1 + \lambda}CO + \frac{\eta}{2}H_2O \qquad (1.1)$$

where:

η = the atomic hydrogen-carbon ratio

λ = the molar ratio of produced carbon dioxide to carbon monoxide

CH_η = the atomic formula for the fuel

Although in-situ combustion has properly been characterized as a high mobility ratio process, it appears to have areal stability with much less fingering tendency than could be expected from mobility ratio considerations alone. The reported areal sweep efficiencies have been around 50% (Farouq Ali, 1972).

In the published literature, initial attempts were directed toward an analytical treatment of the heat flow mechanism without consideration for fluid flow effects (Vogel and Krueger, 1955; Ramey, 1959; Bailey and Larkin, 1960; Chu, 1963; Thomas, 1963; Penberthy and Ramey, 1966; Gottfried, 1966; Perberthy, 1967). All of these treatments were highly idealized insofar as the chemical and physical dynamics of the process were not taken into account. Recently, sophisticated numerical models have been developed which include the complex physico-chemical phenomena with a set of elementary kinetic expressions (Crookston et al., 1979; Youngren, 1980; Coats, 1980).

1.2 Kinetics Aspects

The reaction between fuel and oxygen in a forward combustion process is a heterogeneous flow reaction. For the burning front to move, it is necessary that injected oxidant gas pass through the burning zone. Within the burning zone, a number of known transport processes occur. First, oxygen moves from the bulk gas stream to the fuel interface. Then,

perhaps, the oxygen adsorbs and reacts with the fuel. Combustion products then desorb, and finally transfer into the bulk gas stream. If any of these steps is inherently much slower than the remaining ones, the overall rate will be controlled by that step. Also, the rate of each of the series of steps must be equal in the steady-state condition. However, no useful correlations exist for computation of adsorption and desorption of oxygen in a porous medium.

Unfortunately, consideration of each of these phenomena becomes extremely difficult for even simple reactions. Theoretical expressions for postulated mechanisms often contain ten or more arbitrary constants. Because of the large number of arbitrary constants, several expressions developed for widely different mechanisms will often match experimental data equally well.

The overall in-situ combustion process can be characterized by a simple two-step chain reaction. These steps are fuel deposition and fuel combustion which are essentially competitive (Bousaid and Ramey, 1968; Dabbous and Fulton, 1974; Thomas et al., 1979). However, another type of reaction, low-temperature oxidation of crude oil (LTO reaction), is also important. LTO takes place upon air injection either before or after ignition, when oxygen is available downstream from the combustion front (Ramey, 1959; Moss et al., 1959; Tadema and Weijdema, 1970; Burger, 1976). This may result from: (1) incomplete oxygen consumption in the high temperature combustion zone, (2) air channeling around the front, or (3) a tilted combustion front surface, (Dabbous and Fulton, 1974).

In general, the combustion rate, R_c, of crude oil in a porous medium can be described as follows, (Wilson et al., 1963; Bousaid and Ramey, 1968; Burger and Sahuquet, 1979):

$$R_c = -\frac{dC_f}{dt} = kp_{O_2}{}^m C_f{}^n \tag{1.2}$$

where:

C_f = instantaneous concentration of fuel

k = rate constant

p_{O_2} = partial pressure of oxygen

m,n = reaction orders

The reaction constant, k, is often a function of temperature, T, as expressed in the following equation (Smith, 1970; Carberry, 1976):

$$k = A_r \exp(-E/RT) \tag{1.3}$$

where:

A_r = the Arrhenius constant

E = the activation energy

R = universal gas constant

For heterogeneous reactions, the constant, A_r, is a function of the surface area of the rock (Smith, 1970).

2. LITERATURE REVIEW

Early studies of crude oil oxidation in a porous medium were mostly qualitative. Differential thermal analysis (D.T.A.) was performed on samples of crude oil (Tadema, 1959; Berry, 1968). The resulting thermograms represented the thermal history of each sample as it was heated at a uniform rate (usually $10^{o}C/min$) in a constant air flow (usually 35 scf/hr). These thermograms (Fig. 2.1) indicated the presence of a number of exothermic reactions.

Another method of analysis is Thermogravimetric Analysis (T.G.A.). Here, a sample of crude oil is weighed continuously as it is heated at a constant rate. The resulting curve of weight change vs time or temperature gives the TGA thermogram. A coupling of TGA and DTA thermograms also indicated the occurrence of at least two reactions at different temperatures (Bae, 1977).

Finally, some investigators attempted to measure the kinetic parameters by oxidizing crude oil in a packed bed and analyzing the produced gases (Bousaid and Ramey, 1968; Weijdema, 1968; Dabbous and Fulton, 1974; Thomas *et al.*, 1979). Although the use of an Arrhenius-type equation for the oxidation of crude oil has been questioned by some investigators (e.g., Bae, 1977) this approach has been accepted by others.

Tadema (1959) described the existence of two main reactions, one at a low temperature and one at a higher temperature, which are quite common for a large number of crude oils. About the same time, Gates and Ramey (1958) described a third oxidation reaction which took place at measurable

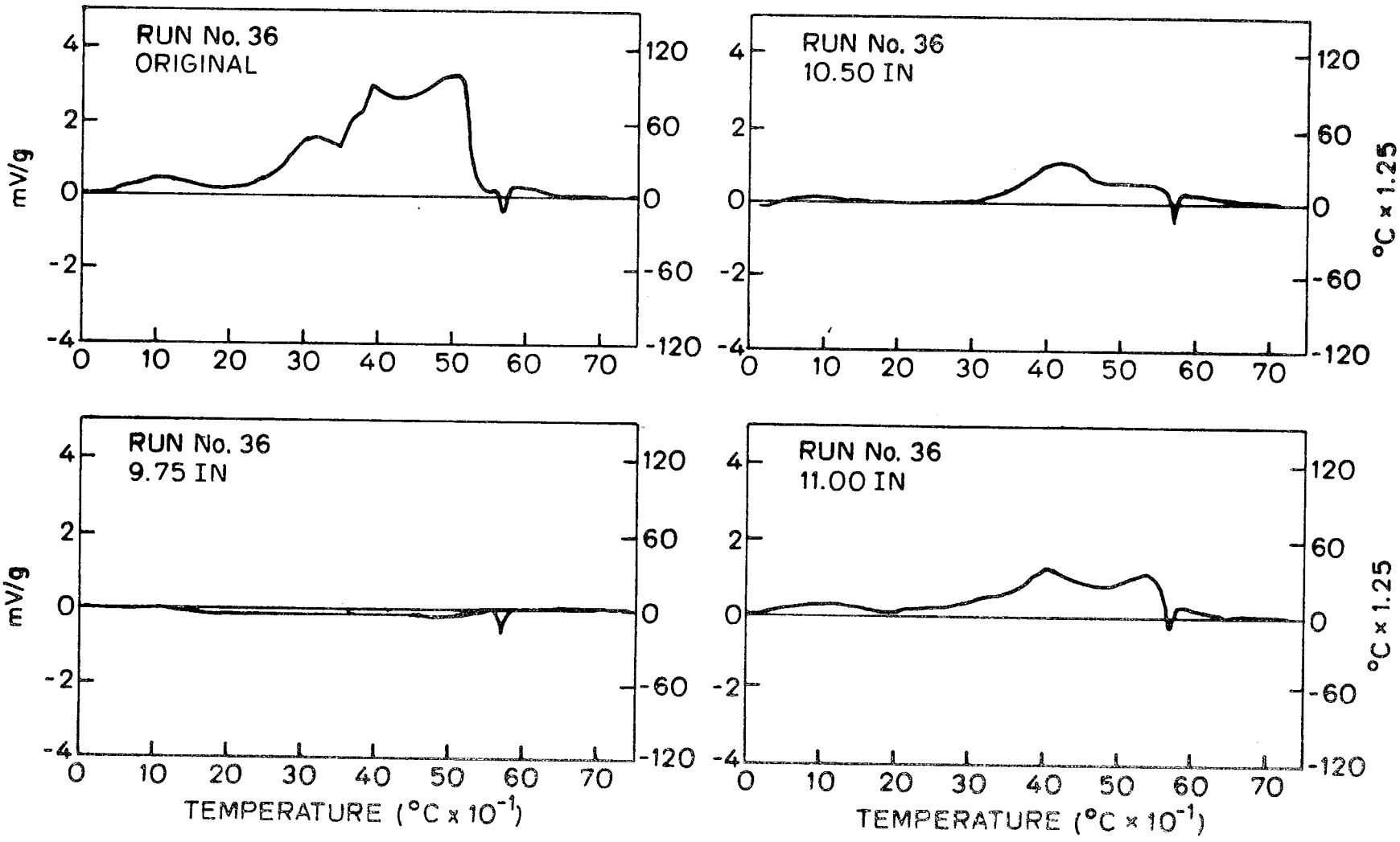

FIG. 2.1 THERMOGRAMS OF THE ORIGINAL OIL AND THE SAMPLES TAKEN ALONG THE COMBUSTION TUBE (BERRY, 1968)

rates at the initial formation temperature during air injection. Later on, work done on kinetics of crude oil oxidation in porous media confirmed the occurrence of three major reactions in in-situ combustion (Bousaid and Ramey, 1968; Weijdema, 1968; Dabbous and Fulton, 1974: Thomas et al., 1979). These were: 1. Fuel Deposition, 2. Fuel Combustion, 3. Low-temperature oxidation.

2.1 Fuel Deposition

The terms coke formation, fuel lay-down, cracking, and fuel deposition of the in-situ combustion literature all describe the process of leaving fuel on the solid matrix as the crude oil moves forward. In this paper, the term fuel deposition will be used.

The quantity of fuel deposited and the reaction rate within the burning zone have been the subjects of intensive study for a number of reasons. First, the maximum oil recovery is the difference between the original oil in place (OOIP) at the start of the operation and the oil consumed as fuel. Second, one of the most important factors in the economic evaluation of any in-situ combustion project is the cost of air compression. Excessive fuel deposition causes the burning front to advance slowly and this incurs large air compression costs.

On the other hand, if the fuel concentration is too low, the heat of combustion will not be sufficient to raise the temperature of the rock and the contained fluids to a level of self-sustained combustion. This may lead to combustion failure.

The mechanism of fuel deposition has been discussed by many investigators. Some believe that the fuel responsible for combustion is carbon which is deposited on the rock after the following pyrolysis reaction:

$$(C_xH_y) \rightarrow xC\downarrow + \frac{y}{2} H_2 \qquad (2.1)$$

Others assume the dominant mechanism is a cracking phenomenon, resulting from the breaking down of molecules due to heat, and leaving a heavy residue called "coke" on the rock:

$$(C_xH_y) \rightarrow C_nH_m\downarrow + C_{x-n}\ H_{y-m} \qquad (2.2)$$

Early measurements of the deposited fuel on the reservoir rock were made in the late 1950's. Ignition studies of coke-bearing samples taken from South Belridge field (Gates and Ramey, 1958) indicated fuel deposits ranging from 1 to 5.4 lb/ft^3 of bulk volume. This was around 15% by weight of the initial oil in place. Extremely high fuel deposits of 8.9 to 14.2 lb/ft^3 were found in several reservoir rock samples which appeared to be composed mainly of claystones or fine silt. The atomic hydrogen-carbon ratio of the coke was determined to be 1.67 and its specific gravity averaged 1.38 (compared to the gravity of the initial oil which was 12.9° API-0.98 specific gravity).

In another field experiment, Moss et al.(1959) achieved a close correspondence between fuel deposition in the field (1.9 lb/ft^3 sand) and in the laboratory (1.8-2.2 lb/ft^3 of sand). This led to extensive work in the laboratories on identification of the quantity and quality of fuel. However, rather than directly measuring the amount of fuel deposited, most investigators estimated the quantity of deposited fuel through stoichiometric equations developed by Nelson and McNiel (1961).

Alexander et al. (1962) did a comprehensive study on the factors affecting fuel availability (or deposition). These factors were original and residual oil saturation, API gravity, viscosity, atomic H/C ratio,

and Conradson carbon residue (ASTM). Although it is doubtful that the first few crude oil properties can be unique correlating parameters, the latter factor, i.e. Conradson carbon residue, should be an indicator of the coke-forming property of the crude oil. The fuel availability showed roughly direct linear dependence on the Conradson carbon residue and an inverse dependence on API gravity. Similar results were obtained by Showalter (1963). However, both the laboratory and field data show that rock lithology could be more significant than oil gravity in determining how much fuel is deposited (Gates and Ramey, 1958; Bousaid and Ramey, 1968).

Alexander et al. (1962) also indicated that high oil saturation and low burning front temperature yield greater fuel deposition. Wilson, et al. (1963) concluded that fuel deposition is independent of initial oil saturation, but instead depends on the residual oil saturation at the steam plateau. In this region steam distillation was found to be the main mechanism for fuel deposition. The amount of oil saturation was found to be nearly constant in this region (Wu and Fulton, 1971). A similar study was carried out in the USSR by Nagorny (1974) in which oil density and air flux were found to be important factors in fuel deposition.

Using TGA thermograms of 15 different crude oils in a wide gravity range (6-38°API) in the presence of both nitrogen and air, Bae (1977) showed that, in general, the oxidation of crude oil starts at higher temperatures and less heat is released as the pressure is lowered. For most of the samples studied, at 50 psig and up to 500°F, the weight loss in the presence of nitrogen or air was around 60%. It was deduced that

distillation was the dominant mechanism for fuel deposition. At higher pressures, less distillation would occur and more fuel would be available for reaction. In Bae's work, only a few crude oils were reactive enough at low temperatures to generate the heat necessary to sustain a low-temperature combustion front.

The importance of the specific surface area was discussed by Poettman, et al. (1967). They deduced that the surface area had a direct effect on fuel deposition characteristics of high-gravity, paraffin-base crude oil. Their results showed that high oil saturation, around 70%, relatively low temperature, approxiamtely 117°C, and air flux, around 0.1cc/cm^{2}-s (12 scf/hr-sq ft), maximizes the amount of fuel deposition (3.65%, carbon weight/rock weight). Also, the minimum fuel required to initiate a combustion wave was found to be about 1% by weight. Given these conditions, sufficient time is necessary to promote the deposition of carbon on sand. Table 2.1 sumarizes results from some studies of the deposition rate.

2.2 Fuel Combustion

Because fuel combustion occurs at the combustion front, investigators have used the data of combustion tube experiments to define the combustion front and its characteristics. Their goal was to obtain correlations relating the combustion front velocity and front temperature to experimental variables such as pressure and air flux. Given such a correlation, the air requirement could then be easily assessed. In their pioneering work, Martin et al. (1958) found a direct relationship between air flux and frontal velocity. They were also able to correlate the frontal velocity with the rate of total oxygen consumption (flux times oxygen consumed).

Table 2.1 FUEL DEPOSITION RATE

$$R_c^{(1)} = A_r \exp(-E/RT) p_{O_2}^{\ m} C_f^{\ n}$$

AUTHORS	CRUDE TYPE	REACTOR BED	A_r (1/s)	E_r (J/gmole)	m	n	p(kPa)
Crawford and Cunningham (1956)	Hydrocarbon vapor	Synthetic catalyst	n.a.(2)	70,300	n.a.	n.a.	n.a.
	Hydrocarbon vapor	Natural clay	n.a.	63,300	n.a.	n.a.	n.a.
Madgwick et al. (1959)	12.4°API oil	Silica sand (100-200 mesh)	n.a.	69,300	n.a.	n.a.	n.a.
Weijdema (1968)	n.a.	Sand		46,000	n.a.	n.a.	4×10^4
Thomas et al. (1979)	27°API	Sand quarry and	3.88×10^6(3)	65,100	0(3)	1(4)	1×10^4
	27°API	Kaolinite clay	3.66×10^6(3)	65,100	0(3)	1(4)	2.7×10^4
	27°API		8.33×10^6(3)	69,100			4.8×10^4

(1) R_c = g fuel deposited on 100 g sand/s

(2) n.a.= not available

(3) If a first order reaction with respect to oxygen partial pressure is assumed, then A_r would be around 0.6-1.8.

(4) $C_f = \phi \rho_o S_o$

This work was supported by Benham and Poettmam (1958) who used Eq. 1.1 combined with a material balance equation to get:

$$\frac{U \cdot Y}{V_f} = \left[\frac{2\lambda + 1}{\lambda + 1} + \frac{\eta}{4}\right] \frac{C_f}{1.109 \times 10^{-3}} \tag{2.3}$$

where:

U = air flux, scf h/ft^2

Y = fraction of oxygen consumed

V_f = front velocity, ft/hr

C_f = deposited fuel lb/ft^3 of formation

Of course, the above equation is another version of the general material balance equation (Penberthy and Ramey, 1966):

$$V_f = \frac{U}{C_f (AFR)} \tag{2.4}$$

where:

AFR = Air-fuel ratio, scf/lb

The same kind of correlation was reported by Moss et al. (1959), Showalter (1963), and Wilson et al. (1963), (see Fig. 7.9).

These relationships could indicate that if the air flux drops below a certain limit in the field, the burning front may extinguish. On the contrary, field tests have indicated that the burning front could remain static for long periods of time, as well as move normal, or counter-current to, the direction of air flow (Ramey, 1971). The front moves in the direction in which fuel, oxidant and temperature were sufficient to permit the reaction to continue.

Wilson and others showed that front temperature increased with air flow but became independent of air flux at sufficiently high pressure. Pressure

was also found not to affect both front temperature and its velocity at high air flux, while at low flux, a higher pressure increases the peak temperature and decreases the burning front velocity (Martin et al., 1958; Wilson et al., 1963). However, the pressure effect is minor.

Berry and Parrish (1960) did a theoretical study on reverse combustion which was reinforced by the experimental data of Wilson et al. (1963). They not only included the effect of pressure and air flux on front temperature, but also studied the effect of heat loss. They found that heat loss reduces the frontal velocity without a change in temperature. Such a study has not been done on forward combustion.

Although little quantitative work has been done on the reaction kinetics involved in forward combustion, extensive literature exists on the oxidation of carbon and oil which indicates first-order reaction dependency on both carbon concentration and oxygen partial pressure. Bousaid and Ramey (1968) reported a study of the carbon burning rate for two types of crude oil. Their findings are in agreement with several other studies. However, the conditions under which they studied the fuel deposition probably do not simulate the sequence of hydrodynamic and thermal effects experienced by a reservoir volume element as a combustion front approaches. Furthermore, the residual hydrocarbon had not been subjected to low temperature oxidation reactions prior to combustion. Bousaid and Ramey did not study the effect of surface area on the rate of reaction.

Dabbous and Fulton (1974) observed that the combustion reaction is first-order with respect to oxygen partial pressure, but second-order with respect to carbon concentration. They also found that this reaction is controlled by diffusion. Although they observed some effects of surface

area of clay additives on the reaction rate, they did not measure them. Table 2.2 summarizes measured combustion rate parameters from several studies.

By using a special sampling probe, Thomas, et al., (1979) were able to obtain gas samples from a combustion tube at different temperatures. They measured the rates of both fuel deposition and fuel combustion. Their work showed that operating pressure had no effect on the activation energy, but that it did affect the Arrhenius constant. However, their data were not accurate enough to detect low-temperature oxidation (LTO) reactions.

2.3 Low-Temperature Oxidation

LTO reactions are characterized by either no carbon oxides or low levels of carbon oxides in the effluent stream. In other words, more oxygen reacts with the hydrocarbons than can be found in the produced gases.

This reaction occurs with the oxygen dissolved in the whole volume of the dispersed oil phase. Oxygen diffusion to the hydrocarbon molecules is faster than the oxidation process (Dabbous and Fulton, 1974).

Some of the products of low-temperature oxidation of oils are alcohols, aldehydes, ketones, acids and peracids. It has also been reported that aldehydes promote the reaction (Crawford, 1968). It appears that the reaction rate is proportional to the specific surface area of the matrix raised to a power of between 0 and 1 (Dabbous and Fulton, 1974; Burger and Sohuquet, 1977). In addition, certain soils and metallic derivatives have catalytic effects on this reaction (Bousaid and Ramey, 1968; Johnson et al., 1968; Crawford, 1968).

Table 2.2 COMBUSTION REACTION RATES

$$R_c^{(1)} = A_r \exp(-E/RT) p_{O_2}^{\ m} C_c^{\ n}$$

AUTHORS	CRUDE TYPE	REACTOR BED	A_r(1/Pa-s)	E(J/gmole)	m	n	p(kPa)
Lewis, et al. (1954)	Metallurgical coke	Fluidized	7.4×10^{-2}	121,400	1	1	1×10^{2}
	Hardwood Charcoal	Fluidized	2.0×10^{-3}	66,500	1	1	1×10^{2}
	Graphite	Fluidized	1.3×10^{3}	205,800	1	1	1×10^{2}
Weisz and Goodwin (1966)	Coke(3)	Sand Pack	6.67×10^{5}(4)	157,300	0(4)	1	1×10^{2}
Weijdema (1968)	n.a.(2)	Sand Pack	n.a.	125,500	n.a.	n.a.	4×10^{3}
Bousaid and Ramey (1968)	13.9°API	Berea sand, 170-230 mesh	2.37×10^{-3}	61,900	1	1	3×10^{2}
	13.9°API	80% Berea, 20% clay	2.43×10^{-4}	48,400	1	1	5×10^{2}
	22.1°API	Berea sand	9.14×10^{-3}	59,800	1	2	2×10^{2}
Dabbous and Fulton (1974)	19.9°API precoked	Berea sand 60 mesh	1.38×10^{-3}	58,900	1	2	2×10^{2}
Thomas, et al. (1979)	27°API	Sand quarry, Kaolinite (5%)	3.0×10^{1}	58,800	1(5)	1	1×10^{4}
			1.8×10^{1}	58,800	1(5)	1	2.8×10^{4}
			4.84×10^{1}	58,800	1(5)	1	4.8×10^{4}

(1) R_c = g carbon burned/100 g sand-s

(2) n.a. = not available

(3) Obtained from chromatographic decolorization of heavy oil (percolation); it was purged at 430°C with nitrogen to remove residual liquid.

(4) This is obtained at high oxygen partial pressure. If a first order dependency on oxygen partial pressure is assumed, the A_r would be 31.3.

(5) Here m is the exponent of $(\phi\rho_f S_f)$ where: $(\phi\rho_f S_f)$ = fuel laid down minus fuel burnt off.

By subjecting a sample of oil sand to a heating schedule, Alexander et al. (1962) found that LTO reactions, over an extended period of time, promote the deposition of coke-like residues on the sand grains. For a 21.8° API crude, the amount of this material was maximized at an LTO reaction temperatrue of 425°F and then it decreased sharply to zero at 700°F. They also found that if the heating rate schedule is decreased, more fuel is deposited as a result of increased LTO reactions. They emphasized that LTO reactions increase the oil viscosity and alter the distillation characteristics of crude oil. The same conclusion was reached by Bae (1977) who found that crude oils generally gain weight in an air atmosphere at low temperatures. Bousaid and Ramey (1968) reported several experiments studying the rate of LTO reaction.

Several authors have indicated that the ignition delay corresponds to the initial part of the oxidation process during which a very small fraction of crude oil is altered. They used the heat released by the oxidation reaction to estimate the spontaneous ignition time for crude oils (Tadema and Weijdema, 1970; Burger, 1976). Dabbous and Fulton (1974) found that light crudes are more susceptible to partial oxidation than are heavy oils. LTO reactions may affect the movement of oil and water and, ultimately, the performance of an in-situ combustion process (Alexander et al., 1962). Some of the reported LTO rates are shown in Table 2.3.

Table 2.3 LTO REACTION RATES

$$R_{O_2}^{(1)} = A_r \exp(-E/RT) p_{O_2}^{m}$$

AUTHORS	CRUDE TYPE	REACTOR BED	A_r (gmole/Pa^m-cc-s)	E(J/gmole)	m	p(kPa)
Weijdema (1968)	n.a.(2)	Sand Pack	n.a.	44,200	n.a.	n.a.
Tadema and Weijdema (1970)	14.4°API	Sand Pack	9.2×10^2	73,700	0.46	n.a.
	12.8°API	Sand Pack	4.0×10^2	72,200	0.45	n.a.
	n.a.	Sand Pack	7.78×10^1	71,900	0.57	n.a.
	n.a.	Sand Pack	3.31	73,900	0.79	n.a.
	n.a.	Sand Pack	2.01×10^4	85,500	0.48	n.a.
	n.a.	Sand Pack	1.24×10^4	78,900	0.31	n.a.
Bousaid and Ramey (1968)	13.9° API	Pressure Bomb	5.1×10^{-2}(3)	53,300	1(3)	1.38×10^3
Dabbous and Fulton (1974)	19.9° API	Sand Pack A' = 0.91 m^2/g	3.51	70,500	0.5(4)	1×10^2
	27.1° API	Sand Pack A' = 0.91 m^2/g	1.6	73,300	0.75(4)	1×10^2
	27.1° API	Sand Pack A' = 0.52 m^2/g	1.25	73,500	0.75(4)	1×10^2
Bardon and Gadelle (1977)	27.0° API	Sand Pack	9.4×10^{-2}	70,700	0.7	9.1×10^3

(1) R_{O_2} = gmole oxygen/s-cc

(2) n.a. = not available

(3) Reported in terms of $(A_r' X_{O_2})$ rather than p_{O_2}, where $A_r' = 8.9 \times 10^5$ min.$^{-1}$ and X_{O_2} = fraction of oxygen concentration. Thus, $A_r = 0.051\ p_{O_2}$

(4) $(A_r' C_{O_2})$ used rather than p_{O_2}, where $A_r' = 0.33 \times 10^6$ min.$^{-1}$ (lit/gmole)$^{0.5}$ and C_{O_2} = gmole/lit
Therefore: $A_r = 3.51 \times p_{O_2}^{0.5}$

3. STATEMENT OF THE PROBLEM

In the previous sections, the interdependency of the different mechanisms involved in in-situ combustion was discussed. As it was shown, the attempts to correlate the laboratory data and to apply these data to the field have not been entirely successful. Part of the reason is the use of combustion stoichiometry which is not adequately defined. The oxidation of multicomponent hydrocarbon mixtures is very complex involving several reactions.

A knowledge of the kinetic data for the various reactions involved is imperative for making meaningful predictions of the effectiveness of any in-situ combustion project. Also, the kinetic model should be based on the oxygen reacted rather than the carbon oxides produced. This is because: (1) low-temperature oxidation reactions consume more oxygen than can be accounted for in the effluent gas; (2) the heat release per mole of oxygen reacted is approximately the same, regardless of the mechanism (Wilson *et al.*, 1963).

The work done on the kinetics of in-situ combustion is limited and sometimes inconclusive. The investigators either have used the regular kinetic models based on the effluent gas composition to estimate the reaction rates (Bousaid and Ramey, 1968; Dabbous and Fulton, 1974), or else they have neglected some of the reactions in their calculations, (Thomas *et al.*, 1979). Thus, due to the scarcity of applicable data in the current literature and also to provide a better understanding of the

reactions occurring at and ahead of the combustion front, it was necessary to undertake new laboratory studies.

The first objective of this investigation was to build an apparatus for measuring the reaction rates involved in in-situ combustion. The second was to measure the effects of variables such as temperature, oxygen partial pressure, flow rate, crude oil type, and lithology on these reaction rates. These kinetic data will provide useful information about the relative importance of the individual oxidation reactions. This, in turn, may lead to an understanding of whether the combustion front moves as a result of fuel dominated reactions or as a result of diffusion control.

The purpose of the investigation was also to demonstrate experimentally the importance of the process variables on the frontal movement and to measure the saturation distribution ahead of the front, the gas produced as the combustion front approaches the deposited fuel, and, finally, the burning front thickness. For these reasons, several combustion tube runs were made. The final goal of the study was a theoretical evaluation of the burning front thickness using the kinetic data.

4. EXPERIMENTAL EQUIPMENT

Two separate kinds of experimental apparatus were constructed. The first was designed for displacement and simulation purposes, and consisted mainly of a linear (vertically downwards) combustion tube with the necessary heating devices, temperature controllers, product separation, gas sampling and analysis equipment. The second experimental apparatus was designed for reaction kinetic studies. It consisted of a combustion cell equipped with a furnace, temperature and flow rate control, and recording equipment, auxiliary flow system and gas analysis equipment.

4.1 Combustion Tube Apparatus

Figure 4.1 shows a schematic diagram of the combustion tube apparatus, with Table 4.1 presenting the combustion tube data gathering equipment. The combustion tube is of stainless steel and has flanges at both ends which are silver soldered to the tube as shown in Fig. 4.2. Two Viton gaskets are used to secure the flanges and two stainless steel wire screens of different mesh are fitted in the bottom flange. The upper screen is of 200 mesh to prevent the sand from entering the production line. The supporting screen is of 10 mesh.

A 1/16" needle tube was inserted through the injection line into the combustion tube and was silver soldered to the center of the 10 mesh screen to secure it in place. For gas sampling purposes, taps were installed on the tube at 21 cm, 41 cm, and 61 cm from the bottom flange.

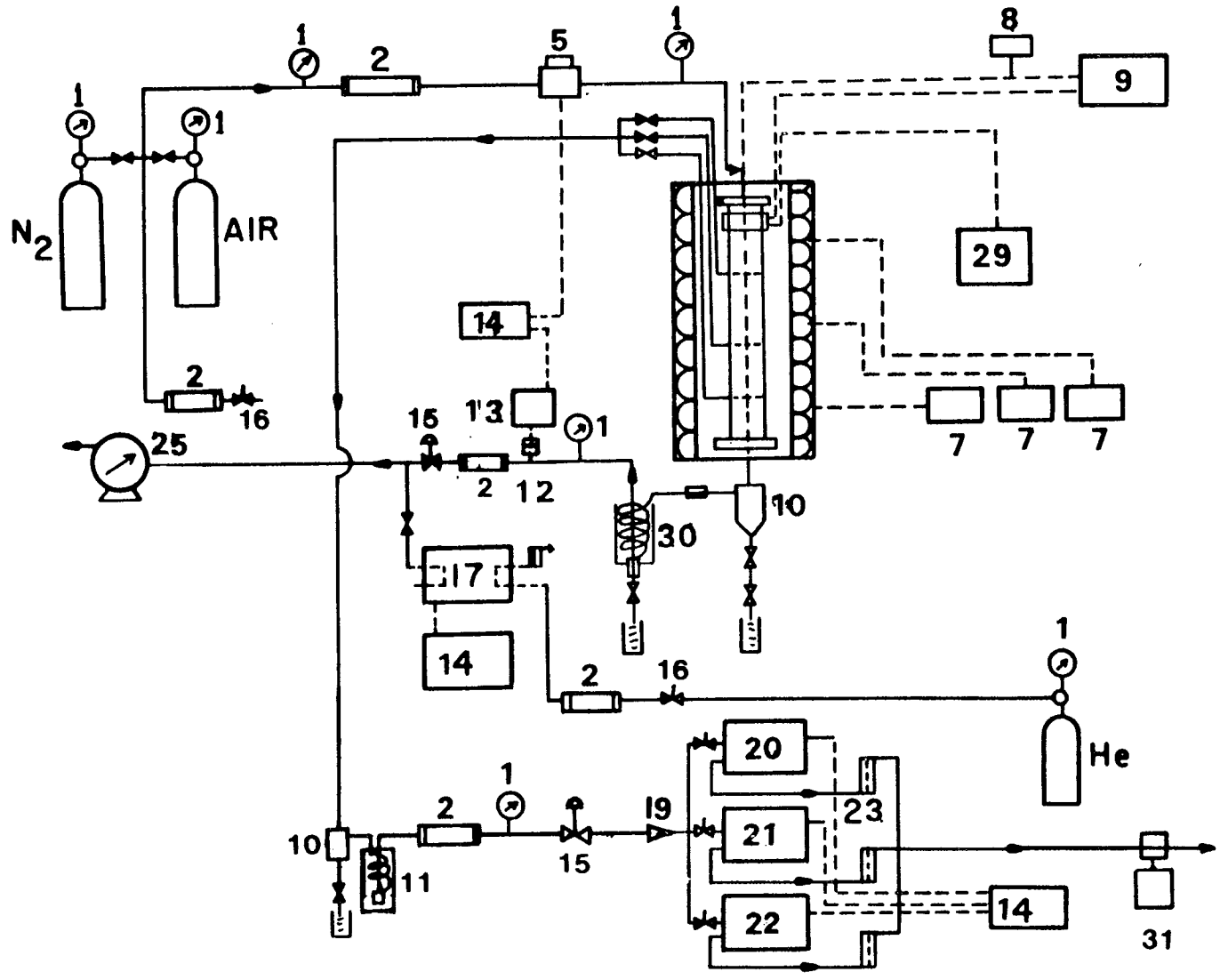

FIG. 41
SCHEMATIC DIAGRAM OF THE COMBUSTION TUBE APPARATUS

EQUIPMENT USED IN THE CIRCUIT (Fig. 4.1)

1. Pressure Gauge
2. Drierite Holder
5. Mass Flow Controller
7. Temperature Controller
8. Digital Temperature Reader
9. Temperature Recorder
10. Separator
11. Ice Bath
12. Pressure Transducer
13. Pressure Indicator
14. Recorder
15. Back-Pressure Regulator
16. Needle Valve
17. Fischer Gas Partitioner
19. 2-μ Filter
20. Carbon Dioxide Analyzer
21. Carbon Monoxide Analyzer
22. Oxygen Analyzer
23. Rotameter
25. Wet Test Meter
29. Variac
30. Condenser
31. Flow Meter

Table 4.1 COMBUSTION TUBE APPARATUS

Combustion Tube	Type 321 Stainless steel 3" O.D. x 0.016" wall, 39.2" length
Pressure Shell	Type 304 Stainless steel 6-5/8" O.D. x 0.28" wall, 44" length
Thermowell	Type 321 Stainless steel needle tube 0.65" O.D. x .009 wall
Thermocouple	Type J Iron constant .04" O.D. x 50" length
Flanges	Type 304 Stainless steel
Mesh	200 Mesh S.S. used at bottom of pack
Temperature Controller	Proportional 10 amp. triac output Range 0-800°F, type "J".
Temperature Reader	Numatron Digital indicator, type "J" thermocouple
Temperature Recorder	Speedomax W 0-1500°F
Gas Sampling Lines	Type 321 Stainless steel needle tube 0.65" O.D. x .009" wall

AIR INLET
ELECTRICAL CONNECTOR
IGNITER
LINER
PRESSURE SHELL
AXIAL THERMOCOUPLE WELL
GAS SAMPLING DEVICE
WIRE SCREEN
200 MESH
10 MESH
FLANGE
GASKET
BOLT AND NUT
PACKING GLAND

FIG. 4.2 COMBUSTION TUBE ASSEMBLY

DETAIL OF GAS SAMPLING DEVICE

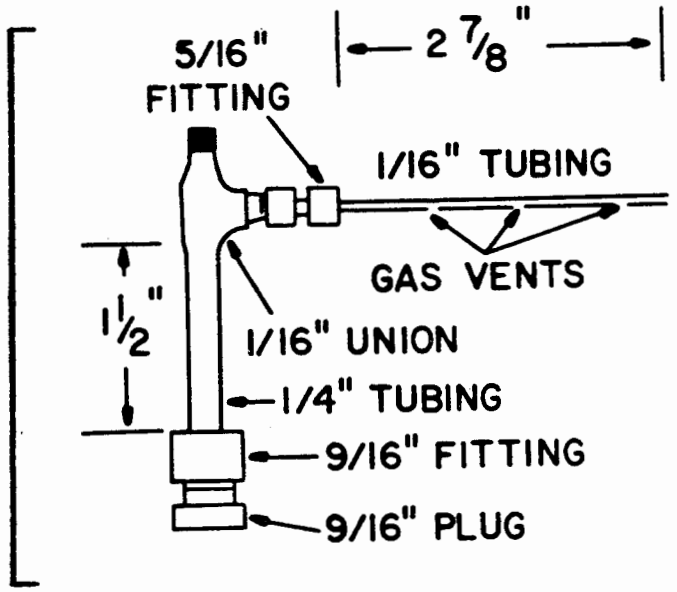

A special gas sampler was designed by soldering a union to a 1/4" tube and connected to the 1/16" needle tube. The latter was inserted into the tube through the top. Three holes were drilled in the bottom of this tubing for gas sampling probes. The 1/4" tubing is used as a liquid trap to prevent plugging of the line. The produced gases can pass through this device to a 1/16" tubing line and to the outside of the Pressure Cell (Fig. 4.2).

The combustion tube is inserted in the pressure shell, and insulated by filling the annular space between the combustion tube and pressure shell with Santocel, a low density, silica gel thermal insulator.

The igniter is clamped around the combustion tube just above the packed sand face. The voltage to the igniter is controlled by a 110 volt variable autotransformer (Variac).

Three electrical heating tapes were wrapped around the pressure shell to heat the combustion tube to simulated reservoir temperature. Three temperature controllers are used to give more uniform temperature along the tube than would one. This step also reduces the possibility of fluid blocking resulting from viscous, high oil saturations.

The temperature in the combustion tube is measured by probing the entire length of the combustion tube with a thermocouple. The thermocouple can move easily in the thermowell located along the axis of the tube and soldered at the bottom to the supporting 10-mesh screen. The soldering was done to prevent the thermowell from bending at the time of packing.

Gas for combustion is supplied by 2000 psi cylinders of compressed gas equipped with a two-stage pressure regulator. All effluent gas and liquid pass through a separator. A two-valve exit system is used to

drain the liquid from the separator.

Originally, an automatic gas-flow control system controlled the inlet flow rate. However, the flow rate was found to be variable when outlet pressure changed, so this controlling stage was replaced by an electronic mass flow controller which was installed in the upstream end. Thus, after passing through the mass flow controller, the gas flows into the combustion tube. At the outlet, it is separated from the produced liquids in the separator. After being cooled in the condenser, it flows through the back pressure regulator and finally to the wet test meter.

4.2 Reaction Kinetics Apparatus

Figure 4.3 shows a flow diagram of the apparatus. Its main components were a combustion cell placed in a furnace, three continuous gas analyzers, and temperature and flow rate measuring equipment.

The combustion cell consisted of a stainless steel tube, 1-1/8" O.D. with 0.020" wall thickness and 5.00" length (Fig. 4.4 and Table 4.2). A coil made up of a 1/8" stainless steel tubing of 0.010" wall thickness was wrapped around the tube to preheat the air. The wrapping also created two air cushions around the tube (Fig. 4.4). This promoted more uniform temperature in the reactor and improved measurement of the actual reactor temperature. The adjustment of the heating coils in the furnace made it possible to get an isothermal plateau about 4" long in the furnace. The combustion cell was placed in this zone. A copper sheet of 0.01" thickness was also wrapped around the reactor to improve heat distribution.

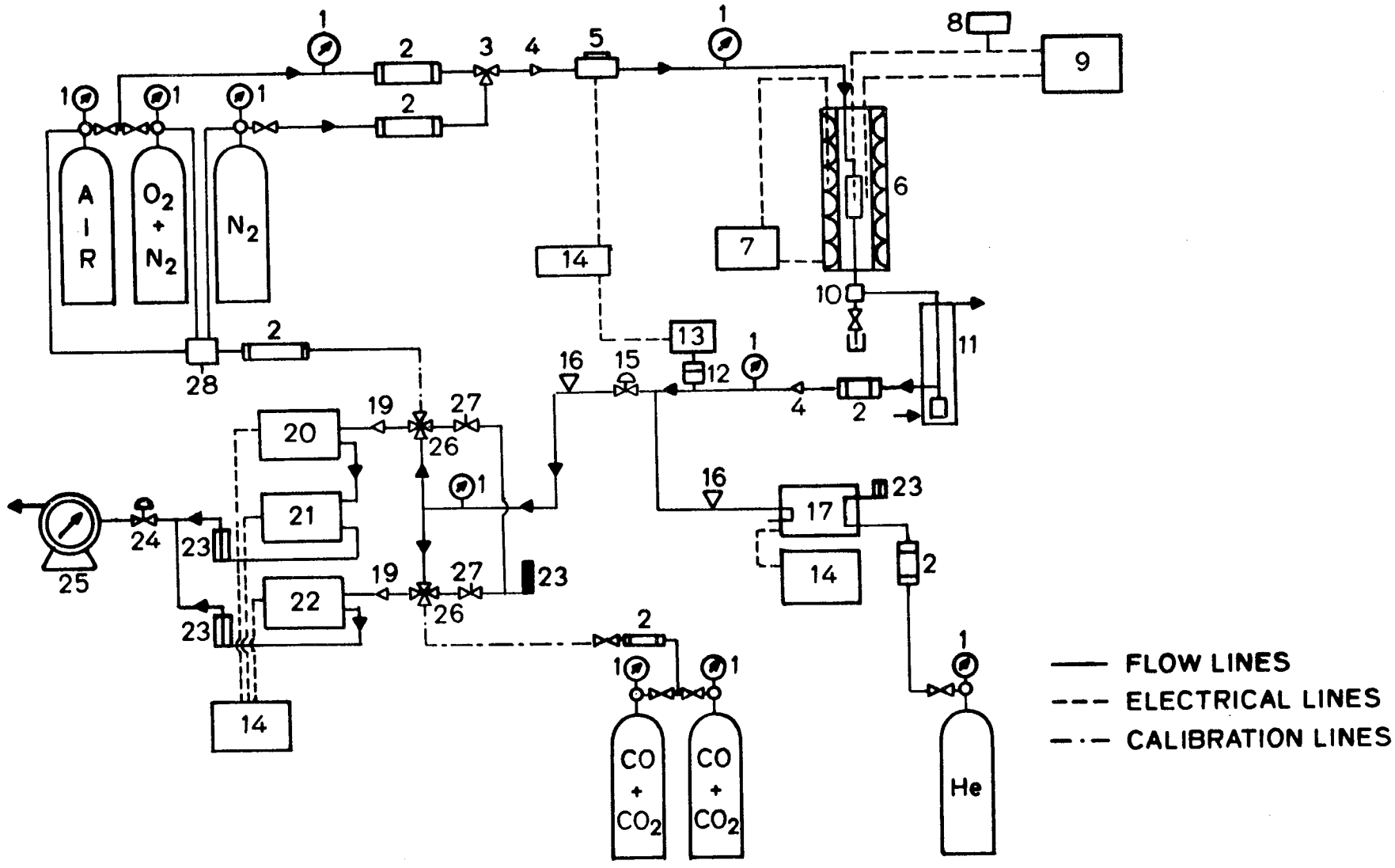

FIG. 4.3

SCHEMATIC DIAGRAM OF APPARATUS FOR KINETICS STUDIES OF IN-SITU COMBUSTION

EQUIPMENT USED IN THE CIRCUIT (Fig. 4.3)

1. Pressure Gauge
2. Drierite
3. 3-Way Valve
4. 60-μ Filter
5. Mass Flow Controller
6. Furnace
7. Temperature Controller
8. Digital Temperature Reader
9. Temperature Reader
10. Separator
11. Ice Bath
12. Pressure Transducer
13. Pressure Indicator
14. Recorder
15. Pressure Regulator
16. Needle Valve
17. Fischer Gas Partitioner
18. Bubble Flow Meter
19. 2-μ Filter
20. Carbon Dioxide Analyzer
21. Carbon Monoxide Analyzer
22. Oxygen Analyzer
23. Rotameter
24. 20-psia Back-Pressure Regulator
25. Wet Test Meter
26. 4-Way Valve
27. 1-psi Relief Valve
28. 5-Way Valve

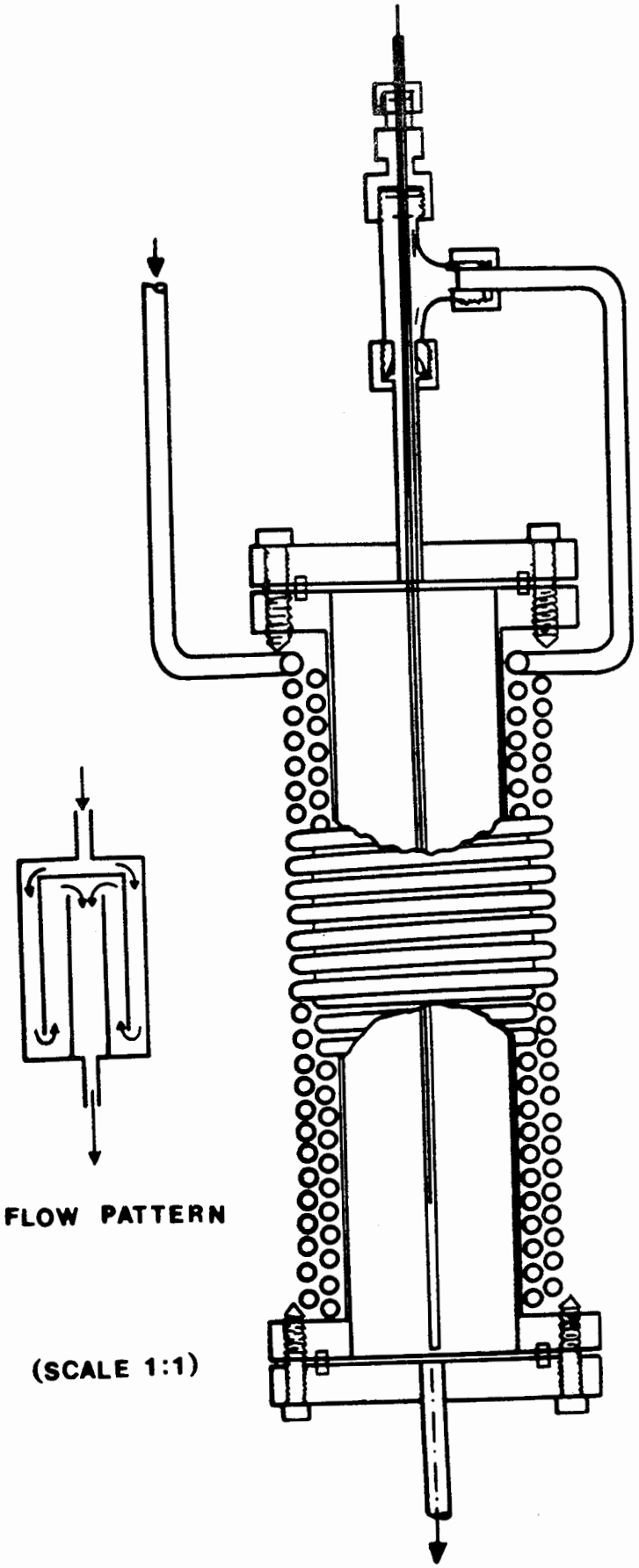

FIG. 4.4
COMBUSTION
CELL

Table 4.2 REACTOR DATA

Combustion Cell	Type 321 Seamless Stainless steel 1-1/8" O.D. x 0.02" wall, 5.00" length
Gas Preheater	Type 347 Stainless steel 1/8" x 0.01", 25.0' length
Thermowell	Type 321 Stainless steel needle tube 0.065" O.D. x 0.009" wall, 20.0" length
Thermocouple	Type J Iron constant 0.04" O.D. x 50.0" length
Flanges	Type 304 Stainless steel 2-1/8" diameter x 1/4" width
Screen	200 Mesh S.S. used at the bottom of the pack
Gaskets	Brass O-rings 1-1/2" O.D. x 0.078" thickness, 1/16" width
Furnace	"Marshall" Furnace model 1046 3" bore x 10" diameter x 20.0" length, 0-2000°F
Temperature Controller	Proportional 10 amp. triac output Range 0-1400°F, type "K".
Temperature Reader	"Numatron" Digital indicator, type "J" thermocouple. (Leeds & Northrup)
Temperature Recorder	"Speedomax W" 0-1500°F (Leeds & Northrup)

To prevent contamination at the bottom of the cell, the bottom flange had several grooves and a ledge (Fig. 4.5). A 200-mesh screen was inserted between the ledge and the O-ring. Flanges were sealed with brass gaskets. A torque wrench was used to tighten the screws uniformly. Before placing the reactor in the furnace, the flanges were insulated with glasswool in order to prevent contact with the furnace wall.

A tube diameter of 1-1/8" O.D. was chosen to obtain a low radial temperature gradient (Appendix A). A thermowell inserted at the center of the reactor could be used to check the isothermal behavior at any time. A thermocouple was also placed around the air preheater, outside of the reactor, to indicate the radial temperature differential.

Table 4.3 presents the major equipment used in the experiments.

4.2-1 Temperature Control

The combination of a digital temperature reader and a temperature recorder was used to check the temperature controller. For most runs, it was necessary to raise the temperature linearly. This was accomplished by using a synchronous motor attached to a gearbox that turned one revolution per day. Because this equipment was installed on top of the circular setting dial of the temperature controller, the desired temperature rate was obtained. Toward the end of the experiments, this apparatus was replaced with a Log/Linear Temperature controller which could be programmed at different rates.

4.2-2 Gas Separation

Two adaptor fittings (1/8" male tube to 1/2" female NPT) were welded together and a valve was connected to them to construct a simple

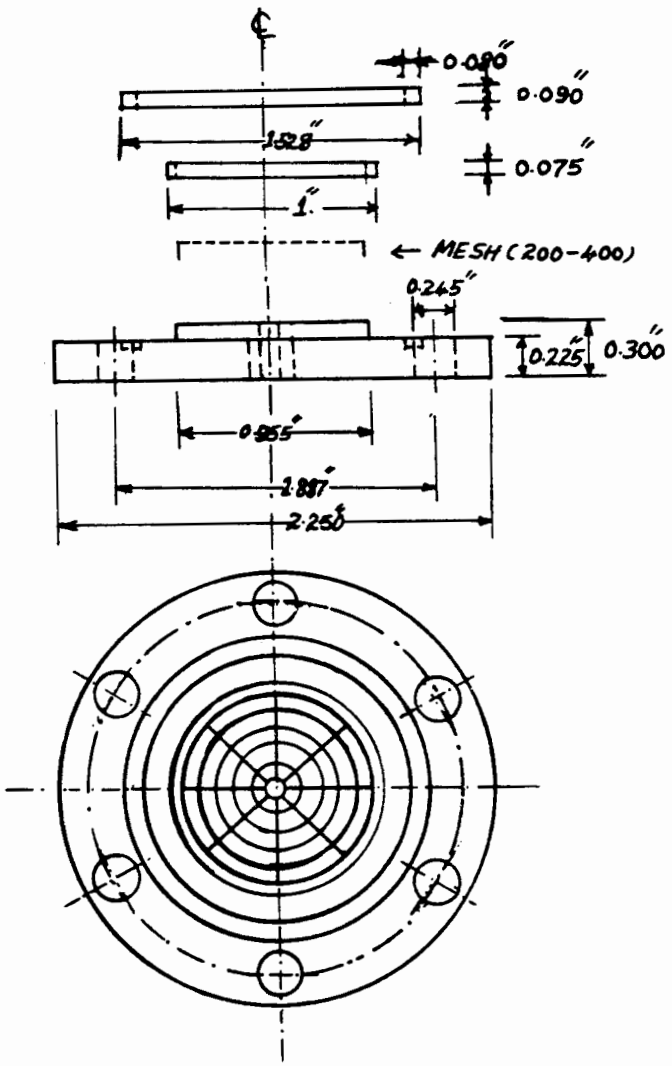

FIG. 4.5 THE BOTTOM FLANGE

Table 4.3 EQUIPMENT IN THE CIRCUIT

Flow Controller	"Matheson" electronic mass flow controller, Model 8240, range 100-5000 sccm, air, with digital output
Gas Analyzers	1. "Beckman" Model 755 Paramagnetic Oxygen analyzer with the 0-5, 0-10, 0-25, 0-50% range and a supressed range of 21-20, 21-19, 21-16, 21-11%. 2. "Beckman" Non-Dispersive infrared Carbon Dioxide analyzer with linearized circuit, 0-5 & 0-20% range. 3. "Beckman" Non-Dispersive infrared Carbon Monoxide analyzer with linearized circuit, 0-2 & 0-10% range. 4. "Fischer" Gas Partitioner for N_2, CO_2, O_2, CH_4, and CO gases.
Recorders	1. "SOLTEC" 3-pen Precision recorder connected to analyzer. 2. "H.P." Strip chart recorder with integrator connected to gas partitioner. 3. "Chessell" 2-pen recorder connected to flow meter and pressure indicator.
Pressure Transducer & Indicator	"Celesco" Pressure transducer and indicator with 0-100 Psi and 0-500 Psi plate.
Flow Meter	1. "Precision Scientific Co." Wet test meter. 2. "Matheson" 0.1-2scfh Rotameter 3. "Matheson" 0.1-2slpm digital flow meter.
Viscometer	"Brookfield" Sunchro-Lectric viscometer cone type high temperature, 0-4000 c.p.
Balance	"Fischer" Gram-Atic Balance accuracy ± 0.0005 g.
Igniter	"POWERSTAT" Variable Auto transformer 0-3000 volts.

Table 4.3 (cont.)

Band Heater	"Norman Associates" expandable wire strap steel construction Bank Heaters, 3" I.D. x 3" width.
Heating Tapes	"BRISKET" heave flexible heating tapes 4 ft and 6 ft long with 1" width.
Furnace	"Marshall" furnace, model 1046, 0-2000°F, used for heating the combustion cell.
Back-Pressure Regulator	1. "Moore" Absolute Pressure Relief valve, model 43R, 0-20 psi. Used after the analyzers. 2. "Tescom" Back-Pressure Regulator No. 26-1700, 0-500 psi used after the combustion cell or after the combustion tube. 3. "Whitey" Micro Needle Valve used in the absence of Pressure regulators.
Temperature Programmer	1. "Teco" Linear, Log Temperature Programmer, model TP-2000, 0-200°C/hr. 2. "Love" Temperature Controller, proportional 10 amp, 0-1400°F in conjunction with "Elremco" motor and gearbox, 1 rpd to rotate the controller dial at 100°F/hr.

separator. A condenser made up of a 1/8" tubing coil in an ice-salt bath, was connected to the separator. The residue of the condensation was collected in a small trap at the bottom of the condenser coil. A mixture of crushed ice and NaCl or $CaCl_2$ decreased the temperature of the condenser to $-20^{o}C$ in order to liquify some of the contaminants. A Drierite holder was installed behind the condenser to absorb the moisture in the gas. Glasswool in the Drierite holder trapped most of the light hydrocarbon in the effluent gas.

4.2-3 Gas Sampling

Figure 4.6 shows a schematic of a gas sampling line. This special setup was designed to prevent disturbances created by unequal pressure during calibration and gas analysis. The back pressure regulator behind the analyzers was adjusted so that the same pressure could be maintained in both calibration and flow lines.

4.2-4 Flow Metering

The gas was supplied by high pressure gas cylinders and the gas flow rate was controlled by an electronic mass flow controller. After maintaining about 10 psi pressure differential across the flow sensor, the required flow rate could be obtained by setting the dial. The flow rate into the analyzers was adjusted with needle valves in front of the analyzers. A wet-test meter and a rotameter were used to check the exit flow rate. Later, for better accuracy, they were replaced by a digital flow meter.

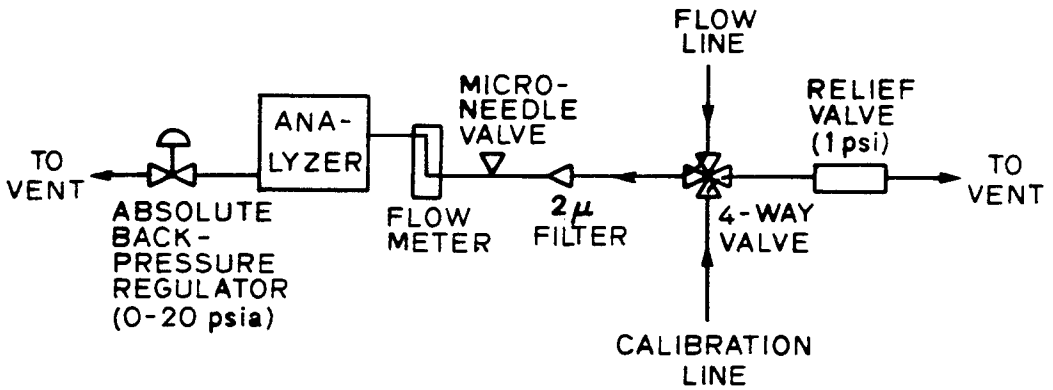

a. FLOWING CONDITION

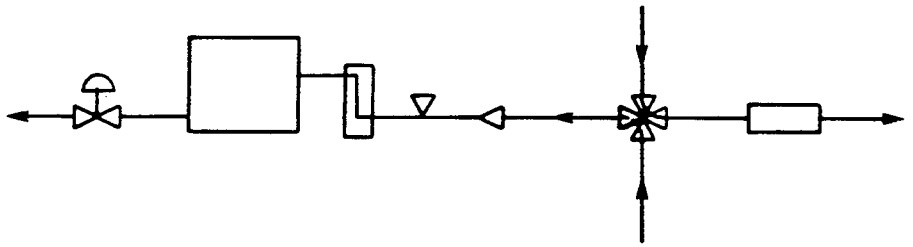

b. CALIBRATION CONDITION

FIG. 4.6 GAS ANALYSIS SETUP

4.2-5 Pressure Regulation

A 0-500 psi adjustable back-pressure regulator was used to obtain the required pressure in the system. Another absolute back-pressure regulator was used to adjust pressure in the analyzers.

5. PROCEDURE

In this section the properties of the crude oils, sand and clay used in the experiments, and also the experimental procedure for preparation of the sand packs are discussed.

5.1 Properties of the Crude Oils

Four different kinds of crude oil were used in the experiments. They were from San Ardo, Lynch Canyon, Huntington Beach (all located in California) and Venezuela. These oils were viscous and heavy. Figure 5.1 shows the viscosity of these oils as a function of temperature. Table 5.1 shows other properties of these oils. Sample distillations for San Ardo and Huntington Beach oils are shown in Figs. 5.2 and 5.3.

Because most of the experiments in this work were run at pressures higher than atmospheric and due to the importance of distillation in in-situ combustion, the distillation data measured at atmospheric pressure were converted to 650 kPa (80 psig) using the published vapor pressure charts for paraffins (Standing 1977). The results are shown in Figs. 5.4 and 5.5 as percent distilled vs temperature. In these calculations, it was assumed that no cracking would take place, and that the hydrocarbons behave like ideal solutions. The calculated incremental volumes distilled at each temperature are also presented on these graphs (at 80 psig pressure). For a more accurate distillation analysis at higher pressures, the flash calculations should be carried out for all crude oil fractions. Also, the presence of steam or inert gases should

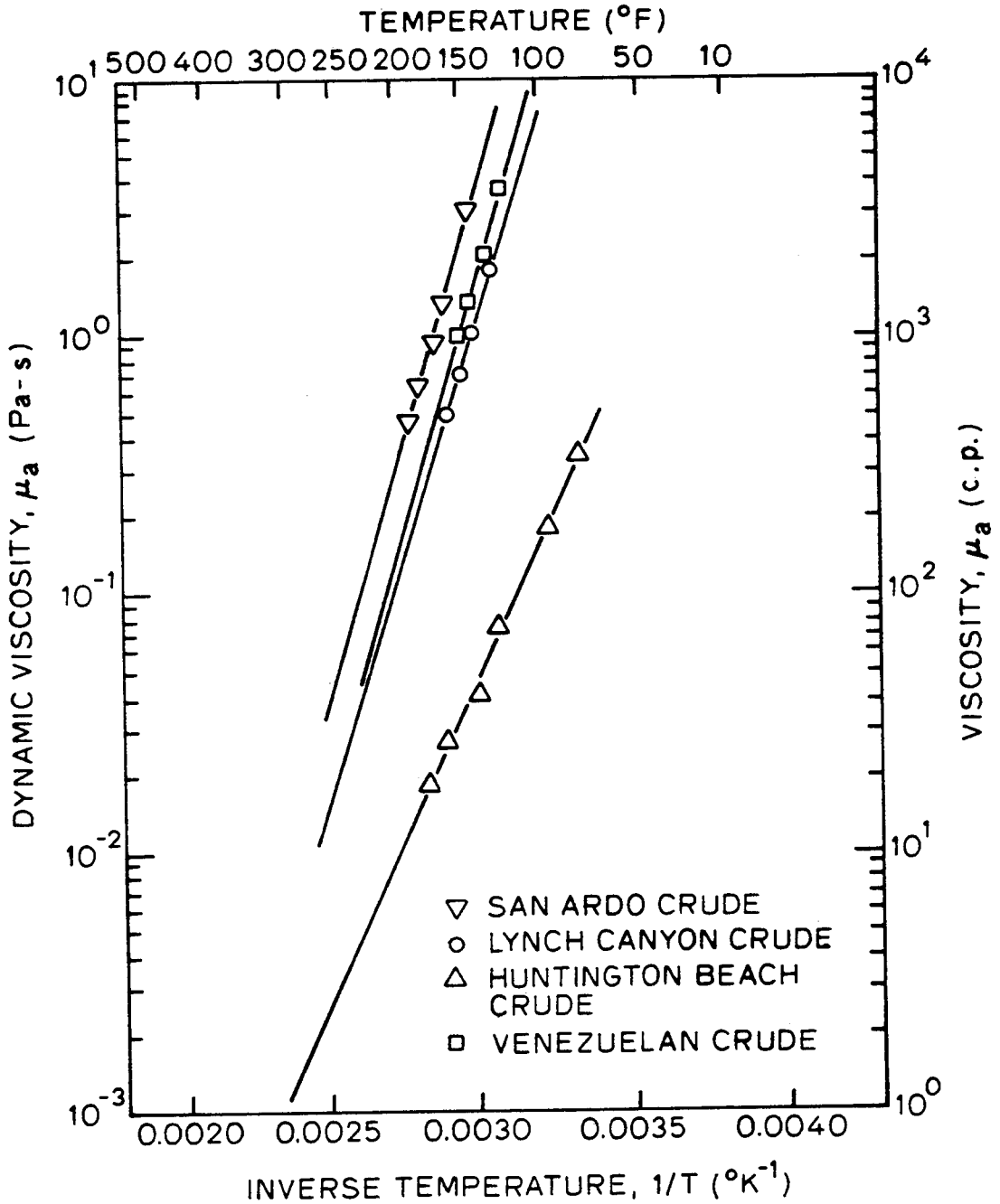

FIG.5.1 OIL VISCOSITY VS 1/T

Table 5.1 CRUDE OIL PROPERTIES[1]

FIELD	ZONE	GRAVITY °API	%C	%H	ATOMIC H/C RATIO	%N	%S	M.W.
San Ardo	Lombardi	11.2	84.94	10.86	1.53	0.96	4.74	593
Venezuela	Jobo Field No. 2	9.5	83.24	10.55	1.52	0.60	4.06	681
Huntington Beach	Lower Main Zone	18.5	84.50	11.53	1.64	0.86	--	386
Lynch Canyon[2]	n.a.	10	74.97	10.81	1.73	0.71	--	435

(1) Obtained by analytical chemistry laboratory.

(2) The properties are those of the displaced crude in combustion Run No. 79-7.

5-485 a
(August 1944)

CRUDE PETROLEUM ANALYSIS

Bureau of Mines .....Bartlesville..... Laboratory
Sample .....58028.....

IDENTIFICATION

San Ardo field
Lombardi sand
2,100-2,250 feet

California
Monterey County
23S-10E

GENERAL CHARACTERISTICS

Specific gravity, ...0.992..... A. P. I. gravity, ...11.1°..... Pour point, ° F., ...80.....
Sulfur, percent .....2.25..... Color, ...brownish black.....
Saybolt Universal viscosity at .....100° F., over 6,000 sec.; ..... Nitrogen, percent, 0.913
at 130° F., over 6,000 sec.

DISTILLATION, BUREAU OF MINES ROUTINE METHOD

STAGE 1—Distillation at atmospheric pressure, ...749..... mm. Hg
First drop, ...178..... ° C. (.....352..... ° F.)

Fraction No.	Cut temp. ° F.	Percent	Sum, percent	Sp. gr., 60/60° F.	° A. P. I., 60° F.	C. I.	Refractive index N_D at 20° C.	Specific dispersion	S. U. visc., 100° F.	Cloud test, ° F.
1	122									
2	167									
3	212									
4	257									
5	302									
6	347									
7	392	1.0	1.0	0.832	38.6	-)				
8	437	1.4	2.4	.861	32.8	53)				
1/ 9	482	4.1	6.5	.867	31.7	-)	1.45473	125.6		
10	527									

STAGE 2—Distillation continued at 40 mm. Hg

11	392	4.9	11.4	0.892	27.1	-	1.48846	141.1	43	Below 5
12	437	5.5	16.9	.909	24.2	58	1.49896	155.4	57	Below 5
13	482	6.3	23.2	.930	20.7	64	1.51060	161.6	99	Below 5
2/ 14	527	3.2	26.4	.946	18.1	-	1.51865	-	200	Below 5
15	572									
Residuum.		72.0	98.4	1.025	6.6					

Ramsbottom carbon residue: Residuum, ...3.3.... percent; crude, ...2.5.... percent.
Equivalent Conradson carbon residue: Residuum, ...4.6.... percent.

APPROXIMATE SUMMARY

	Percent	Sp. gr.	° A. P. I.	Viscosity
Light gasoline				
Total gasoline and naphtha				
Kerosine distillate				
Gas oil	11.7	0.875	30.2	
Nonviscous lubricating distillate	8.5	.901-.931	25.6-20.5	50-100
Medium lubricating distillate	4.6	.931-.946	20.5-18.1	100-200
Viscous lubricating distillate	1.6	.946-.951	18.1-17.3	Above 200
Residuum	72.0	1.025	6.6	
Distillation loss	1.6			

U. S. GOVERNMENT PRINTING OFFICE 16—[illegible]

1/ Distillation discontinued at 482° F.
2/ Distillation discontinued at 509° F.

Fig. 5.2: DISTILLATION ANALYSIS OF THE SAN ARDO CRUDE OIL

6-435 a
(August 1955)

CRUDE PETROLEUM ANALYSIS

Bureau of Mines Bartlesville Laboratory
Sample 55141

IDENTIFICATION

Huntington Beach field
Jones sand, offshore (Upper Miocene)
6,300 feet

California
Orange County

GENERAL CHARACTERISTICS

Specific gravity, 0.945 A. P. I. gravity, 18.2° Pour point, ° F., 15
Sulfur, percent 1.46 Color, brownish black
Saybolt Universal viscosity at 100° F., 870 sec.; at 130° F., 400 sec. Nitrogen, percent, 0.830

DISTILLATION, BUREAU OF MINES ROUTINE METHOD

STAGE 1—Distillation at atmospheric pressure, 756 mm. Hg
First drop, 71 ° C. (160 ° F.)

Fraction No.	Cut temp. ° F.	Percent	Sum, percent	Sp. gr., 60/60° F.	° A. P. I., 60° F.	C. I.	Refractive index N_D at 20° C.	Specific dispersion	S. U. visc., 100° F.	Cloud test, ° F.
1	122									
2	167									
3	212	1.7	1.7	0.749	57.4	-)				
4	257	3.0	4.7	.763	54.0	33)	1.41593	122.7		
5	302	3.3	8.0	.783	49.2	35	1.42922	126.1		
6	347	2.6	10.6	.805	44.1	39	1.44154	130.5		
7	392	3.0	13.6	.829	39.2	43	1.45399	135.6		
8	437	3.5	17.1	.849	35.2	47	1.46534	141.5		
9	482	4.4	21.5	.862	32.7	48	1.47332	151.5		
10	527	9.0	30.5	.872	30.8	48	1.48202	158.8		
STAGE 2—Distillation continued at 40 mm. Hg										
11	392	1.0	31.5	0.880	29.3	48	1.48696	142.5	43	Below 5
12	437	3.3	34.8	.897	26.3	52	1.49610	149.2	55	10
13	482	5.7	40.5	.916	23.0	58	1.50672	142.5	87	20
14	527	4.4	44.9	.927	21.1	60	1.51560	-	200	45
1/ 15	572	6.8	51.7	.950	17.5	-	-	-	Over 400	55
Residuum.		48.2	99.9	1.022	7.0					

Ramsbottom carbon residue: Residuum, 10.9 percent; crude, 5.7 percent.
Equivalent Conradson carbon residue: Residuum, 13.4 percent.

APPROXIMATE SUMMARY

	Percent	Sp. gr.	° A. P. I.	Viscosity
Light gasoline	1.7	0.749	57.4	
Total gasoline and naphtha	10.6	0.778	50.4	
Kerosine distillate	-	-	-	
Gas oil	21.8	.861	32.8	
Nonviscous lubricating distillate	5.9	.891-.917	27.3-22.8	50-100
Medium lubricating distillate	4.4	.917-.927	22.8-21.1	100-200
Viscous lubricating distillate	9.0	.927-.963	21.1-15.4	Above 200
Residuum	48.2	1.022	7.0	
Distillation loss	.1			

1/ Distillation discontinued at 565° F. U.S. GOVERNMENT PRINTING OFFICE 16—87330-2

Fig. 5.3: DISTILLATION ANALYSIS OF THE HUNTINGTON BEACH CRUDE OIL

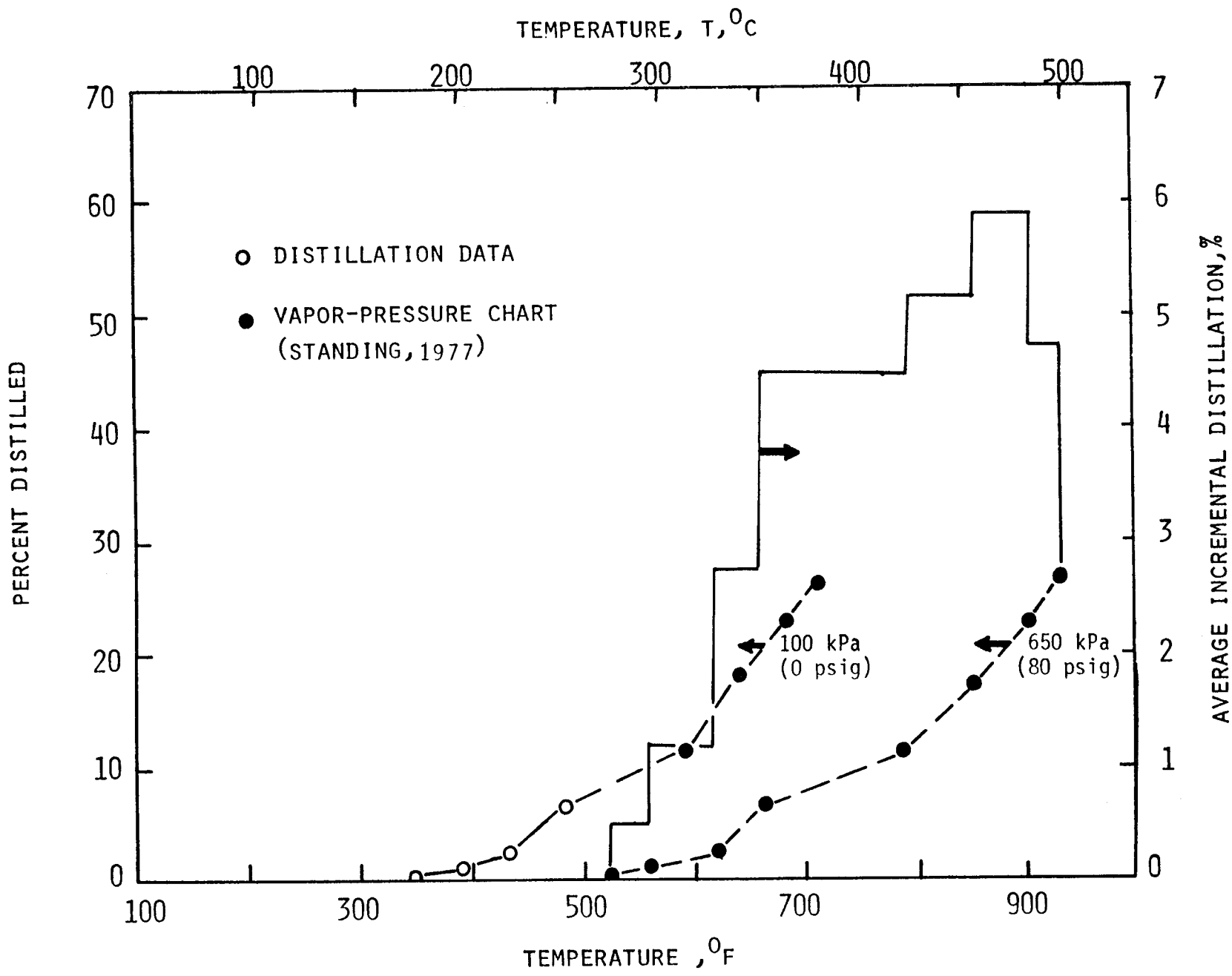

Fig. 5.4: DISTILLATION ANALYSIS OF SAN ARDO OIL

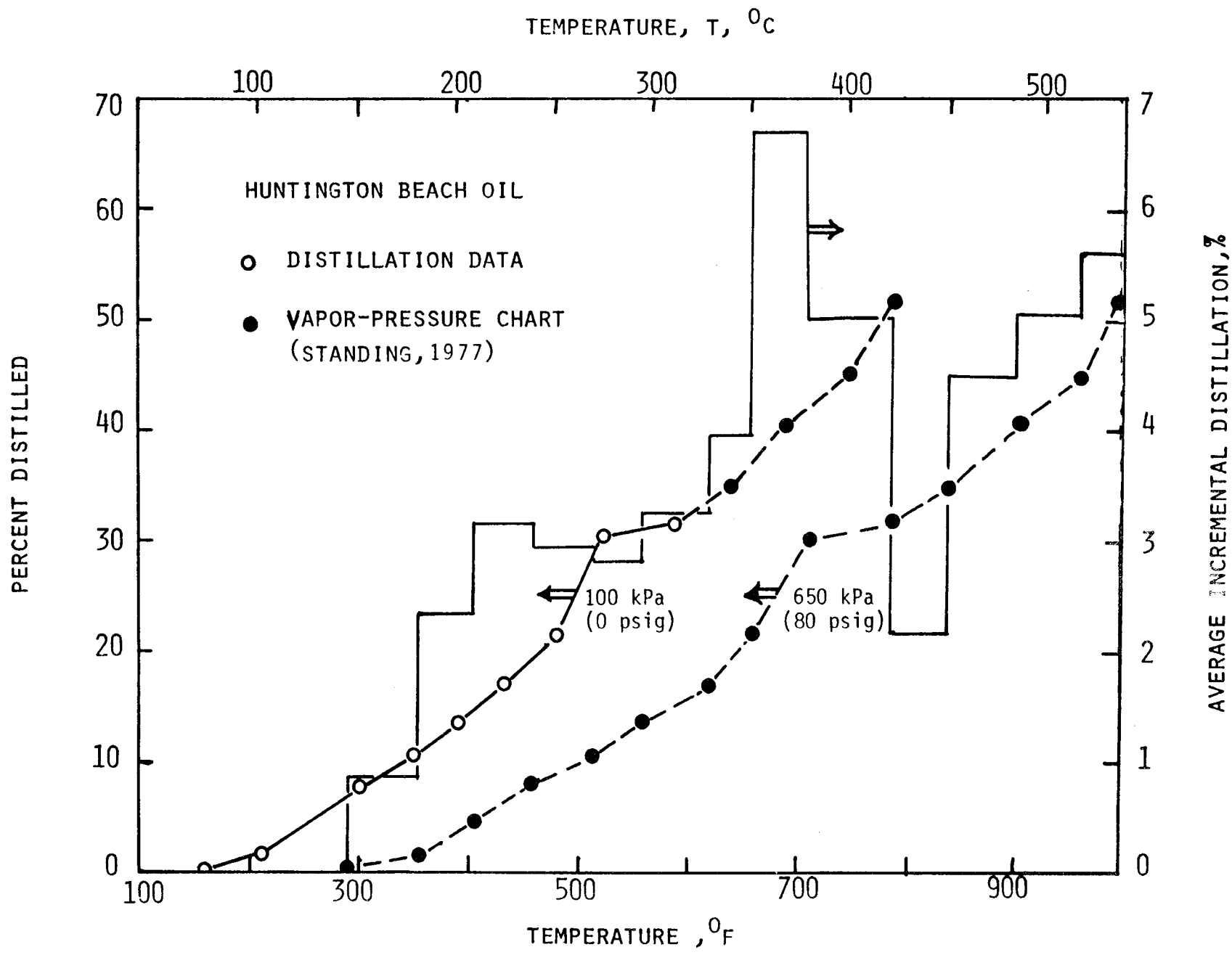

Fig. 5.5: DISTILLATION ANALYSIS OF HUNTINGTON BEACH OIL

be taken into account, because they would tend to lower the vapor pressure of the fractions distilled and consequently change their boiling points.

These figures qualitatively show the amount of vaporized crude oil as the temperature of the oil sand is increased. Notice that the incremental oil vaporized starts from zero and reaches a peak before it drops to zero. A similar trend was observed in the gases produced vs temperature during the kinetic runs. This point will be discussed later.

5.2 Properties of the Sand Pack

Most of the combustion and kinetic runs were made with a mixture of sand and oil. Table 5.2 shows a sieve analysis of the sand. To study the effect of clay, some runs were conducted using a mixture of clay and sand with oil. The fire clay used was analyzed using x-ray diffraction and was found to contain mostly kaolinite. The diffraction pattern of this clay is shown in Fig. 5.6, along with the kaolinite peaks (shown as "K").

In some runs, the original cores obtained from the parent reservoirs were packed in the combustion cell (from Venezuela and Lynch Canyon). A sieve analysis for the latter is shown in Table 5.2. The Venezuelan sand had an average grain size of 150μ. Also, about 20% clay (grain size around 55μ) was present in the matrix.

5.3 Preparation of the Combustion Tube

The combustion tube was prepared by first mixing the sand, oil, and water to yield the desired fluid saturations. This mixture was then

Table 5.2

INITIAL PACK CONDITIONS FOR TUBE RUNS

Sieve Analysis

Sieve Size	Per Cent by Weight Retained
20	0.40
24	41.40
28	57.70
32	0.43
60	0.05
Pan	0.02
	100.00

Type of Core	Unconsolidated
Type of Sand	Ottowa Sand (Unisil Corp.) graded 20-30
Type of Clay	Fire Clay, Mix - Kwik (Lone Star Ind.)

Sieve Analysis of the Burned Core From Lynch Canyon

Sieve Size	Per Cent by Weight Retained
48	29.18
65	63.53
100	.90
120	.95
200	3.12
270	.35
Pan	1.97
	100.00

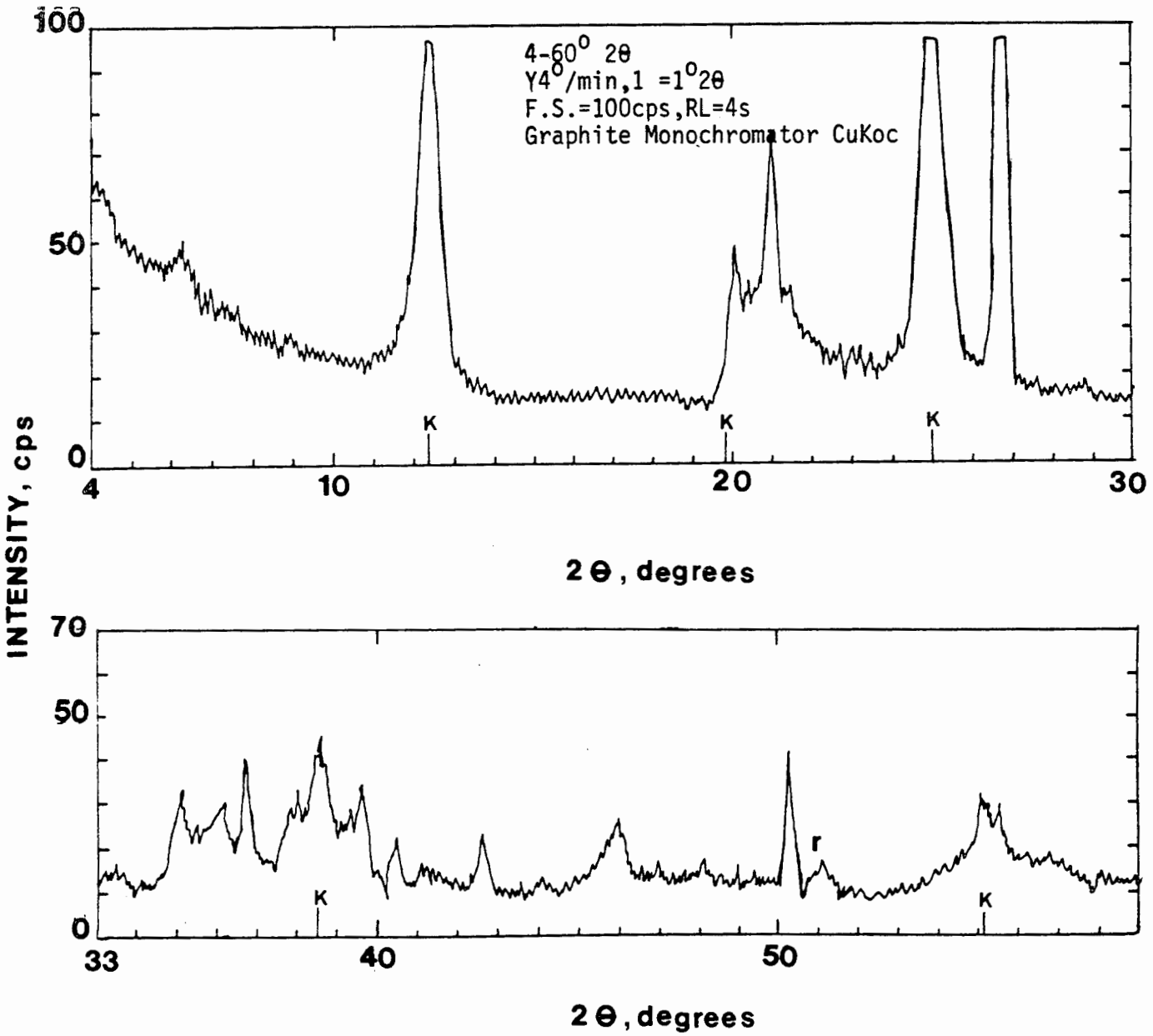

Fig. 5.6: THE X-RAY DIFFRACTION PATTERN OF THE CLAY USED IN THE EXPERIMENTS

carefully tamped into the combustion tube with a steel rod to avoid moving the axial thermowell. For fast, uniform ignition, three cc of linseed oil was added to the top of the sand in the tube before bolting the top flange assembly. The tube was then leak-tested and positioned in the pressure shell. Finally, it was heated overnight at the desired reservoir temperature to get uniform fluid distribution.

For ignition, air flow was established through the pack and the igniter was turned on while the thermocouple was measuring the temperature at the sand face. The ignition could be observed on the temperature recorder by the change of slope on the temperature-time chart. Usually, after a stable front was formed, the igniter was turned off.

Produced gas rate, inlet and outlet pressures, and produced gas composition and temperature (as a function of distance from the top of the pack) were measured periodically. All of the data-taking operations were repeated during the run until the burning front was close to the bottom flange. The run was then terminated.

Several heterogeneous packs were prepared to determine the residual oil saturation at the steam plateau, and to monitor the fuel availability and the effect of temperature and pressure upon it. One section was oil sand, while the neighboring sections had no oil. Hence the displaced oil could move into that portion of the tube that was originally dry. As a result, it was possible to see the behavior of the front in these sections. Also, some combustion runs were ceased to measure the oil, water, and coke saturations at the front and at nearby sections. The procedure for analyzing the volume of the produced oil is discussed below.

5.3-1 Volume Measurement and Analysis of the Produced Liquids in Combustion Tube Runs

In most thermal recovery processes, surfactants, whether originally present in the crude oil, or produced later as a result of oil oxidation, tend to emulsify the crude oil. Consequently, in most combustion tube runs, the produced oil samples consisted of emulsions of water in oil.

After these samples were weighed, a few drops of a special demulsifier (RP-890, Treatolite, provided by Petrolite Co., Brea, California) were added. Then, 5cc gasoline or toluene was mixed into each sample to make the oil less viscous. Finally, a centrifuge separated the oil and water.

The amount of produced liquids was double-checked with an overall material balance. Generally, the results of these calculations agreed by ± 1 g.

A few samples of untreated produced oil were used for gravity and viscosity measurements and some samples were sent to a microanalytic laboratory to analyze the carbon, hydrogen, nitrogen, sulfur and oxygen contents. The results of chemical analysis of the produced oils in combustion runs are summarized on Table 7.1.

5.4 Preparation of the Kinetic Cell

The combustion cell was tamped with the oil sand (around 40 g). Then dry sand was added to fill the tube. No water was added to the oil sand because the published work has shown little effect of initial water saturation on the fuel availability (Alexander et al., 1962). After leak testing, the tube was placed in the furnace. Two sets of temperature histories were applied to this system to determine reaction rate

data; they were: (1) constant-temperature steps, and (2) variable-temperature, increasing at a constant rate.

5.4-1 Constant-Temperature Runs

The bed was brought to the desired temperature level while nitrogen was flowing through the system. This would commonly last 1 to 1.5 hours. Then air was admitted to the bed. This was continued until no change could be seen in the exit gas concentration, and the process would be repeated at a higher temperature at the same pressure and flow rate, and again at a higher temperature until all fuel has burnt. Similar runs were made at different pressures and flow rates.

Although this method is straightforward, it is time consuming (40 to 50 hours) and does not simulate true frontal behavior in which each element of reservoir is under high temperature for a short period of time; therefore, variable-temperature runs were conducted.

5.4-2 Variable-Temperature Runs

If the bed is subjected to a linear rise in temperature (such as in Differential Thermal Analysis) while air is flowing through the cell, it is possible to get useful information regarding the kinetics of the reactions (Appendix C). However, this heat rate should be slow enough to give a minimum temperature differential across the reactor (Appendix A). This process was continued until there were no carbon oxide gases in the effluent line. This type of run is very similar to the behavior of a reservoir element ahead of the combustion front. Although the heating rate is non-linear for the reservoir element, it is, on the average, around 150 to 200°C per hour. A heating rate of 55°C

per hour was chosen to improve heat transfer (see Appendix A) and to provide an experiment of reasonable duration. The temperature history described is similar to that observed in a long tube run with a combustion front velocity of approximately 1 ft/day. Practically, this type of run is similar to a summation of constant-temperature runs at different temperature levels.

6. OPERATION

The problems encountered during running the experiments and the initial and final pack conditions for both the combustion tube and the kinetic cell will be discussed in this section.

6.1 Operation of the Combustion Tube

The major problem encountered in combustion runs was blocking, either in the main tube or in the gas sampling lines. As the front moves, an oil bank grows ahead of the steam plateau. The growth of this zone can be observed through the large pressure drop across the combustion tube. This can be seen in Figs. 6.1 and 6.2.

If the oil saturation is high, blocking may occur. Increasing the ambient temperature and letting the oil drain overnight can help circumvent this problem. In Run No. 79-3 (initial gas saturation 15%), neither of these remedies worked after blocking had stopped gas flow completely, and consequently the combustion run failed.

When gas sampling is done through the sampling line, the fluid may enter these lines and block them. This occurred in Run No. 79-7. However, if the pressure in these lines remains constant by means of a pressure regulator set at the line pressure, it is possible, at a very low flow rate, to prevent liquid from blocking the line.

The combination of two valves at the bottom of the condenser helped to drain it effectively. Often, it was necessary to put some back

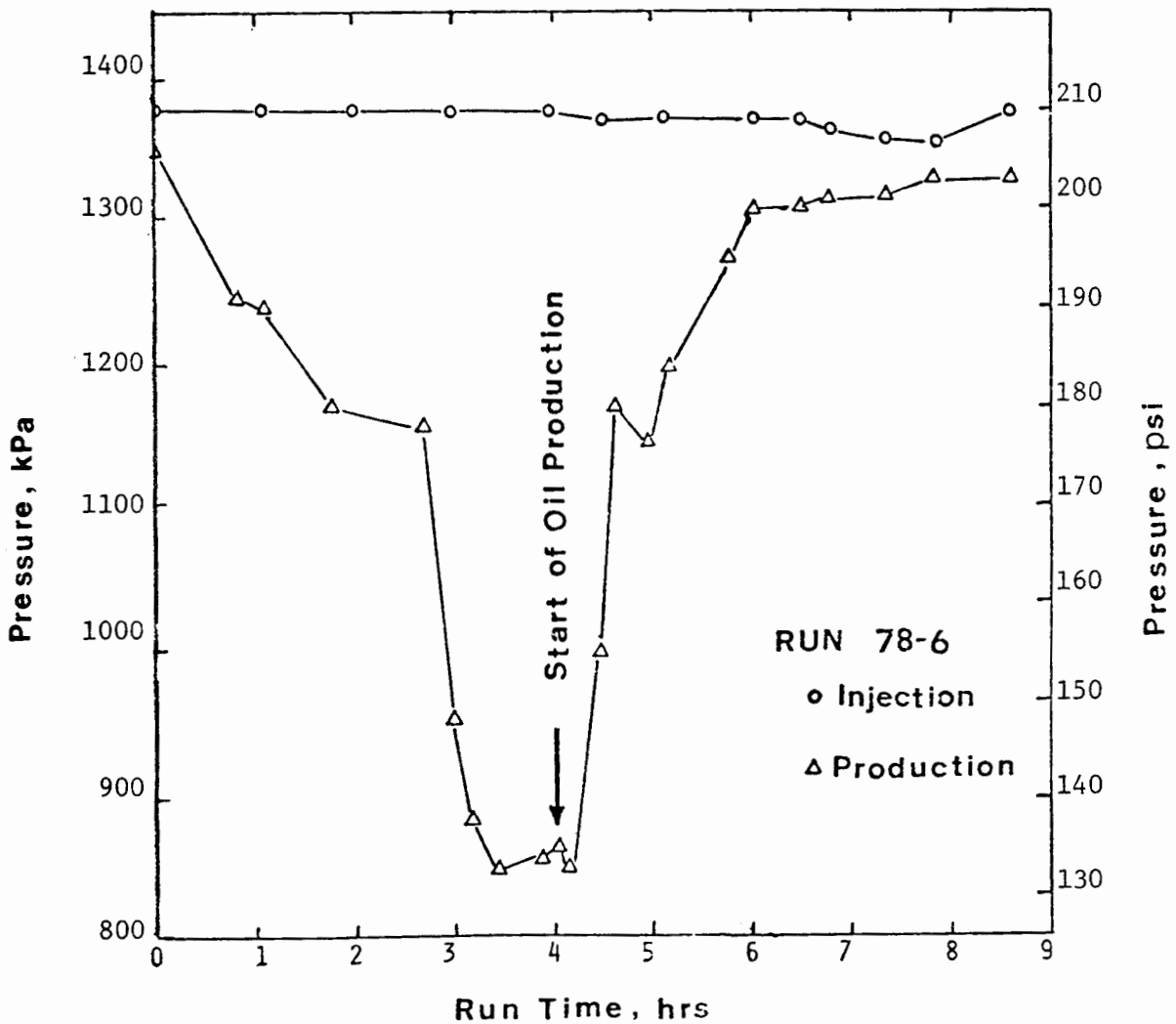

Fig. 6.1: PRESSURE BUILDUP OBSERVED IN RUN NO. 78-6

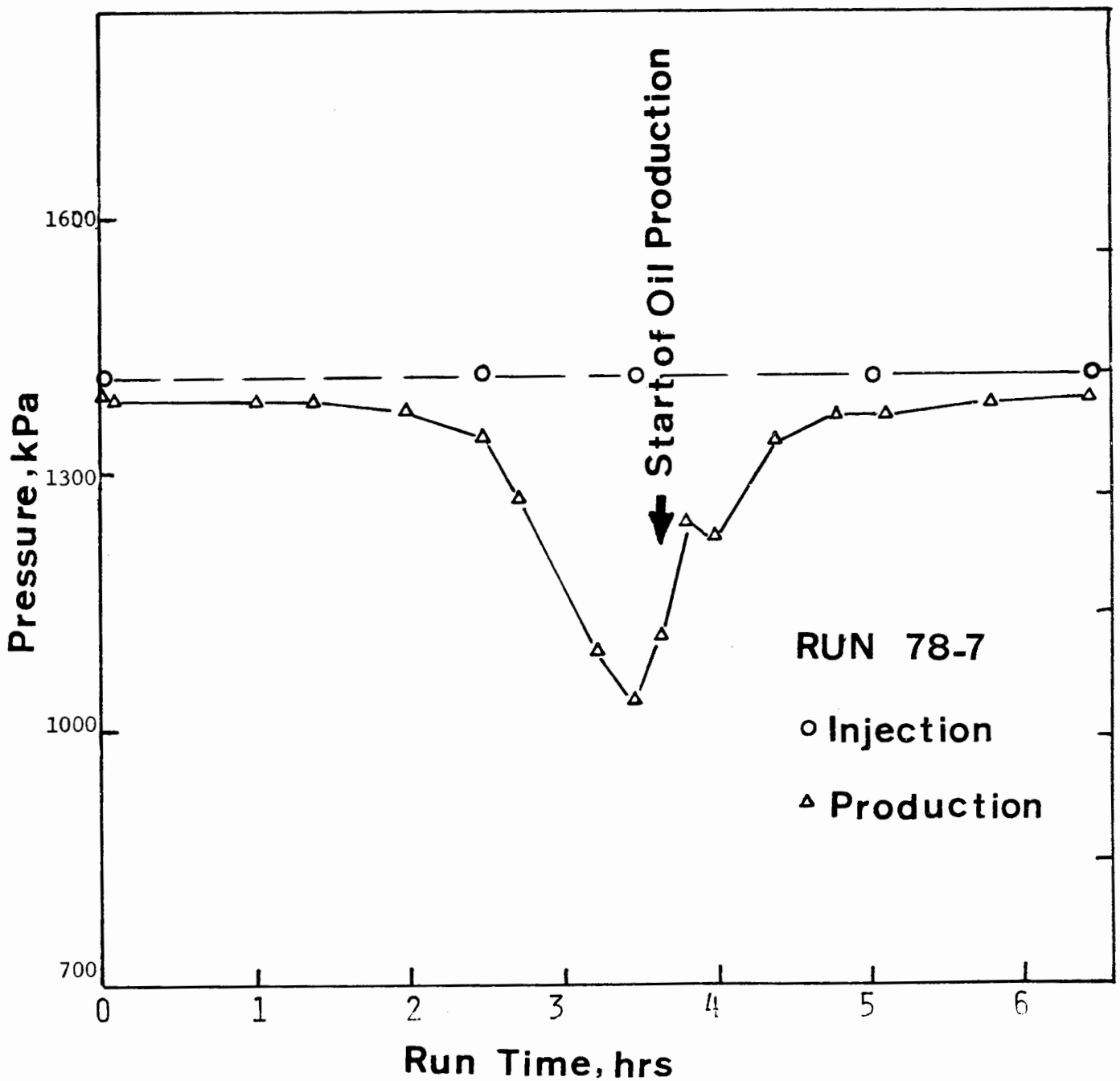

Fig. 6.2: PRESSURE BUILDUP OBSERVED IN RUN NO. 78-7

pressure on the liquid in the separator because of the high viscosity of the oil. This could be done by opening the top valve very slightly while the bottom one was full open.

Following each run, the burned volume (sand and clay) was weighed and produced liquids were analyzed for oil, water, and sediments. Table 6.1 summarizes this information. Thus it was possible to make a material balance calculation. The overall recovery material balance in the tube runs was quite satisfactory.

Table 6.2 shows the initial pack conditions for both homogeneous and heterogeneous packs. As shown, different process variables were tried to investigate their effects on the frontal behavior. Among these were: oil and water saturation, flow rate, pressure, ambient temperature, clay content, and different types of oil.

6.2 Operation of the Reaction Kinetic Apparatus

The operating pressure and flow rate were held constant throughout each run. The back-pressure regulator never digressed more than ±1 psi from the set pressure. The maximum pressure drop was 2 psi. The mass flow controller maintained a constant injection rate. However, due to drift in the electric mass flow controller, the actual flow rate was about 1% lower than the set flow rate at later periods.

The oil saturation in the sand pack (below 15 percent) and the bed thickness (Table 6.3) were chosen so that the oxygen consumption and therefore the heat generation in the sand pack could be minimized (Appendix A). The oxygen consumption never exceeded 15% of the inlet concentration. This also helped maintain an isothermal bed in the reaction zone.

Table 6.1a

GROSS RECOVERY AND PACK DATA FOR COMBUSTION RUNS

RUN NO.	ORIGINAL OIL IN PLACE, g	OIL PRO-DUCED, g	WATER IN PLACE, g	WATER PRO-DUCED, g	SAND g	CLAY g	LENGTH OF THE PACK, cm
78-1	433	275	465	420	5674	67	79
78-2	607	390	290	360	5625	79	80
78-3	416	310	225	216	5100	27	82
78-4	650	478	0	134	4708	498	82.5
78-5	418	255	0	69	4302	461	83.5
78-6	648	496	310	330	5381	319	80
78-7	464	340	271	260	4771	308	71
79-6	414	307	503	470	5833	350	79
79-7	431*	186	569*	547	4838**	---	72.5
80-1	444	212	322	199	5674	0	81

* Estimated

** Total recovered

Table 6.1b

RECOVERY OF TUBE RUNS

RUN NO.	78-2	78-3	78-4	78-5	78-6	78-7
SAND & CLAY, WT.%	99.7	99.7	98.8	99.74	96.4	----
HYDROCARBON, WT.% (oil, fuel, coke)	77.4	101.1	90.40	97.4	91	96.5
WATER, WT.%	102.6	67.7	148.0	96.3	92.5	88.8
OVERALL, WT.% (sand, clay, H.C., water)	98.7	98.1	97.9	99.5	95.0	----

Table 6.2a

INITIAL PACK CONDITIONS FOR TUBE RUNS: HOMOGENEOUS RUNS

RUN NO.	TYPE OF OIL	ϕ, % p.v.	S_o, % p.v.	S_w, % p.v.	S_g, % p.v.	OIL/SAND+CLAY wt. %	CLAY/SAND wt. %	INPUT p kPa.	AMB.TEMP. ^oC
78-1	San Ardo	38.5	32.7	23.5	43.8	7.54	1.2	690	52-77
78-2	San Ardo	40	43.7	20.3	37	9.96	1.2	690	54-82
78-3	San Ardo	47.8	24.1	12.7	63.2	8.12	7.0	690	76-104
78-4	San Ardo	46.4	39.2	0	60.8	12.48	10.6	690 - 850	62-65
78-5	San Ardo	51.5	29.0	0	71	8.77	10.7	690	26-27
78-6	San Ardo	39	48	22	30	11.37	5.9	1360	62-64
78-7	San Ardo	39.7	37.8	21.4	40.8	9.14	6.4	1360	62-64
79-5	Venezuela	47.5	36.6	23.2	40.2	7.93	---	690	62-64
79-7	Lynch Canyon	27.4	31.3	41.3	27.4	8.17	---	680 - 1020	62-71
80-1	San Ardo	41	31	21	48	7.83	0	690	93-126

Table 6.2b

INITIAL PACK CONDITIONS FOR TUBE RUNS: HETEROGENEOUS RUNS

RUN NO.	TYPE OF OIL	ϕ, % p.v.	S_o, % p.v.	S_w, % p.v.	S_g, % p.v.	OIL/SAND+CLAY wt. %	CLAY/SAND wt. %	INPUT p kPa.	AMB.TEMP. °C
79-1	San Ardo	49.6 (top)	67.8	27	5.1	24.4	10	884	62-64
		33.6 (bot.)	0	50.8	49.2	10	10		
79-2	San Ardo	39.3 (top)	37.8	43.1	19.1	8.96	7.67	690	62-64
		34.5 (bot.)	0	53	47	0	8.57		
79-3	San Ardo	36.8 (top)	44	41.5	14.5	9.28	8.5	690 - 1380	62-64
		32.6 (mid.)	0	50	50	0	8.5		
		36.8 (bot.)	44	41.5	14.5	9.28	8.5		
79-4	San Ardo	40.2 (top)	37.4	41.1	21.5	9.24	7.67	690	62-64
		33.7 (bot.)	0	47	53	0	8.57		
79-6	San Ardo	36.2 (top)	43.1	39.9	17	9.01	6	690 - 1020	62-64
		31.8 (mid.)	0	43.5	56.5	0	6		
		36.2 (bot.)	43.1	39.9	17	9.01	6		

Figure 6.3 shows the temperature profile along the kinetic cell observed in isothermal run no. 111 at each temperature level. Before air injection, the temperature was very uniform. However, due to exothermic reactions in the presence of air, the bottom of the reactor became hotter than the top. The amount of heat rise closely resembles similar behavior observed in a Differential Thermal Analysis. The heat generation in the pack did not cause the bed temperature to exceed the average temperature by more than $3^{o}C$. However, at higher oil saturation or with more reactive oil or a thicker bed, the heat generation caused hot spots to form in the bed. If the bed had not been subjected to gas drive, these hot spots could have easily led to spontaneous ignition.

An example is shown in Fig. 6.4 where the bed temperature along with the programmed temperature is graphed on the right ordinate. The produced carbon dioxide and carbon monoxide (shown as "square" and "cross" signs) and consumed oxygen (shown as "circle" sign) are graphed on the left ordinate. The high level of oxygen consumption at low temperatures and consequently the exponential heat rise in the bed led to the spontaneous ignition. The data obtained under these conditions were discarded due to the uncertainty of both the average temperature and the gas analysis.

When the oil in the original matrix was used, blocking would generally occur due to high oil saturation. Under these circumstances, the bed would be kept under high pressure gas (nitrogen) and warm ambient temperature (around $70^{o}C$) until gas could flow easily. Then a gas drive (N_2) followed until oil no longer flowed; the experiment was then continued. Some runs could not be concluded because of ice blocking in

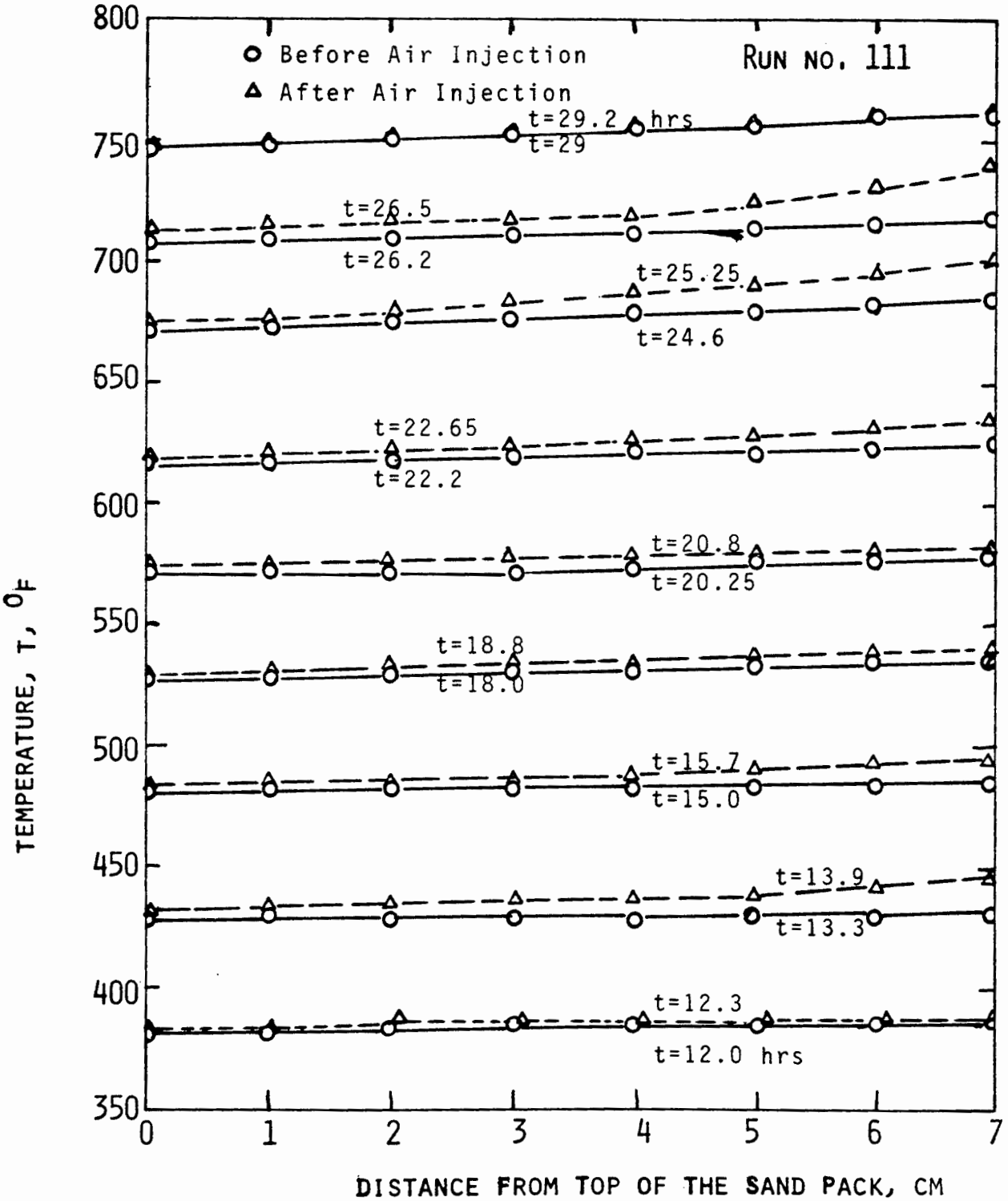

Fig. 6.3: TEMPERATURE PROFILES ALONG THE SAND PACK

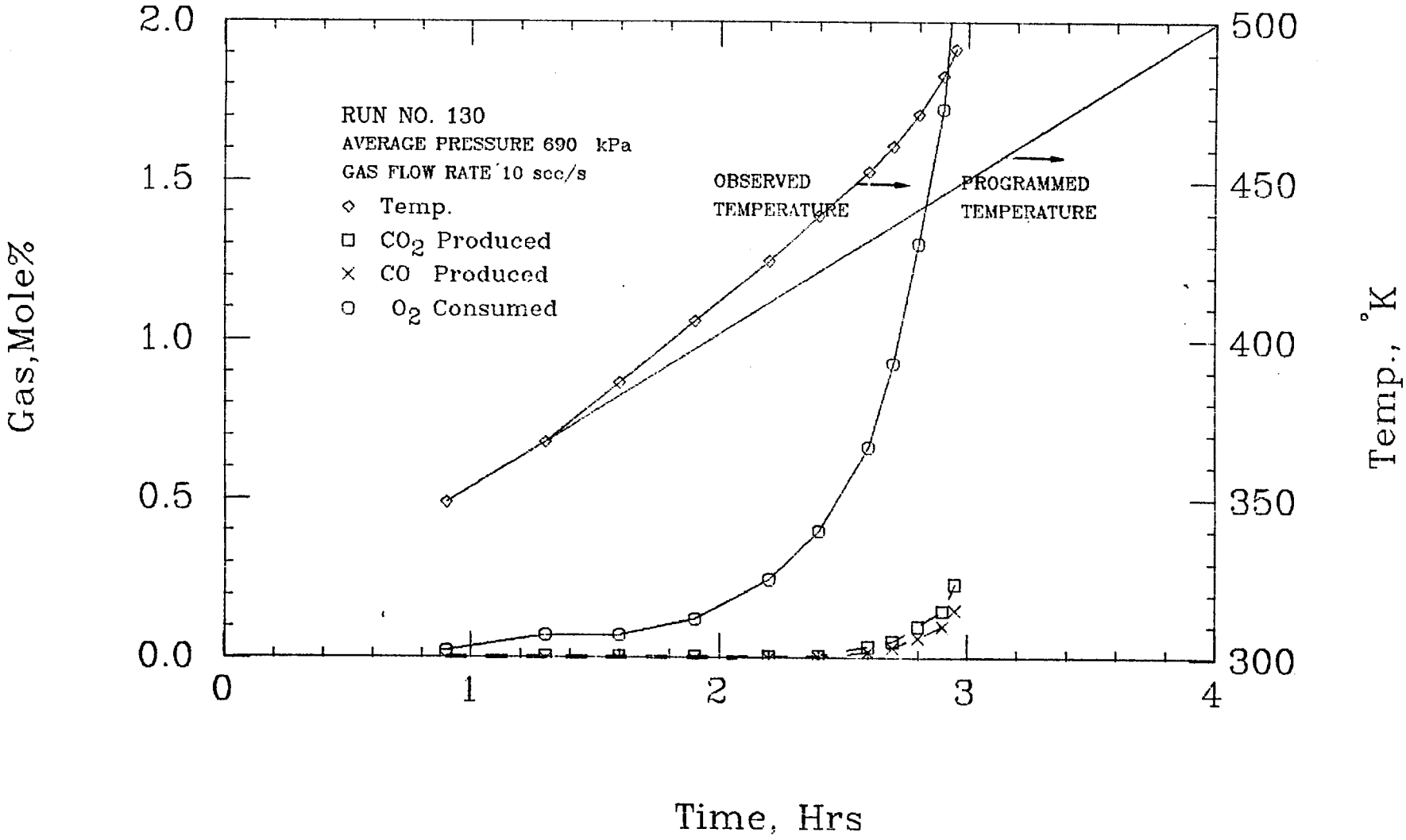

Fig. 6.4: GAS COMPOSITION AND TEMPERATURE FOR RUN NO. 130

the condenser coil. The ice was formed from the hot water droplets which were not trapped in the separator. This problem was partially solved by keeping the separator in another ice bath. By pulling the coil out of the ice bath and keeping it at room temperature for a short period of time, later blockings were circumvented.

Because the oxygen analyzer was sensitive to ambient pressure change, it was necessary to calibrate it frequently. The special drop mentioned previously helped prevent disturbances in the analyzer during calibration. Care was taken to maintain the same gas flow rate in the analyzers during and after calibration.

Table 6.3 presents the initial pack conditions for different kinetic runs. A variety of parameters were tested in different runs to observe their effects on the reaction rates.

6.3 Accuracy of Measurements

The accuracy in the gas analysis was ± 0.5% of the full range. The analyzers had the following ranges: 0-5 and 0-20% for CO_2, 0-2 and 0-10% for CO and 20-21, 19-21, 16-21 and 11-21% for O_2 (in some runs a mixture of 8.3% oxygen and balance nitrogen were injected; the analyzer range for these runs was 0-10%). Because of the low level of combustion, in most runs the most sensitive ranges of the analyzers were used. Thus the accuracy was very high.

The thermocouples and temperature readers were tested for precision and repeatability. It was found that the temperature reader was accurate within ± 1°F. But the temperature recorder showed some drift at high temperatures (in the range of 700-1000°F). Therefore, the data from the temperature recorder were used only for interpolation.

Table 6.3

INITIAL CONDITIONS FOR KINETICS RUNS

RUN NO.	OIL USED	FLOW RATE scc/s	AVG.PRESSURE kPa	INJ.OXYGEN Mole%	CONDITION	BURNED FUEL g	FUEL/SAND RATIO wt.%	BED THICKNESS cm
101	SAN ARDO	16.7	690	21	ISOTHERMAL	2.402	2.69	9
102	SAN ARDO	16.7	690	21	NON-ISOTHERMAL	0.401	1.72	2
103	SAMPLE NO. 8 (79-4)	8.3	690	21	NON-ISOTHERMAL	0.924	4.57	2
104	HUNTINGTON BEACH	8.3	690	21	NON-ISOTHERMAL	0.866	3.64	2
105	SAMPLE NO. 5 (79-3)	16.7	690	21	NON-ISOTHERMAL	0.577	9.07	1
106	SAMPLE NO. 13 (7903)	16.7	550	21	NON-ISOTHERMAL	3.701	7.76	2.3
107	SAN ARDO	16.7	550	21	ISOTHERMAL	0.604	2.81	2.1
108	VENEZUELA	8.3	550	21	NON-ISOTHERMAL	0.514	4.48	1.2
109	SAMPLE NO. 68 (80-1)	16.7	550	8.3	NON-ISOTHERMAL	1.458	3.89	4.2
110	HUNTINGTON BEACH	7.5	550	8.3	NON-ISOTHERMAL	1.777	3.99	4.3
111	VENEZUELA	8.3	415	8.3	ISOTHERMAL	1.894	3.56	5.5
112	VENEZUELA	8.3	415	8.3	NON-ISOTHERMAL	1.234	3.75	3.5
113	SAMPLE NO. 68 (80-1)	8.3	275	8.3	NON-ISOTHERMAL	0.725	3.72	2.5
114	SAN ARDO (clay added)	8.3	550	21	NON-ISOTHERMAL	0.775	3.45	2.5
115	SAN ARDO (clay added)	8.5	275	8.3	NON-ISOTHERMAL	0.677	3.39	2
116	HUNTINGTON BEACH	10.0	550	21	ISOTHERMAL	1.88	3.80	4.5
117	HUNTINGTON BEACH	10.0	1035	21	NON-ISOTHERMAL	1.260	3.16	4
118	HUNTINGTON BEACH	10.0	138	21	NON-ISOTHERMAL	0.730	3.41	2.2
119	HUNTINGTON BEACH	10.0	552	21	NON-ISOTHERMAL	1.035	3.52	3
120	HUNTINGTON BEACH	10.0	1104	21	NON-ISOTHERMAL	0.984	3.63	2.5
121	HUNTINGTON BEACH	10.0	690	21	NON-ISOTHERMAL	0.757	3.41	2.2
122	HUNTINGTON BEACH	10.0	138	8.3	NON-ISOTHERMAL	1.103	3.44	3
123	HUNTINGTON BEACH	10.0	17	21	NON-ISOTHERMAL	1.177	3.75	3
124	HUNTINGTON BEACH	10.0	235	21	NON-ISOTHERMAL	1.441	3.32	4
125	VENEZUELA	10.0	828	21	NON-ISOTHERMAL	0.784	3.22	2.5
126	VENEZUELA (original core)	10	690	21	NON-ISOTHERMAL	10.242*	----	4
127	SAN ARDO	10	690	21	NON-ISOTHERMAL	0.916	2.54	3
128	HUNTINGTON BEACH	10	41	21	NON-ISOTHERMAL	0.931	3.2	2.7
129	SAN ARDO	10	138	21	NON-ISOTHERMAL	0.814	2.55	3.1
130	LYNCH CANYON (original core)	10	690	21	NON-ISOTHERMAL	-----	----	3.3
131	LYNCH CANYON (original core)	10	690	21	NON-ISOTHERMAL	3.321*	----	1.6

*Total weight reduction of oil sand including water loss.

7. ANALYSIS OF PRODUCTS AND RESULTS OF COMBUSTION RUNS

The in-situ combustion process had a considerable effect on the properties of the produced oil. These effects along with some correlations obtained during this study are reported here.

7.1 Properties of Produced Oils

The combustion process lowered the specific gravity and viscosity of produced oil in all runs (Figs. 7.1-7.3). As a run continued, the produced oil became progressively less viscous. This is a result of the cracking and distillation of crude oil in porous medium and subsequent dissolving of the light hydrocarbons in the oil. Table 7.1 shows an increase in atomic hydrogen-carbon ratio and oxygen content of the produced crude oil compared to the original crude. This is another indication of the cracking and the oxidation of crude oil.

7.2 Oil Production-Burned Volume Correlation

Figures 7.4 and 7.5 present the cumulative water and oil recoveries as functions of time. They are graphed as percentages of total fluid produced and not as percentages of fluid originally in place. These two differ by the amount of fuel consumed during experiments. The abscissa on these graphs is percent volume burned. This can be obtained by finding the ratio of the front distance from the sand face to the original pack length.

Folowing Gates and Ramey (1980), data of total oil produced vs volume burned were plotted in Fig. 7.6. These data not only match the

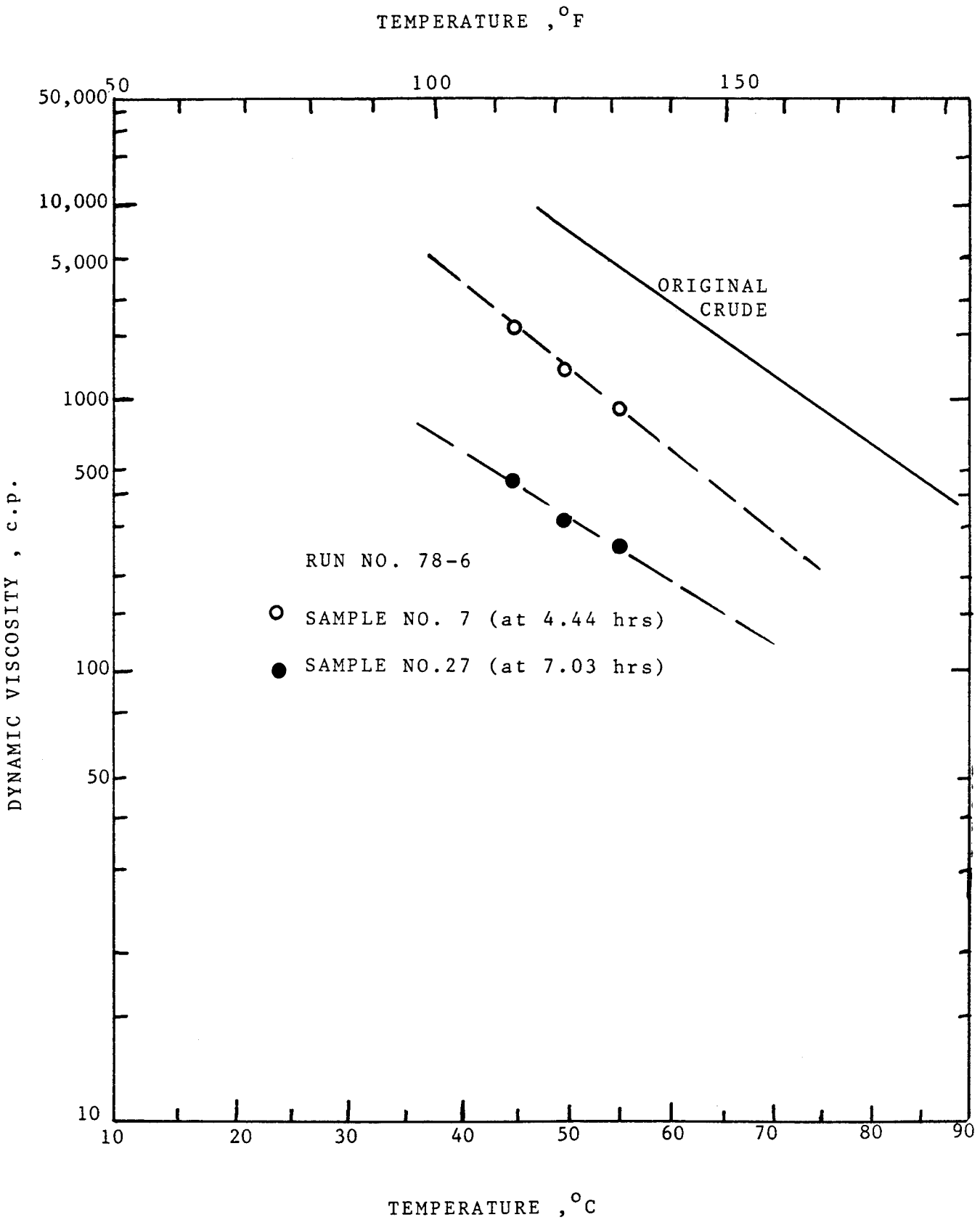

Fig. 7.1: PRODUCED OIL VISCOSITY IN RUN NO. 78-6

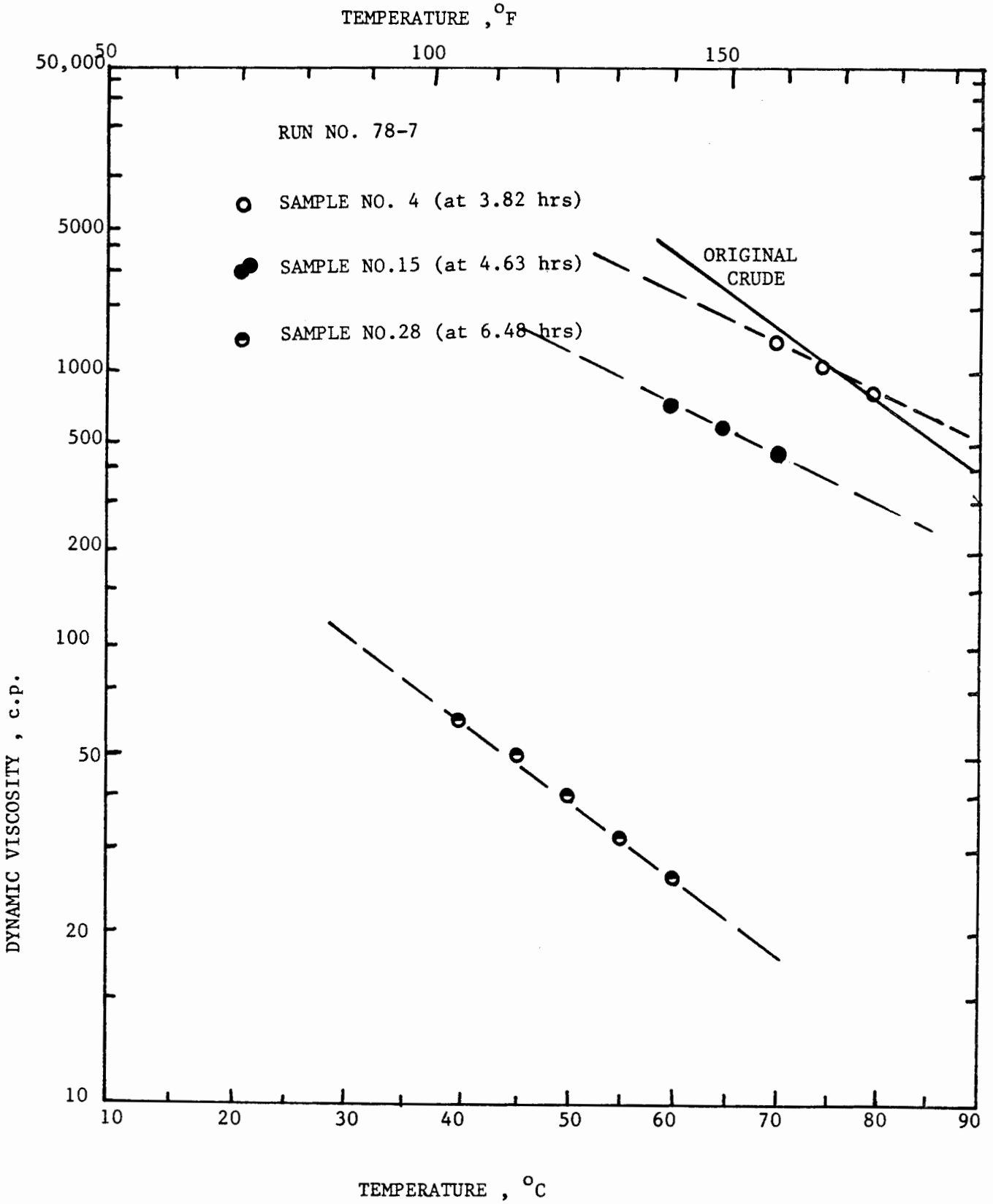

Fig. 7.2: PRODUCED OIL VISCOSITY IN RUN NO. 78-7

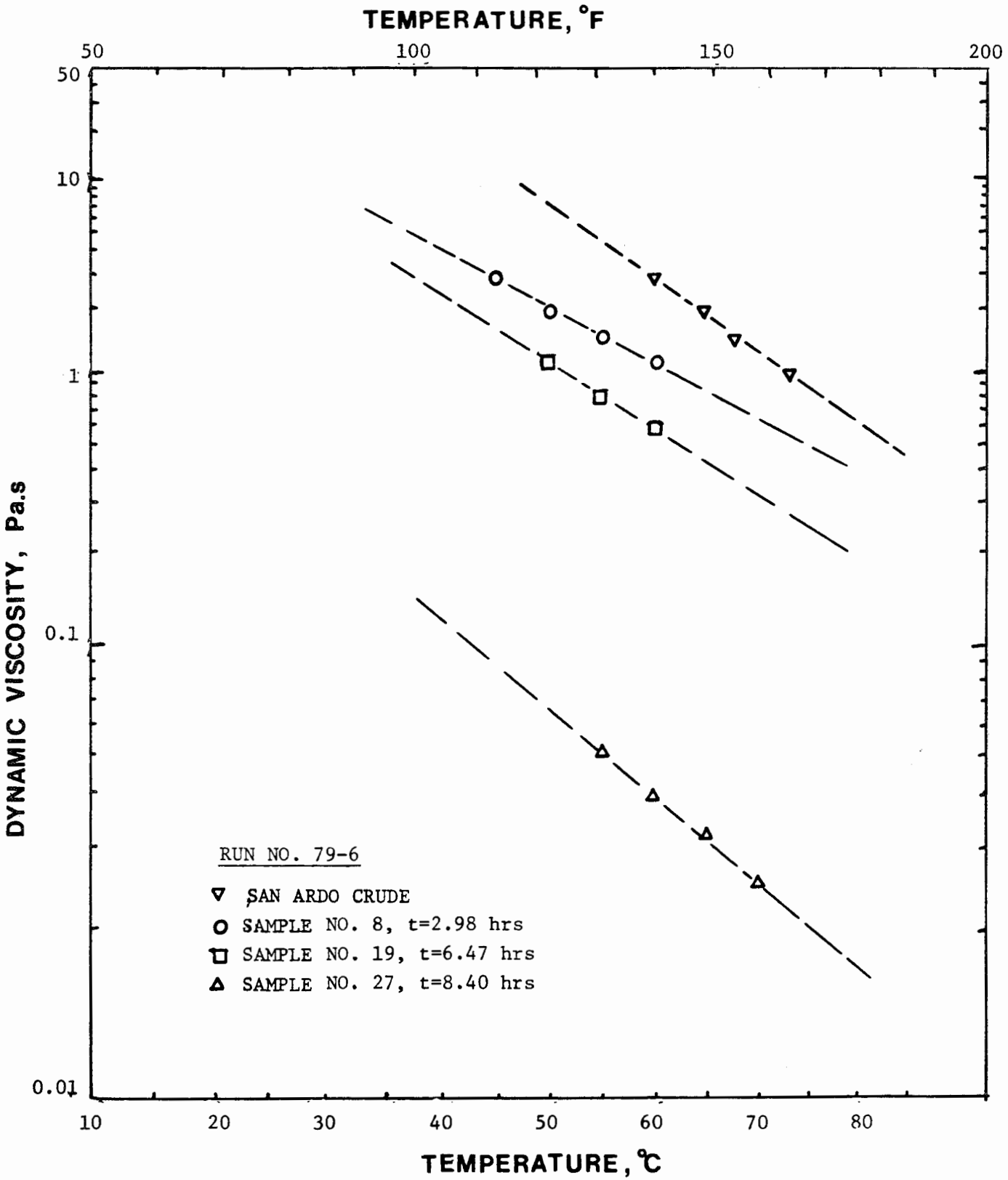

Fig. 7.3: PRODUCED OIL VISCOSITY IN RUN NO. 79-6

Table 7.1

PRODUCED OIL CHARACTERISTICS

Run	Sample	%C	%H	%N	%S	% Ash (O_2?)	°API	Atomic H/C
79-2		79.28	11.09	0.68	2.31	0.07	13.5	1.68
79-4		78.87	11.19	0.59	2.18	0.14	14	1.7
79-5		72.58	10.26	0.69	3.28	0.59		1.96
79-6	2	85.18	13.2	0.1	1.15	0.4	12.2	1.86
79-6	18	62.86	11.01	0.65		0.16		2.1
79-7	15	82.75	10.43					1.51

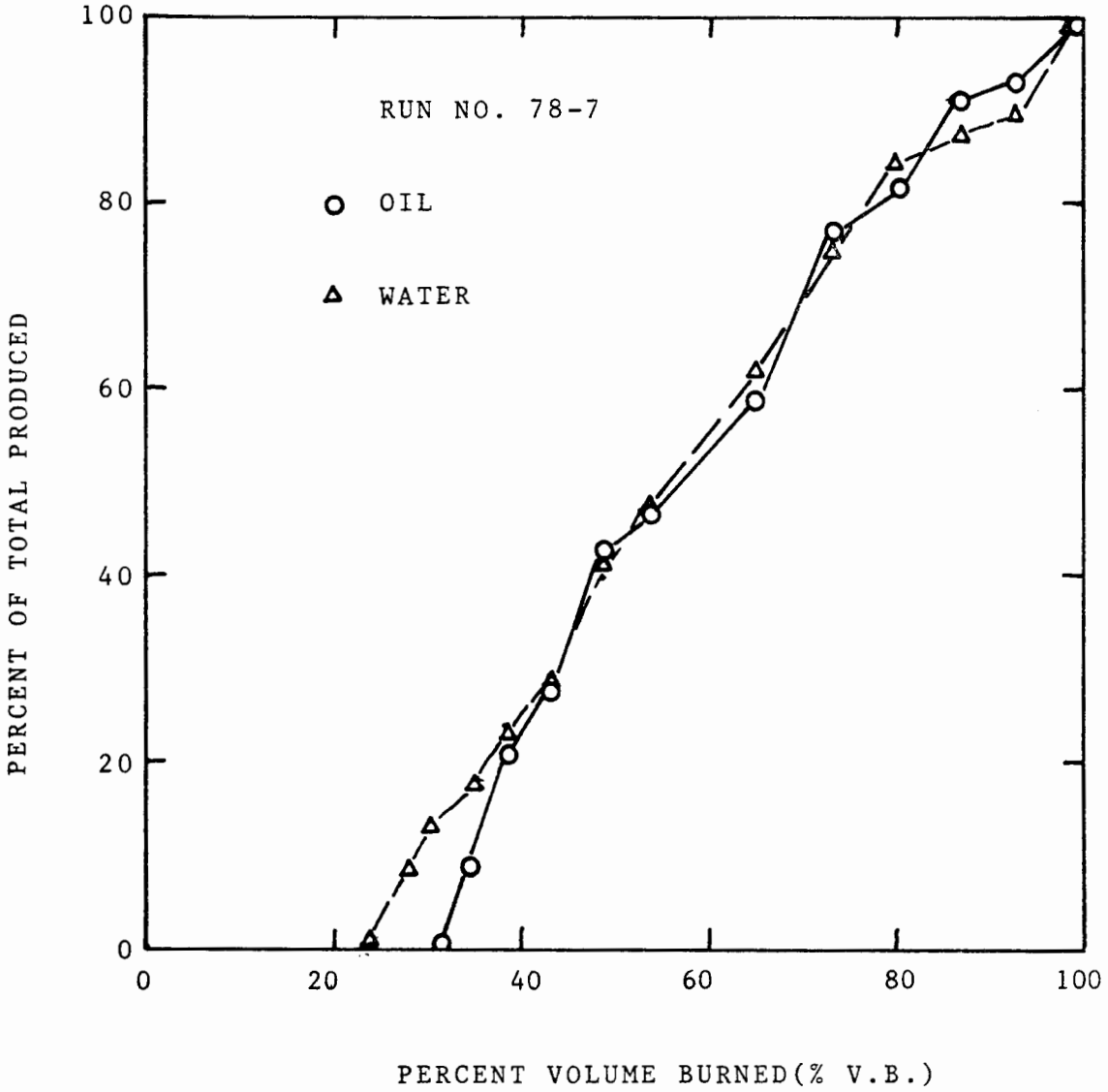

Fig. 7.4: PERCENT RECOVERY VS PERCENT VOLUME BURNED FOR RUN NO. 78-7

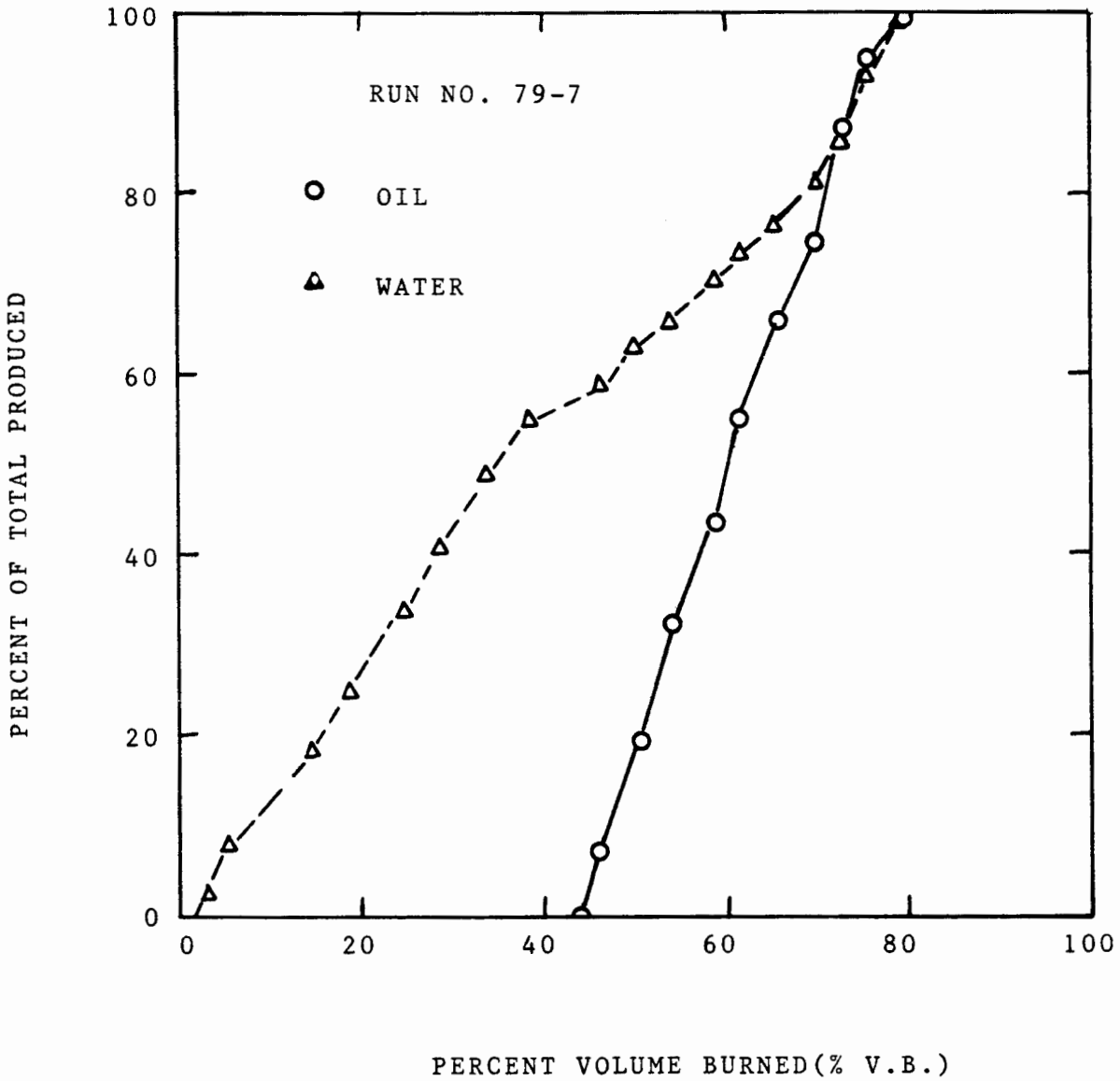

Fig. 7.5 PERCENT RECOVERY VS PERCENT VOLUME BURNED FOR RUN NO. 79-7

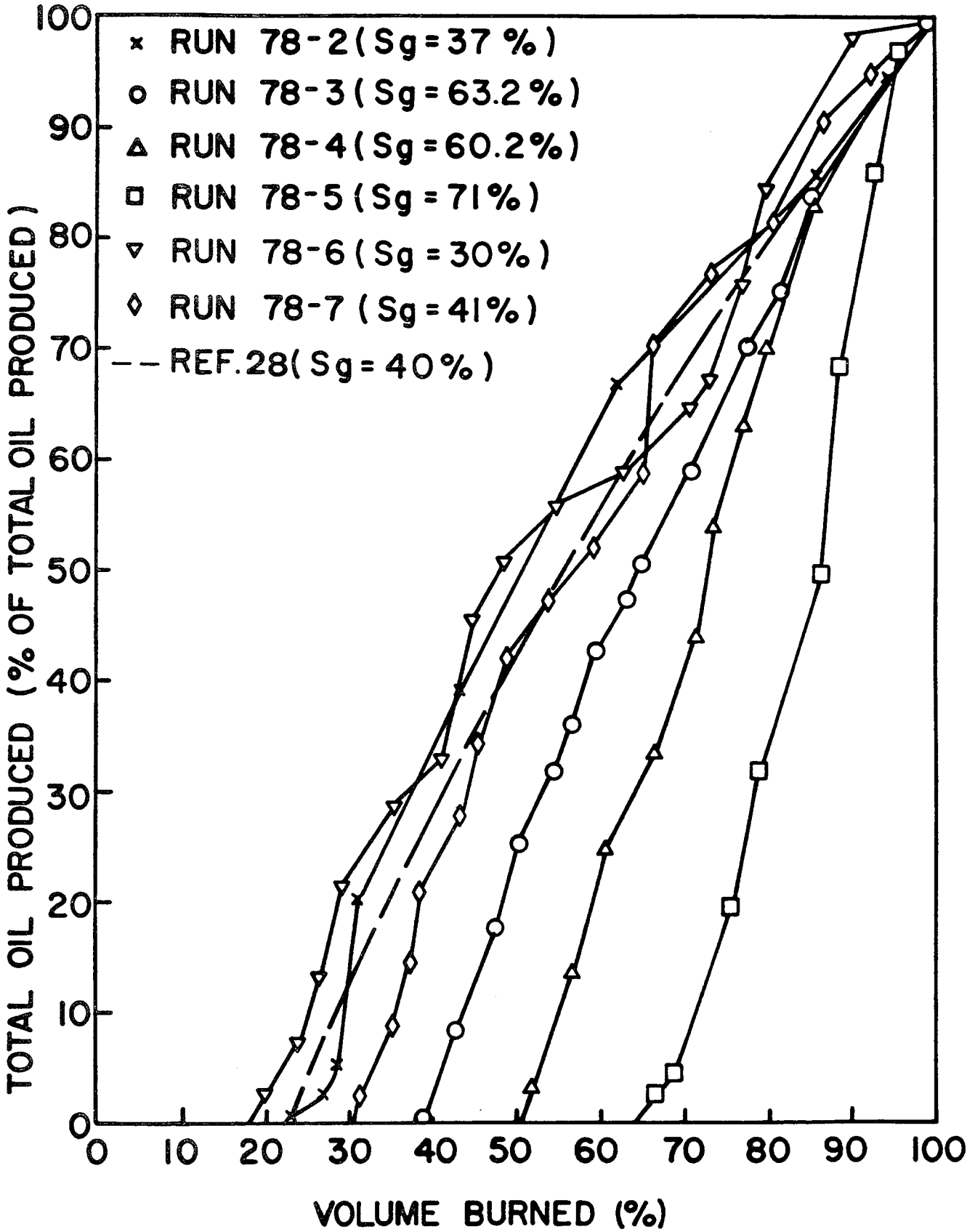

Fig. 7.6: OIL PRODUCED VS VOLUME BURNED

published data, they also extend the range of the gas saturation from a maximum of 50% to a maximum of 70%. If we plot volume burned at the start of oil production vs gas saturation, we get Fig. 7.7. The limiting gas saturation was assumed to be between 85-90% (assuming that the minimum oil saturation for combustion is 10-15% and no water is present). The following equation fits the data of Fig. 7.7.

$$\text{Volume Burned, V.B.\%} = 0.293\ Sg(\%) + 0.00928\ S_g^{\ 2} \qquad (7.1)$$

The straight line shown in Fig. 7.7 illustrates the piston-like displacement. The data indicate that oil production always starts before the burning front has moved far enough to fill up the gas space with displaced liquids. The burning front velocity was found to be directly proportional to the air flow rate.

7.3 Effect of Air Flux on Frontal Velocity

If steady, adiabatic burning is assumed, the theoretical relationship between frontal velocity, V_f, and air flux, U, may be expressed by Eq. (2.4).

It appears that a correlation exists between the burning frontal velocity and the air flux at the front. Although most investigators found a direct relationship between these two parameters, it appears that the product of oxygen ultilization times air flux should be correlated with frontal velocity. This is because the former is proportional to the rate of oxidation. Also, at higher air flux, lower oxygen utilization is reported. A straight line can be drawn through all of the reported data. These lines can be divided into two categories: (a) those with a zero intercept (Fig. 7.8), (b) those with an intercept

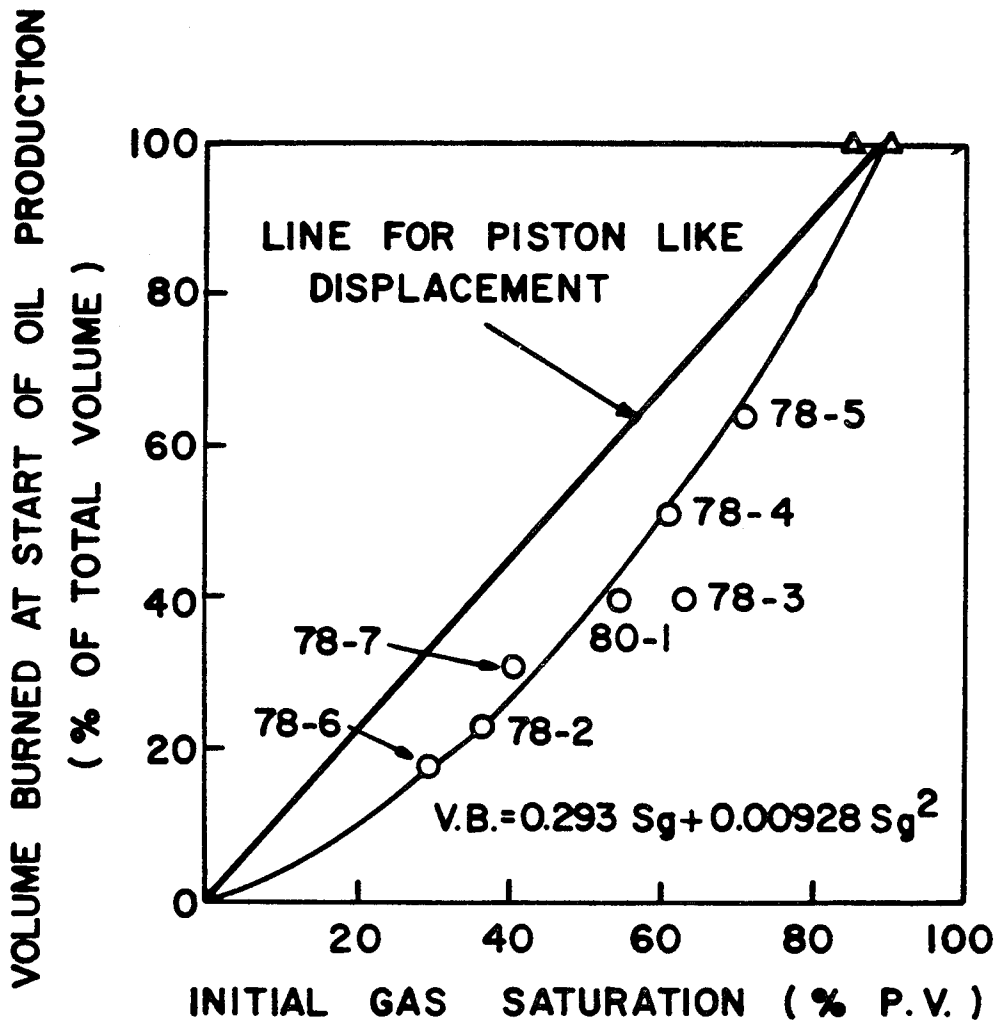

Fig. 7.7: VOLUME BURNED VS GAS SATURATION

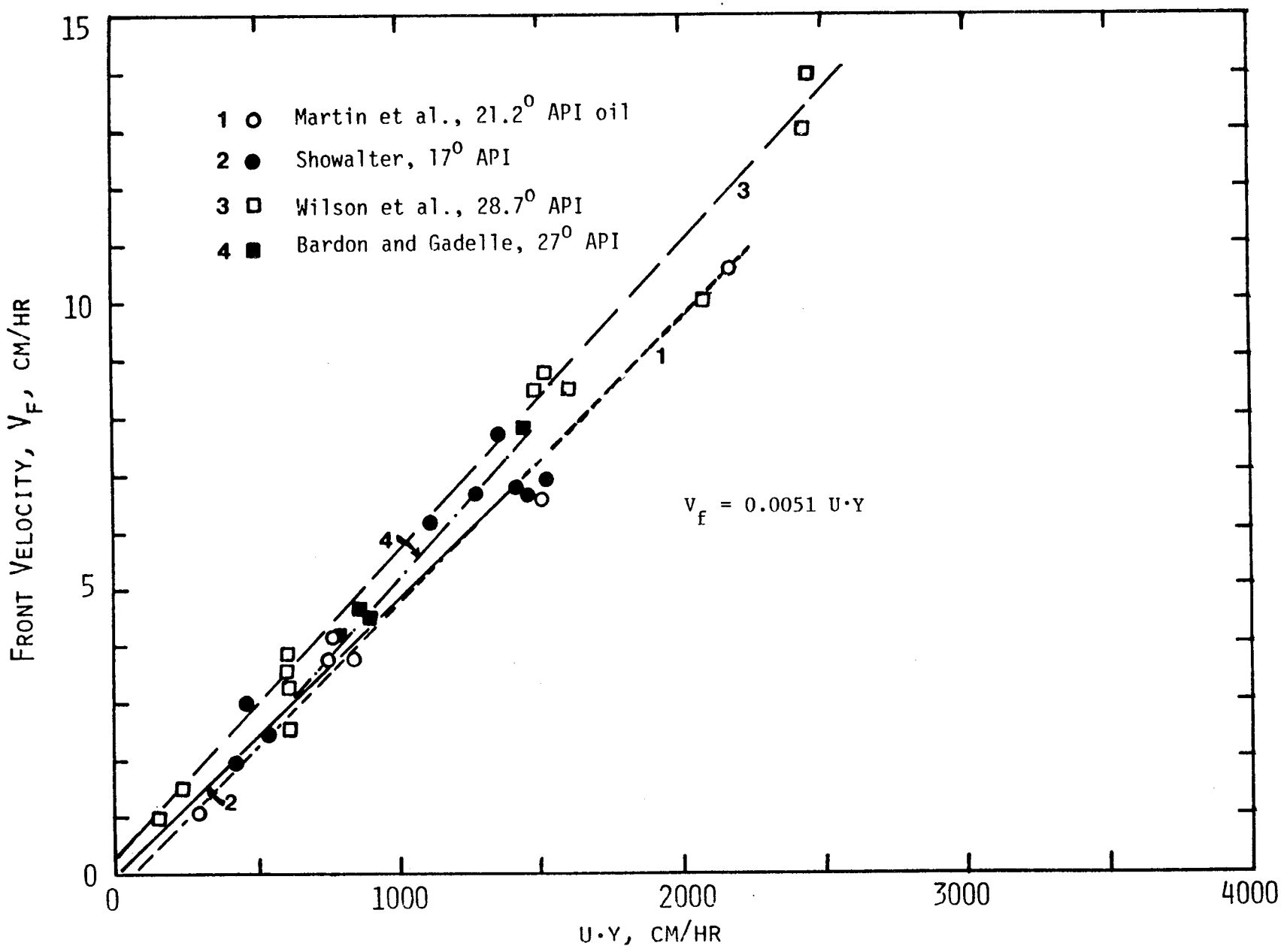

Fig. 7.8: EFFECT OF GAS FLUX ON FRONT VELOCITY

other than zero (Fig. 7.9). In these figures, U is the air flux (scc/cm^2-hr), Y is the oxygen utilization, and V_f is the burning front velocity (cm/hr). Interestingly enough, the first group of data were obtained under near adiabatic conditions, while some heat losses were associated with the second group. Although no study has been done to correlate heat loss to front velocity and air flux, it is felt that the correlating parameter in these two graphs may be the heat loss coefficient. The minimum air requirement is directly proportional to the heat loss. Any intercept in this curve would indicate the amount of heat loss in the tube.

The following equation is the result of a least square technique applied to all the available data obtained under adiabatic conditions (Fig. 7.8).

$$V_f = 0.0051\ U \cdot Y \tag{7.2}$$

This shows that the frontal velocity was about 200 times slower than the gas flux.

The results of the work reported here using San Ardo crude are presented in Fig. 7.9. These data fit into the following equation:

$$V_f = 0.0061\ U \cdot Y - 8.7273 \tag{7.3}$$

Figure 7.10 presents all the results obtained for different crude oils used in this work. The runs with no (or very little) clay in their matrices and those with different oil or at higher pressure, showed some scatter and were excluded from this curve fit. In fact, the front velocity seems to be almost independent of gas flux for runs without clay.

The intercept for this curve can be interpreted as minimum air requirement for sustaining the combustion front under experimental

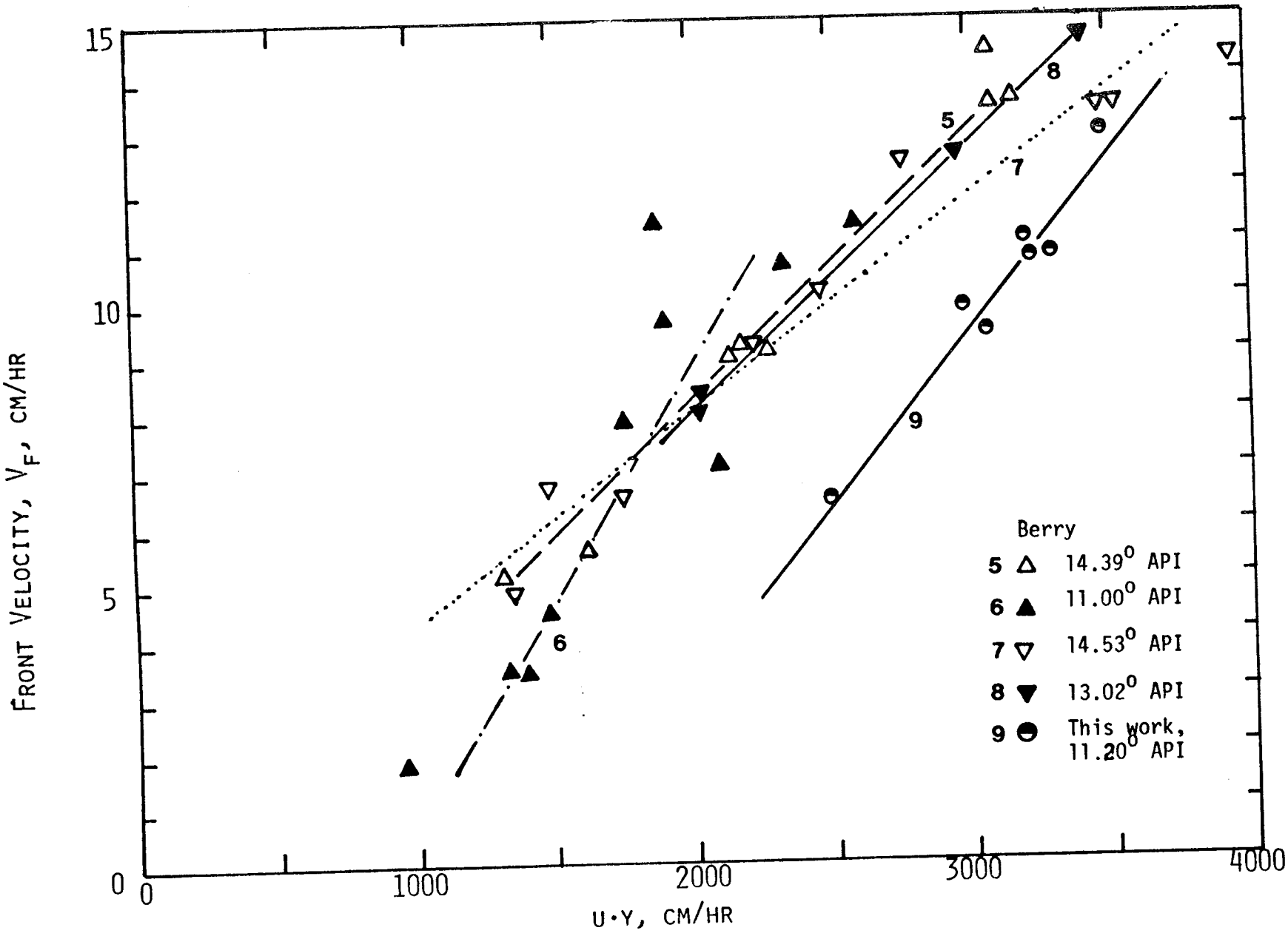

Fig. 7.9: EFFECT OF GAS FLUX ON FRONT VELOCITY

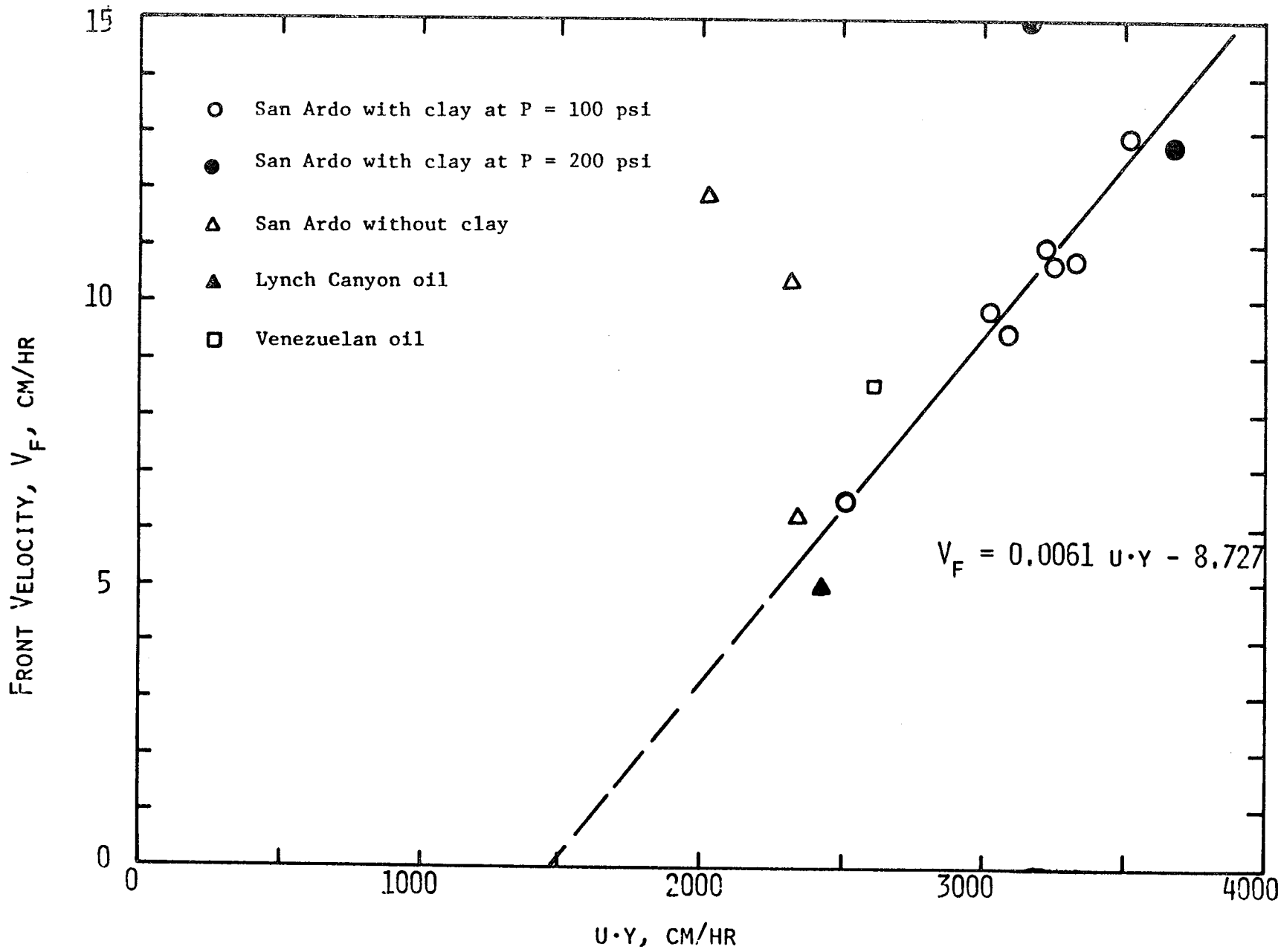

Fig. 7.10: EFFECT OF GAS FLUX ON FRONT VELOCITY

conditions. Assuming 100% efficiency, this value is equivalent to 45 scf/hr-ft^2. Martin et al. (1959) reported a value between 4 to 10 scf/hr-ft^2 for the minimum air requirement in their experiment, while Penberthy and Ramey's (1966) figure was around 30 scf/hr-ft^2. These differences are probably due to the relative heat loss of the equipment used by these authors.

7.4 Effect of Clay on Frontal Temperature

Clay was found to have a profound effect on the frontal behavior. Runs No. 78-3 and Run No. 80-1 had almost the same initial conditions except that the latter had no clay. The average frontal temperature for Run No. 78-3 was around 950°F (Fig. 7.11), but Run No. 80-1 had an average frontal temperature of 650°F (Fig. 7.12) and low oxygen utilization. Considerable coke was left behind the front in Run No. 80-1 while clean sand was obtained in Run. No. 78-3.

Because the igniter was not turned off after the combustion front was established in Run No. 80-1, the temperature profiles ahead of the front had low slopes. This conclusion is in agreement with the results of Penberthy and Ramey (1966).

7.5 Measurement of the Burning Front Thickness

In Runs No. 78-7 and 80-1, the gas sampling probes were installed on the combustion tube to get a detailed analysis of the produced gases as the burning front passed these probes. The produced gas analysis from the probes are shown in Figs. 7-13-7.16. The instantaneous temperature transverse data are graphed in Fig. 7.17.

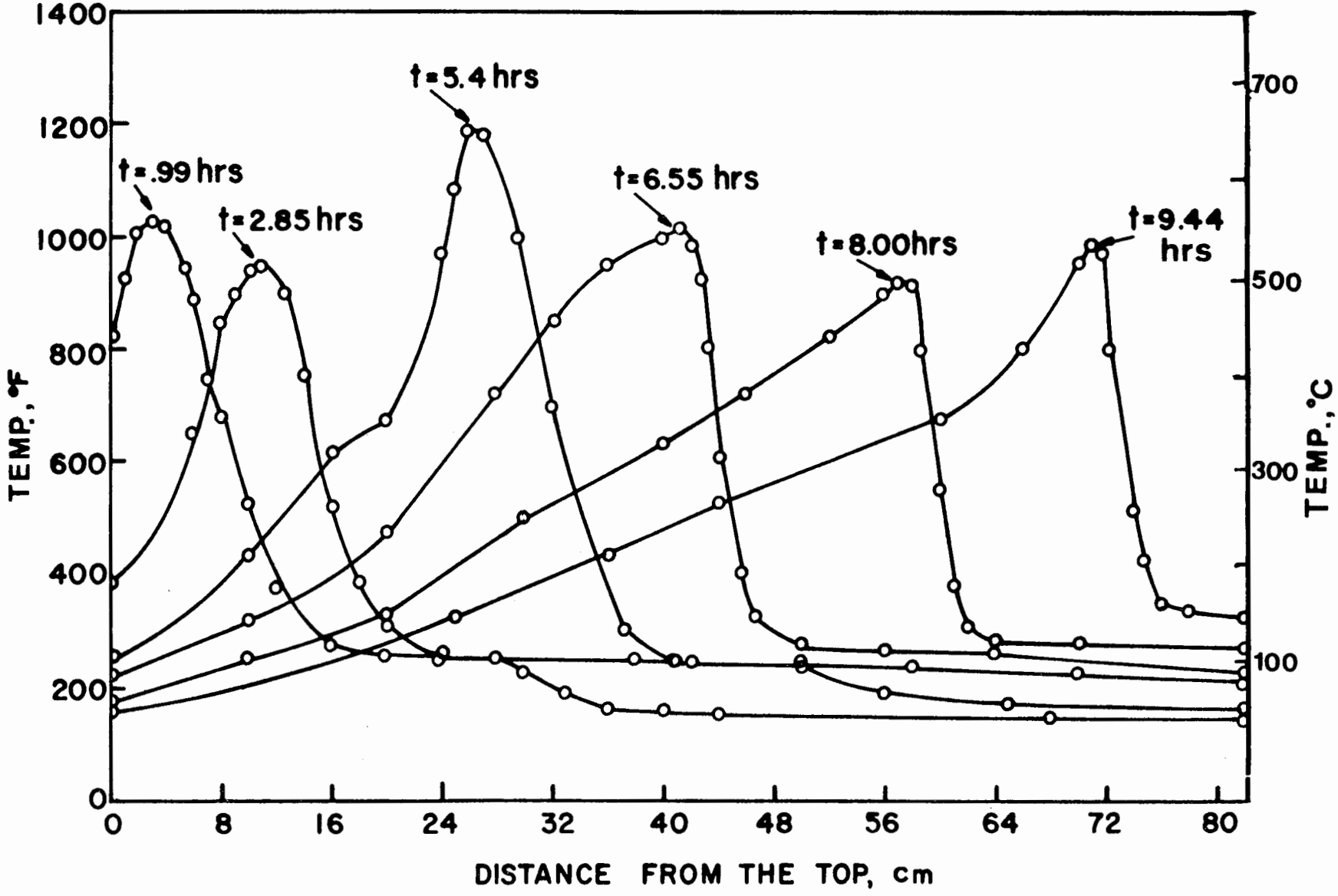

Fig. 7.11: TEMPERATURE PROFILE FOR RUN NO. 78-3

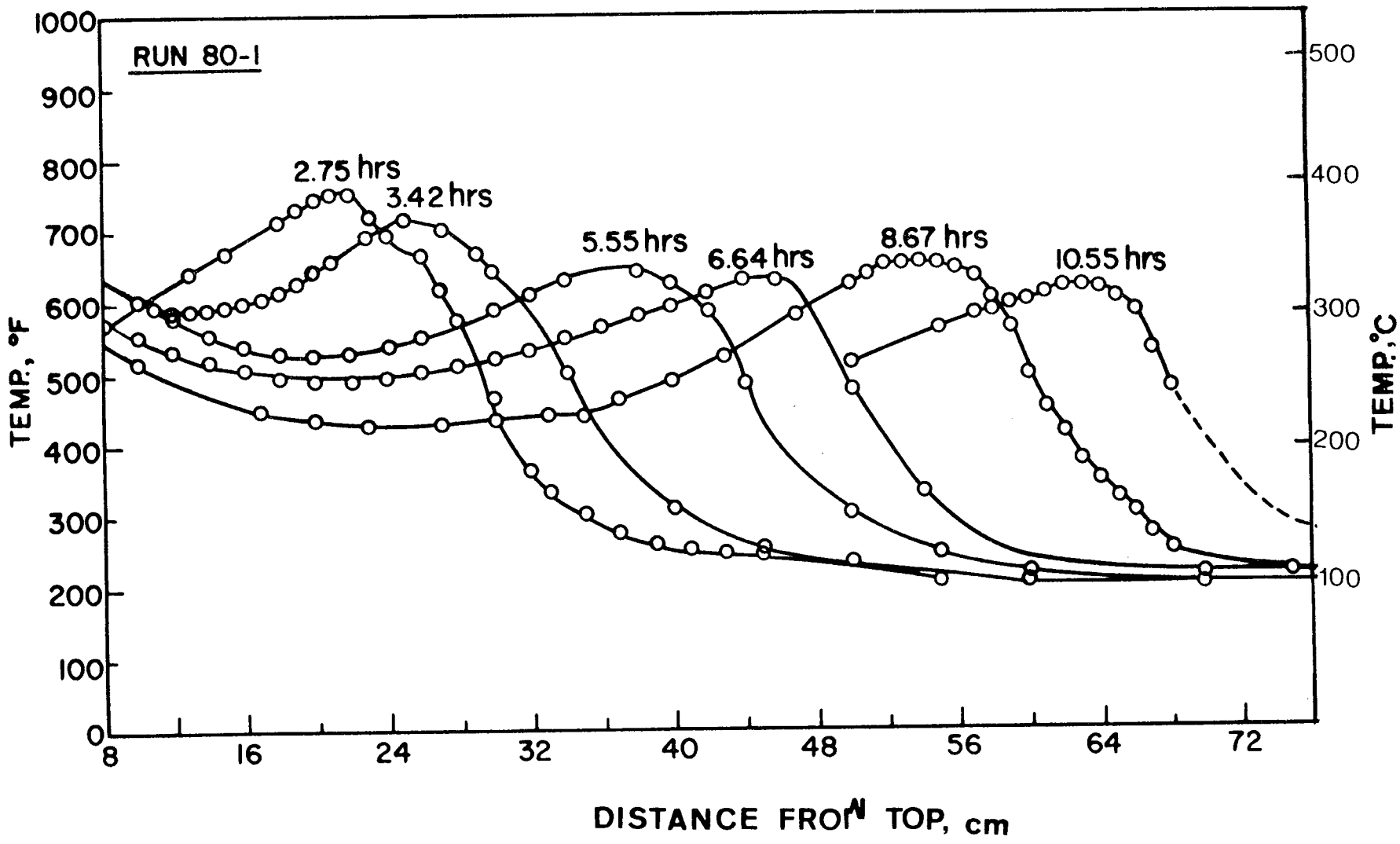

Fig. 7.12: TEMPERATURE PROFILES FOR RUN NO. 80-1

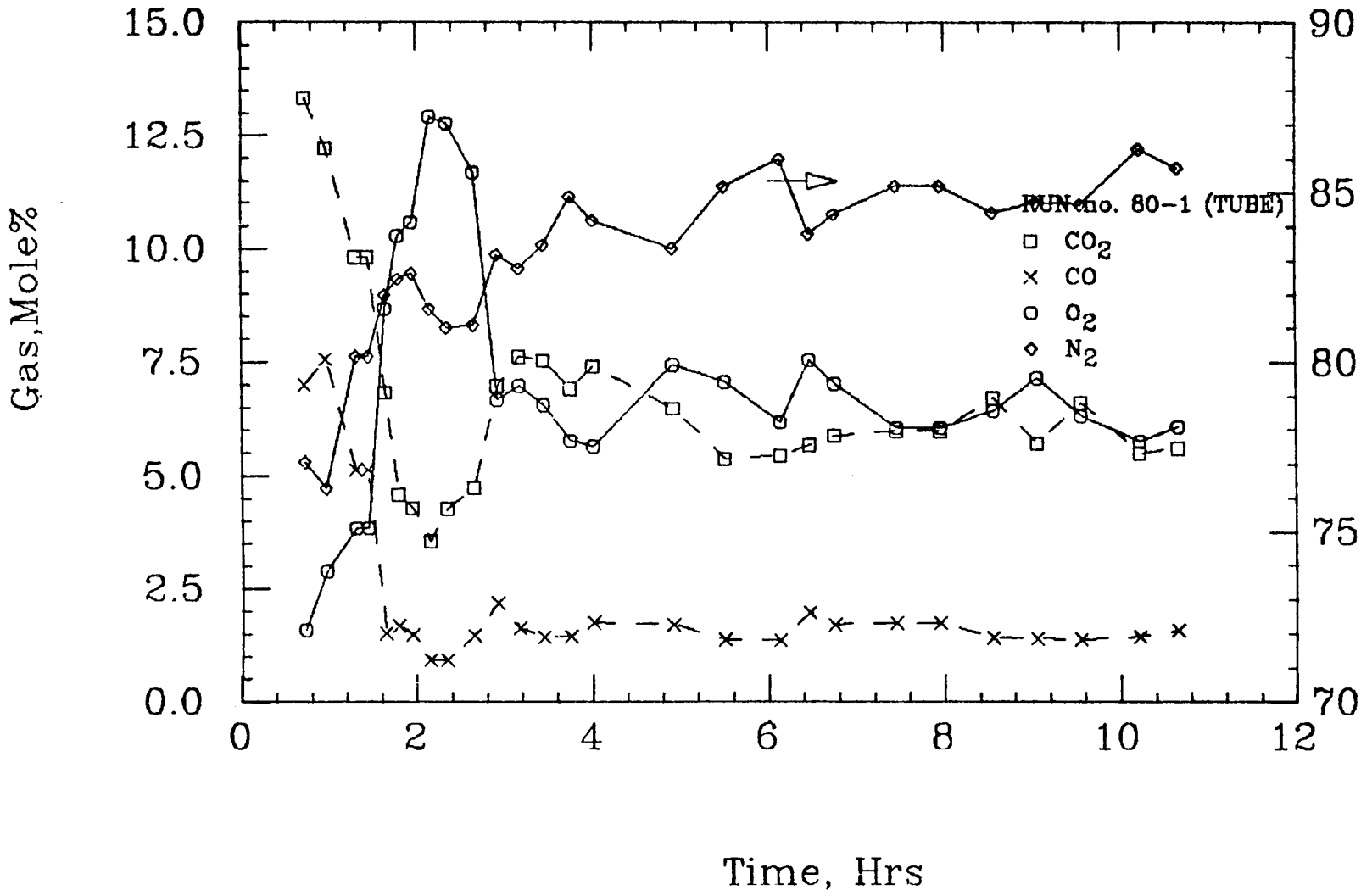

Fig. 7.13: PRODUCED GAS COMPOSITION VS TIME FOR RUN NO. 80-1 (FROM THE TUBE)

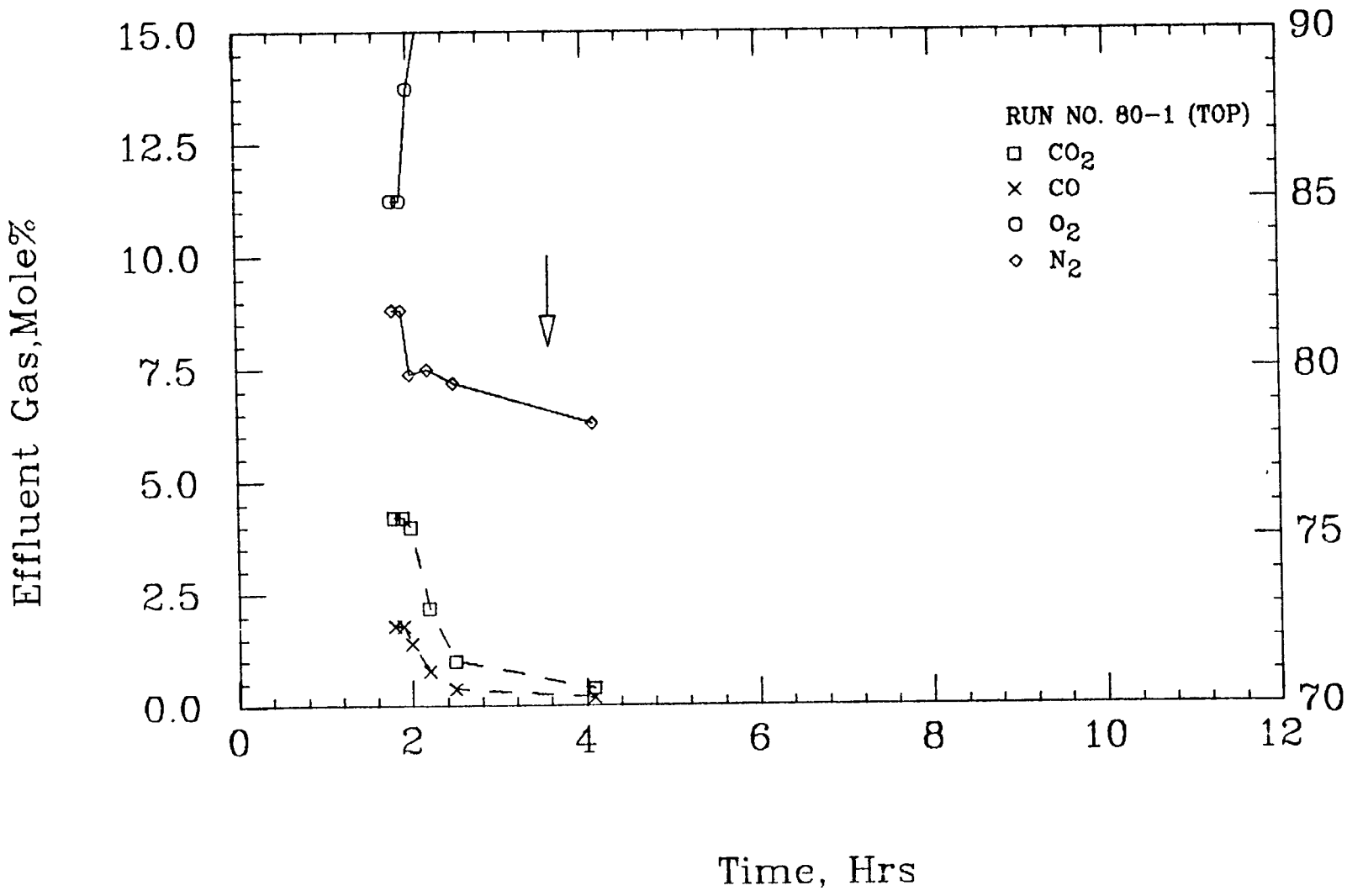

Fig. 7.14: PRODUCED GAS COMPOSITION VS TIME FOR RUN NO. 80-1 (FROM THE TOP GAS PROBE)

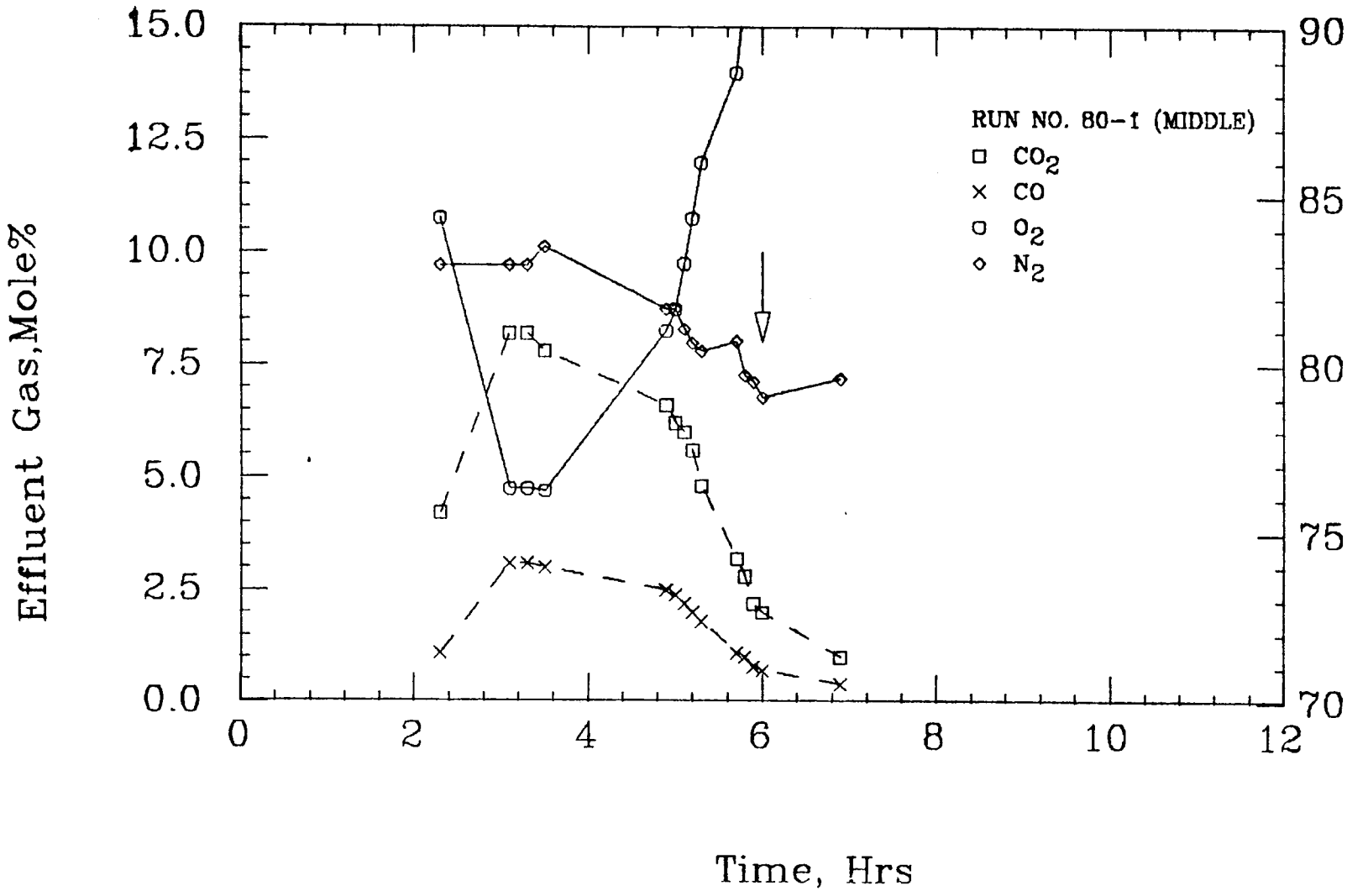

Fig. 7.15: PRODUCED GAS COMPOSITION VS TIME FOR RUN NO. 80-1 (middle probe)

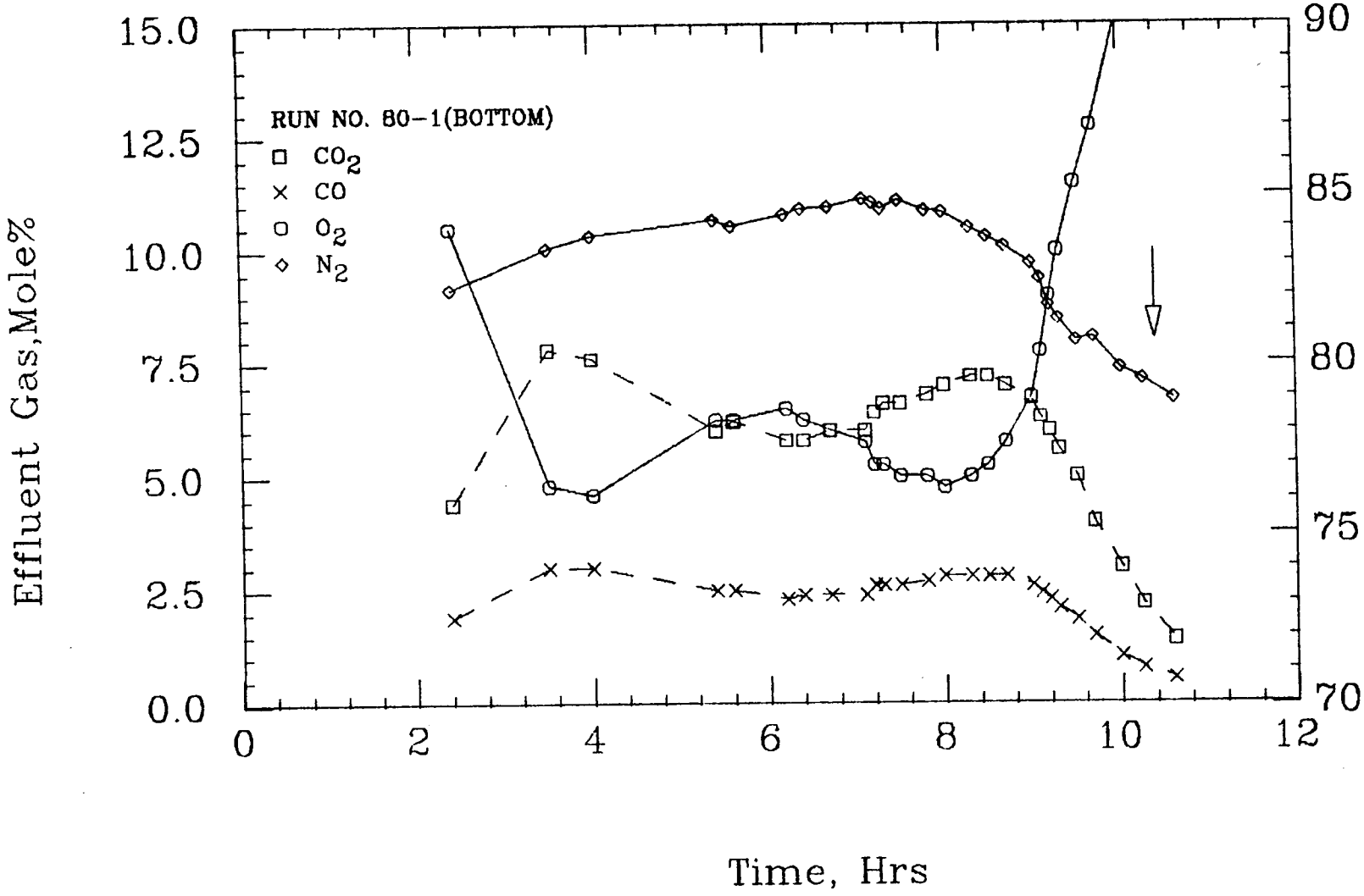

Fig. 7.16: PRODUCED GAS COMPOSTION VS TIME FOR RUN NO. 80-1 (FROM THE BOTTOM PROBE)

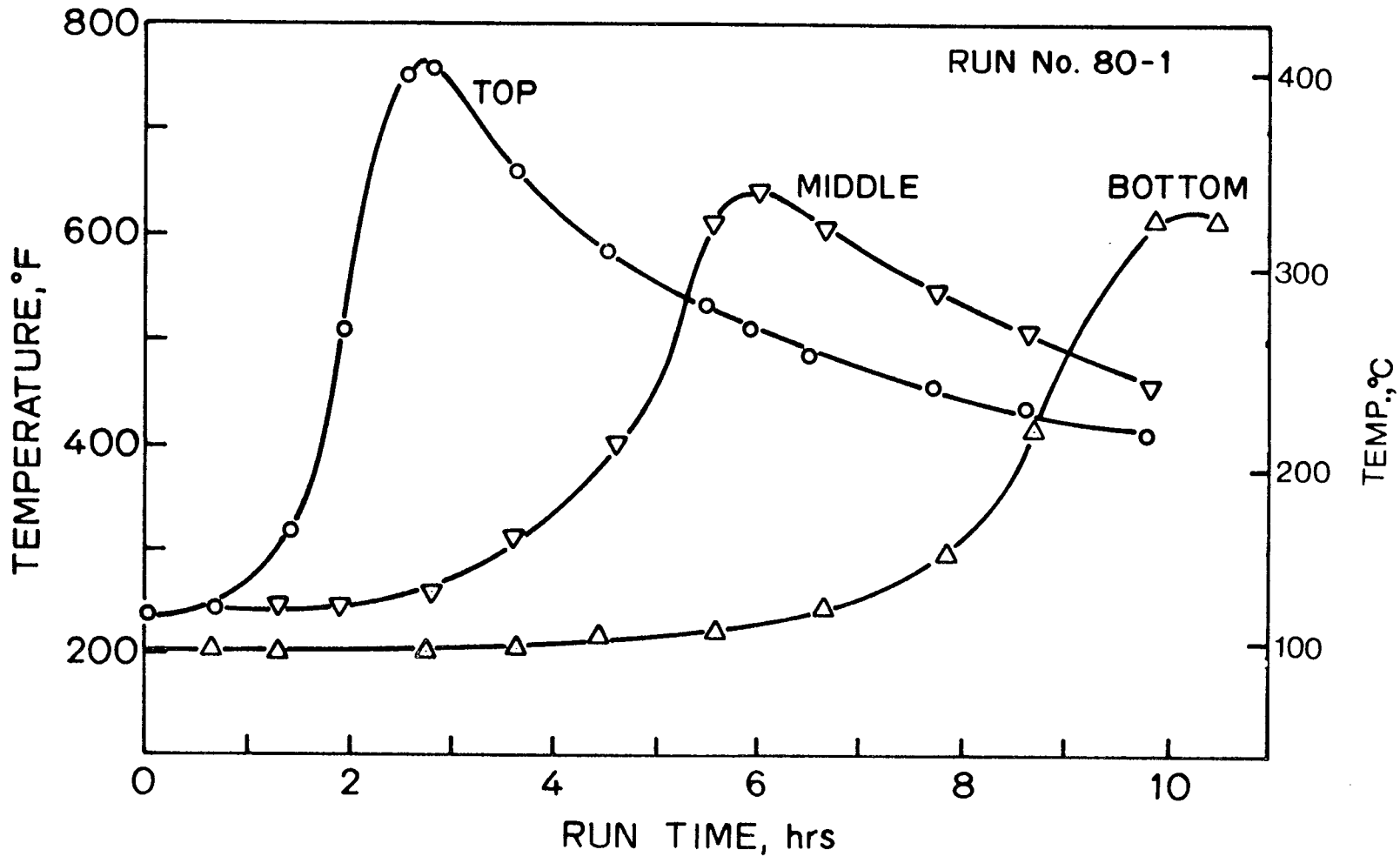

Fig. 7.17: TEMPERATURE PROFILES AT GAS SAMPLING POINTS VS TIME

As the combustion front approached the sampling probe, the probe gas showed an increase in carbon oxides from values near that observed at the exit of the combustion tube toward a maximum. The exit combustion gas from the outflow end of the combustion tube represents a mixture of gases which have passed through various portions of the burning front at various temperatures. Since the probe was located half-way between the wall and axis of the combustion tube, it would be expected that the combustion temperature would be higher than the average combustion temperature for the entire cross-section of the combustion tube. Thus the arrival time of the burning front at the kinetic probe (t_1) was taken to be the time when carbon oxides were at a maximum. The burning front had completely passed the kinetic probe when carbon dioxide reached zero volume percentage of the probe gas (at time t_2). However, it was found that due to low-temperature combustion in Run No. 80-1, some carbon oxides were produced even behind the front. Therefore, t_2 was taken as the time when the temperature of the probe is maximum (this is shown by arrows in Fig. 7.13-7.16). It appears that, in reality, this assumption is more reasonable than the zero carbon oxides assumption previously mentioned (Bousaid, 1967).

The time required for the burning front to pass the probe is the difference between t_1 and t_2. Multiplying this value by the burning front velocity, we arrive at the burning front thickness. Table 7.2 summarizes this process for Run No. 80-1. The front thickness for this Run was found to range from 7.4 to 10.9 cm with an average of 8.8 cm. This is four times greater than the one calculated by Bousaid (1967). However, in his experiment, the front temperature was around 900°F. Thus, it appears that the higher the front temperature, the thinner the front.

Table 7.2

BURNING FRONT THICKNESS CALCULATIONS FOR RUN NO. 80-1

SAMPLING PROBE	t_1, hrs	t_2, hrs	t, hrs	V_f, cm/hr	FRONT THICKNESS, cm
TOP	1.85	2.75	0.90	8.3	7.4
MIDDLE	4.25	6	1.75	6.25	10.9
BOTTOM	8.5	10.25	1.75	4.7	8.2
AVERAGE					8.8

We can analyze the effect of the combustion reaction within the combustion tube by comparing the gas composition at any two points. For example, our gas analyses can be made from the upstream probe at a certain time. Shortly afterward (by a time difference amounting to the residence time) a gas analysis can be made from the downstream probe. The difference in compositions of these samples gives us the reaction rates. When this process is repeated, the net effect of temperature rise in the section between these probes can be observed. Figure 7.18 illustrates the gases produced in the zone between the middle and bottom probes. As can be seen, there are two peaks in this graph at low and at high temperatures. This is a general characteristic of the oxidation kinetics of crude oil in porous media. The detailed data for Fig. 7.18 are shown in Table 7.3.

For the complete data regarding the operating conditions of the combustion runs as well as the results of gas analyses concerning the effluent gas composition, atomic hydrogen-carbon ratio, amount of water formed, fuel concentration and air-fuel ratio, see Fassihi et al. (1980).

7.6 Fuel Content of the Bed

Using an oil sand zone on top of a dry sand zone, the heterogeneous runs were conducted to calculate the minimum fuel availability for combustion, the effect of distillation on fuel availability, and the quality of the fuel at the front. The operating conditions for these experiments are graphed vs run time in Figs. 7.19-7.21, where the right ordinate shows both the injected gas pressure and the frontal temperature. The gas flow rate and the front location are plotted on the left ordinate.

Table 7.3: PROBE TEMPERATURES AND PRODUCED GASES WITHIN THE MIDDLE SECTOR OF THE TUBE IN RUN NO. 80-1

RUN TIME	PROBE TEMPERATURE °C		CO	CO_2	O_2
Hrs.	Middle	Bottom	Mole %	Mole %	Mole%
4.8	430	220	.1	0	1.5
5	470	220	.1	.2	2.5
5.2	515	220	.5	.4	3.7
5.4	565	220	.95	1.75	5
5.6	620	220	1.25	2.7	6.7
5.8	635	225	1.4	3.25	8.5
6	640	225	1.65	3.85	10.8
6.2	635	230	1.7	3.75	13.5
6.4	620	240	1.9	4.3	14.7
6.6	615	245	1.95	4.7	15
6.8	610	250	1.95	4.85	15.2
7	585	255	1.9	4.85	15.5
7.2	575	260	2.2	5.3	15.6
7.4	560	270	2.3	5.4	15.9
7.6	550	280	2.35	5.95	16.1
7.8	540	295	2.5	6.1	16.2
8	532	310	2.6	6.4	16.3
8.2	525	330	2.7	6.75	16.1
8.4	515	360	2.75	7	15.9
8.6	510	395	2.8	7.1	15.5
8.8	500	425	2.75	6.8	15
9	490	485	2.55	6.5	14.2
9.2	480	530	2.3	6	12
9.4	475	565	2.1	5.3	10.4
9.6	465	585	1.7	4.4	8.5
9.8	455	605	1.35	3.6	7
10	445	620	1.05	3	6
10.2	440	620	.8	2.3	5
10.4	437	615	.7	1.8	3.5
10.6	427	600	.6	1.5	2.8

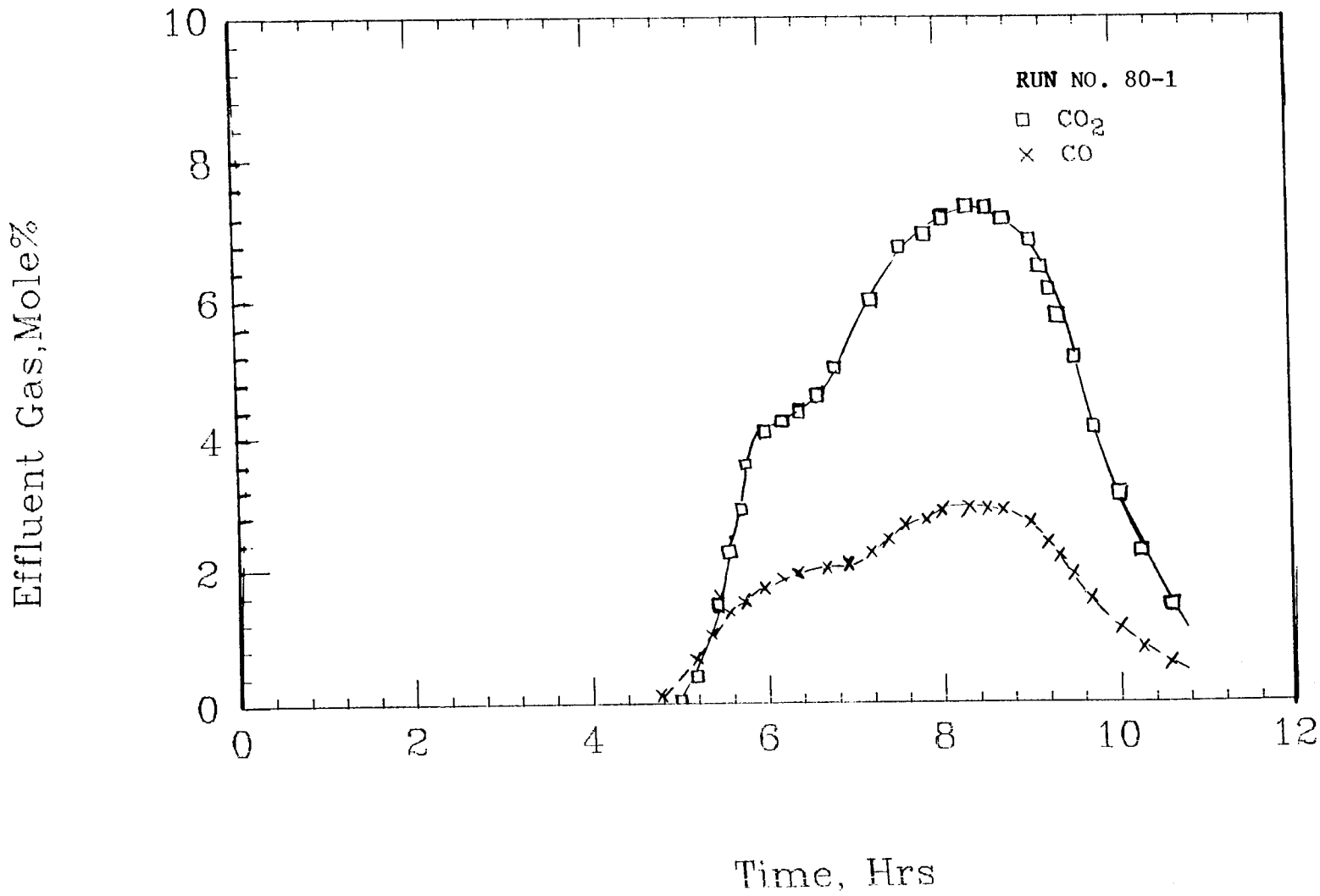

Fig. 7.18: GASES PRODUCED WITHIN THE MIDDLE SECTION OF THE COMBUSTION TUBE

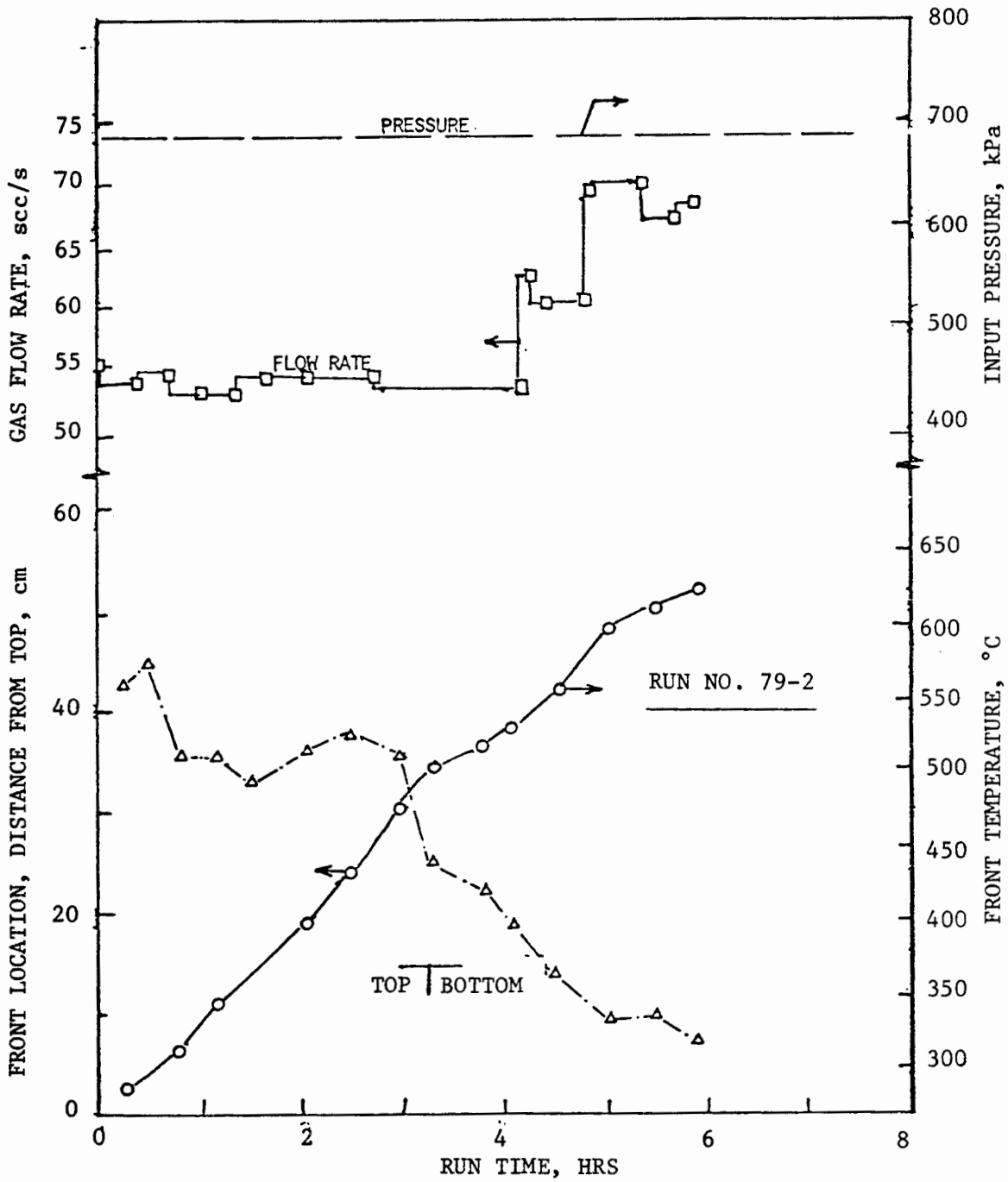

Fig. 7.19: OPERATING CONDITIONS FOR RUN NO. 79-2

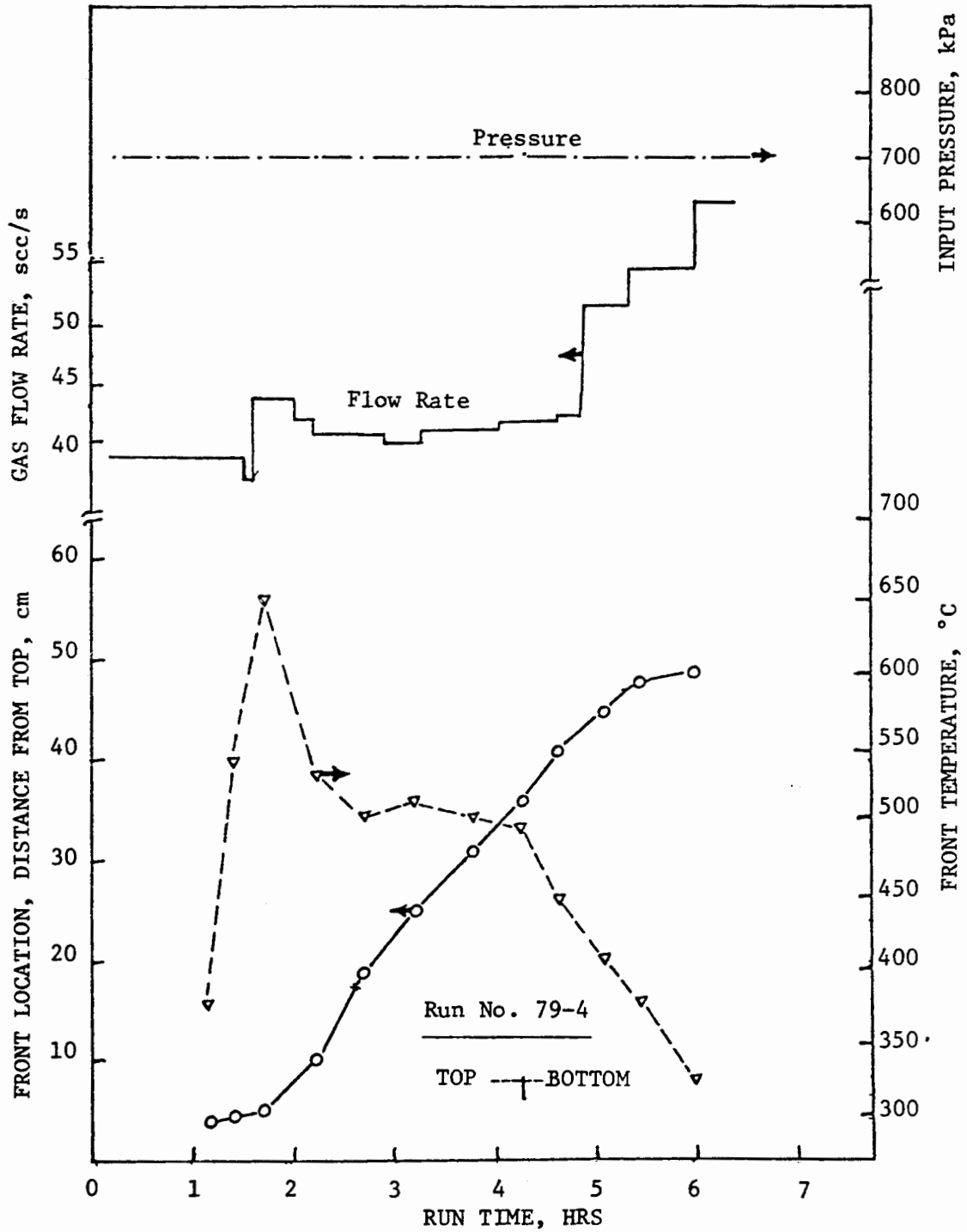

Fig. 7.20: OPERATING CONDITIONS FOR RUN NO. 79-4

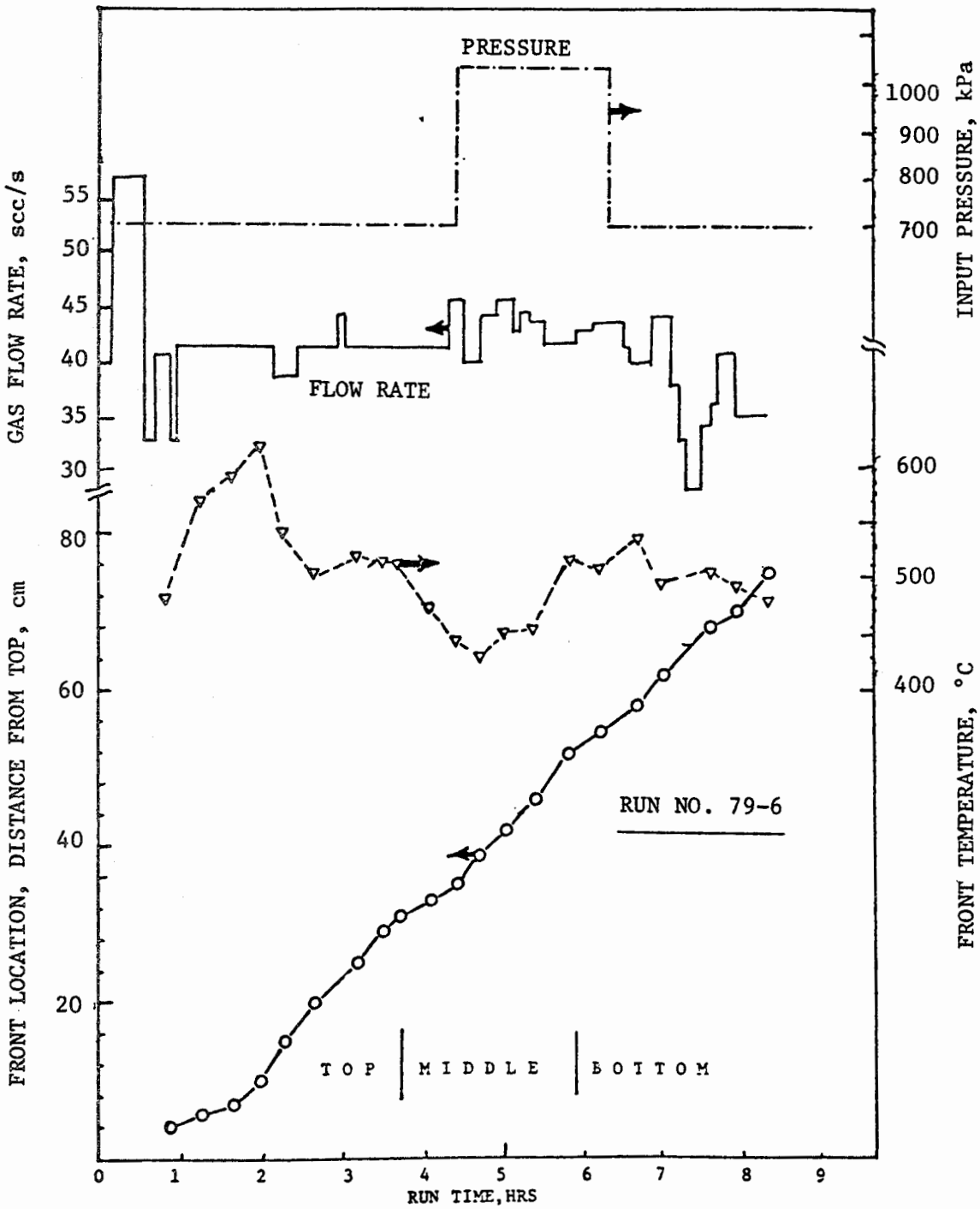

Fig. 7.21: OPERATING CONDITIONS FOR RUN NO. 79-6

7.6-1 Measurement of the Fuel Saturation

In Runs No. 79-2 and 79-4, combustion was continued until the front passed the interface between the oil zone and the dry zone. Then, it was found that the temperature dropped at a constant rate and finally combustion ceased (Figs. 7.19 and 7.20). The samples taken along the combustion tube were analyzed using ASTM methods. Figure 7.22 illustrates the saturation profiles of different substances such as water, oil, and "coke." Here, the term "coke" signifies a solid material around the sand which could not be extracted unless burned. Assuming the average oil saturation in the steam plateau is the residual oil saturation, then

$$S_{or} = 3 \text{ g oil/100 g sand}$$

This is equivalent to 15% of pore volume.

7.6-2 Effect of Pressure on Fuel Deposition

In Run No. 79-6 there were three zones (Table 6.2), an oil zone (Top), a dry zone (Middle) and then another oil zone (Bottom). Useful information was obtained concerning the effect of pressure on the frontal behavior and fuel availability. Comparing Figs. 7.20 and 7.21 we see that increasing the air flow rate had no effect on front temperature, but as soon as pressure increased, so did temperature. This can be related to steam distillation. The higher the pressure, the lower the distillation effect. Hence more fuel is available for combustion and, as a result, a higher burning temperature is obtained.

The results of the effluent gas analyses showed that combustion was failing in Run No. 7906 before the pressure was increased (Fig. 7.23).

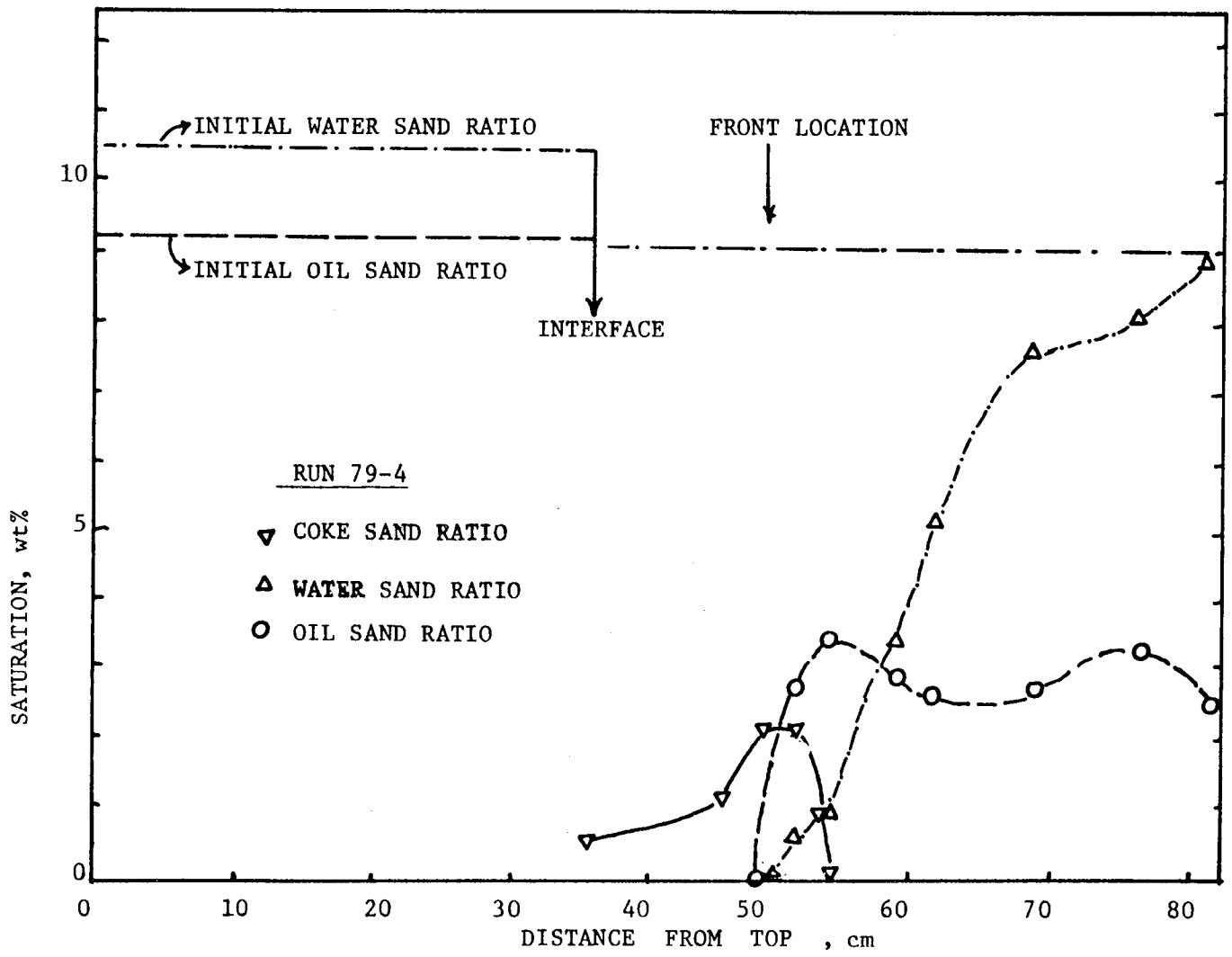

Fig. 7.22: SATURATION DISTRIBUTION

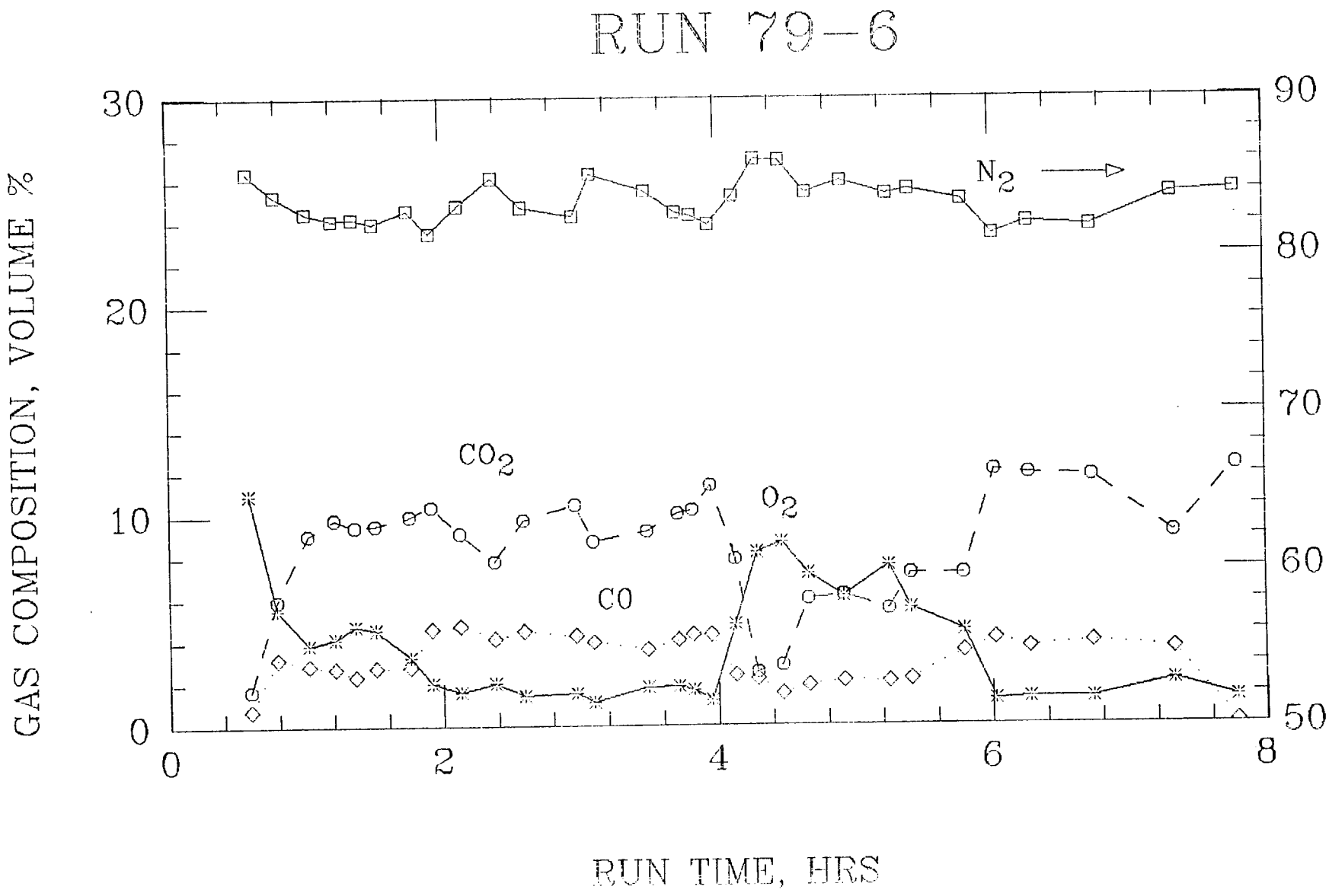

Fig. 7.23: EFFLUENT GAS COMPOSITION VS TIME

Also, in this run, the production slowed down when the combustion front was moving through the middle section of the pack (Fig. 7.24).

7.7 Discussion of Results of Combustion Tube Runs

Table 7.4 summarizes the results of combustion tube runs for both homogeneous and heterogeneous runs. This table shows that the fuel concentration in the sand pack varied between 1.4-2.4 lb/ft^3 bulk volume and the air-fuel ratio ranged between 155 and 316 scf/lb. Also, the amount of air required to sweep an acre-foot was found to be around 15 MMscf. These results are comparable to the reported data obtained in both field combustion projects and laboratory experiments. For example, the average AFR was found to be 350 scf/lb fuel in a field experiment (Gates and Ramey, 1958). Notice that the theoretical minimum amount of air required to clean a cubic foot of unconsolidated sand by combustion is about 135 scf (Martin *et al.*, 1958).

7.8 Conclusions from the Combustion Tube Runs

1. The effects of process variables on frontal behavior were assessed and it was found that both pressure and clay content have a significant effect on the amount of fuel deposited. Higher pressure leads to less distillation and, hence, more fuel is available for combustion. The frontal temperature was higher in tube runs in which clay was used.

2. Correlations were obtained for the oil produced as a function of volume burned and initial gas saturation. In general, the oil displacement efficiency was found to be higher than the displacement efficiency observed in a normal piston-like displacement.

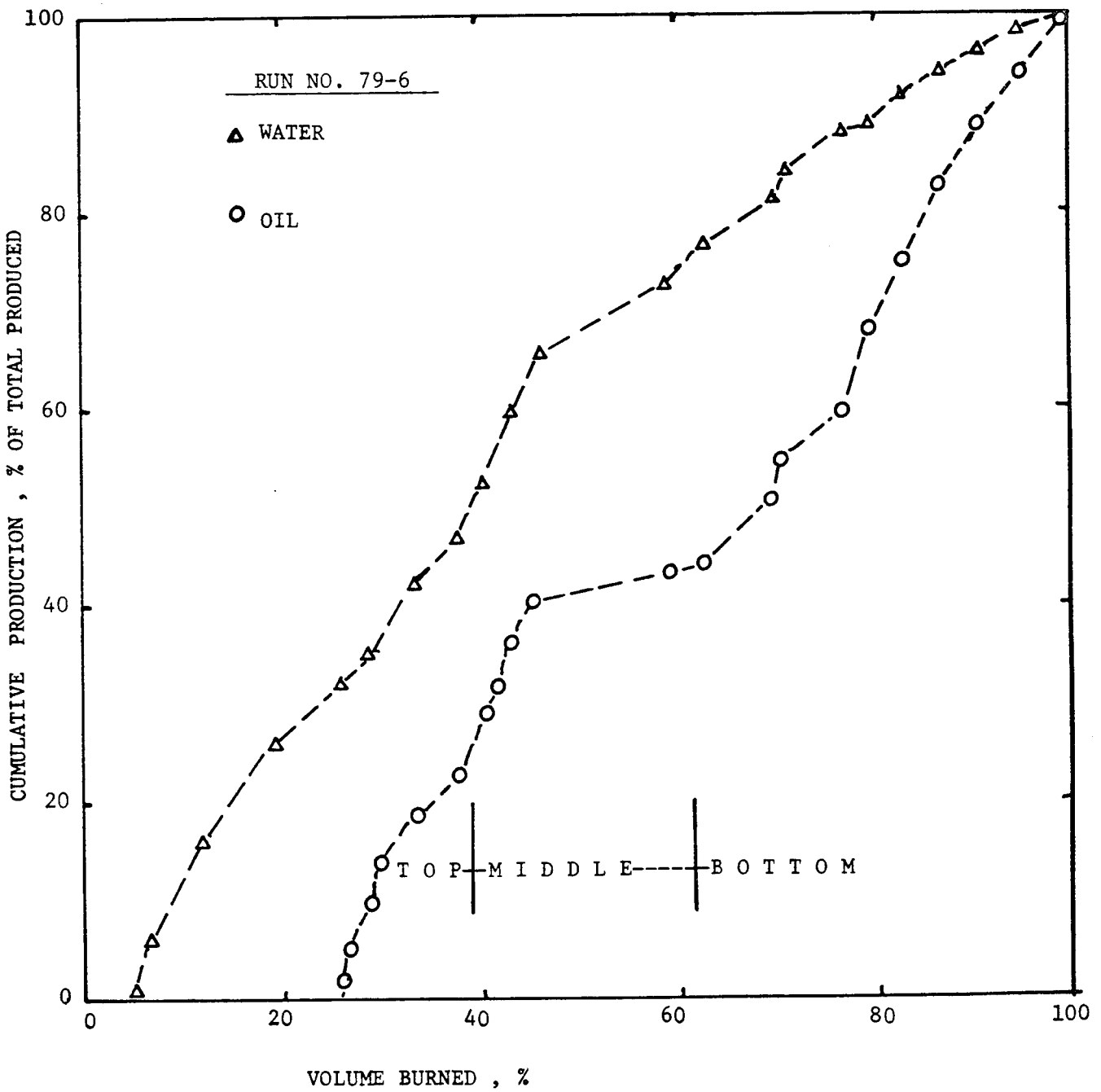

Fig. 7-24: PRODUCTION VS VOLUME BURNED FOR RUN NO. 79-6

Table 7.4

SUMMARY OF COMBUSTION TUBE RUN RESULTS

RUN NO.	AIR FLUX	AVG. BURNING FRONT TEMP.	BURNING FRONT VELOCITY	PRODUCED GAS ANALYSIS, VOL%				ATOMIC H/C RATIO	lb.FUEL BURNED PER HOUR	FUEL CONCENTRATION	AIR/FUEL RATIO	AIR/SAND RATIO
	scc/s(scf/hr-ft ^{2})	°C	cm/hr	CO_2	CO	O_2	N_2	fraction	lb/hr	lb/ft ^{3} bulk(bbl/Acre-ft)	scf/lb	MMscf/Acre-ft
78-1	29.1-34.6(83.2)	488	11.8	10.7	1.5	4.4	82.3	1.93	0.019	1.07(137)	230	10.73
78-2	34.1(91.5)	482	10.4	10.6	6.1	3.7	78.7	0.86	0.025	1.53(196)	177	11.76
78-3	26.4-31.1(114.6)	510	10.8	12.5	4.7	1.1	80.7	1.29	0.025	1.44(185)	170	10.65
78-4	33-37.6(88.3)	538	6.5-12.3	14.7	3.5	1.9	78.8	0.66	0.024	2.22(285)	168.5	16.29
78-5	38.8-4.5(122.7)	variable	13	14.5	5.2	1.4	78.8	0.67	0.036	1.80(231)	162.5	12.80
78-6	43.2(114.4)	518	15.4	12.9	5.2	2.2	78.4	0.68	0.033	1.38(178)	164	9.90
78-7	48.7(129)	471	12.8	14.8	2.9	1.4	79.9	0.45	0.040	1.95(25)	155	12.9
79-1	45.6(120.7)	501	10.8	14.2	3.8	2.5	78.8	0.52	0.034	2.06(264)	168	15.1
79-2	43.2(114.4)	510	9.45	13.2	3.4	2.5	79.1	0.74	0.032	2.14(224)	172	16.1
79-4	43.2(114.4)	501	11	11.5	4.9	1.6	80.9	1.55	0.032	1.83(235)	175	14.2
79-6	41.7(110.2)	510	9.8	10.1	3.7	2.2	82.7	2.3	0.028	1.78(228)	203	16.6
79-7	33.(87.4)	593	5	11.5	2.3	1.8	82.9	2.1	0.024	2.4(307)	210	20.7
80-1	41.6(110.3)	343	6.25	6.3	1.5	6.5	84.8	4.4	0.018	1.85(233)	316	25.1
79-5	33.9(89.8)	600	8.49	13.8	2.6	1.2	81.0	1.27	0.025	1.99(250)	178	15.5

3. The frontal velocity was found to be proportional to the rate of oxygen utilization and dependent upon the heat loss. For adiabatic systems, the front moves about 200 times more slowly than the gas flux. For non-adiabatic systems, heat loss causes the front to move differently. However, the minimum air requirement to sustain the combustion front from any system can be estimated directly from the oxygen utilization rate-frontal velocity graph.

4. Detailed kinetic data can be obtained by simultaneously analyzing the gases produced at different sections of the combustion tube and differentiating these data. The burning front thickness can also be calculated by measuring the gases produced at each section.

5. The movement of the combustion front is a result of the interaction of several parameters such as flow rate, pressure, and rock matrix on the fuel deposition. The degree of interaction, in turn, depends on the reaction governing the combustion process. Therefore, the kinetics of these reactions should be investigated.

8. ANALYSIS OF THE RESULTS OF KINETICS RUNS

As was mentioned earlier, two sets of experiments were carried out in kinetics runs. In this chapter, the results of both constant temperature and variable-temperature runs are discussed. Also, some parameters such as molar CO_2/CO ratio and apparent H/C ratio are graphed vs reaction temperature to identify the reactions occurring. Finally, a model is proposed to analyze these reactions and the results are discussed.

8.1 Isothermal Runs

A model was developed by Weijdema (1968) for essentially constant-temperature runs. Originally he assumed a first order reaction rate with respect to fuel concentration. This model is generalized and is presented in Appendix C. Based on this model, if we plot the logarithm of the oxygen reacted with the fuel ($\Delta\gamma$) vs time at each temperature level, a straight line can be obtained. From the slope and intercept of this line we can evaluate E, the energy of activation, and the other kinetic constants.

The data for two isothermal runs are presented on Figs. 8.1 and 8.2a, b and c. Each portion of the diagram plots the data obtained at a specific temperature level vs the run time. The mole percentages of the produced carbon dioxide are shown by squares and the mole percentages of the produced carbon monoxide are shown by crosses. The circles represent the mole percentages of the consumed oxygen and the diamonds represent the sand temperature (in ^{o}C). The changes in

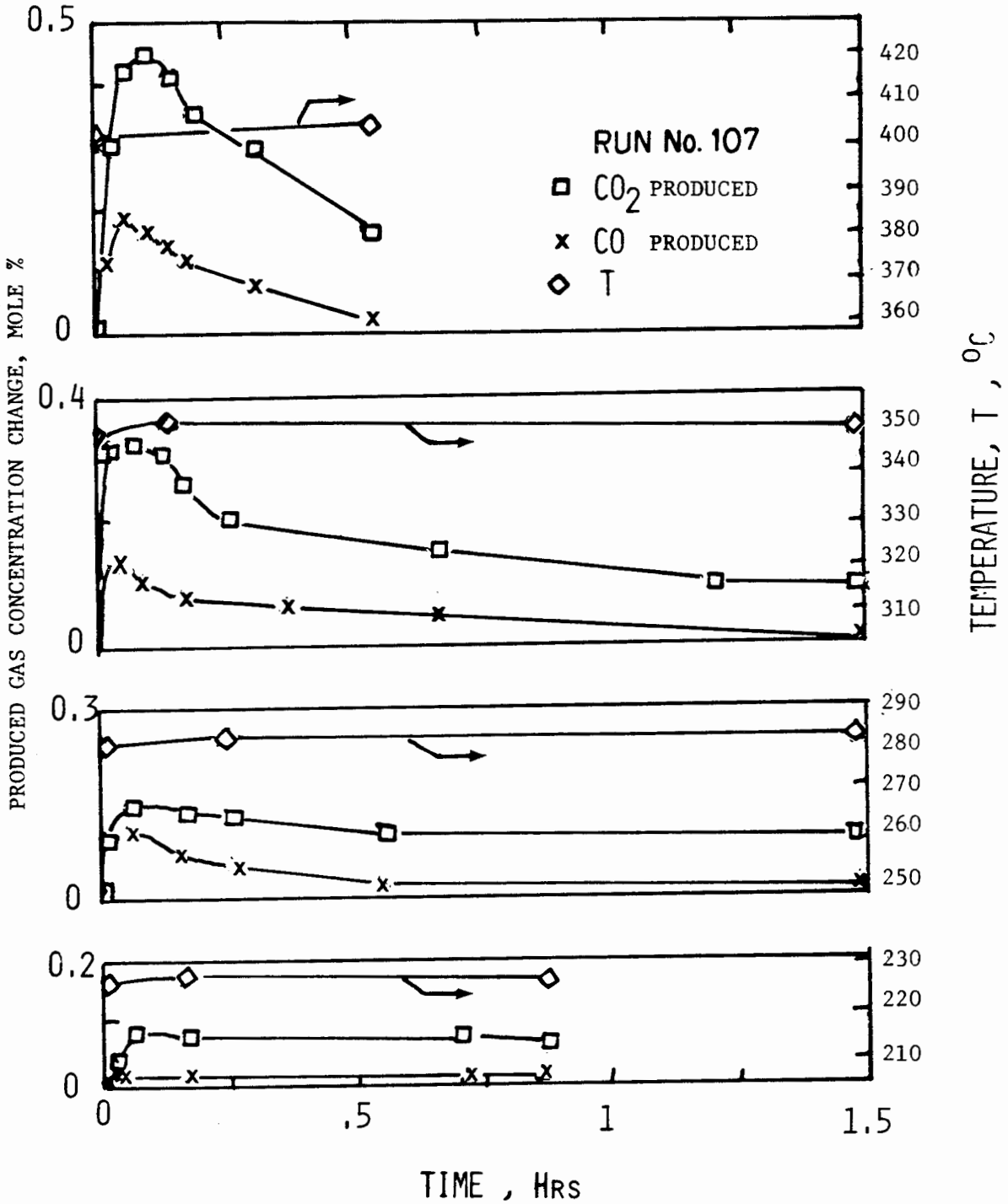

Fig. 8.1: GAS COMPOSITION AND TEMPERATURE VS TIME FOR ISOTHERMAL RUN NO. 107

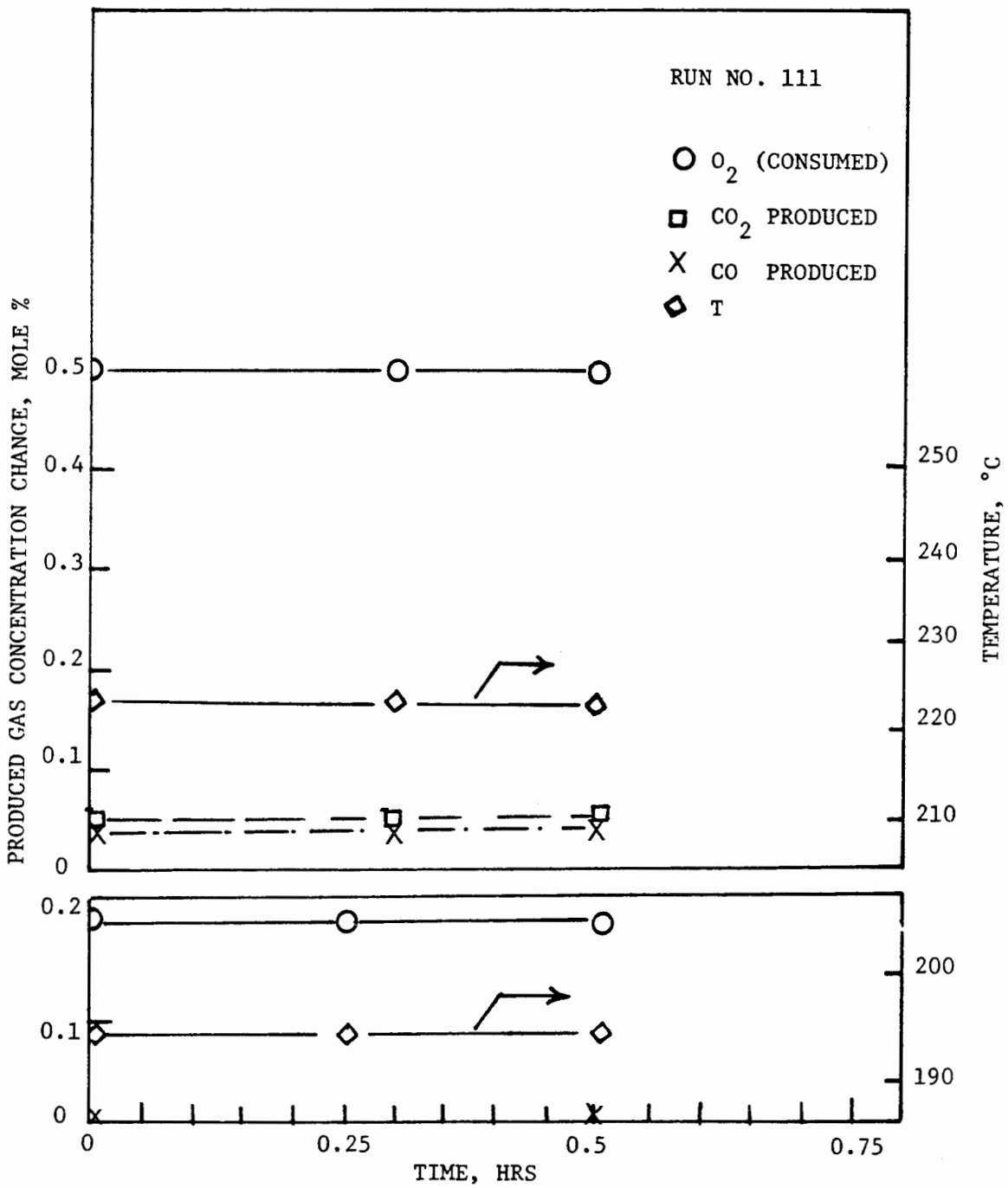

Fig. 8.2a: DATA FOR ISOTHERMAL RUN NO. 111

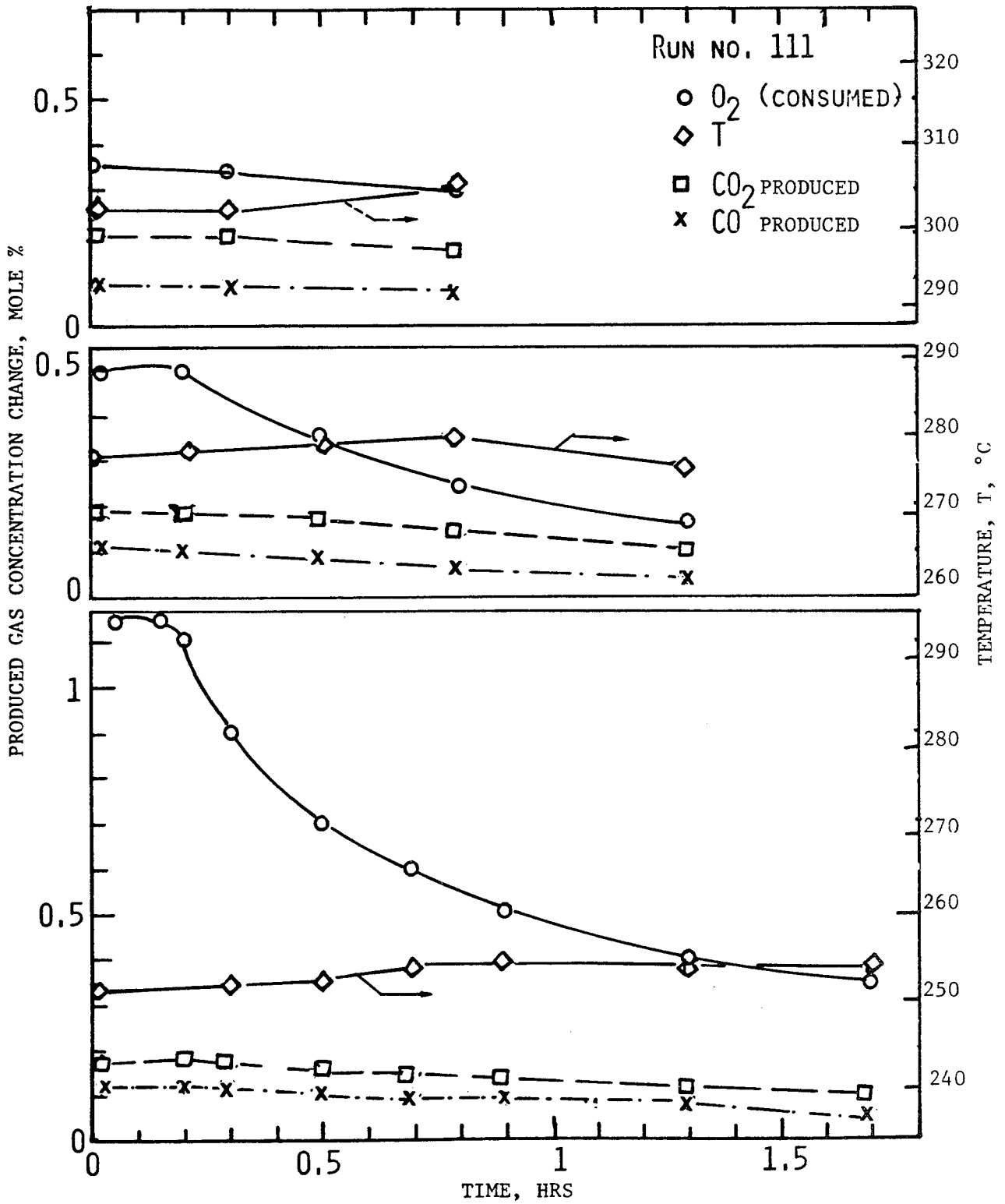

Fig. 8.2b: DATA FOR ISOTHERMAL RUN NO. 111

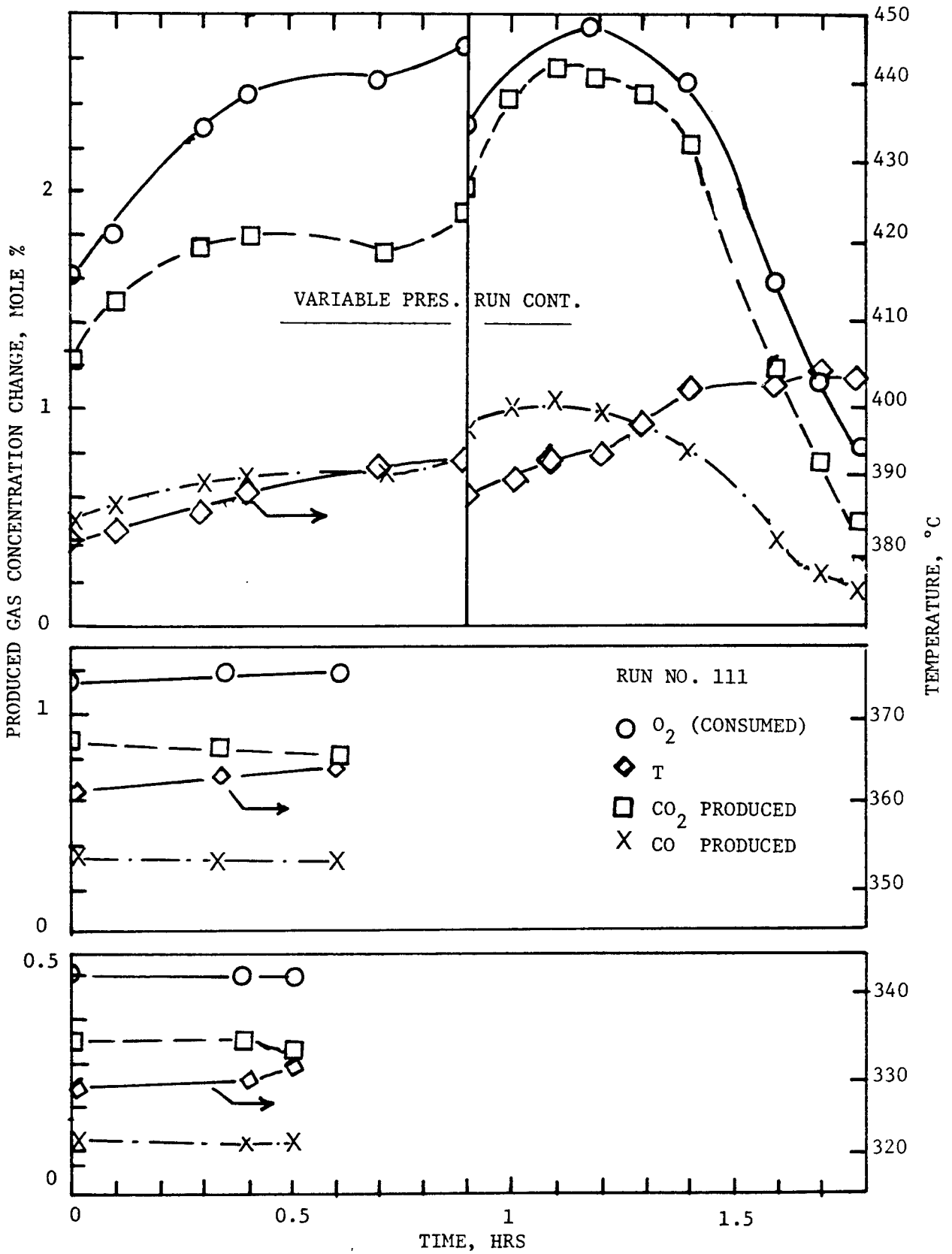

Fig. 8.2c: DATA FOR ISOTHERMAL RUN NO. 111

produced gas concentration at each temperature level are plotted against the left ordinate and the sand temperatures are plotted against the ordinate on the right. Each abscissa represents the oxidation time during which the fuel was in contact with air at a given temperature level. Unless otherwise stated, the nomenclature mentioned above will be used throughout this report.

The isothermal data in Fig. 8.1 for Run No. 107 exhibit unusual reaction kinetic results. When the temperature is raised, the reaction rate increases (more carbon oxides are produced) as expected; however, based on usual kinetic theory, one would expect the exit gas composition to level off to a nearly constant value. Although this seems to occur at 230°C, at higher temperatures the reaction rate gradually diminishes toward zero. This implies that the reactant has disappeared. However, at higher temperatures, there is another rapid rise in the reaction rate followed by another decline towards zero.

In another experiment, Run No. 111, in which a more reactive oil from Venezuela was used, the same kinetic behavior was observed (Fig. 8.2). At temperatures higher than 370°C (Fig. 8.2c), ignition occurred. To control the temperature rise resulting from oxidation, the run was stopped by injecting nitrogen instead of air for 5 minutes. This halted the combustion reaction. When air was reinjected into the reactor, the combustion reaction caused the temperature to rise again. It appears that the reactor did not behave isothermally at this temperature level (395°C). Therefore, the accuracy of those measurements is doubtful.

The overall result indicated by these figures is that the system acts as though the amount of material available to react increases with

temperature. Also, since the relative portions of reacting carbon and hydrogen vary with temperature level, the chemical nature of the material available to react changes with temperature. This type of behavior was originally observed by Bousaid and Ramey (1968), but has not been considered in previous kinetic models. Therefore, a new kinetic model formulation is needed.

8.2 Variable Temperature Runs

Figures 8.3-8.6 present gas composition and temperature vs time for non-isothermal experiments using four different crude oils. In these figures, as before, the consumed oxygen (shown by $\Delta\gamma$) and the produced carbon dioxide and carbon monoxide are plotted against the left ordinate while the ordinate on the right represents the temperature of the sand pack (in ^{o}K). The abscissa shows the run time (in hours) from the beginning of air injection.

Although the gas injection rate was held constant during each run, the effluent gas flow rate was variable. This was due to the difference between the number of moles of reacting and producing gases. Therefore, the measured oxygen consumed needed to be adjusted to include this change in flow rate. Using Eq. C-6 in Appendix C, the actual oxygen consumed was calculated and is shown as $\Delta\gamma$ in the following figures.

There are two apparent peaks in the production of carbon oxides at different temperatures. This result, as well as the results of Differential Thermal Analysis, confirms the existence of at least two reactions. At high temperatures (around 700°K), the amount of consumed oxygen is comparable to the amount of produced carbon oxides (i.e., CO_2 + 0.5 CO). But at low temperatures, the oxygen consumed is greater than the carbon oxides produced. At even lower temperatures, some oxygen is consumed but no carbon oxides are produced.

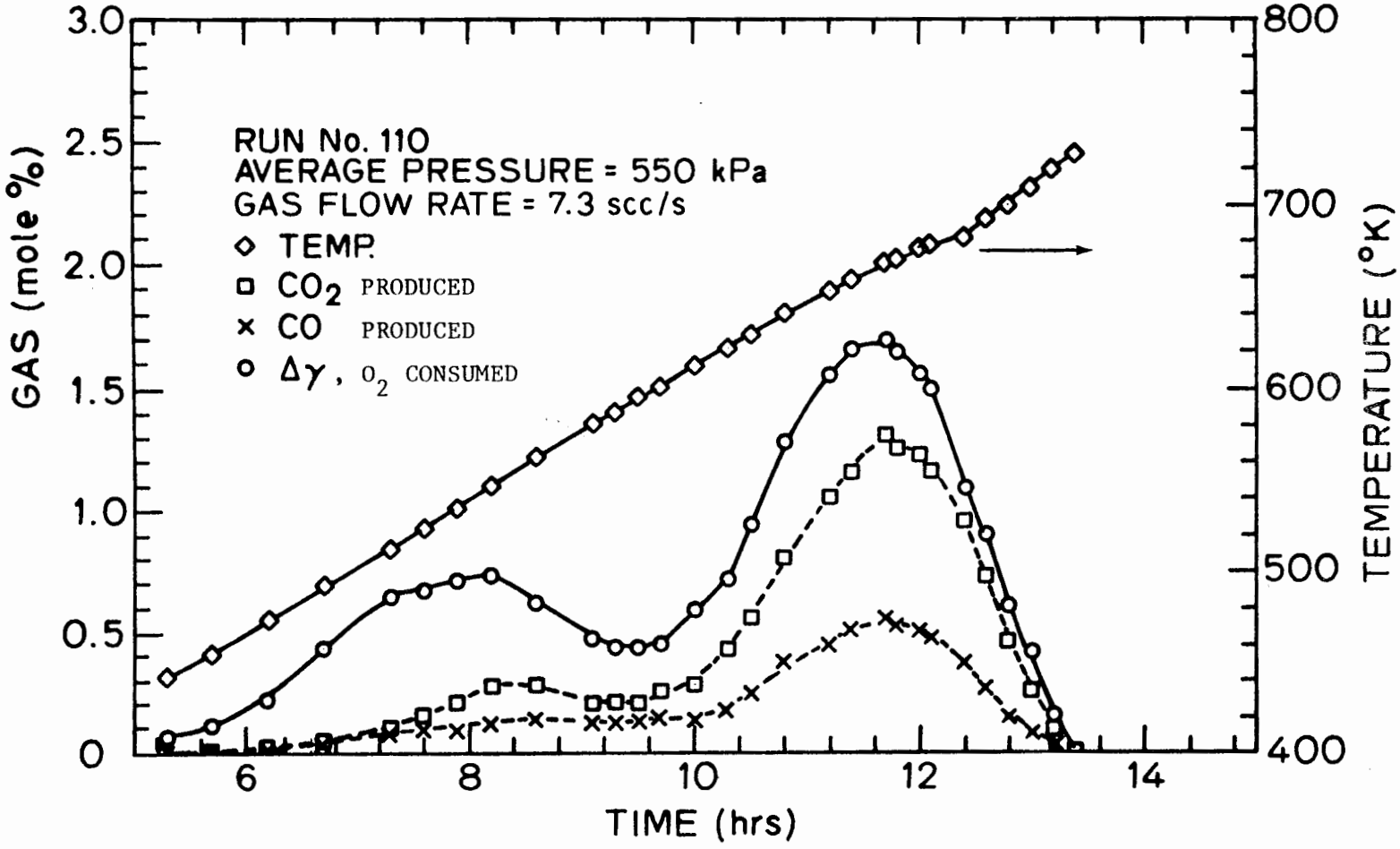

Fig.8.3: GAS COMPOSITION AND TEMPERATURE VS TIME FOR HUNTINGTON BEACH OIL

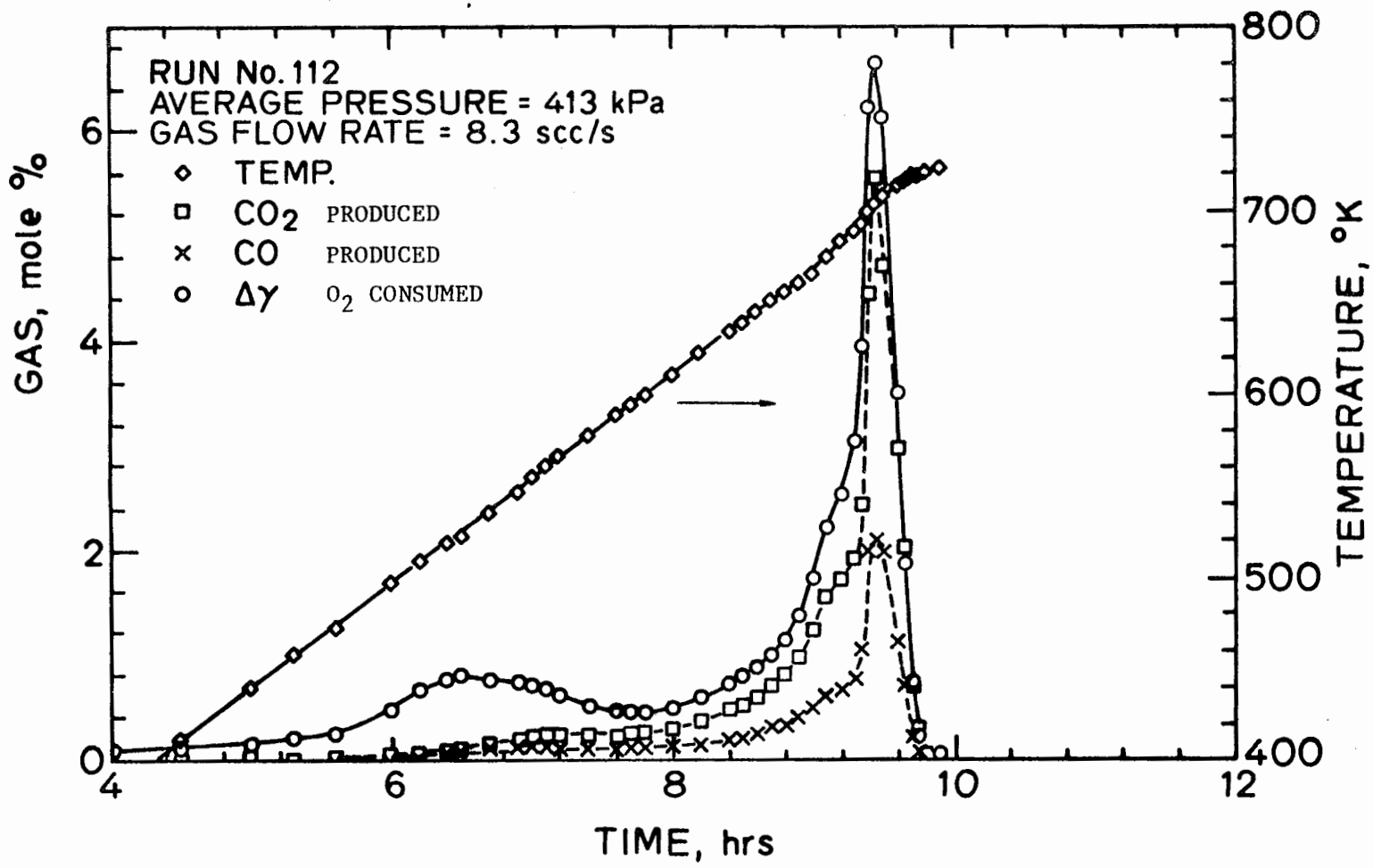

Fig. 8.4: GAS COMPOSITION AND TEMPERATURE FOR VENEZUELAN OIL

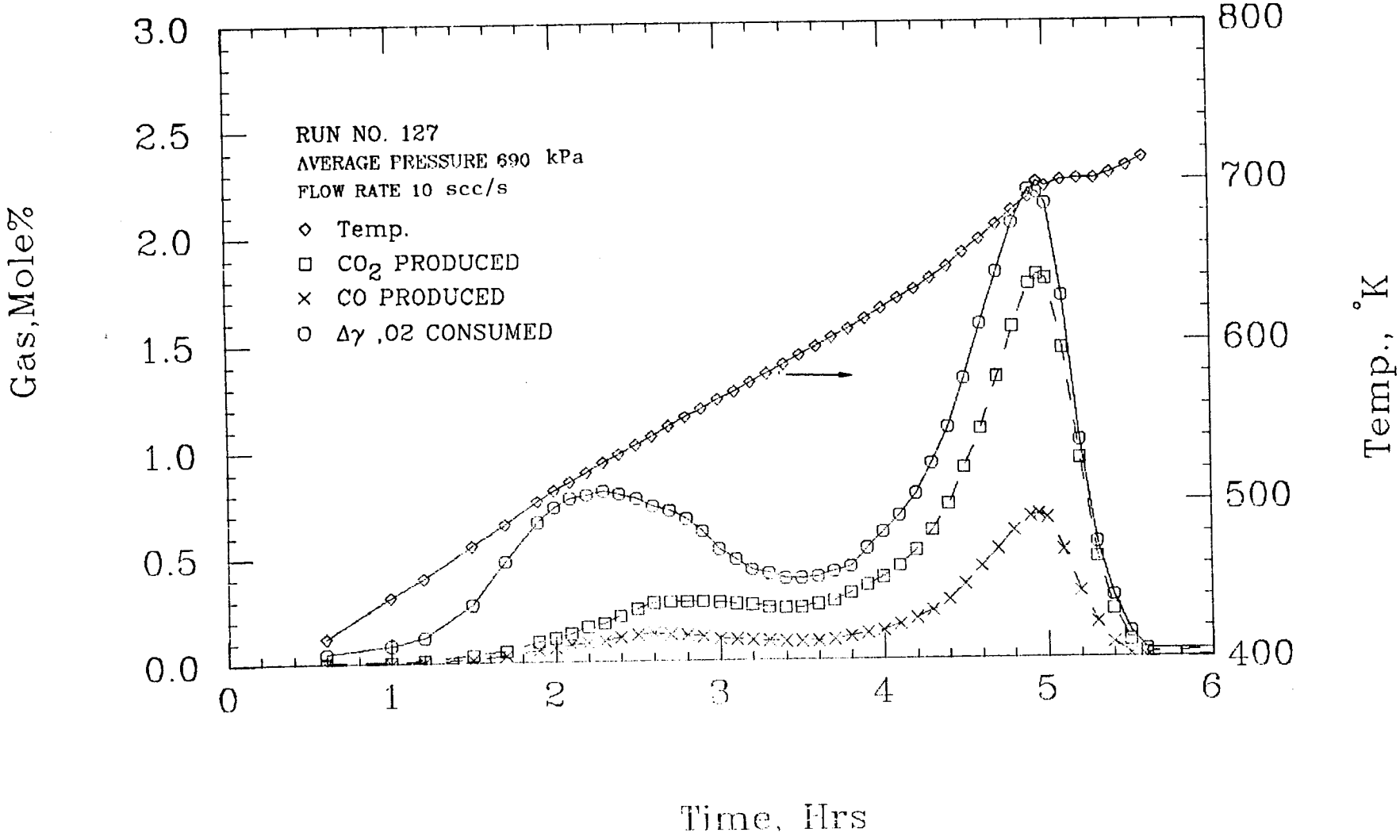

Fig. 8.5: GAS COMPOSITION AND TEMPERATURE FOR SAN ARDO OIL

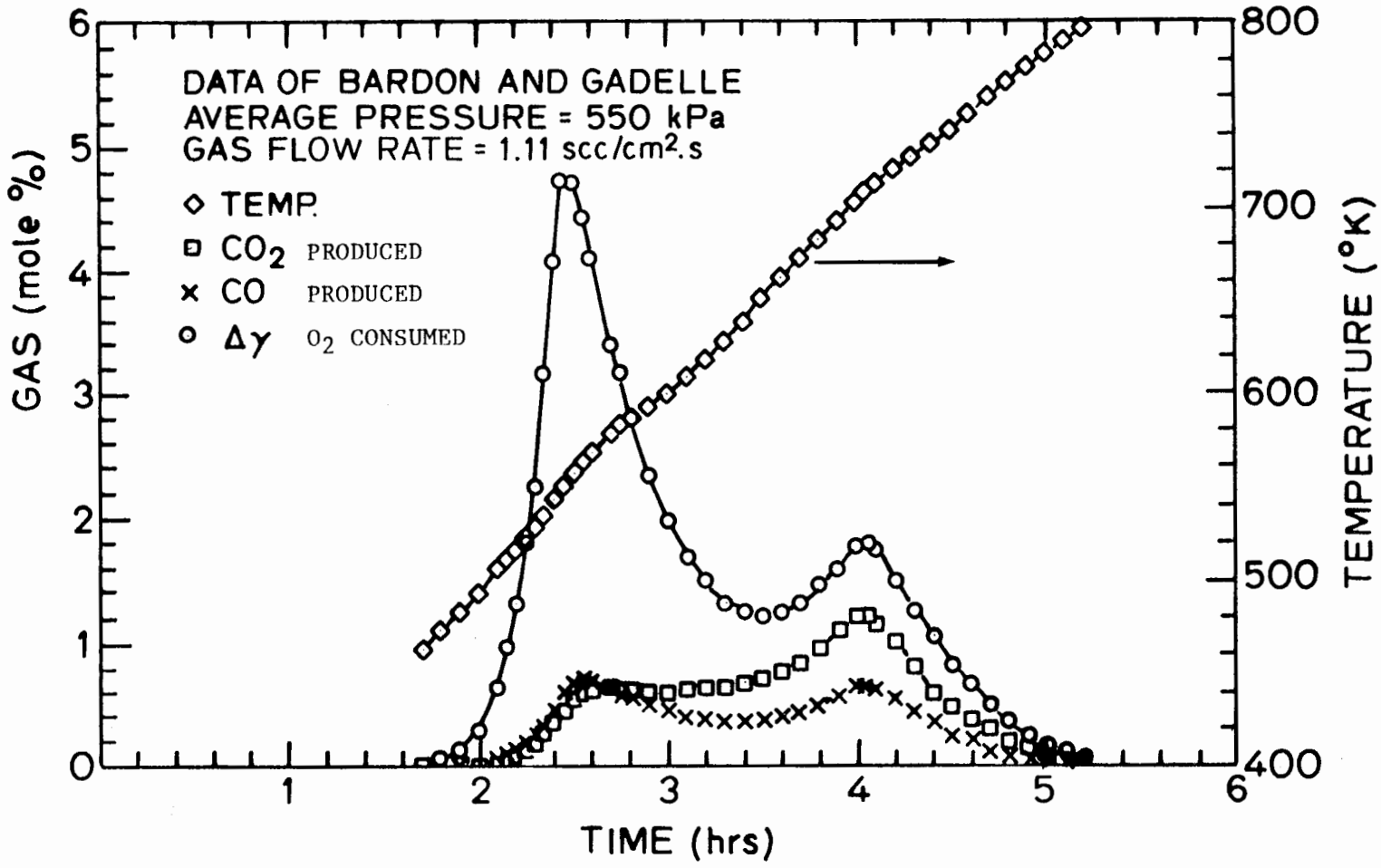

Fig. 8.6: GAS COMPOSITION AND TEMPERATURE FOR FRENCH OIL

The first peak in the gas concentration graphs corresponds to the oil oxidation at low temperatures while the second peak corresponds to the fuel combustion at high temperatures. Comparing Figs. 8.3-8.6, it is clear that the first peak may be smaller or higher than the second one depending on the nature of the crude oil. For example, for the heavy viscous Venezuelan oil, the combustion peak is much higher than the low-temperature peak (Fig. 8.4). This indicates the propensity of this crude oil for fuel deposition. In contrast, the French oil (Fig. 8.6), due to its high reactivity with oxygen at low temperatures, has a first peak which is much higher than the second case. (This figure is taken from the data of Bardon and Gadelle, 1977, who used a 27° API French oil. The properties of this oil are described in Table 8.8.

To understand the effects of pyrolysis on the combustion reaction, Bardon and Gadelle heated two samples of oil sand at $350^{o}C$, one for one hour and the other one for five hours, while nitrogen was flowing. Then, they subjected these samples to a heating schedule in the presence of air (similar to the non-isothermal runs mentioned herein previously). The resulting gas compostion data (Figs. 6 and 7 of their report) showed that for the sample heated for one hour, the first peak was much smaller than the corresponding peak using the original oil, and for the sample heated for five hours, the first peak virtually disappeared. These findings were in agreement with those of Tadema (1959) who found that subjecting the oil sand to prolonged heating at $350^{o}C$, caused the first peak in DTA thermograms to disappear.

Bardon and Gadelle concluded that during pyrolysis, the light fractions of the oil are eliminated by stripping; the medium and heavy fractions are transformed by cracking, giving volatile products and

heavy residues. As a result, during air oxidation, when there is lack of oxidizable fuel at low temperatures, the first peak disappears. This may explain why some oils have such a small low-temperature peak (Fig. 8.4). For these oils, there is not enough fuel to be oxidized at low temperatures because very little pyrolysis occurs. Consequently, the oxygen consumption is very low. The unusual behavior observed in Runs No. 107 and 111 can be explained by this pyrolysis reaction.

To investigate these reactions and the chemical nature of the fuel burned, and to see the importance of distillation and pyrolysis on these reactions, the apparent hydrogen-carbon ratio and the molar carbon dioxide-carbon monoxide ratio were calculated. The results of these calculations are discussed in subsequent paragraphs.

8.3 Molar CO_2/CO Ratio

The molar ratios of the carbon oxides (λ) produced by the oxidation reactions of crude oil at different temperatures are shown as triangles in Figs. 8.7-8.10. The changes in λ indicate the transition between reactions at different temperatures (Lewis *et al.*, 1954).

8.3-1 Effect of Temperature on λ

It appears that the value of λ has two distinct regions; below $600^{\circ}K$ ($620^{\circ}F$), λ is variable, increasing from 0.8 to 2.0. At higher temperatures, it is nearly constant at around 2-3, depending on the pressure. The calculated λ's at very low and very high temperatures were excluded because of the lower accuracy in measurement of small concentration carbon oxides produced.

The fact that λ is almost constant at high temperatures indicates that carbon oxides are being produced by the same reaction. By the same token, the reactions at low temperatures must be numerous and non-unique because below $600^{\circ}K$, λ varies with temperature.

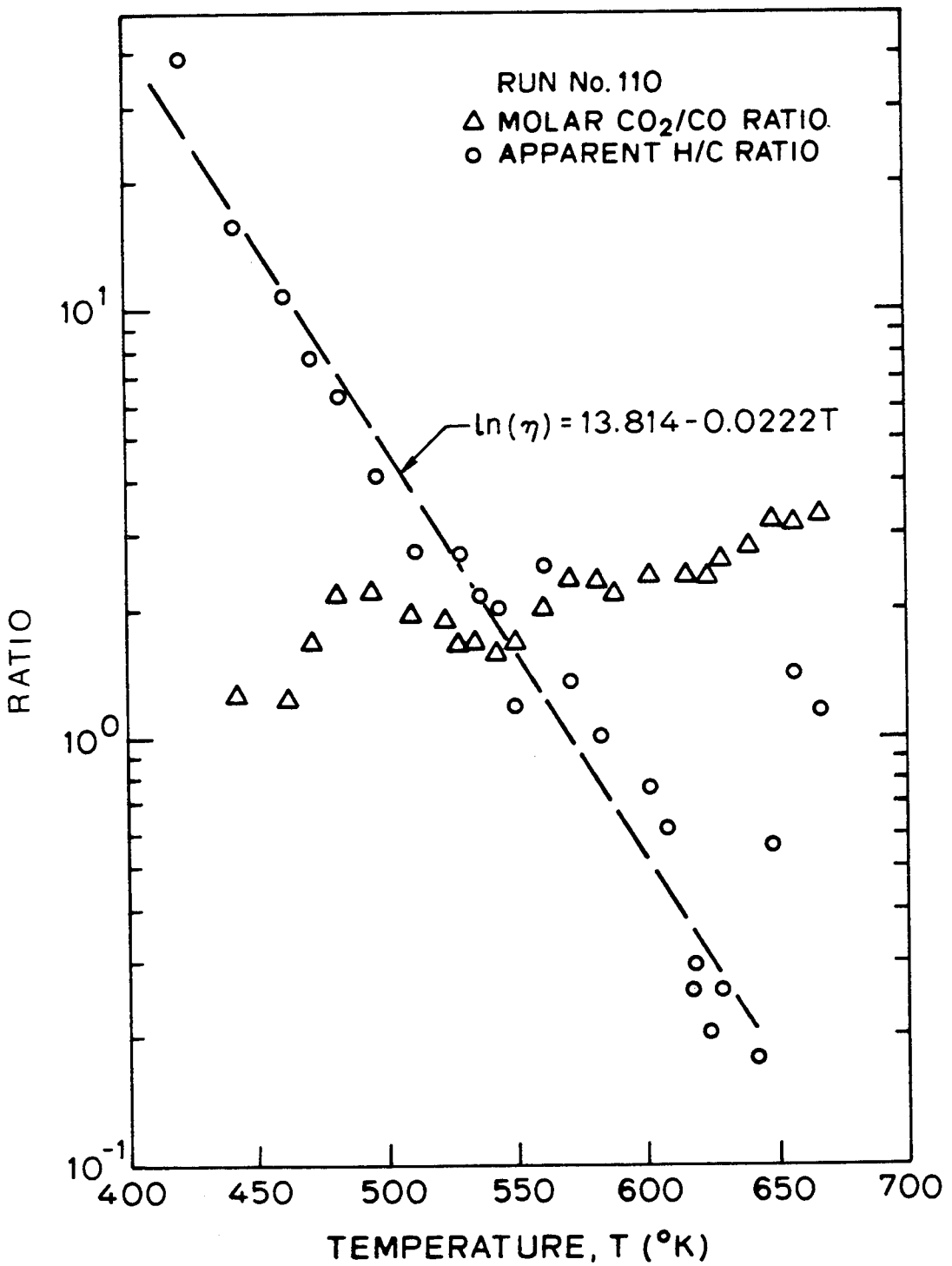

Fig. 8.7: MOLAR CO_2/CO RATIO AND APPARENT H/C RATIO VS TEMPERATURE FOR HUNTINGTON BEACH OIL

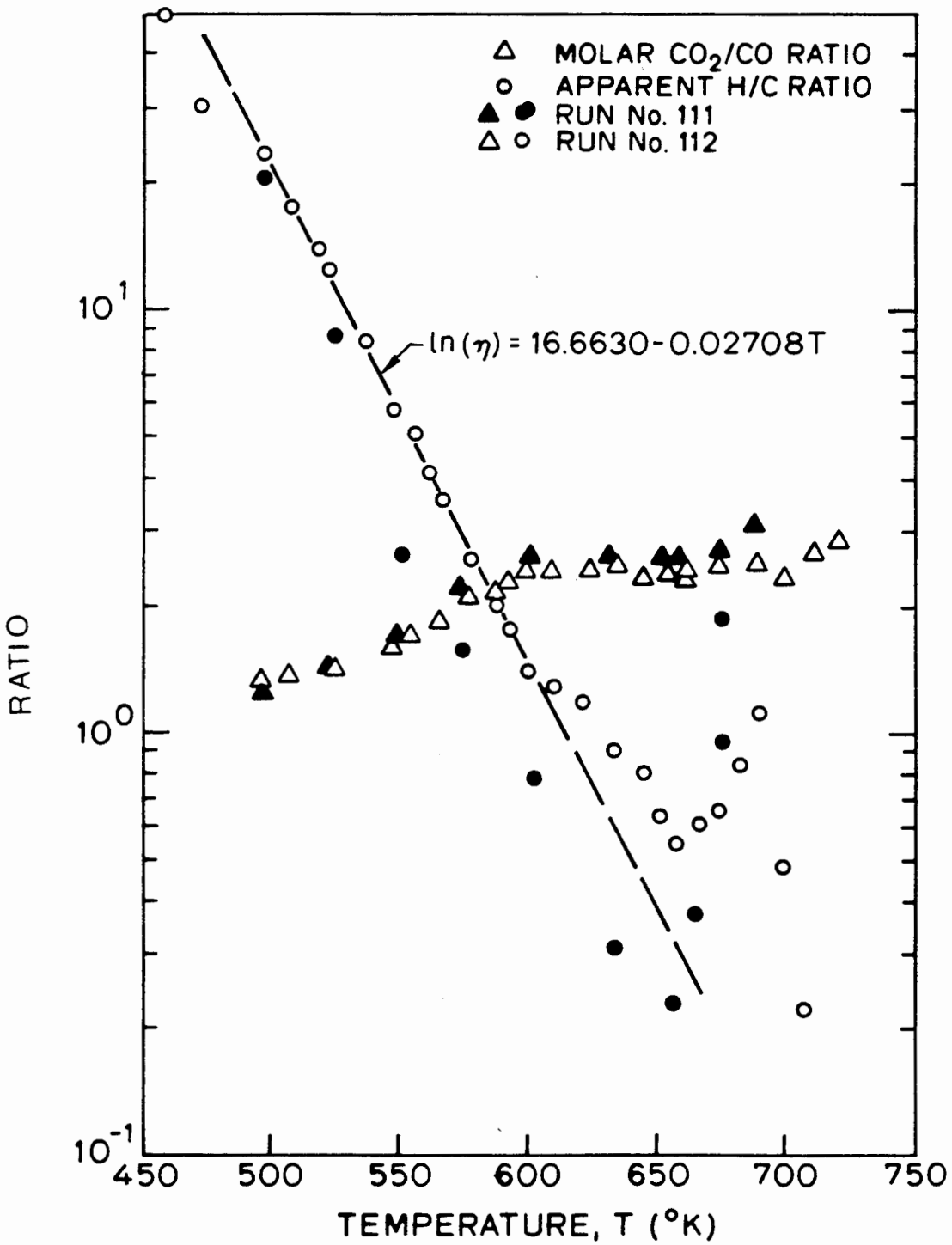

Fig. 8.8: MOLAR CO_2/CO RATIO AND APPARENT H/C RATIO FOR VENEZUELAN OIL

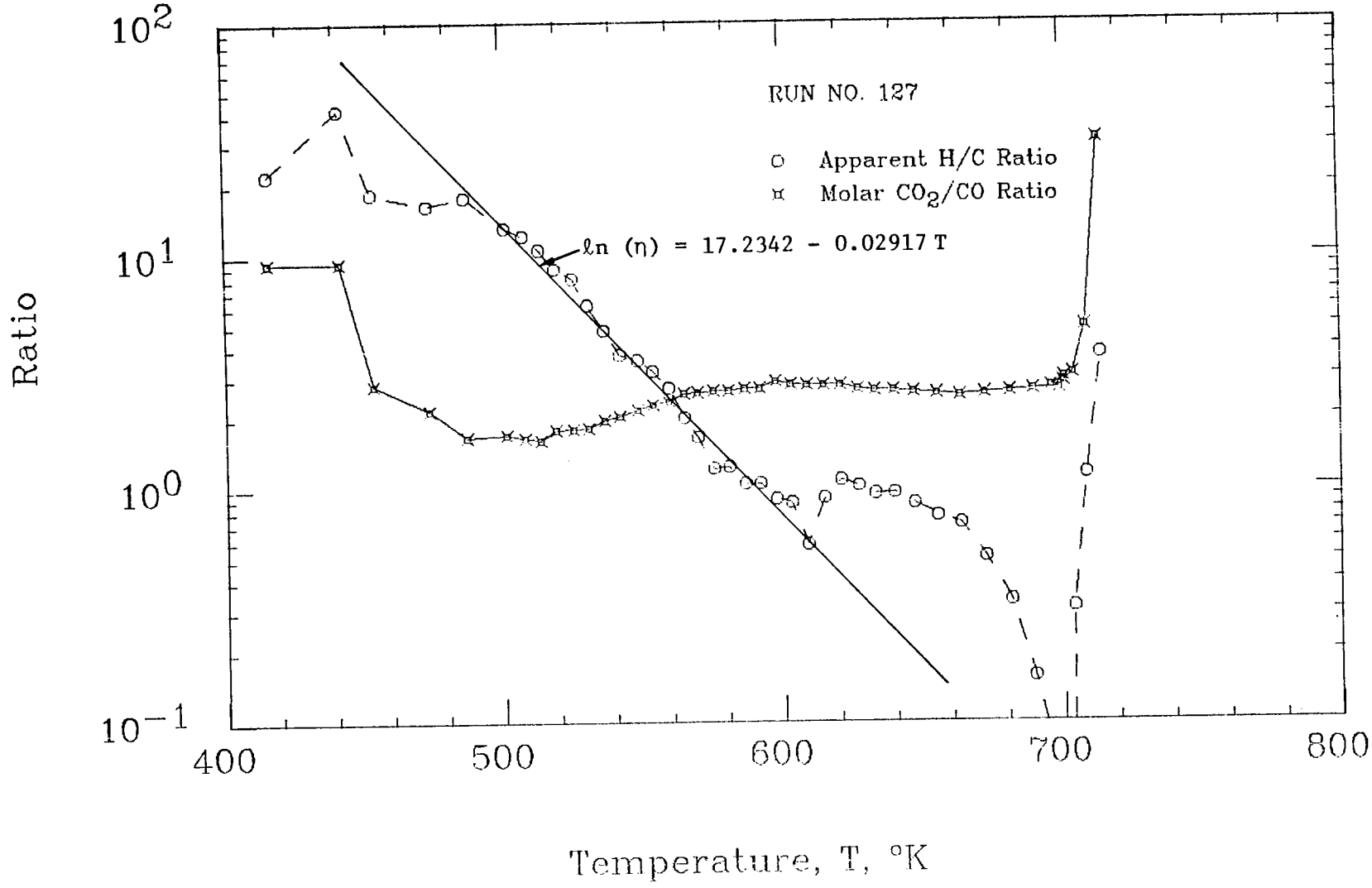

Fig. 8.9: MOLAR CO_2/CO RATIO AND APPARENT H/C RATIO FOR SAN ARDO OIL

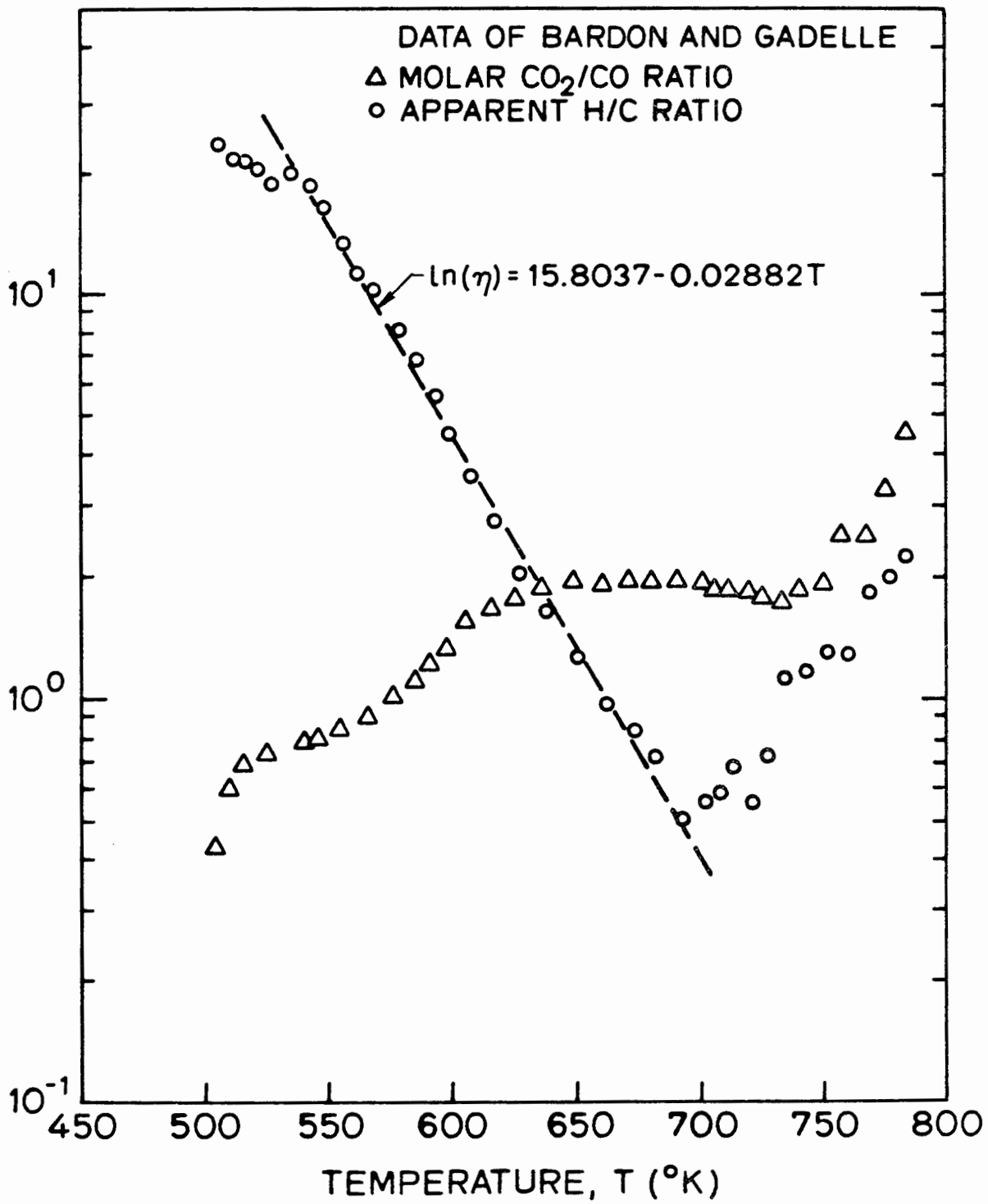

Fig. 8.10: MOLAR CO_2/CO RATIO AND APPARENT H/C RATIO FOR FRENCH OIL

Lewis et al. (1954) reported that the molar ratio of $CO/(CO + CO_2)$ for combustion reactions of charcoal, graphite, and coal in a fluidized bed is around 0.25 (i.e., $\lambda = 3$). The fact that this number is near the value of λ obtained at high temperatures, indicates that the fuel burned in the combustion reaction is a heavy residue and is similar to carbon in chemical characteristics.

In Fig. 8.8, the calculated λ's for an isothermal run (shown as dark triangles) are compared to the λ's obtained in a non-isothermal run (shown as clear triangles). Generally, the longer heating schedule and residence time of isothermal runs resulted in greater carbon dioxide production and greater values of λ compared to non-isothermal runs. Apparently, the larger residence times resulted in more nearly equilibrium conditions.

8.3-2 Effect of Pressure on λ

The average values of λ calculated at high temperatures in different runs are graphed vs partial pressure of oxygen in Fig. 8.11. It appears that λ increases slightly with higher pressure. The straight line shown is drawn through the data obtained using Huntington Beach oil and has the following equation:

$$\lambda = 0.228 \ \ell n \ p_{O_2} + 1.404 \qquad (8.1)$$

where

p_{O_2} = Partial Pressure of Oxygen, kPa

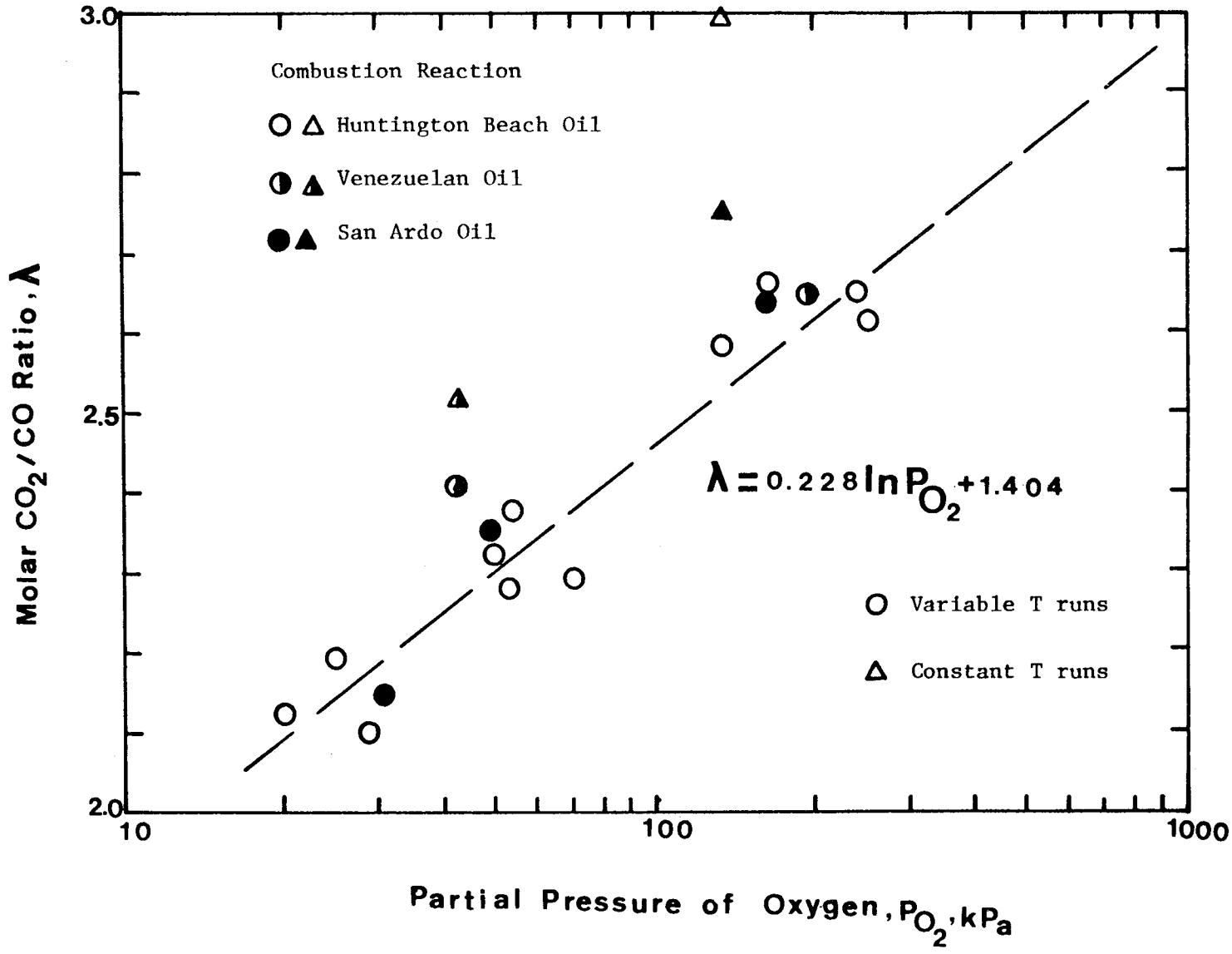

Fig. 8.11: MOLAR CO_2/CO RATIO VS PRESSURE

This pattern is in accordance with the findings of Dabbous and Fulton (1974). However, Bousaid and Ramey (1968) did not find any effect of pressure on λ.

This pressure dependency of λ may be due to the occurrence of the following reactions:

$$CO + 1/2\ O_2 \rightleftharpoons CO_2 \tag{8.2}$$

$$2CO \rightleftharpoons CO_2 + C \tag{8.3}$$

Calculated thermodynamic equilibrium constants (Kanury, 1977, pp. 366-368) for the above reactions showed that the second reaction is more likely to occur at pressures and temperatures encountered in the experiments. In fact, at 800°K, by calculation the following relationship exists between λ and the partial pressure of CO_2, p_{CO_2}:

$$\lambda = 0.971\ (p_{CO_2})^{1/2} \tag{8.4}$$

Similar equations cna be derived for λ at different temperatures using the published values of the equilibrium constant for this reaction (Kanury, 1977). However, the occurrences of reaction 8.3 cannot fully explain the observed behavior shown on Fig. 8.11 because Eqs. 8.1 and 8.4 have different constants.

8.4 The Apparent H/C Ratio, η

The apparent hydrogen-carbon ratio of the fuel consumed, η, was calculated from the analysis of the produced gases for each combustion run as a function of temperature. These calculations were based on the assumption that all the oxygen not observed in the exit gas had reacted to form water. This assumption is not rigorous because of the occurence of LTO reactions.

The apparent H/C ratio is a useful correlating tool (Alexander, et al., 1962). Burger and Sahuquet (1972) showed that η and λ can be used to estimate the heat of combustion. The relationship between η and produced gas composition is:

$$\eta = \frac{4[(\gamma_i/\nu_i)\nu_o - CO_2 - 0.5\ CO - \gamma_o]}{(CO_2 + CO)} \tag{8.5}$$

where:

γ_o = concentration of produced oxygen, mole %

γ_i = concentration of injected oxygen, mole %

ν_i, ν_o = concentration of injected and produced nitrogen, mole %

The calculated H/C ratios for four runs are graphed as circles in Figs. 8.7-8.10. The values of η at both very high and very low temperatures should be discarded due to less accurate measurement of the small concentration of gases produced.

In most runs, a general decrease in the apparent H/C ratio with an increase in temperature was observed and was found to follow a simple semilogarithmic relationship.

$$\ln \eta = a + bT \tag{8.6}$$

where a and b are constants shown in Table 8.1.

8.4-1 Effect of Distillation on η

The atomic H/C ratios of the distillation cuts of crude oils used were calculated to investigate whether distillation in porous medium is responsible for lowering η (see Watson and Nelson, 1935, on methodology). Figure 8.12 shows the H/C ratios of different fractions of Huntington Beach crude oil. The η for the original crude is also graphed.

As shown in Fig. 8.12, the H/C ratios of distillation cuts only dropped from 1.95 to 1.5 as the temperature was increased. This drop is much less than the one observed in kinetic experiments (Figs. 8.7-8.10). In these runs, at temperatures below 560°K, η was higher than the atomic H/C ratio of the parent oil. However, as the temperature was increased, η decreased more until it reached a minimum (around 0.5). This may be due to further pyrolysis of the fuel at higher temperatures.

8.4-2 Effect of Pyrolysis on η

Burger and Sahuquet (1977a) studied the effect of pyrolysis on the atomic H/C ratio of the fuel. Their study consisted of subjecting a sample of crude oil to a heating rate (500°C/hr) in the presence of nitrogen and then measuring the hydrogen and carbon content of the residue at each temperature. The results are reproduced in Fig. 8.13. As shown, the carbon content of fuel was almost constant at all temperatures, but the hydrogen content was only constant up to around 300°C, after which it decreased as the temperature was increased. Hence, they observed that η decreased linearly with an increase in temperature.

Table 8.1: CONSTANTS OF THE CORRELATION

$$\ln \eta = a + bT$$

CRUDE TYPE	a	b
Huntington Beach	13.8140	0.02220
Venezuela	16.6630	0.02708
French Oil	15.8037	0.02382
San Ardo	17.2342	0.02917

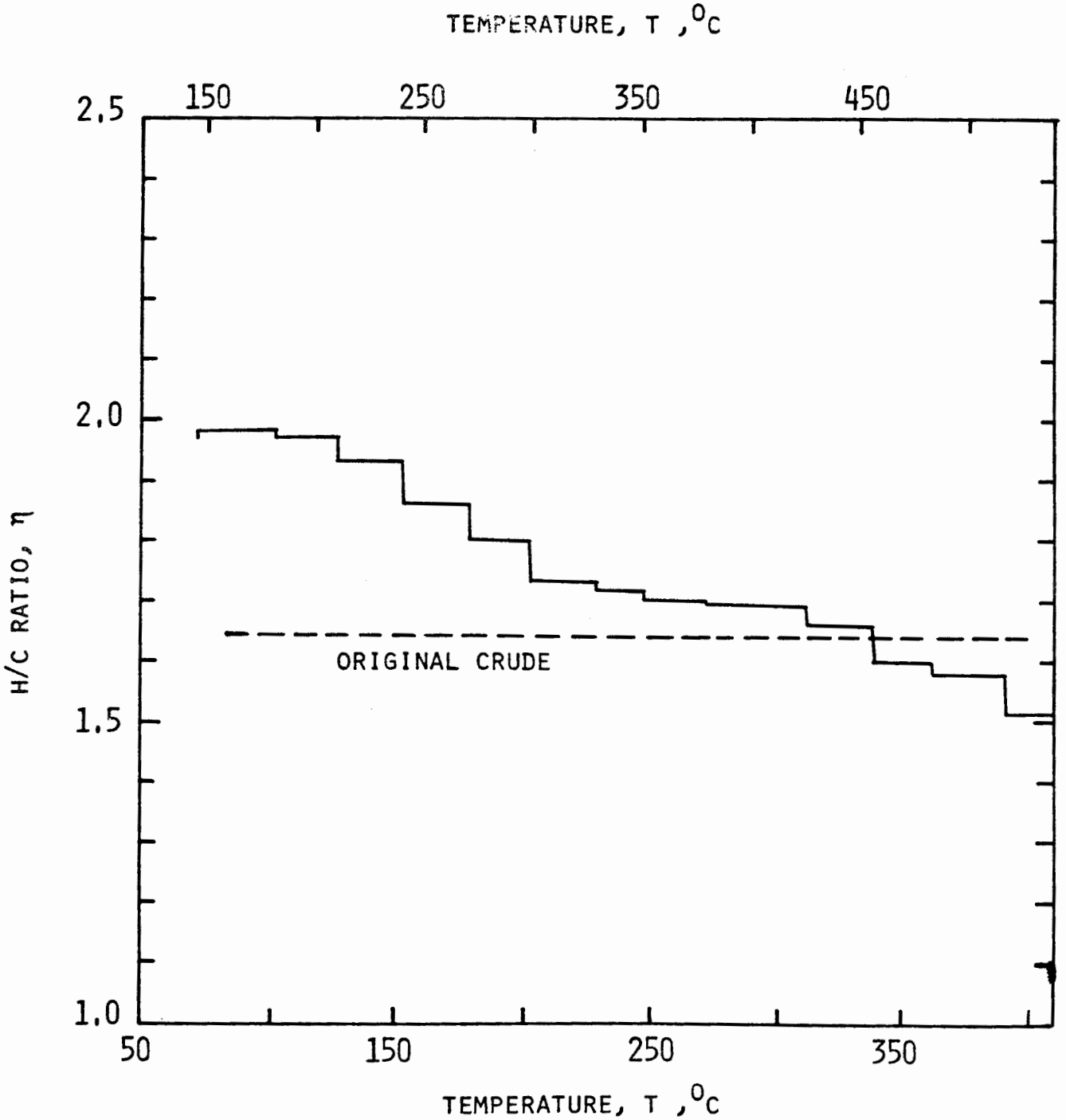

Fig. 8.12: ATOMIC H/C RATIO OF THE FRACTIONS OF HUNTINGTON BEACH CRUDE DISTILLED (THE LOWER AND UPPER ABSCISSAE ARE FOR DISTILLATION AT 0 AND 80 PSIG RESPECTIVELY, REFER TO FIG. 5.3)

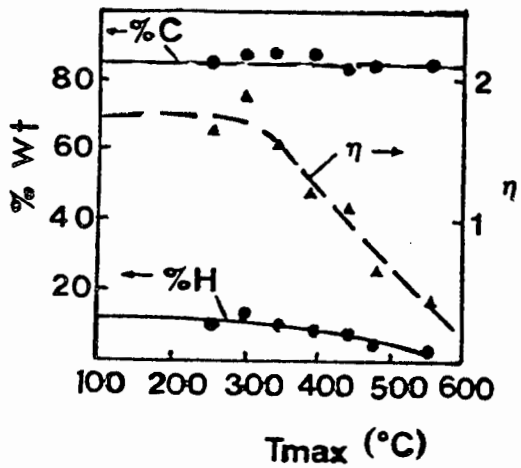

Fig. 8.13: ALTERATION OF RESIDUAL OIL IN THE PRESENCE OF NITROGEN DURING HEATING TO A MAXIMUM TEMPERATURE T_{max} OF A MIXTURE OF CRUSHED SILICA AND OIL. HEATING RATE = 500° C/hr. (Burger, J., 1972)

As a result of the preceding sections, the following conclusions can be drawn:

At lower temperatures, the crude oil undergoes an oxidation reaction without generating carbon oxides.

As the temperature is raised, distillation coupled with pyrolysis produces hydrogen gas and some light hydrocarbons in the gas phase. A major part of these hydrocarbons are produced without being oxidized. However, oxygen reacts with the remainder of these gases and hence, medium-temperature oxidation occurs.

At higher temperatures, this reaction is completed and a heterogeneous reaction begins. Here, the reactants are oxygen in the gas phase and heavy residue of oil deposited on the solid matrix.

8.5 Modelling of the Reactions

In Appendix C, a model is developed based on Weijdema's kinetic equation (1968). In this model, the temperature can be increased linearly with time, and by proper graphing of the variables, a semi-log straight line should result. The variable temperature runs were made to test this model. Using the data in Run No. 110, the relative reaction rate (Appendix C) was calculated and is graphed in Fig. 8.14. Note that the high temperature data fall on a straight line as predicted by Weijdema's model but at lower temperatures (increasing values of 1/T) a departure from the straight line is observed. It is clear from these data that Weijdema's single-reaction model does not adequately describe the reaction kinetics observed.

At high temperatures the amount of carbon oxides formed closely matches the amount of oxygen consumed, but at medium temperatures the oxygen consumed is greater than the carbon oxides formed. Finally,

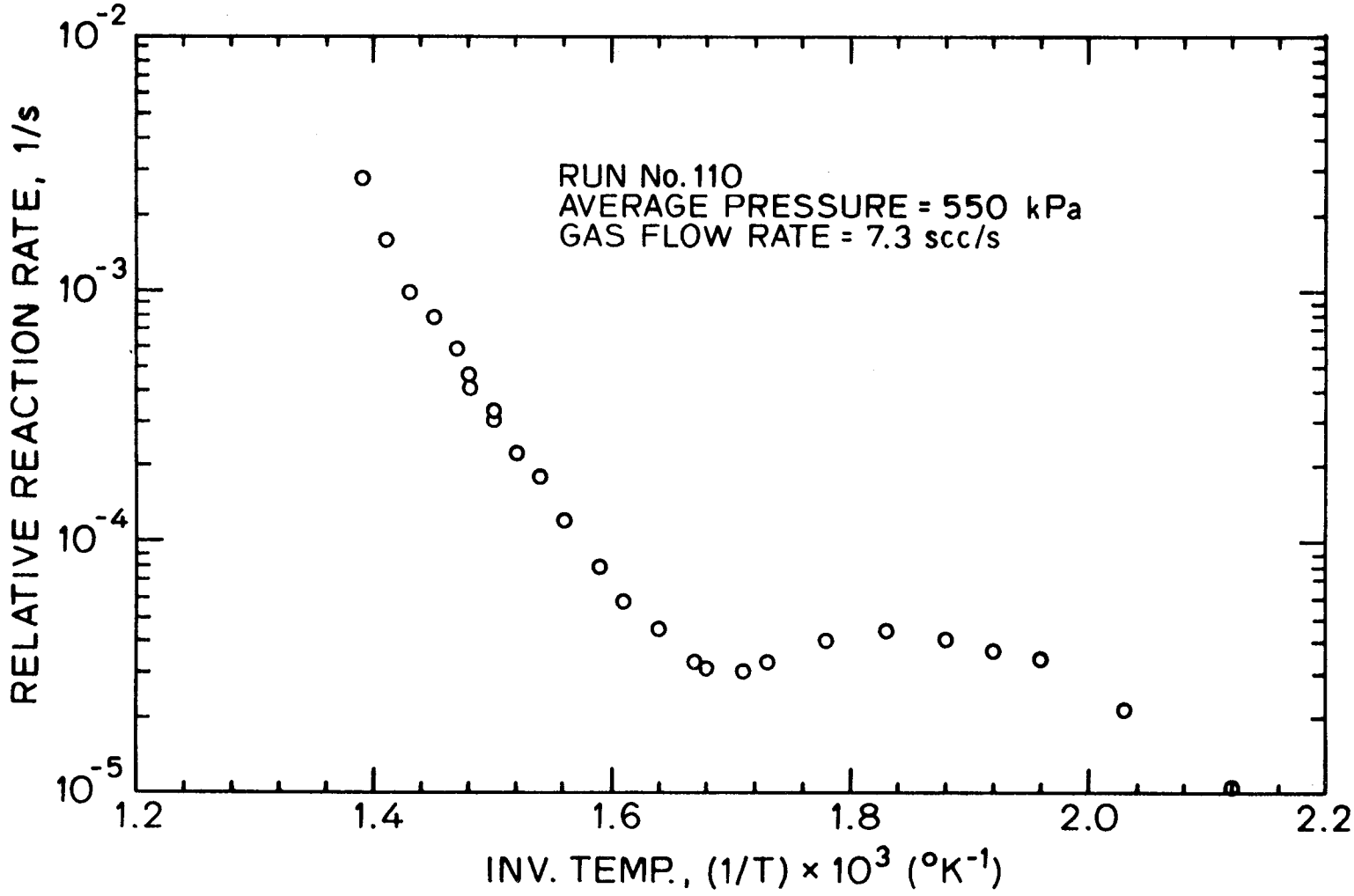

Fig. 8.14: RELATIVE REACTION RATE VS INVERSE TEMPERATURE FOR RUN NO. 110

at low temperatures, oxygen is consumed with no carbon oxide formation. This pattern is the basis of an analysis of the data for these separate reactions as described in the following paragraphs.

A straight line was drawn through the high temperature data. From the slope of that line an activation energy, E = 135 kJ/mole, is obtained (Fig. 8.15a, curve I). It was assumed that this reaction also occurs at lower temperatures according to an extrapolation of the high temperature data. The method used is described in Appendix D.

By subtracting the amount of oxygen consumed in the high temperature reaction from the original $\Delta\gamma$ curve (Fig. 8.16a) a new curve (Fig. 8.16a, curve II) is obtained which describes the oxidation behavior at the medium temperature range, and curve III in Fig. 16b is obtained which describes the production of carbon oxides in the medium temperature range.

From curve II of Fig. 8.16a, a calculation of the relative reaction rate, $(\Delta\gamma)/\int_t^\infty \Delta\gamma dt'$ as a function of 1/T leads to the curve labelled II in Fig. 8.15b (the open triangles). The data are not linear. However, a computation of an equivalent term for the carbon oxides formed, $\delta/\int_t^\infty \delta dt'$, where $\delta = CO_2 + o.5CO$, from curve III, Fig. 8.16b, shows a definite straight line (curve III, Fig. 8.15b). An activation energy of E = 84 kJ/mole is calculated from the slope of this line. In this figure, although the data scatters considerably, it appears reasonable to assume the oxygen consumption curve in the medium temperature range follows the same slope as the carbon oxides curve. Using this assumption, the oxygen consumption can be calculated and subtracted from curve II of Fig. 8.16a and the remainder is represented in curve V (Fig. 8.16c).

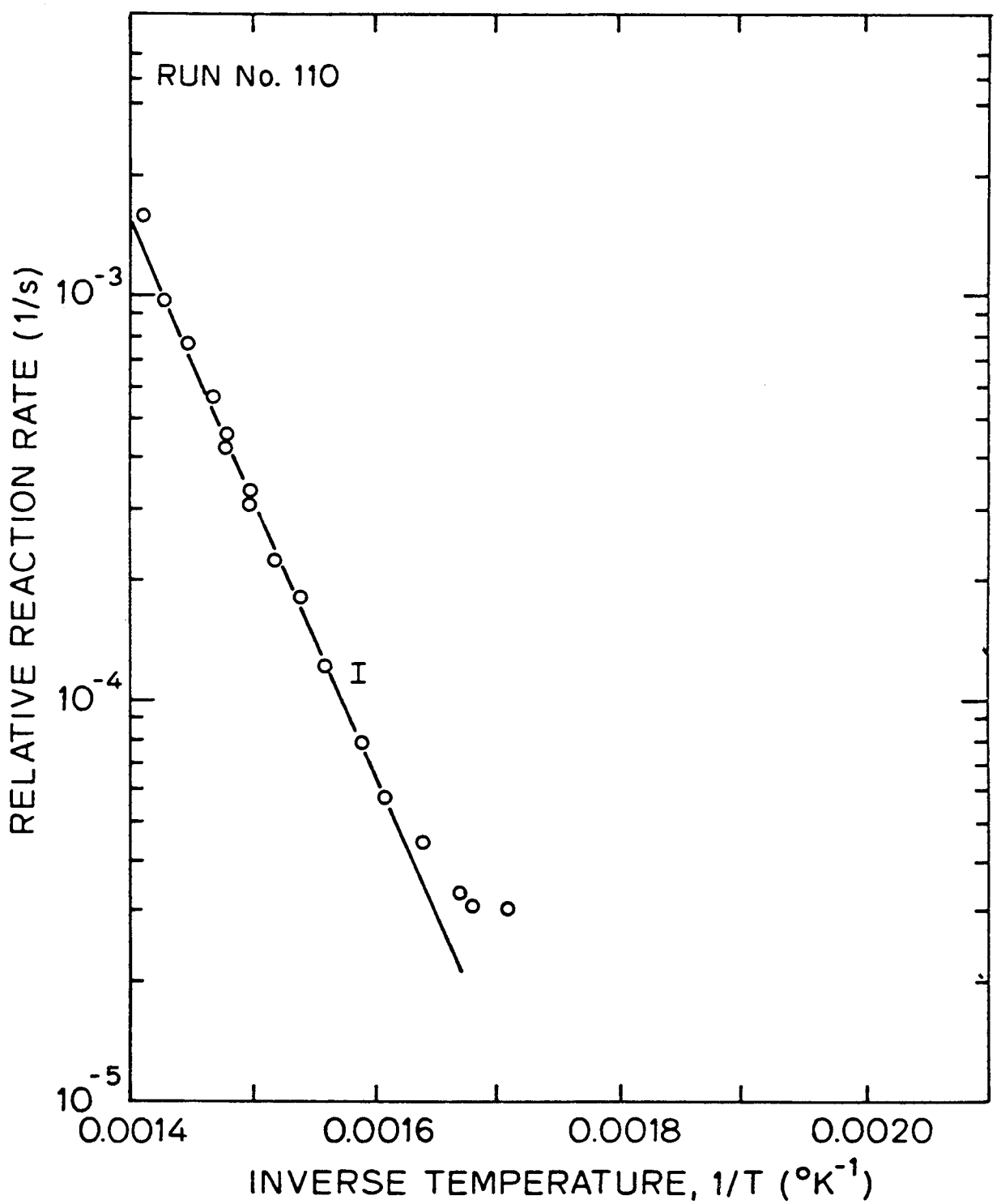

Fig. 8.15a: ARRHENIUS PLOT FOR COMBUSTION REACTION RATE (RUN NO. 110)

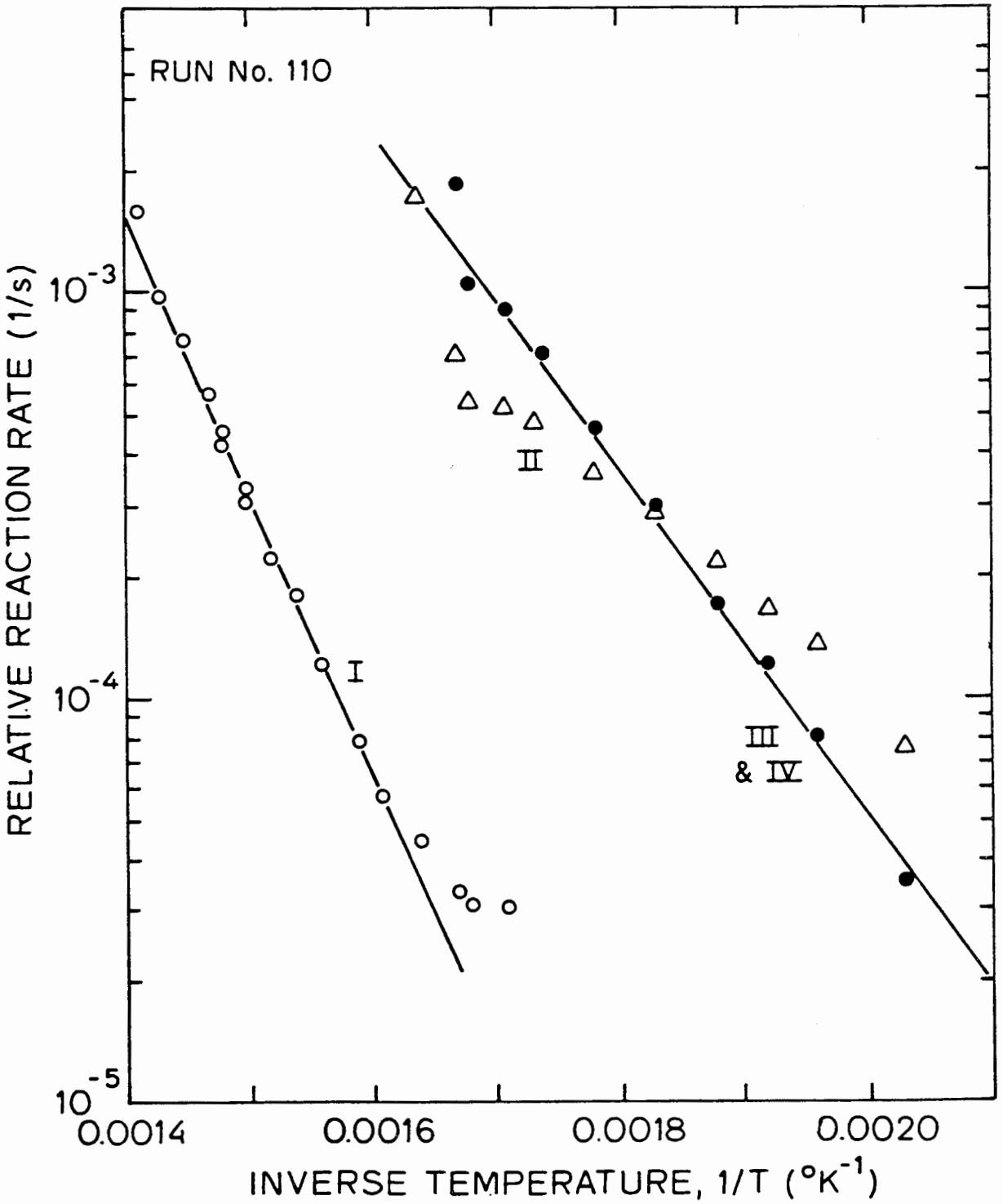

Fig. 8.15b: ARRHENIUS PLOT FOR FUEL COMBUSTION AND DEPOSITION REACTION RATES (RUN NO. 110)

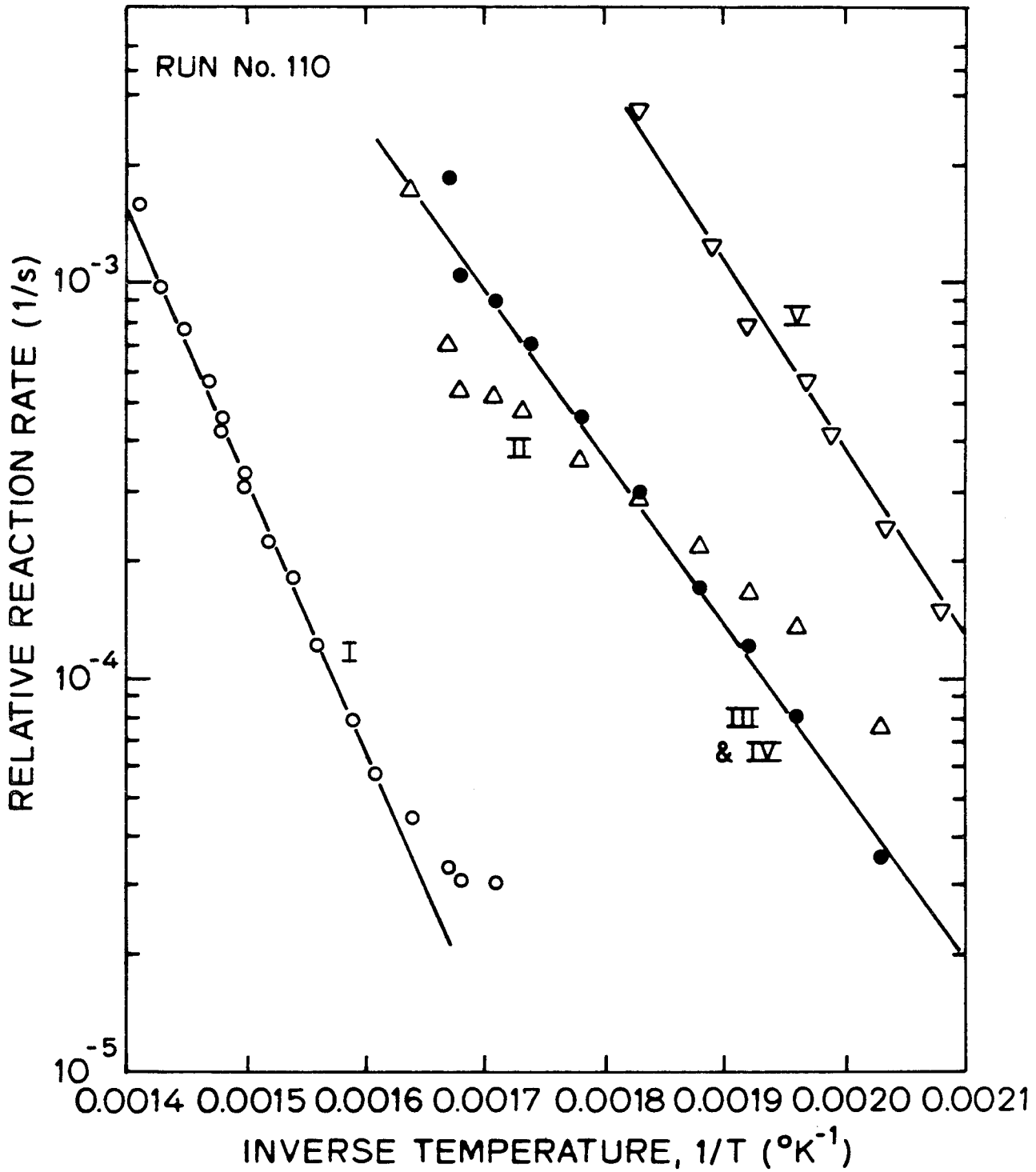

Fig. 8.15c: ARRHENIUS PLOT FOR RUN NO. 110

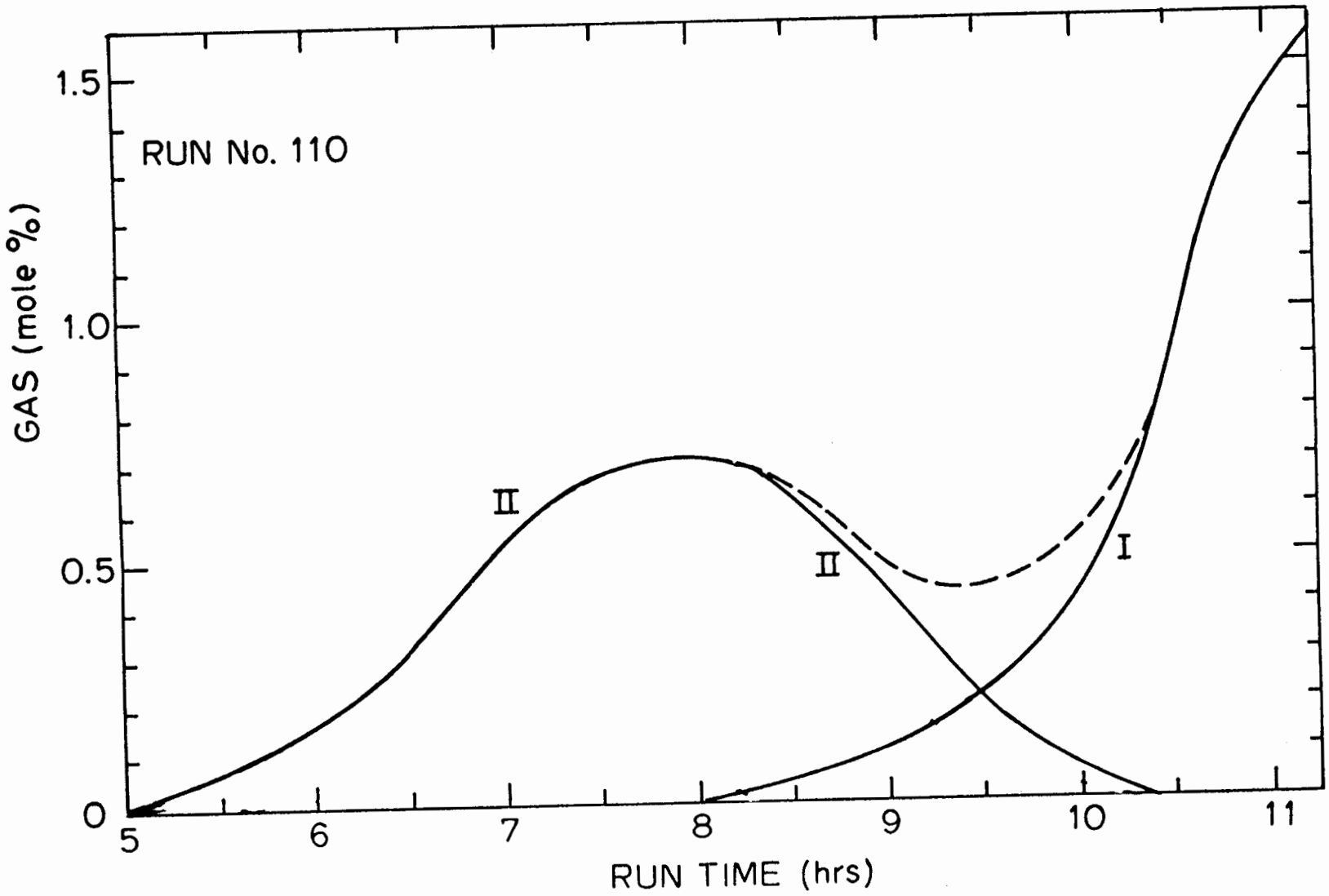

Fig. 8.16a: DECOMPOSITION OF THE CONSUMED OXYGEN IN FUEL COMBUSTION REACTION

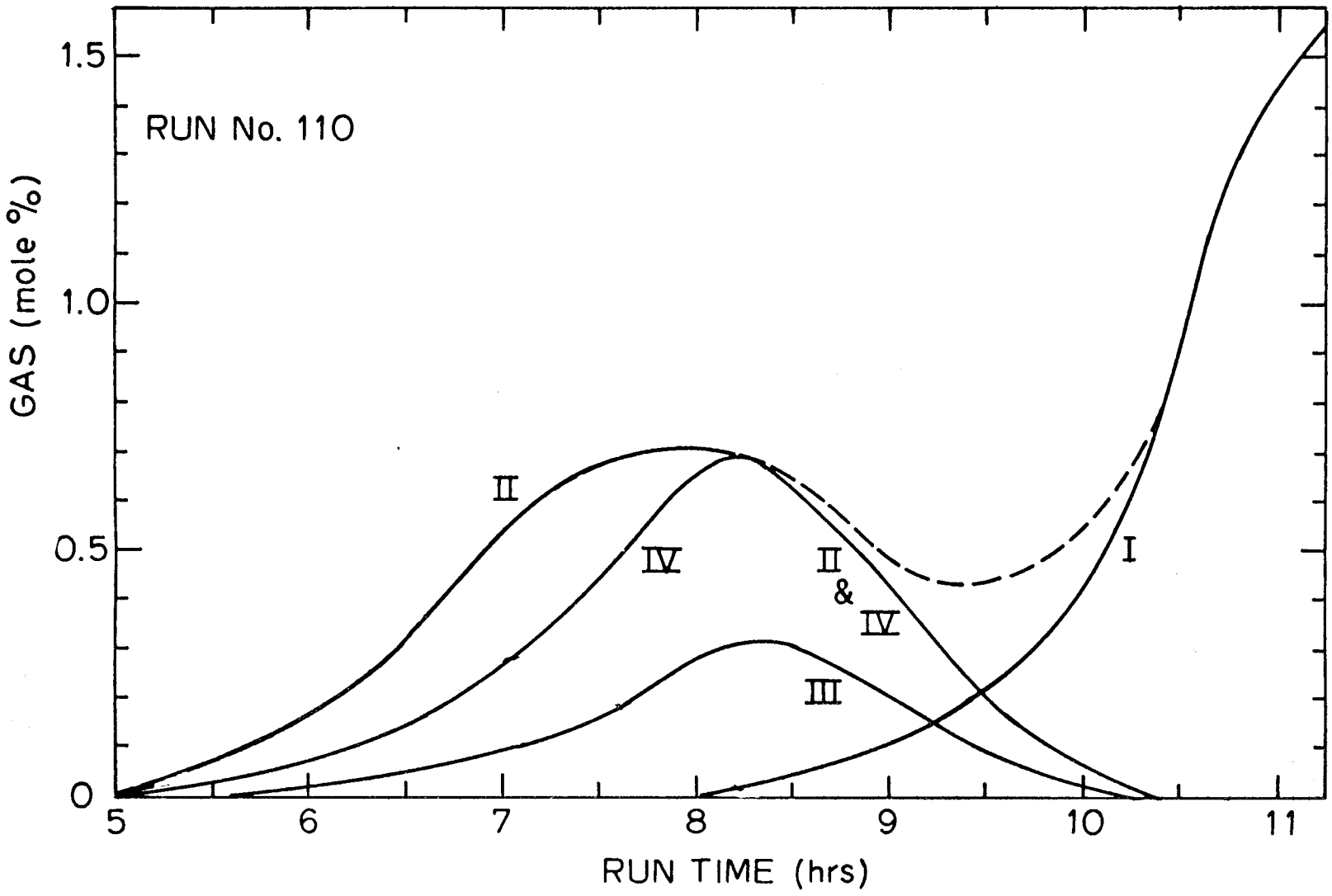

Fig. 8.16b: DECOMPOSITION OF THE CONSUMED OXYGEN IN MIDDLE-TEMPERATURE REACTION

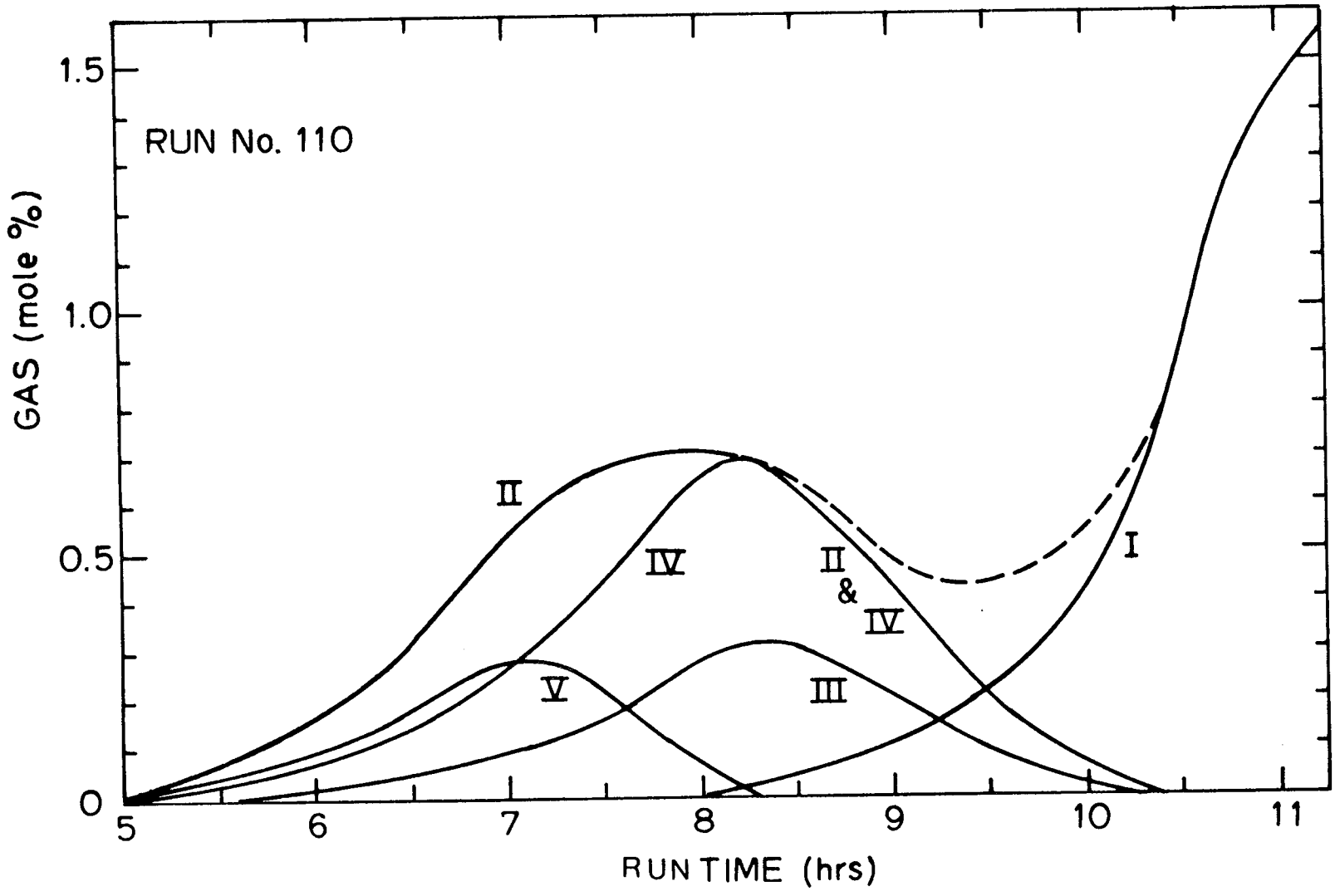

Fig. 8.16c: DECOMPOSITION OF THE CONSUMED OXYGEN IN LTO REACTION

When the data from curve V, Fig. 8.16c is evaluated using the Weijdema integral, $\Delta\gamma/\int_t^\infty \Delta\gamma dt'$, and the result is graphed on Fig. 8.15c, a straight line (curve V) is formed which describes the low-temperature oxidation reaction. The activation energy calculated from the slope of this line is E = 93 kJ/mole.

Using the computer interactively, this same analysis was applied to other experiments. The results always fit straight lines. However, for different crude oils, the order of the reaction with respect to fuel concentration, n, was different. Figures 8.17 through 8.20 show the corresponding Arrhenius plots and produced gases for two other crude oils.

8.6 Repeatability and Accuracy of Experiments

In general, all runs were repeatable. For example, using the same fuel in Runs No. 109 and 113, it was found that the resulting Arrhenius plots matched very closely. The same procedure was followed in matching the other results and the repeatability of the tests was confirmed.

To verify that the activation energies and the reaction orders derived from the analyses were reasonable, the amounts of oxygen consumed in the three reactions were superimposed upon one another and the results were compared to the experimental oxygen consumption curves. Figures 8.21 and 8.22 show computed $\Delta\gamma$ curves (solid line) compared to the experimental data. The match was good for these and other similar data.

The trapezoidal rule was used to integrate the area under the oxygen consumption curve. This caused some errors when there was a sharp change in gas concentration. It also introduced some errors into the calculations of curve fitting and extrapolation of the reaction rates to lower temperatures. These calculations were especially sensitive to the choice of the point at which the relative reaction rate

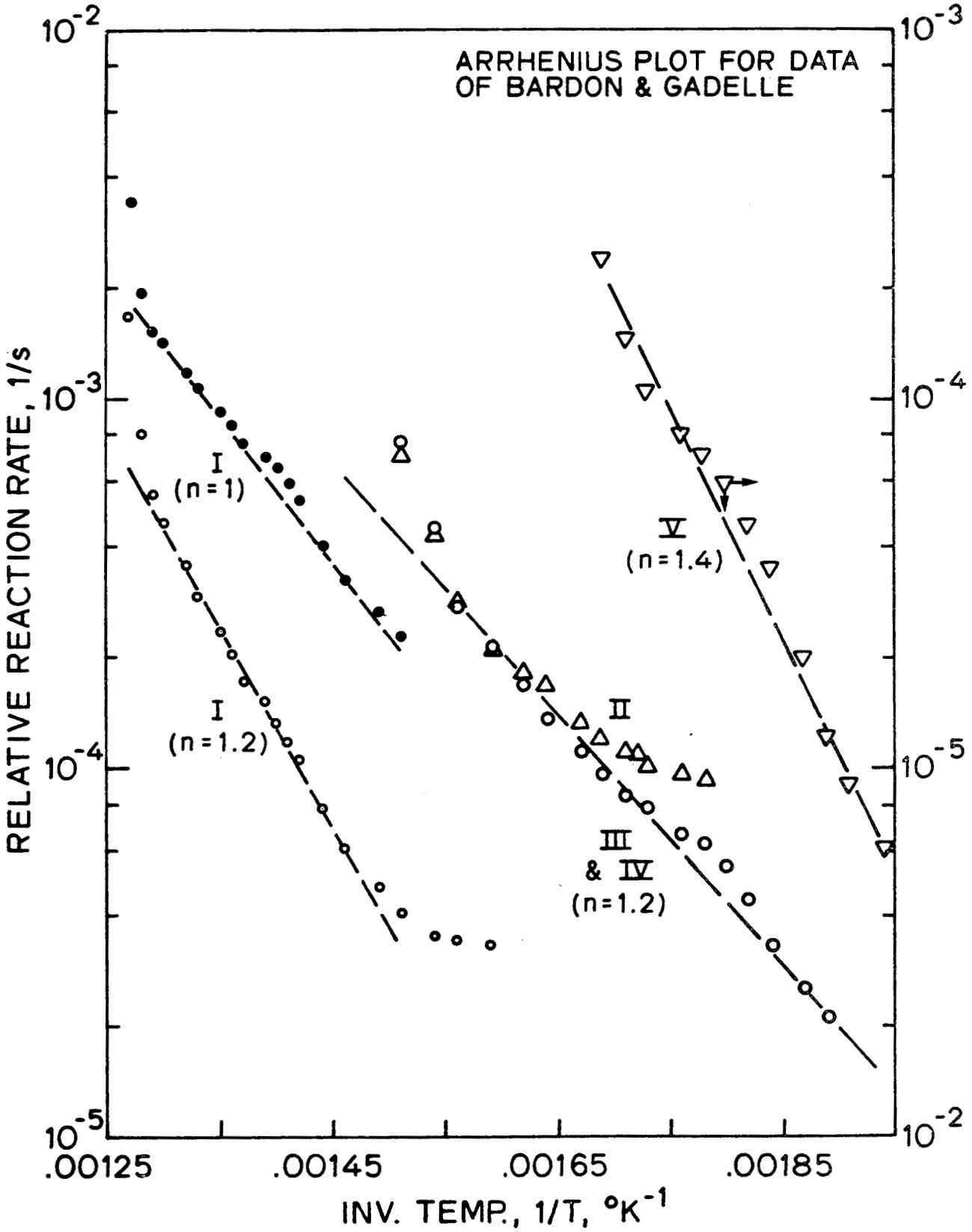

Fig. 8.17: ARRHENIUS PLOT FOR FRENCH OIL

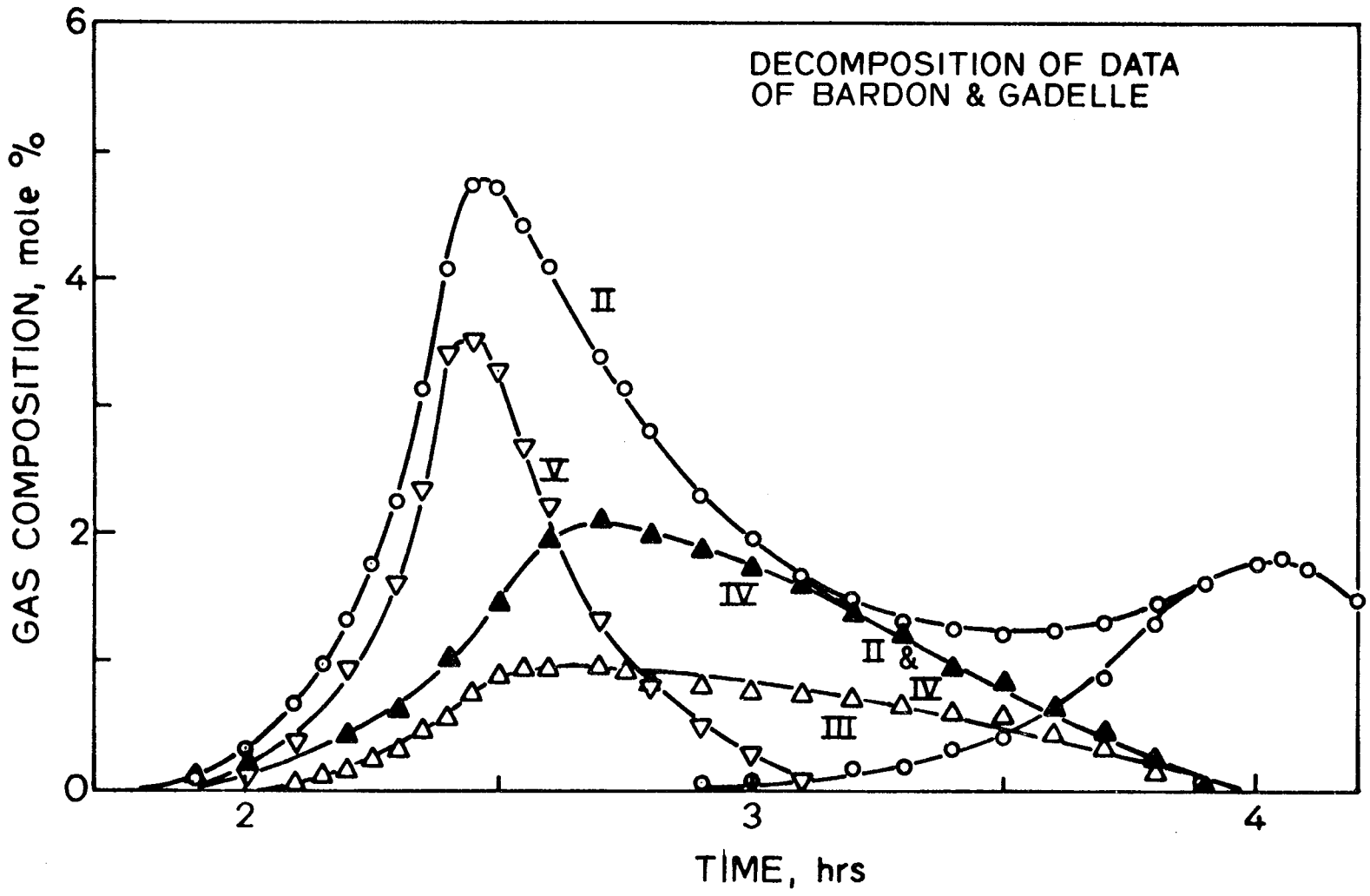

Fig. 8.18: DECOMPOSITION OF THE PRODUCED GASES GRAPHED IN FIG. 8.6

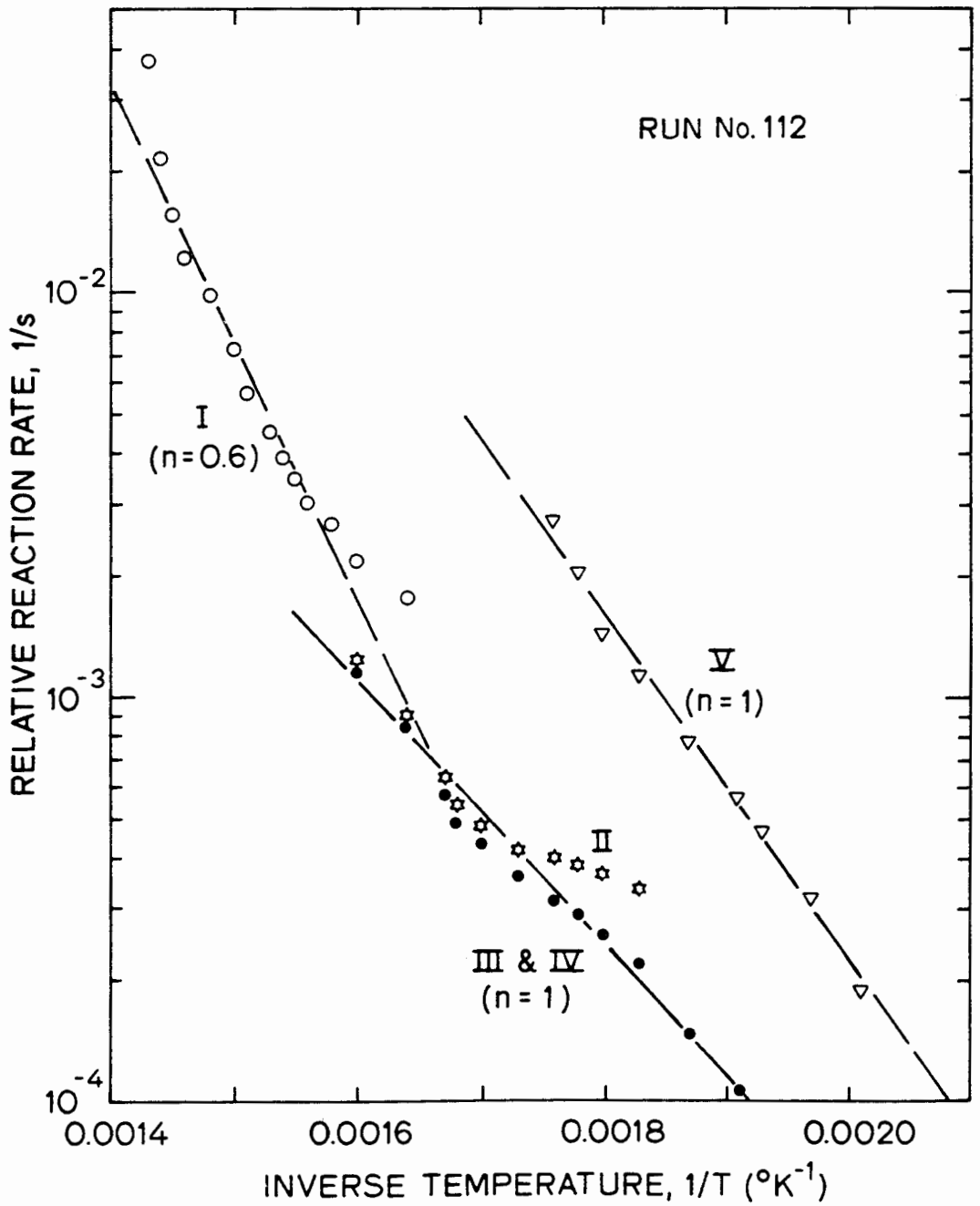

Fig. 8.19: ARRHENIUS PLOT FOR VENEZUELAN OIL

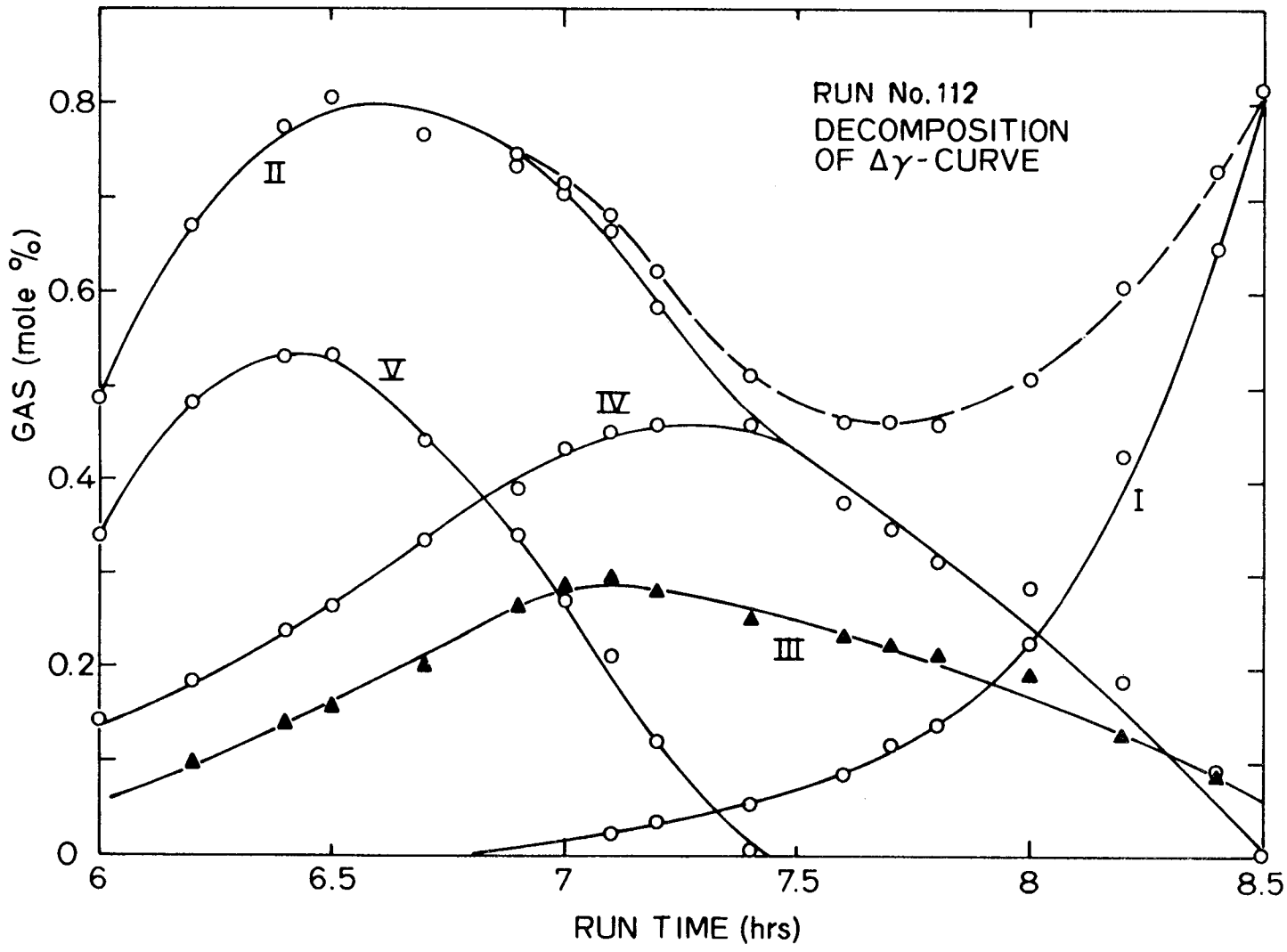

Fig. 8.20: DECOMPOSITION OF GASES PRODUCED IN RUN NO. 112

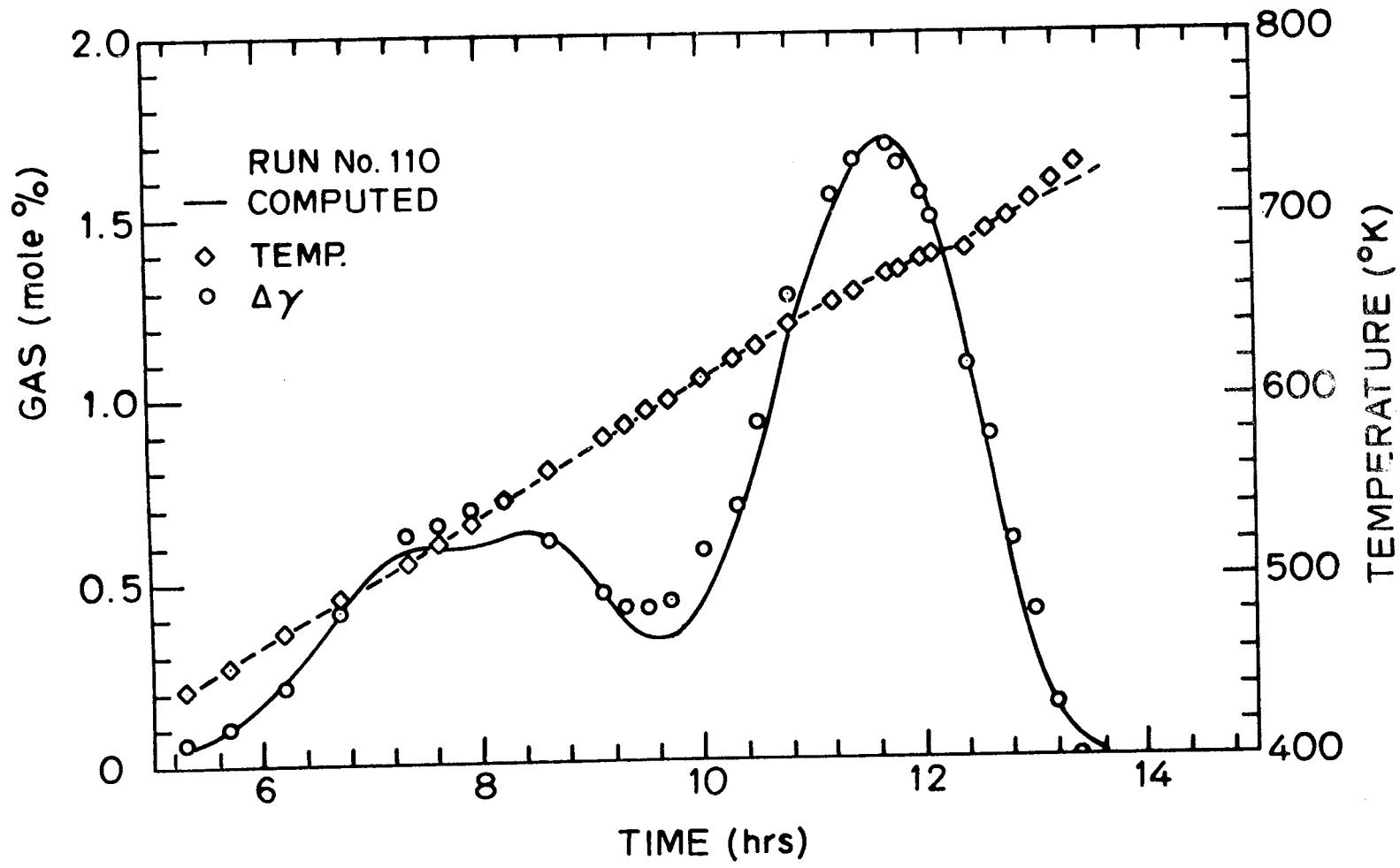

Fig. 8.21: MATCH BETWEEN EXPERIMENTAL DATA AND THE PROPOSED KINETIC MODEL (RUN NO. 110)

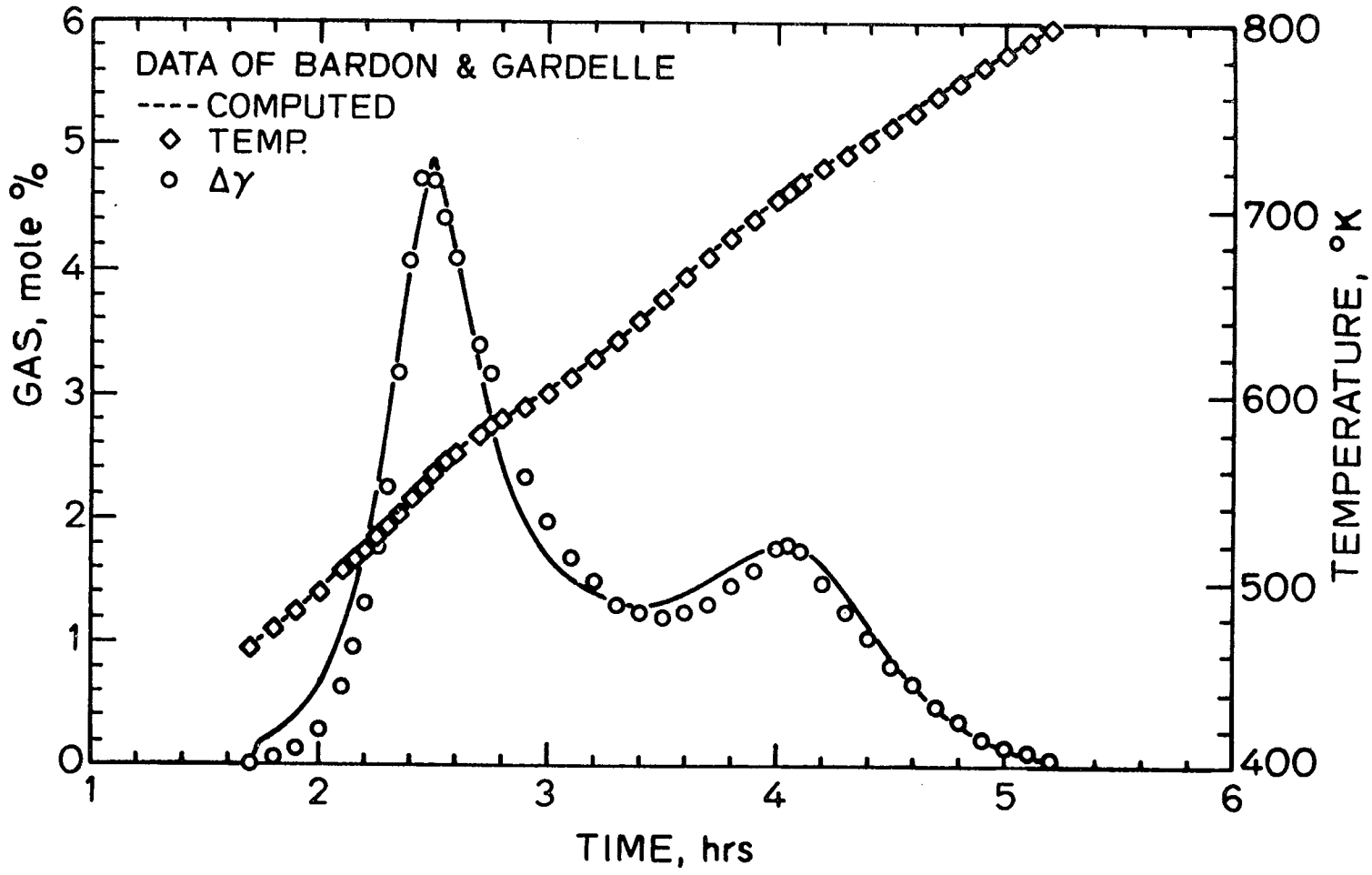

Fig. 8.22: MATCH BETWEEN EXPERIMENTAL DATA AND THE KINETIC MODEL (FRENCH OIL)

curve would deviate from the straight line (Appendix C). Thus, in some runs, using the same fuel, but at different partial pressure of oxygen, the calculated activation energies were not the same (Table 8.2). This in turn led to the evaluation of a wrong intercept. Therefore, to normalize the data, first, the activation energies which were quite different from the average value, were discarded. Then, using the average value of the calculated activation energies, straight lines of the same slope were drawn through the experimental data points on the Arrhenius plot (Fig. 8.23). This was achieved by selecting an arbitrary data point at the mid-range of the abscissa as the focal point. For a combination reaction (Fig. 8.23), this point was 1.5×10^{-3} °K^{-1}. The corresponding points for fuel deposition (Fig. 8.24) and LTO reaction (Fig. 8.25) were 1.8×10^{-3} and 1.93×10^{-3} °K^{-1}, respectively. The relative reaction rates evaluated at the focal points for the above three reactions are shown in column 5 of Tables 8.2-8.4. Finally, the true intercept at each pressure was computed (column 6 of Tables 8.2-8.4).

8.7 Evaluation of Arrhenius Constant

Appendix C shows that by plotting the true intercept (i.e., $A_r p_{O_2}{}^m$) with respect to partial pressure of oxygen (i.e., p_{O_2}), we can evaluate both the Arrhenius constant, A_r, and the reaction order with respect to oxygen partial pressure, m. Figures 8.26-8.28 illustrate this method for all three reactions. The final reaction rate equations are shown on Tables 8.2-8.4.

Following the same procedure, the reaction kinetic parameters were evaluated for other crude oils used in the experiments. For these crude

Table 8.2: FUEL COMBUSTION REACTION RATE*
(Huntington Beach Crude Oil)

Run No.	$A_r p_{O_2}^m$ 1/s x 10^{-6}	E/R ^oK x 10^{-4}	p_{O_2} kPa	RRR(1.5×10^{-3}) 1/s x 10^{+4}	True Intercept 1/s x 10^{-6}
110	13.30	1.628	54.2	3.45	12.336
117	23.88	1.616	238.7	7.00	25.030
118	7.912	1.611	50.3	2.5	8.940
119	21.07	1.643	137.0	4.1	14.660
120	25.97	1.627	253.0	6.4	22.884
121	18.29	1.628	166.2	4.5	16.090
122	4.03	1.619	19.9	1.15	4.112
124	7.585	1.602	70.5	2.72	9.726
128	4.858	1.608	30.0	1.60	5.721
Average:		1.620			

* $R_c = 6 \times 10^5 \exp(-135{,}000/RT)\, p_{O_2}^{0.66}\, C_f$

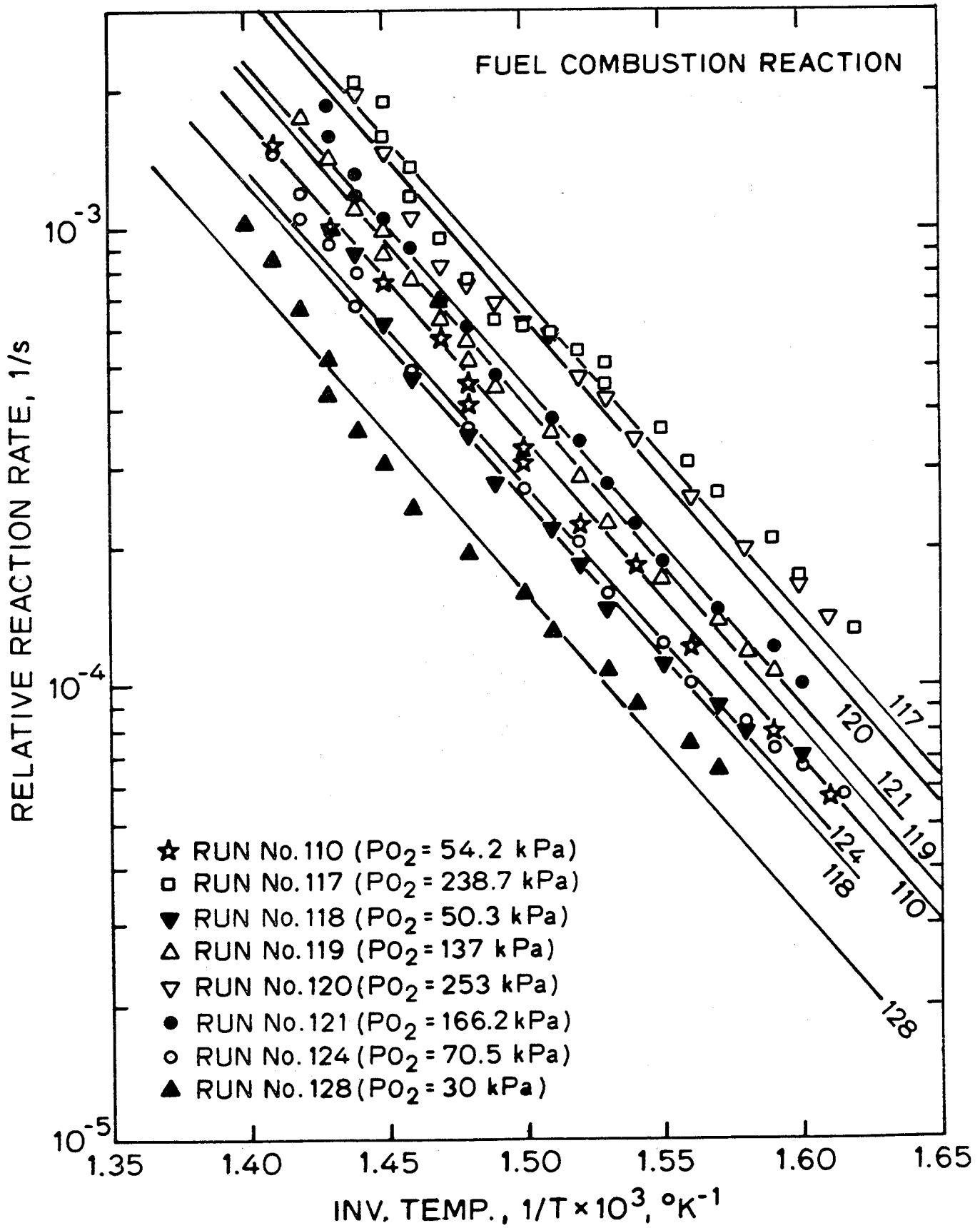

Fig. 8.23: ARRHENIUS PLOT FOR FUEL COMBUSTION REACTION (HUNTINGTON BEACH OIL)

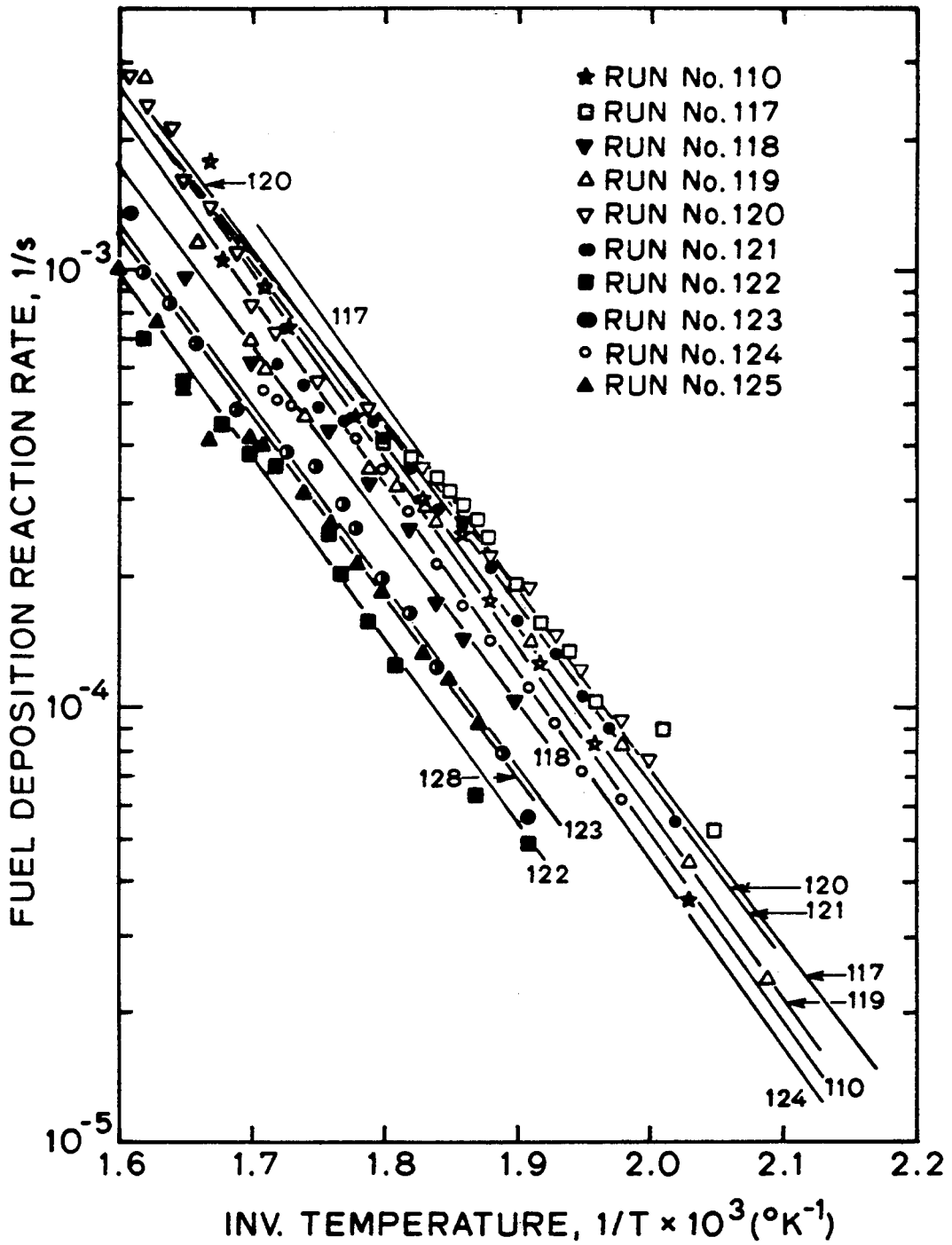

Fig. 8.24: ARRHENIUS PLOT FOR FUEL DEPOSITION REACTION (HUNTINGTON BEACH OIL)

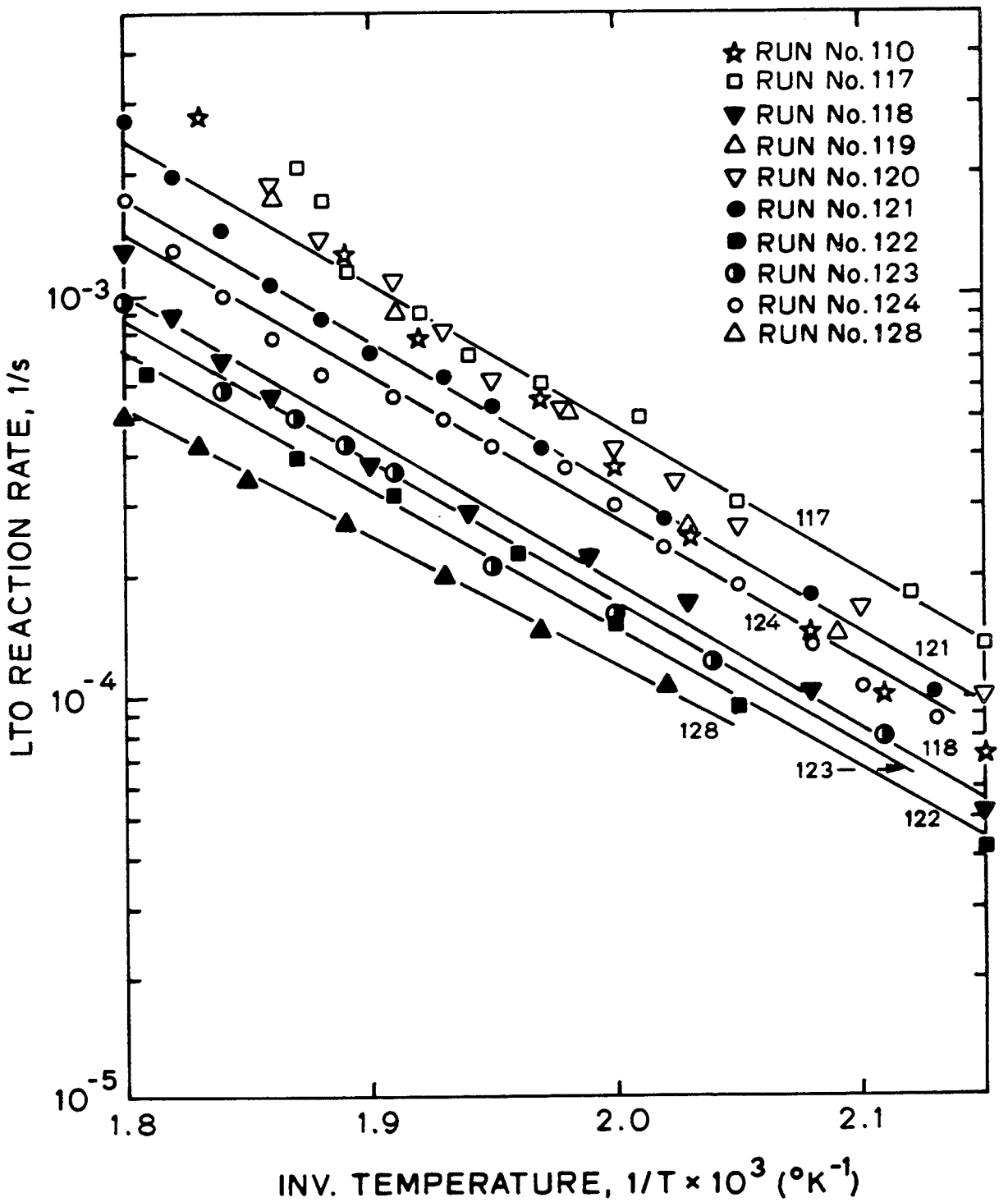

Fig. 8.25: ARRHENIUS PLOT FOR LTO REACTION (HUNTINGTON BEACH OIL)

Table 8.3: FUEL DEPOSITION REACTION RATE*
(Huntington Beach Crude Oil)

Run No.	$A_r p_{O_2}^m$ 1/s x 10^{-3}	E/R °K x 10^{-3}	p_{O_2} kPa	RRR(1.8×10^{-3}) 1/s x 10^{+4}	True Intercept 1/s x 10^{-3}
110	31.480	10.120	54.2	3.62	10.593**
117	11.630	9.430	238.7	5.00	14.631
118	5.664	9.372	50.3	2.60	7.608
119	21.8	9.857	137	4.3	12.582
120	2.981	8.743	253	4.4	12.87
121	5.63	9.128	166.2	4.2	12.29
122	5.928	9.746	19.9	1.42	4.155
123	6.79	9.675	24.6	1.88	5.501
124	18.040	9.901	70.5	3.2	9.364
128	5.05	9.535	30	1.78	5.208
Average:		9.551			

* $R_f = 1.2 \times 10^3 \exp(-80{,}000/RT)\, p_{O_2}^{0.46}\, C_f$

** This was not included in the curve fit

Table 8.4: LOW-TEMPERATURE OXIDATION RATE*
(Huntington Beach Crude Oil)

Run No.	$A_r p_{O_2}^m$ 1/s x 10^{-3}	E/R ^oK x 10^{-3}	p_{O_2} kPa	RRR(1.95×10^{-3}) 1/s x 10^{+4}	True Intercept 1/s x 10^{-3}
110	1896.	11.15	54.2**	--	--
117	5.915	8.176	238.7	7.	4.678
118	3.851	8.403	50.3	1.85	1.236
119	22.62	8.945	137.**	--	--
120	117.3	9.716	253.**	--	--
121	4.385	8.198	166.2	5.	3.342
122	1.170	7.948	19.9	2.2	1.470
123	1.978	8.135	24.6	1.55	1.036
124	3.445	8.172	70.5	4.1	2.740
128	0.31	7.38	30.0	1.73	1.156
Average:		8.059			

* $R = 1.9 \times 10^2 \exp(^{-67,000/RT}) \, p_{O_2}^{0.57} \, C_f$

** This was not included in the curve fit

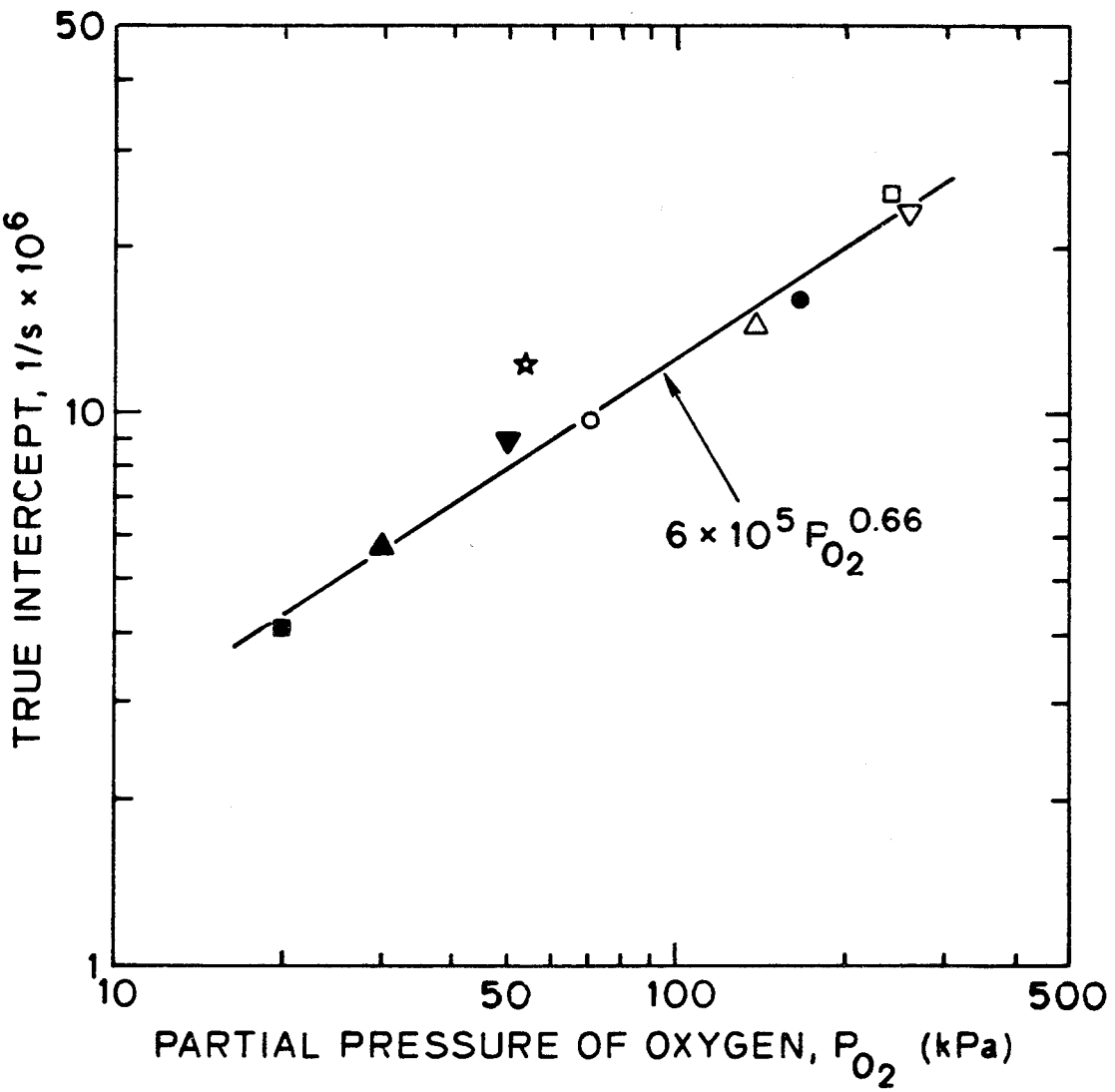

Fig. 8.26: PLOT OF INTERCEPT VS PRESSURE FOR COMBUSTION REACTION (HUNTINGTON BEACH OIL)

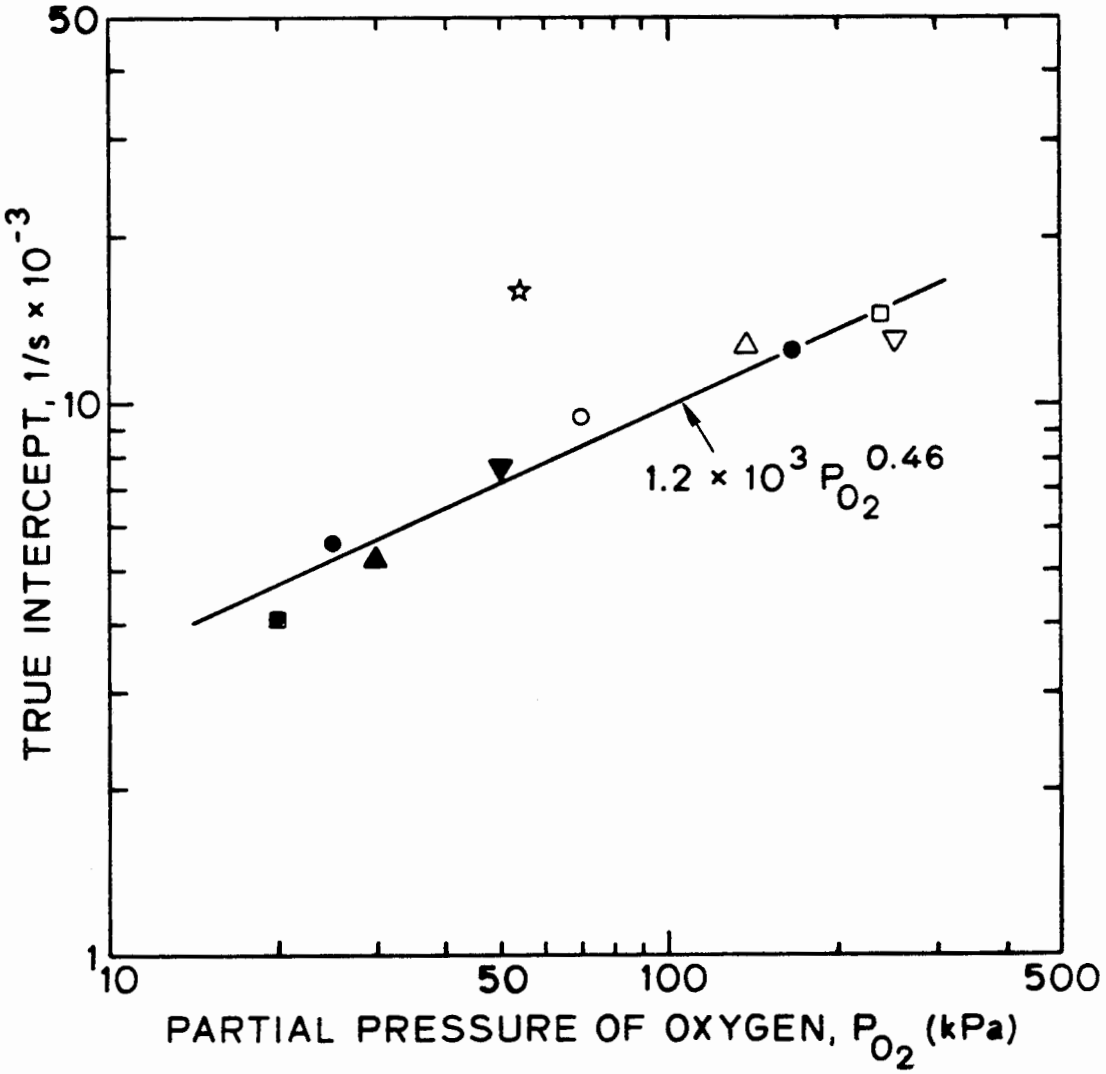

Fig. 8.27: PLOT OF INTERCEPT VS PRESSURE FOR FUEL DEPOSITION REACTION (HUNTINGTON BEACH OIL)

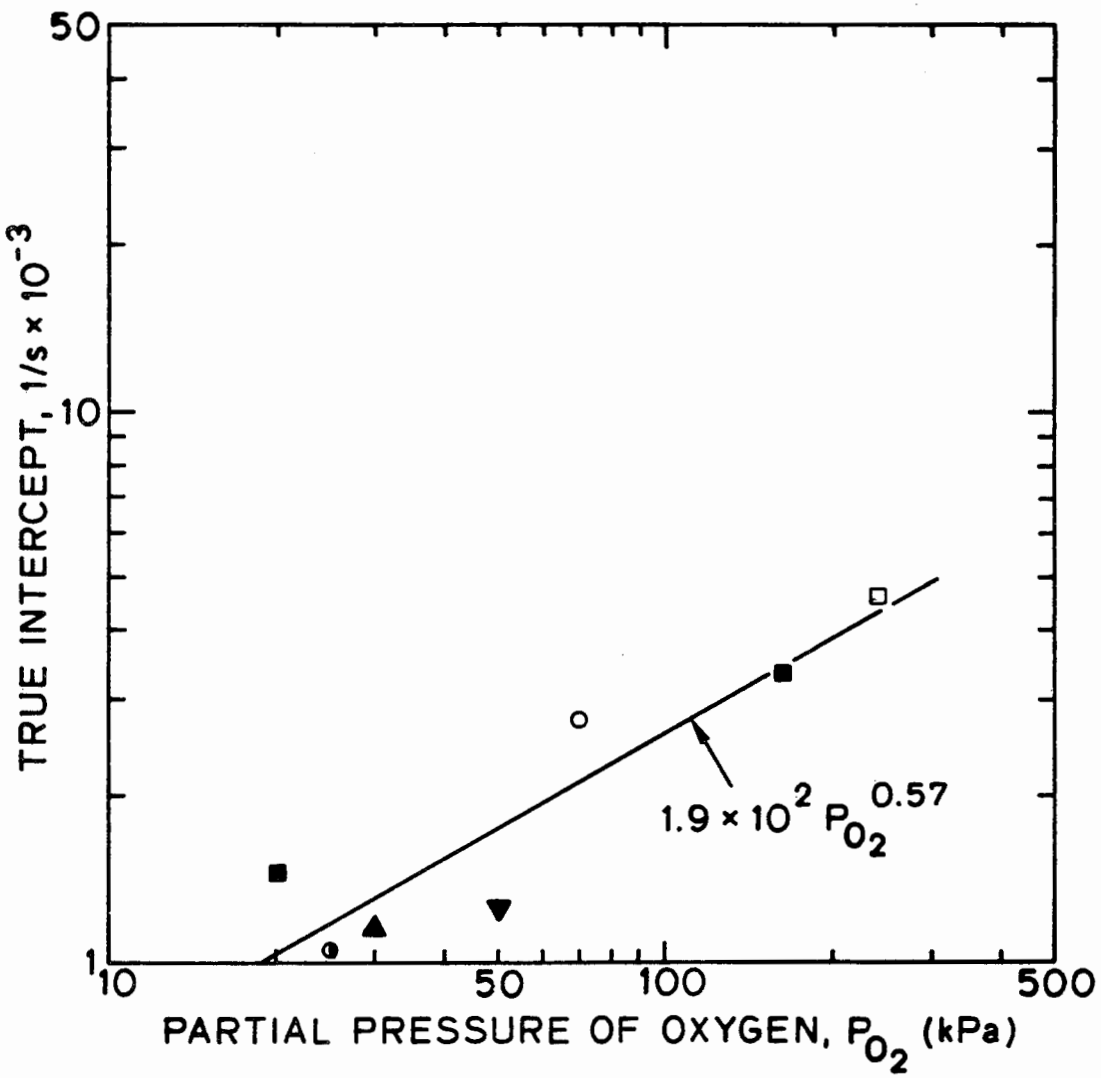

Fig. 8.28: PLOT OF INTERCEPT VS PRESSURE FOR LTO REACTION (HUNTINGTON BEACH OIL)

oils, only two runs were conducted. Figures 8.29-8.31 show the straight lines obtained for different reactions using San Ardo and Venezuelan oils. The true intercepts of these lines are plotted on Figs. 8.32-8.33. The entire suite of kinetic data for these crude oils are given on Tables 8.5-8.6. The results show the applicability of the proposed model in evaluation of kinetic parameters for oxidation of crude oil in porous medium.

8.8 Diffusion Effects

As was stated in the introduction, the first step in the reaction mechanism of crude oil oxidation in a porous medium is the diffusion of oxygen from the bulk gas stream to the fuel on the rock. Using correlations for prediction of the diffusion rate, it was found that the chemical reaction step is much slower than the diffusion step (Appendix F). Therefore, the overall rate appears to be kinetically controlled. Later, this notion was substantiated experimentally when a two-fold increase in the air flow rate did not cause any change in reaction constants.

8.9 Effect of Lithology on the Reactions

Investigators have reported the effects of clay content, metallic additives, and surface area of the rock on fuel deposition. Some experiments were run using either the original core or a mixture of sand and clay to study these effects quantitatively. The results of these experiments along with those of Bardon and Gadelle (1977) who also studied the effect of metallic additives on these reactions are reported here.

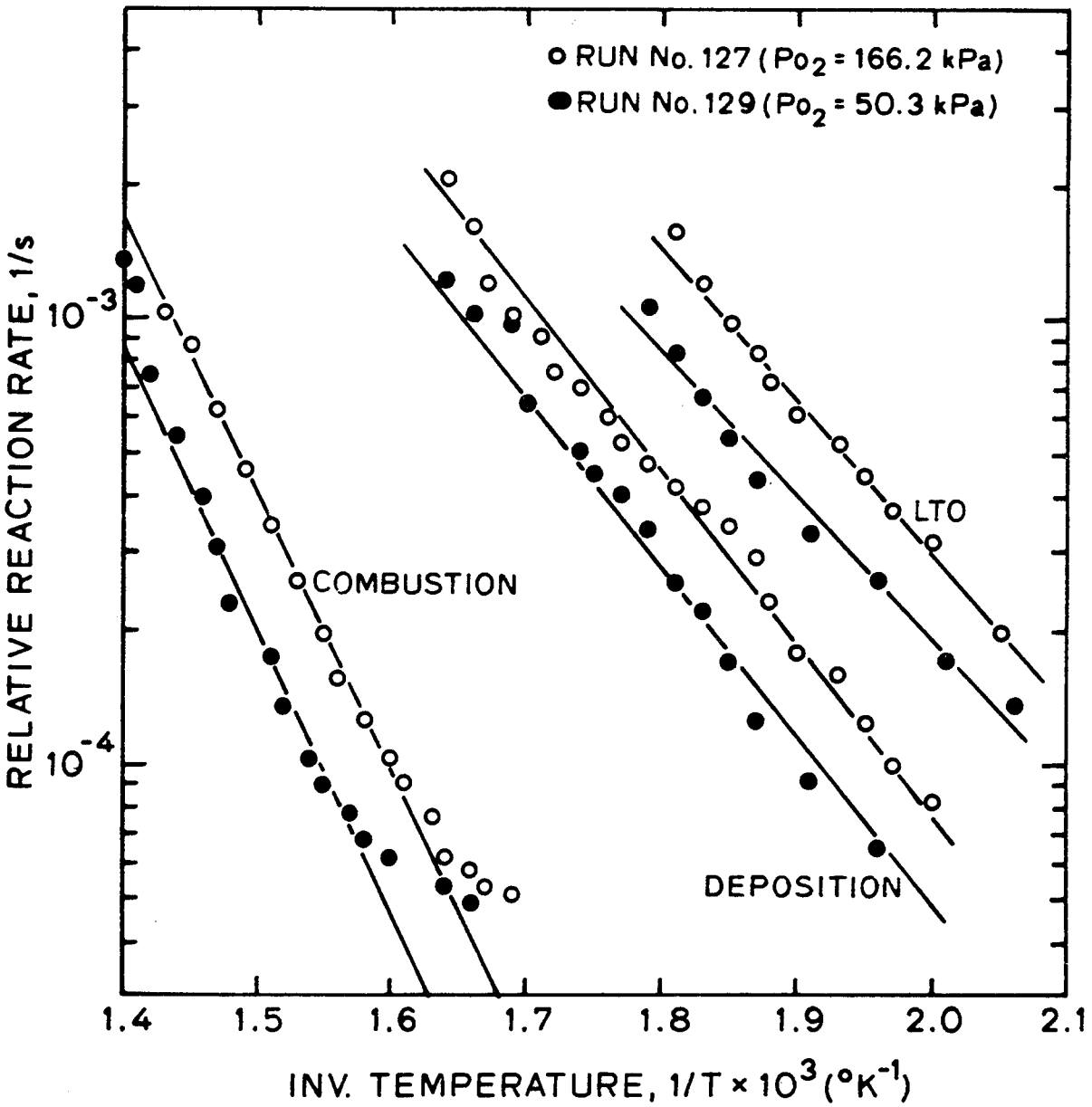

Fig. 8.29: ARRHENIUS PLOT FOR DIFFERENT REACTIONS (SAN ARDO OIL)

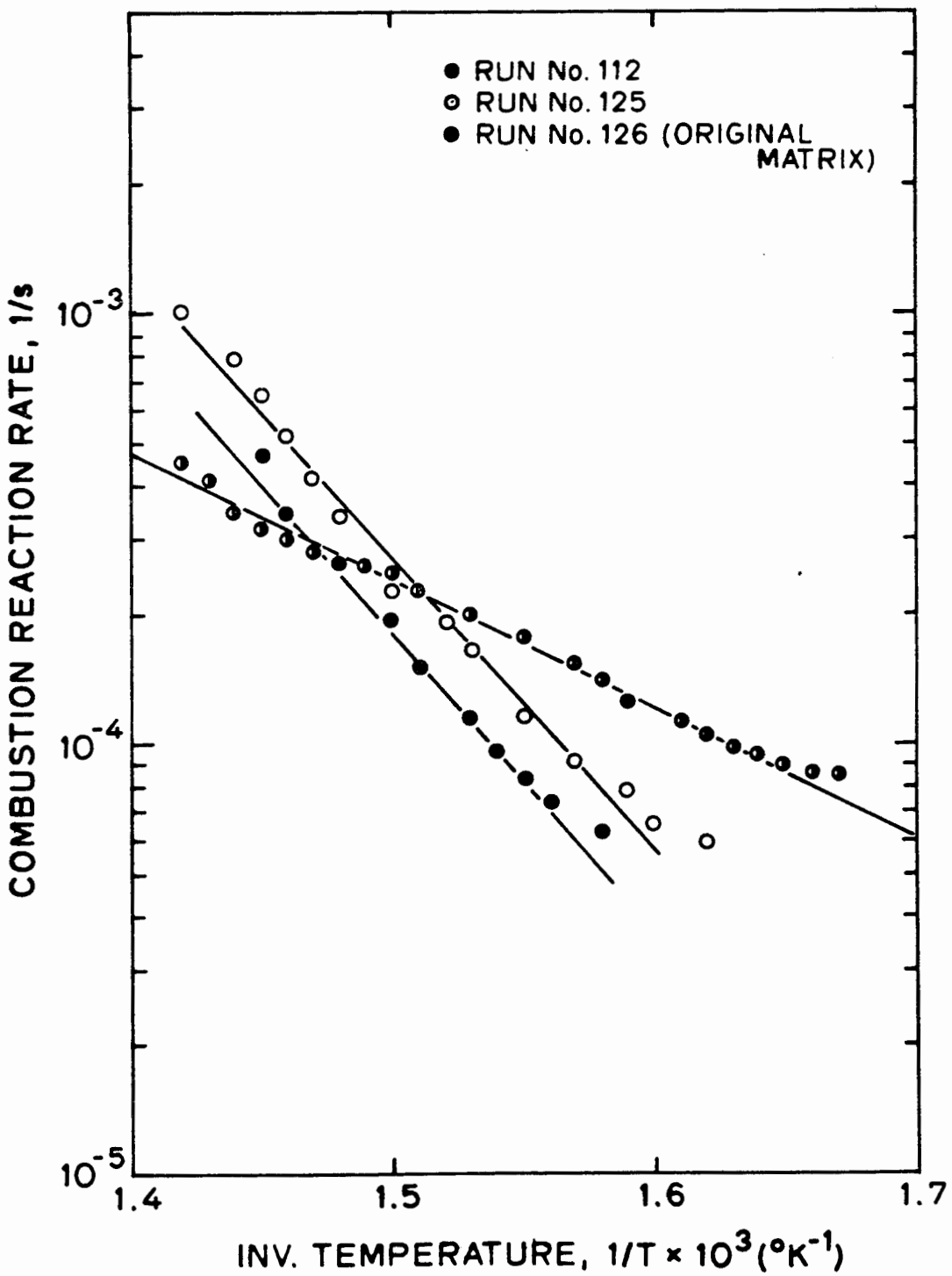

Fig. 8.30: ARRHENIUS PLOT FOR COMBUSTION REACTION (VENEZUELAN OIL)

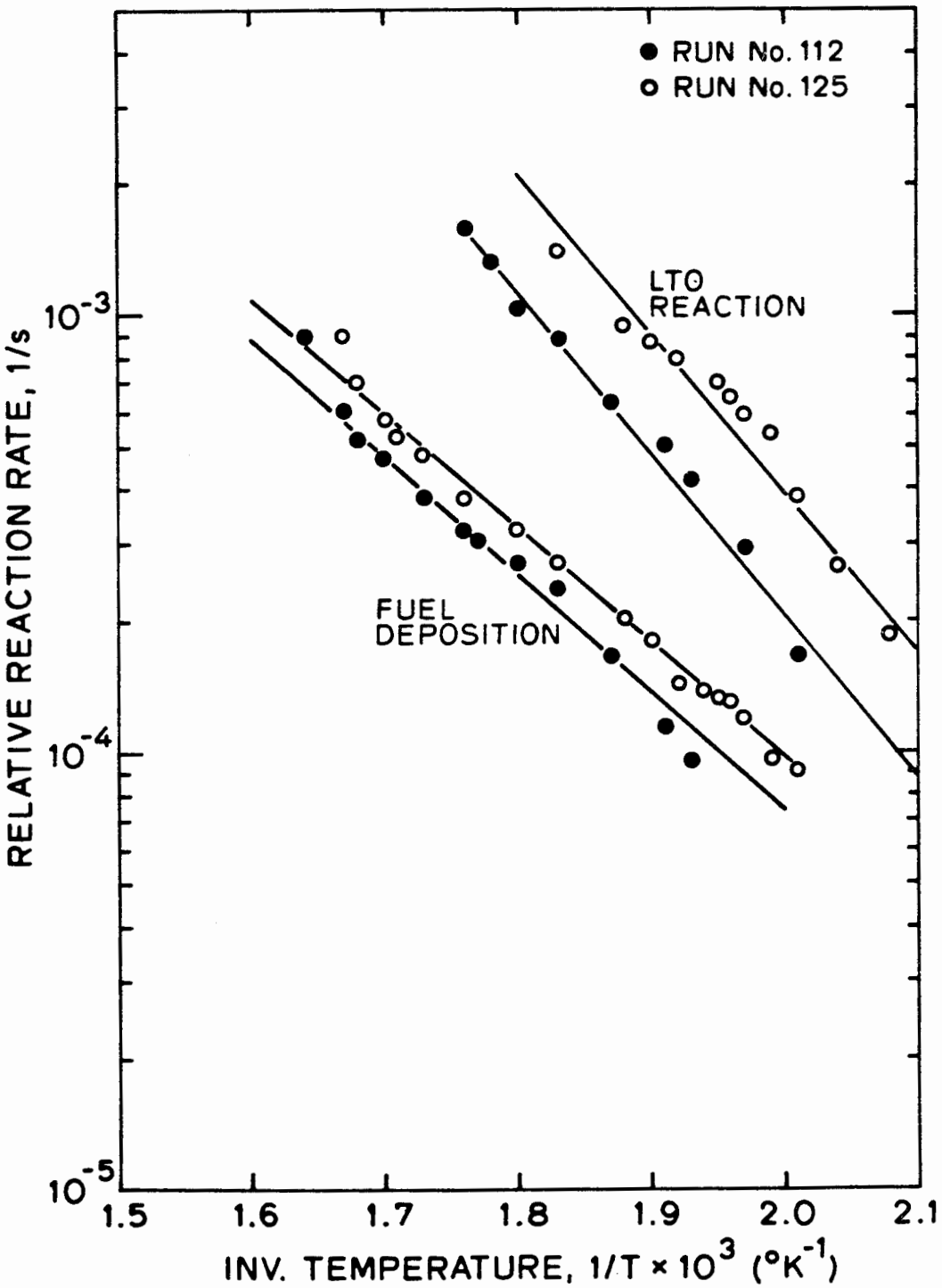

Fig. 8.31: ARRHENIUS PLOT FOR DIFFERENT REACTIONS (VENEZUELAN OIL)

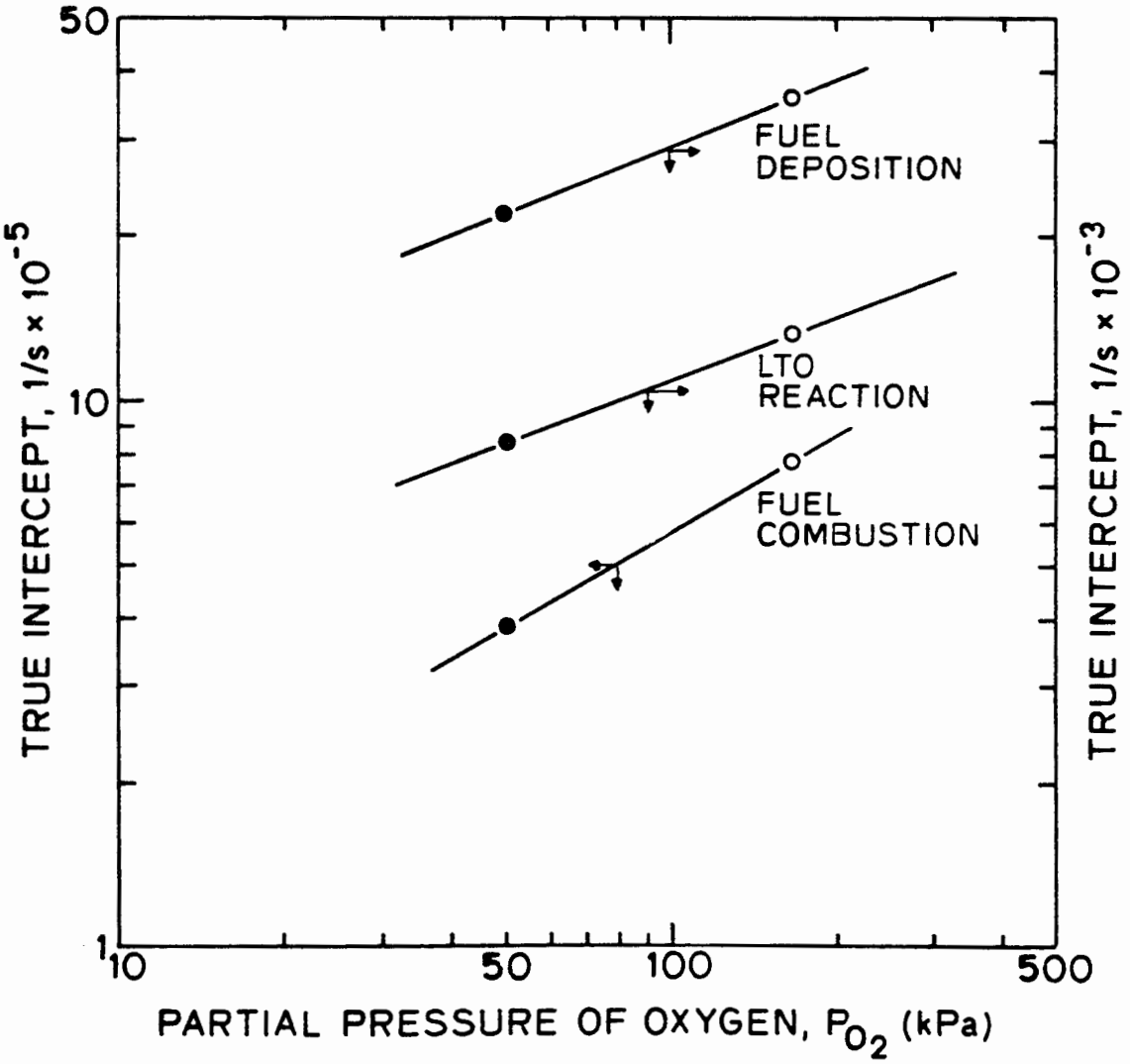

Fig. 8.32: PLOT OF INTERCEPT VS PRESSURE (SAN ARDO OIL)

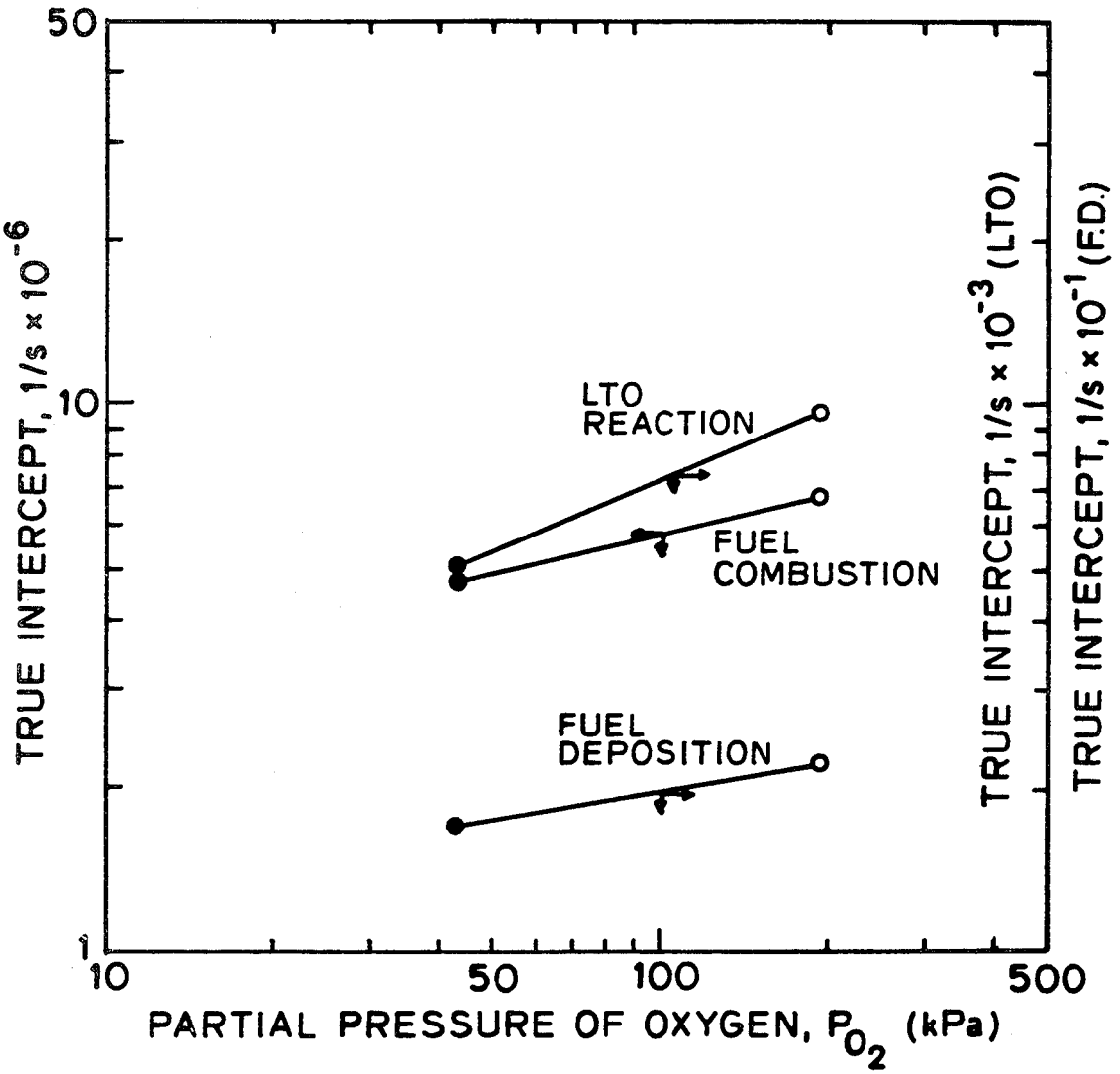

Fig. 8.33: PLOT OF INTERCEPT VS PRESSURE (VENEZUELAN OIL)

Table 8.5: KINETIC DATA FOR SAN ARDO CRUDE OIL

1. Fuel Combustion Rate*

Run No.	$A_r p_{O_2}^m$ 1/s x 10^{-5}	E/R °K x 10^{-4}	p_{O_2} kPa	RRR(1.5×10^{-3}) 1/s x 10^4	True Intercept 1/s x 10^{-5}
127	6.705	1.416	166.2	4	7.675
129	4.495	1.433	50.3	2	3.838
Average:		1.425			

* $R_c = 4 \times 10^4 \exp(-120{,}000/RT)\ P_{O_2}^{0.58}\ C_f$

2. Fuel Deposition Rate**

Run No.	$A_r p_{O_2}^m$ 1/s x 10^{-3}	E/R °K x 10^{-3}	p_{O_2} kPa	RRR(1.8×10^{-3}) 1/s x 10^4	True Intercept 1/s x 10^{-3}
127	3.965	8.884	166.2	4.5	3.564
129	1.975	8.766	50.3	2.75	2.178
Average:		8.825			

** $R_f = 4.5 \times 10^2 \exp(-74{,}000/RT)\ P_{O_2}^{0.4} C_f$

3. Low-Temperature Oxidation Rate***

Run No.	$A_r p_{O_2}^m$ 1/s x 10^{-3}	E/R °K x 10^{-3}	p_{O_2} kPa	RRR(1.95×10^{-3}) 1/s x 10^{+4}	True Intercept 1/s x 10^{-2}
127	1.964	7.847	166.2	4.4	13.19
129	0.563	7.450	50.3	2.8	8.39
Average:		7.648			

*** $R = 1.9 \times 10^2 \exp(-64{,}000/RT)\ P_{O_2}^{0.4} C_f$

Table 8.6: KINETIC DATA FOR VENEZUELAN OIL

1. Fuel Combustion Rate*

Run No.	$A_r p_{O_2}^m$ 1/s x 10^{-6}	E/R °K x 10^{-4}	p_{O_2} kPa
112*	4.72	1.597	43
125*	6.674	1.597	195
126	7.326×10^{-6}	0.687	166

* $R_c = 2 \times 10^6 \exp(-133{,}000/RT)\ p_{O_2}^{0.23}\ C_f$

2. Fuel Deposition Rate**

Run No.	$A_r p_{O_2}^m$ 1/s x 10^{-1}	E/R °K x 10^{-3}	p_{O_2} kPa	RRR(1.8×10^{-3}) 1/s x 10^{+4}	True Intercept 1/s x 10^{-1}
112**	2.102	6.288	43	2.52	1.69
125**	1.747	6.060	195	3.28	2.20
126+	$2.848 \times 10^{+5}$	9.73	166	--	--
Average:		6.174			

** $R_f = 8.8 \exp(-51{,}000/RT)\ p_{O_2}^{0.18}\ C_f$

3. Low Temperature Oxidation Rate***

Run No.	$A_r p_{O_2}^m$ 1/s x 10^{-3}	E/R °K x 10^{-3}	p_{O_2} kPa	RRR(1.95×10^{-3}) 1/s x 10^{+4}	True Intercept 1/s x 10^{-3}
112	5.942	8.594	43	3.12	5.034
125	8.343	8.429	195	5.9	9.519
126+	1.929×10^3	1.067×10^1	166	--	--
Average:		8.511			

*** $R = 1. \times 10^3 \exp(-70{,}000/RT)\ p_{O_2}^{0.42}\ C_f$

\+ This was not included in the curve fit

8.9-1 Effect of Matrix

Some experiments were run using the oil in the original core. These cores were obtained from the Jobo field in Venezuela and from Lynch Canyon field in California (Figs. 8.34 and 8.35). The corresponding graphs showing the molar CO_2/CO ratio and apparent H/C ratio for these runs are shown in Figs. 8.36 and 8.37. The CO_2/CO ratio was higher for these runs than for the runs using the sand mix.

The reaction rates were calculated using the kinetic model previously mentioned. The Arrhenius plots for these runs are shown in Figs. 8.38 and 8.39. (The combustion reaction rate of Venezuelan oil was graphed on Fig. 8.24 for comparison.) Table 8.6 and 8.7 present the calculated kinetic constants for these reactions.

Figure 8.24 clearly shows that the activation energy for combustion reaction in the original core is much lower than in the sand mix. The sieve analysis for these matrices confirmed that the sand grains were much finer than the sand mix used in the runs. There were even some silts in these cores.

Bardon and Gadelle (1977) investigated the effects of matrix on the oxidation reactions of a French oil. The properties of this oil along with the matrix and pack conditions are shown in Tables 8.8-8.9. In their first kinetic experiment (Run No. 1), they used a sand mix of varying grain size while a finer sand was used in their second run (Table 8.9). They also conducted an experiment using the original core (Run No. 4). Their data were analyzed using the proposed kinetic model and the resulting Arrhenius graphs are presented in Figs. 8.40-8.42.

As is shown, the increase in the surface area (finer sand) resulted in a smaller Arrhenius constant for both fuel deposition and fuel

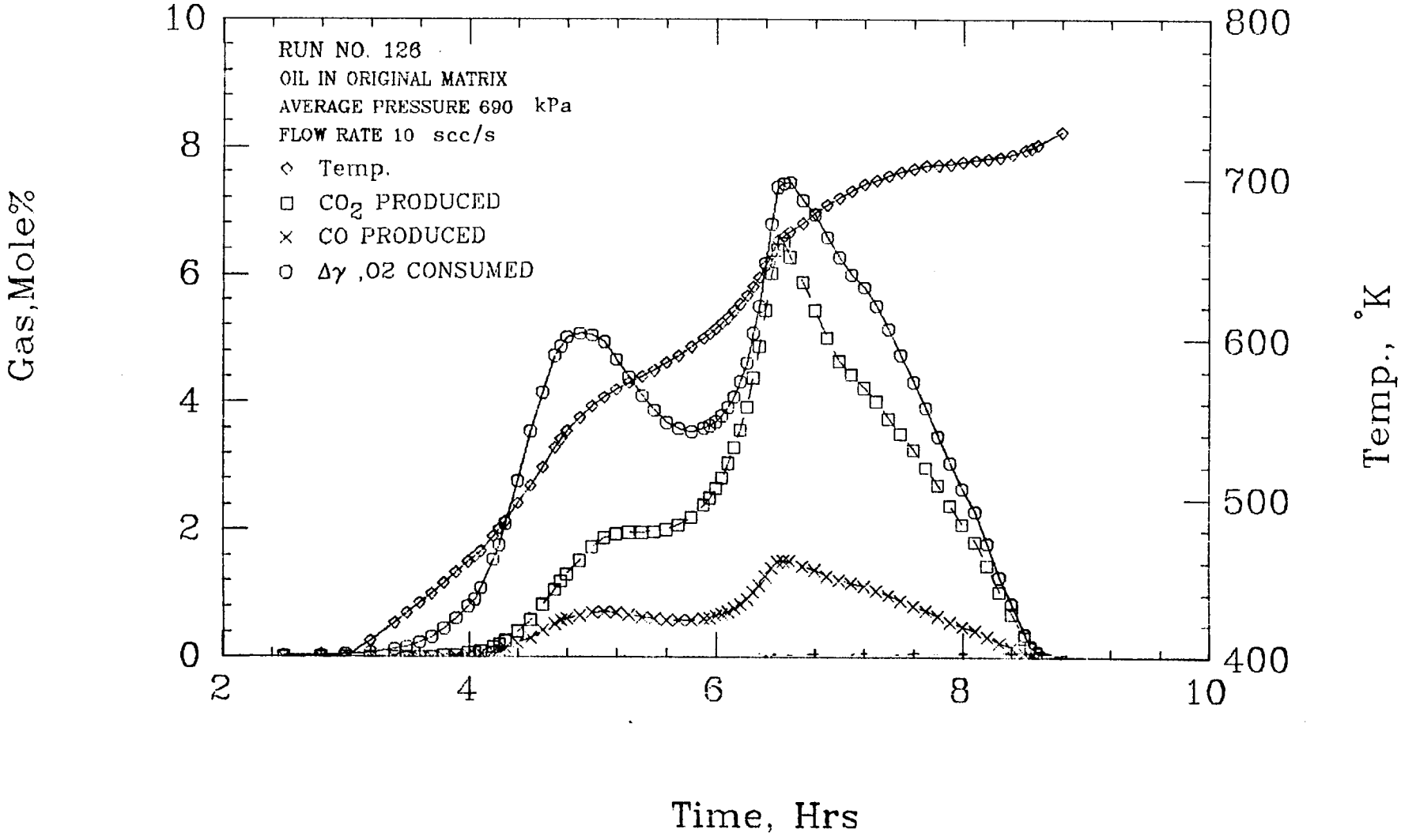

Fig. 8.34: GAS COMPOSITION AND TEMPERATURE VS TIME FOR VENEZUELAN OIL IN ORIGINAL CORE

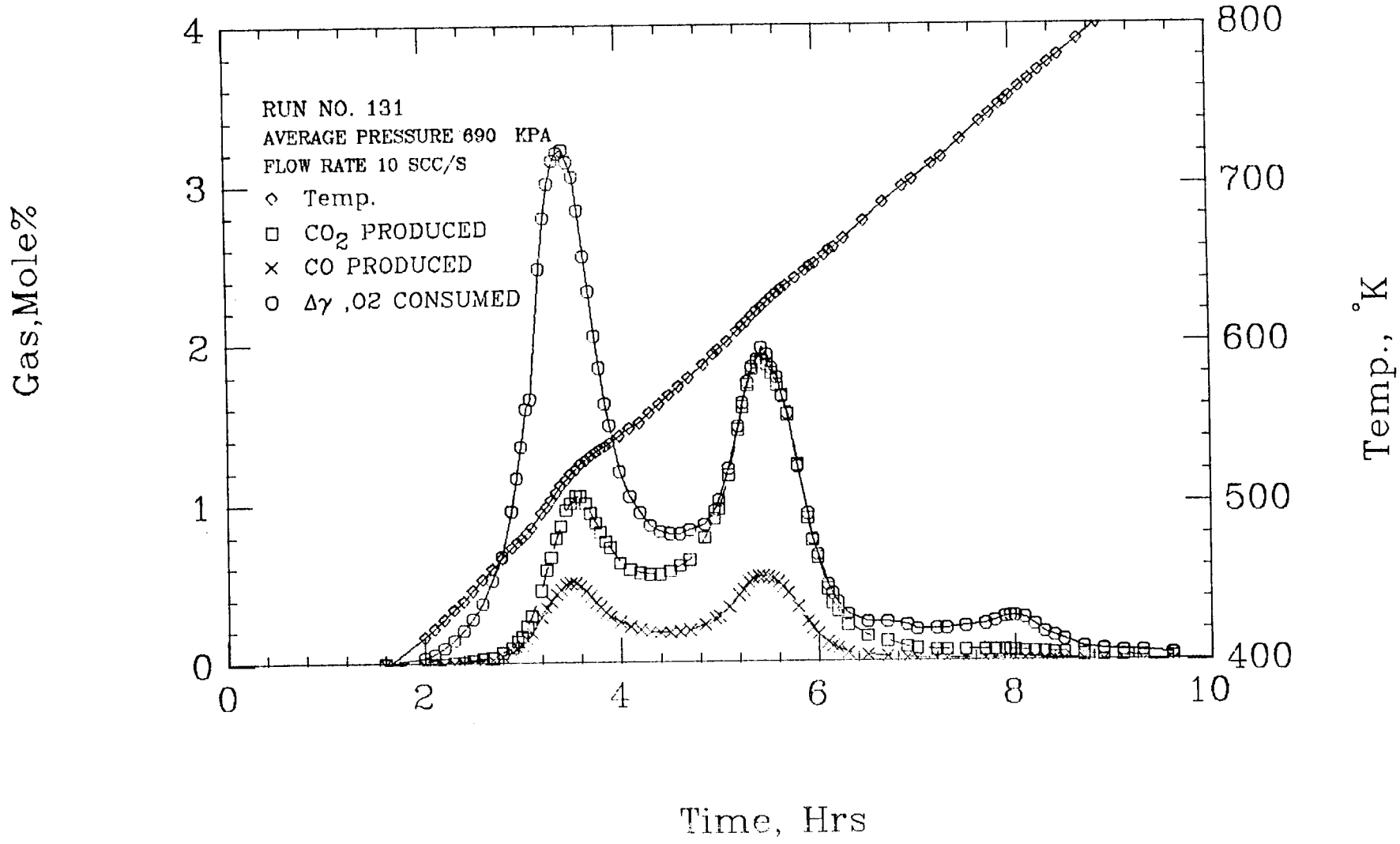

Fig. 8.35: GAS COMPOSITION AND TEMPERATURE VS TIME FOR LYNCH CANYON OIL IN ORIGINAL CORE

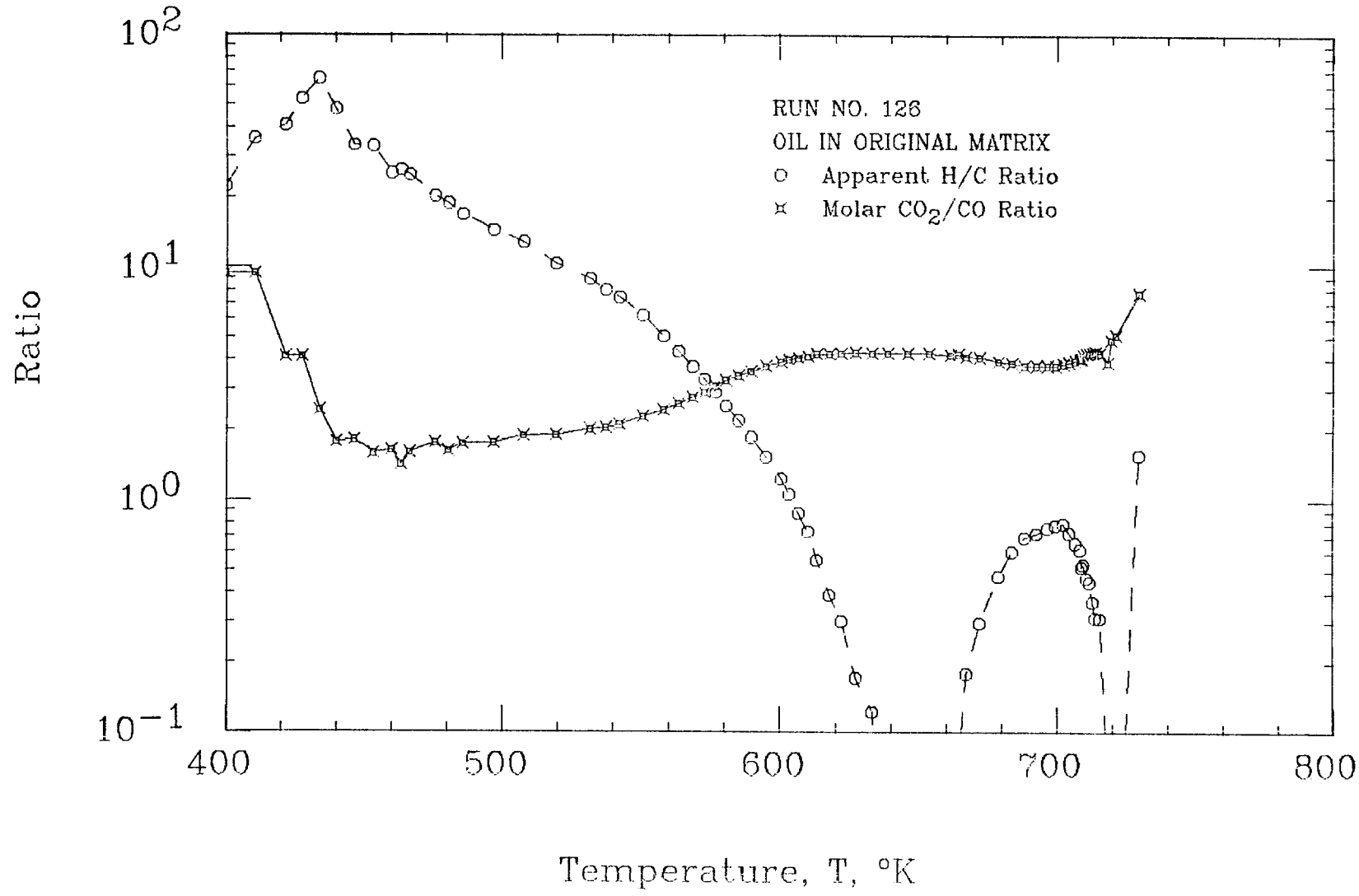

Fig. 8.36: MOLAR CO_2/CO RATIO AND APPARENT H/C RATIO VS TEMPERATURE FOR VENEZUELAN OIL IN ORIGINAL CORE

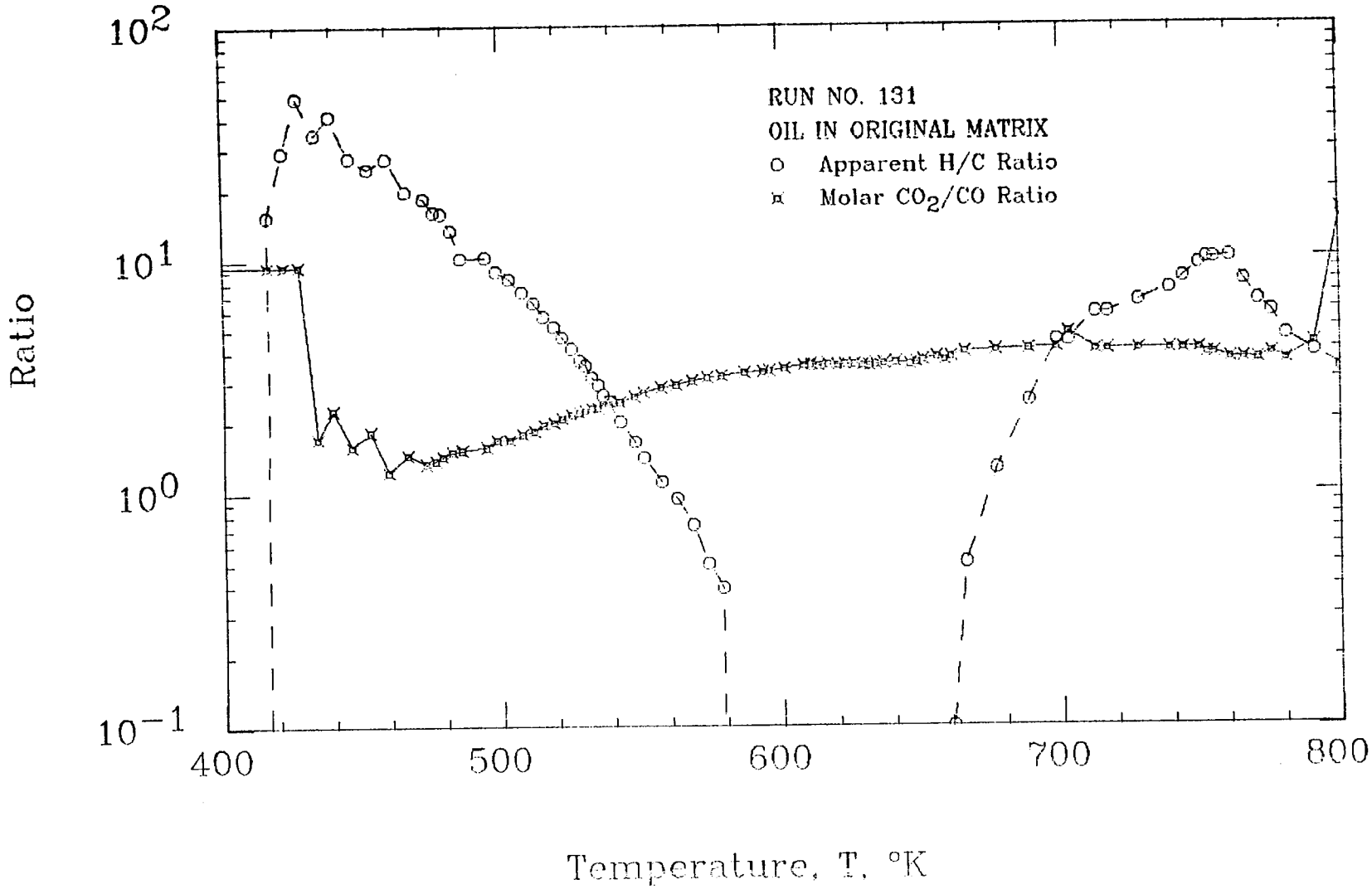

Fig. 8.37: MOLAR CO_2/CO RATIO AND APPARENT H/C RATIO VS TEMPERATURE FOR LYNCH CANYON OIL IN ORIGINAL CORE

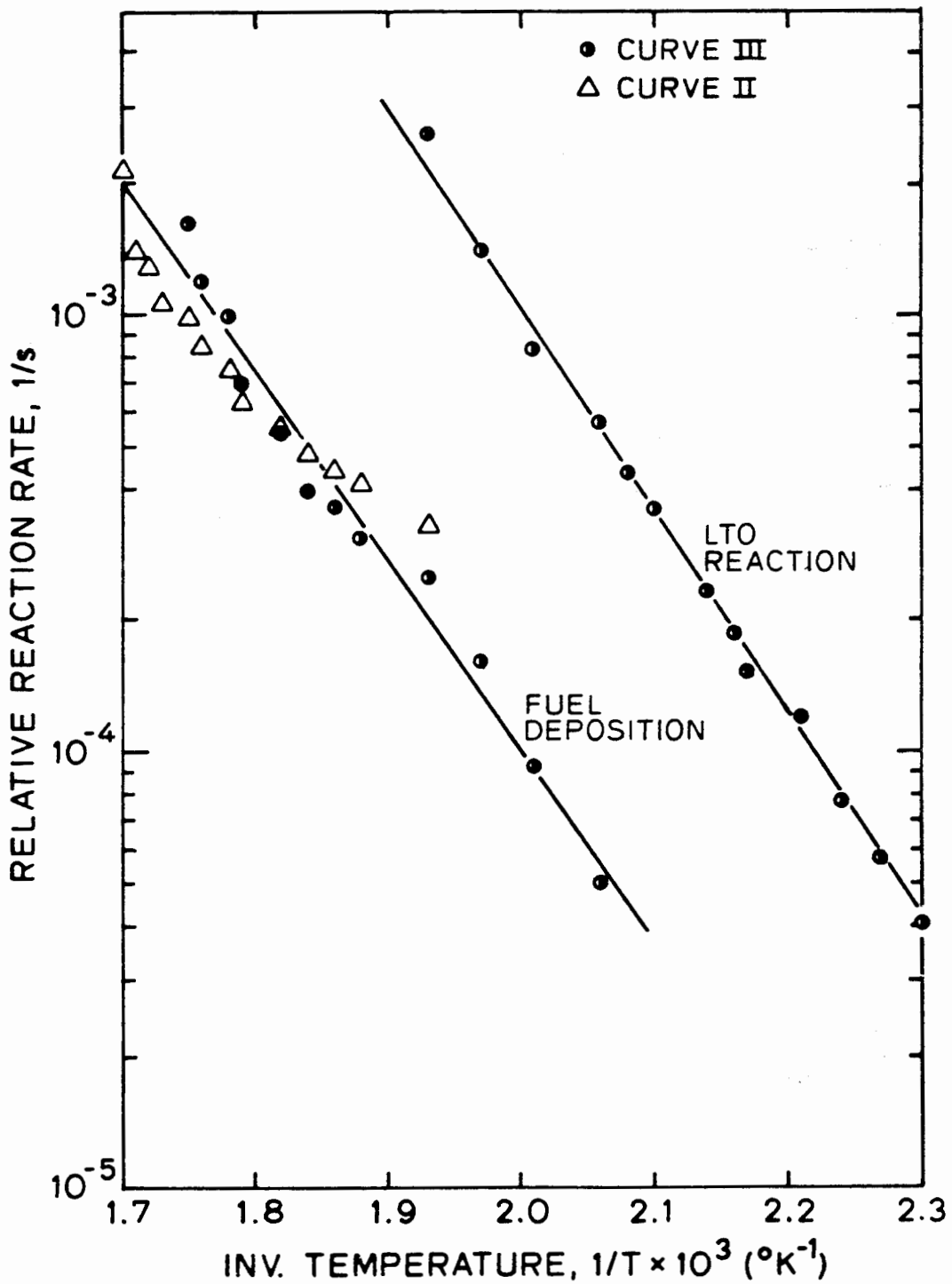

Fig. 8.38: ARRHENIUS PLOT FOR RUN NO. 126 (ORIGINAL CORE)

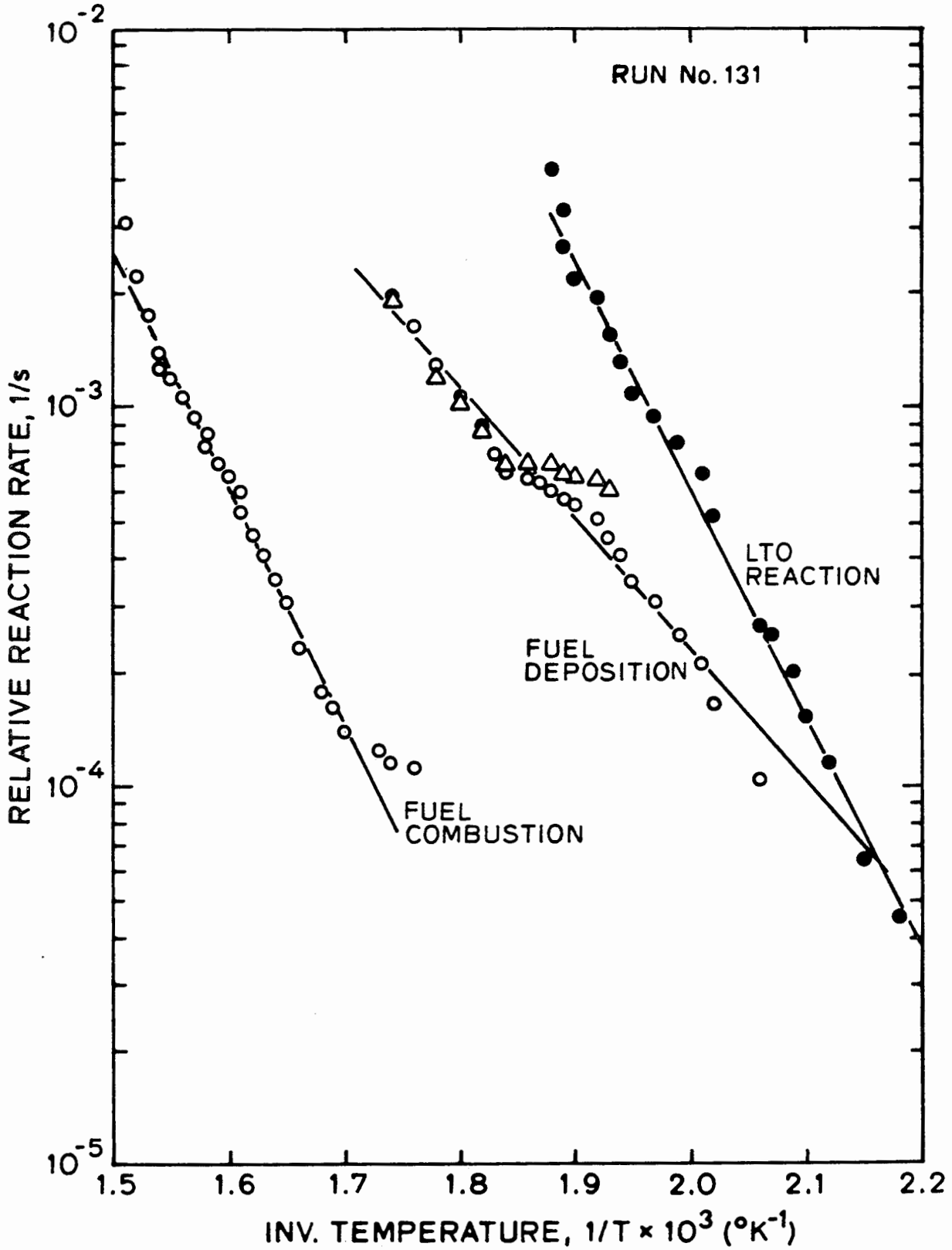

Fig. 8.39: ARRHENIUS PLOT FOR LYNCH CANYON OIL

Table 8.7

KINETIC DATA FOR LYNCH CANYON OIL (Run No. 131)

	FUEL COMBUSTION	FUEL DEPOSITION	LTO REACTION
Intercept, 1/s	7.785×10^6	1.984×10^3	6.808×10^8
E, J/gmole	1.209×10^5	6.645×10^4	1.153×10^5

Table 8.8

THE PROPERTIES OF THE FRENCH CRUDE OIL
USED BY BARDON AND GADELLE (1977)

Density	:	0.891 g/cm^3 (27° API)
Viscosity	:	80 - 100 c.p.
Chemical nature	:	51% saturated hydrocarbons
		32% aromatics
		17% heavy compounds { 16.5% resins, 0.5% asphaltenes }
Distillation Curve	:	< 215°C 7.7% (wt)
		215 - 360°C 24.7
		260 - 400°C 6.5
		> 400°C 61.1

Table 8-9

INITIAL PACK CONDITIONS FOR RUNS CONDUCTED BY BARDON AND GADELLE (1977)

Oil Content	3.5% by wt. (4.75% in Run No. 2)
Sand Type	Ottawa
Air Flux	40 m^3/m^2-hr
Pressure	550 kPa.
Heating Rate	100°C/hr

Sieve Analysis of the Pack

GRAIN SIZE DISTRIBUTION	SAND MIX	ORIGINAL MATRIX	SILICA
	RUN NO. 1	RUN NO. 4	RUN NO. 2
< 125μ	0.7	1.6	
125 - 160μ	10.1	13.8	
160 - 200μ	21.6	12.9	
200 - 250μ	33.0	20.1	
250 - 315μ	23.9	15.8	
315 - 400μ	8.9	29.9	100
> 400μ	1.8	5.9	
Kaolinite		4 - 5%	

Note: In Run No. 3 the grain size was the same as in Run No. 1

Table 8.10: ANALYSIS OF DATA OF BARDON AND GADELLE

1. Combustion Reaction*

Bed	Intercept, 1/s	E/R $^{o}K \times 10^{-4}$	n
Sand Mix*	6.25×10^{3}	1.264	1.2
Silica*	1.241×10^{4}	1.277	1.2
Original Matrix	2.287×10^{1}	0.844	1.2
Sand Mix + 2000 PPm Cu	2.8481×10^{-1}	0.486	1.2

* $R_c = ArP_{O_2}^{m} \exp(-105{,}000/RT)\ C_f^{1.2}$

2. Fuel Deposition Reaction**

Bed	Intercept, 1/s	E/R $^{o}K \times 10^{-3}$	n
Sand Mix**	3.56×10^{1}	7.546	1.2
Silica**	8.896×10^{1}	7.712	1.2
Original Matrix	1.811×10^{4}	10.361	1.2
Sand Mix + 2000 PPm Cu	7.46×10^{6}	11.485	0.7

** $R_f = ArP_{O_2}^{m} \exp(-63{,}500/RT)\ C_f^{1.2}$

3. Low-Temperature oxidation Reaction***

Bed	Intercept	E/R $^{o}K \times 10^{-4}$	n
Sand Mix***	5.610×10^{6}	1.415	1.4
Silica	--	--	--
Original Matrix	1.027×10^{9}	1.444	1
Sand Mix + 2000PPm Cu	1.209×10^{8}	1.320	1

*** $R = ArP_{O_2}^{m} \exp(120{,}000/RT)\ C_f^{1.4}$

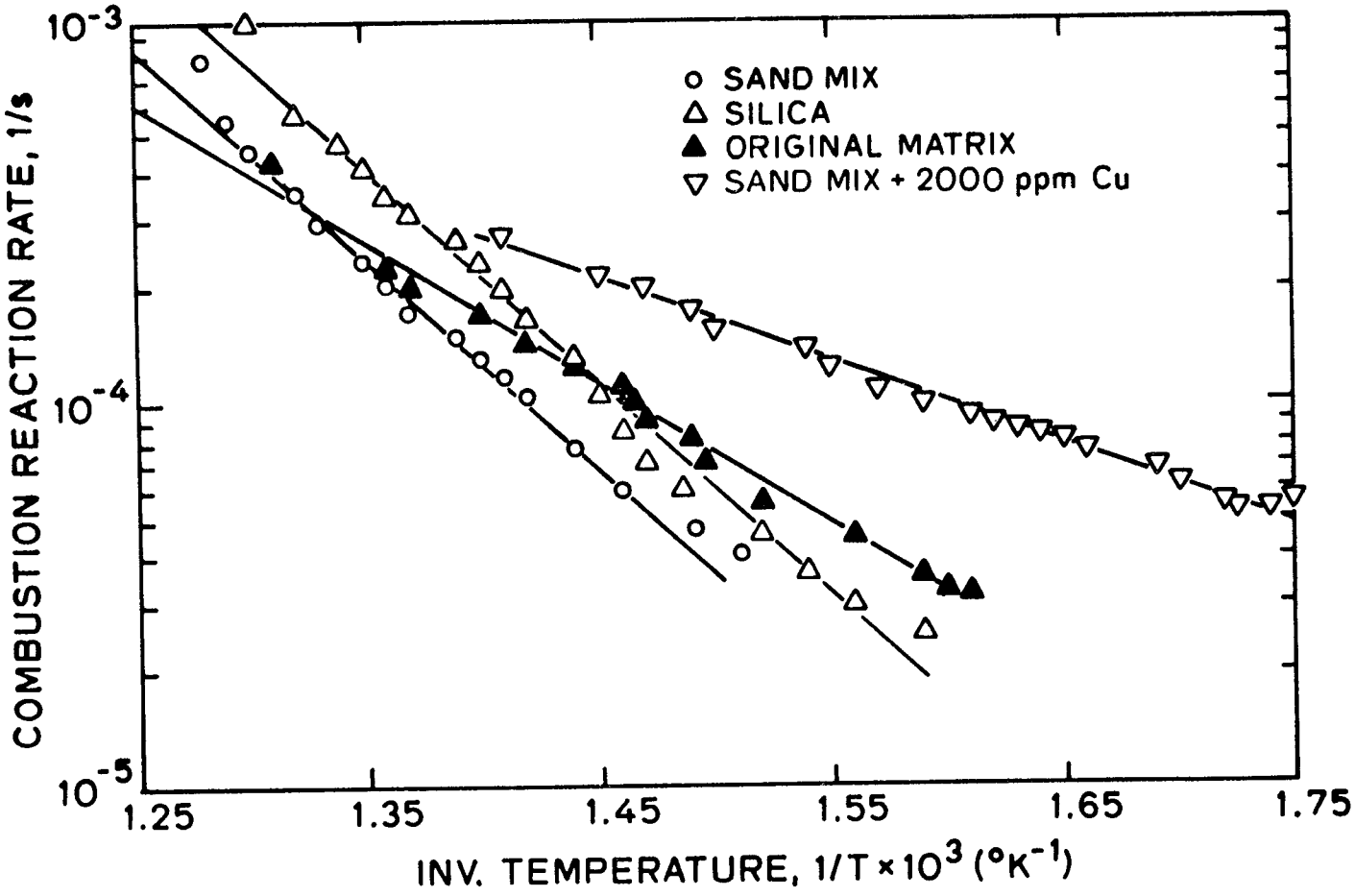

Fig. 8.40: ARRHENIUS PLOT FOR COMBUSTION REACTION (FRENCH OIL)

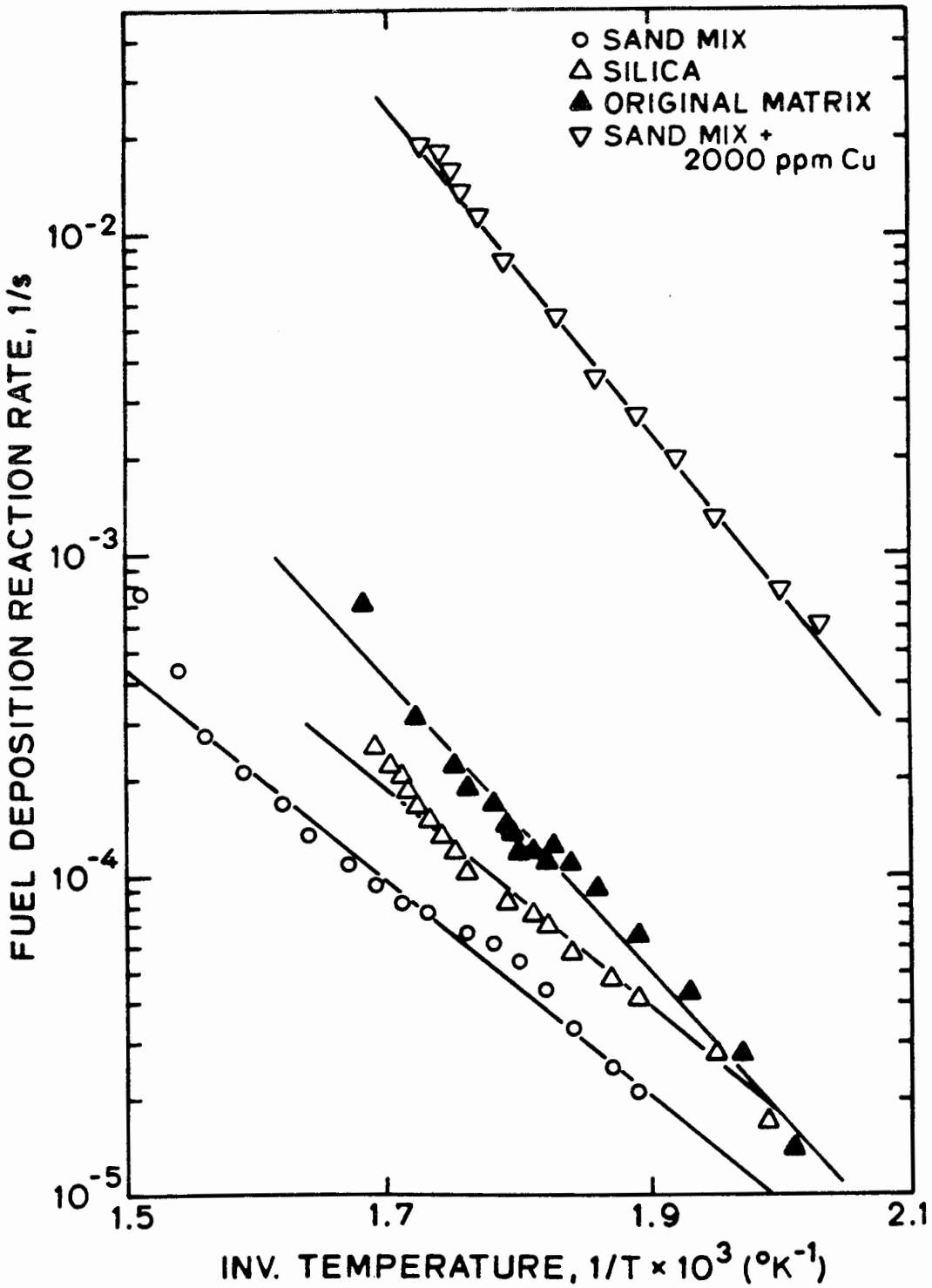

Fig. 8.41: ARRHENIUS PLOT FOR FUEL DEPOSITION REACTION (FRENCH OIL)

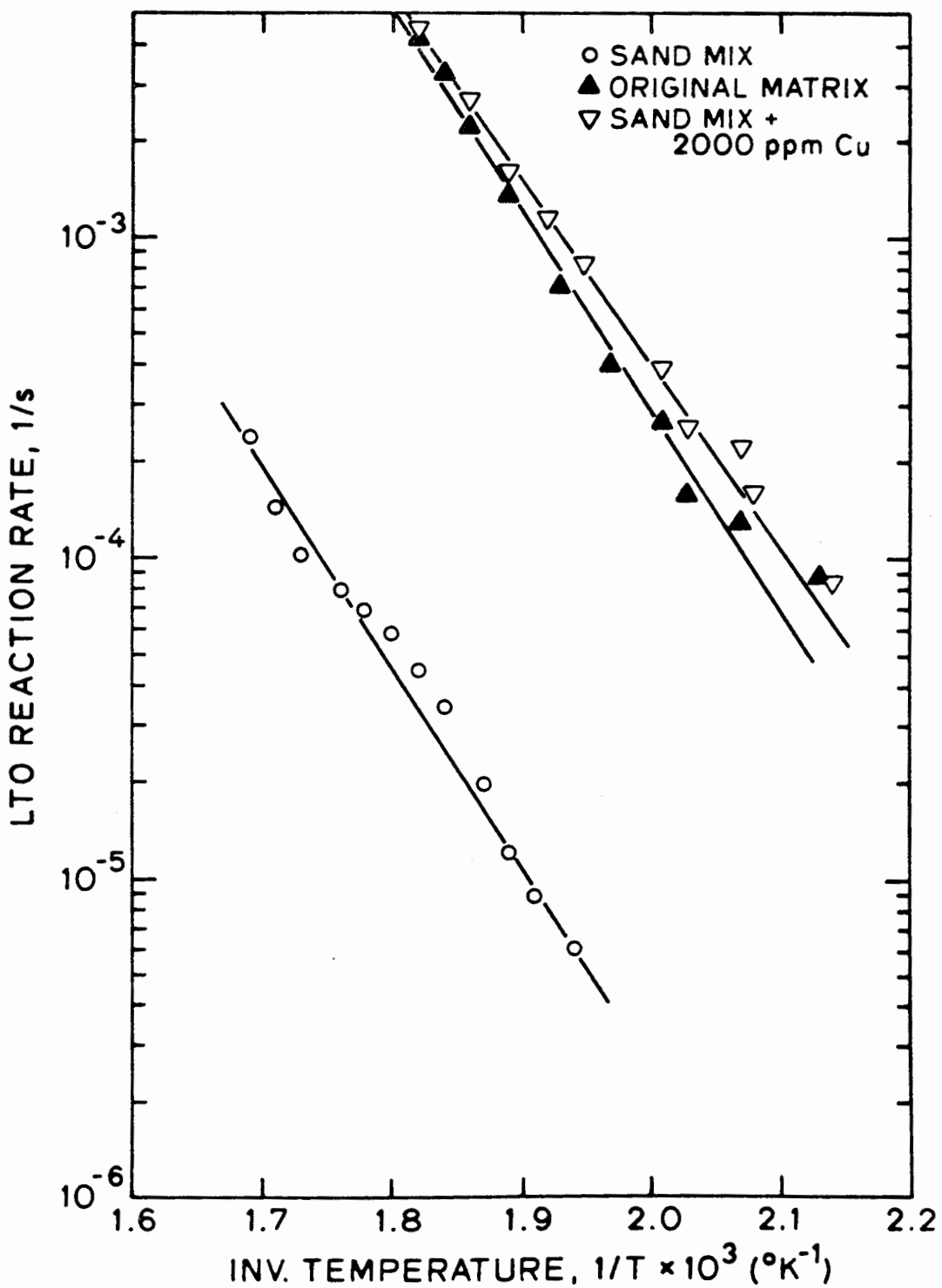

Fig. 8.42: ARRHENIUS PLOT FOR LTO REACTION (FRENCH OIL)

combustion without any change in activation energy (Table 8.10). This surface area dependency shows that the heterogeneous combustion reaction is apparently the result of burning some layers of fuel deposited on the rock. However, using the original matrix, both the Arrhenius constant and activation energy change. This is attributed to the presence of about 5% kaolinite in the matrix. Therefore, the effect of clay was studied.

8.9-2 Effect of Clay

In Runs No. 114 and 115, 5% clay was added to the sand pack and the normal procedure for a kinetic run was conducted. In both runs, the low-temperature peak (Fig. 8.43) was found to be higher than the corresponding peaks in Runs No. 127 and 129 in which no clay was used (Fig. 8.5). This implies that in the presence of clay, more fuel is available for oxidation reactions. This may be due to adsorption of hydrocarbons on the clay surface and, hence, low distillation and pyrolysis in porous medium.

The Arrhenius plot for the runs in which clay was used showed that the combustion reaction has a lower dependency on fuel concentration (i.e., $n < 1$) and a smaller activation energy than the ones obtained without clay (i.e., a catalytic effect). These results are shown in Table 8.11 and are in accordance with the ones previously obtained for French oil (Table 8.11). Bousaid and Ramey (1968) also pointed out the catalytic effect of clay on the combustion reaction. They reported that the addition of 20% clay to sand caused a 10% reduction in the energy of activation of the combustion reaction.

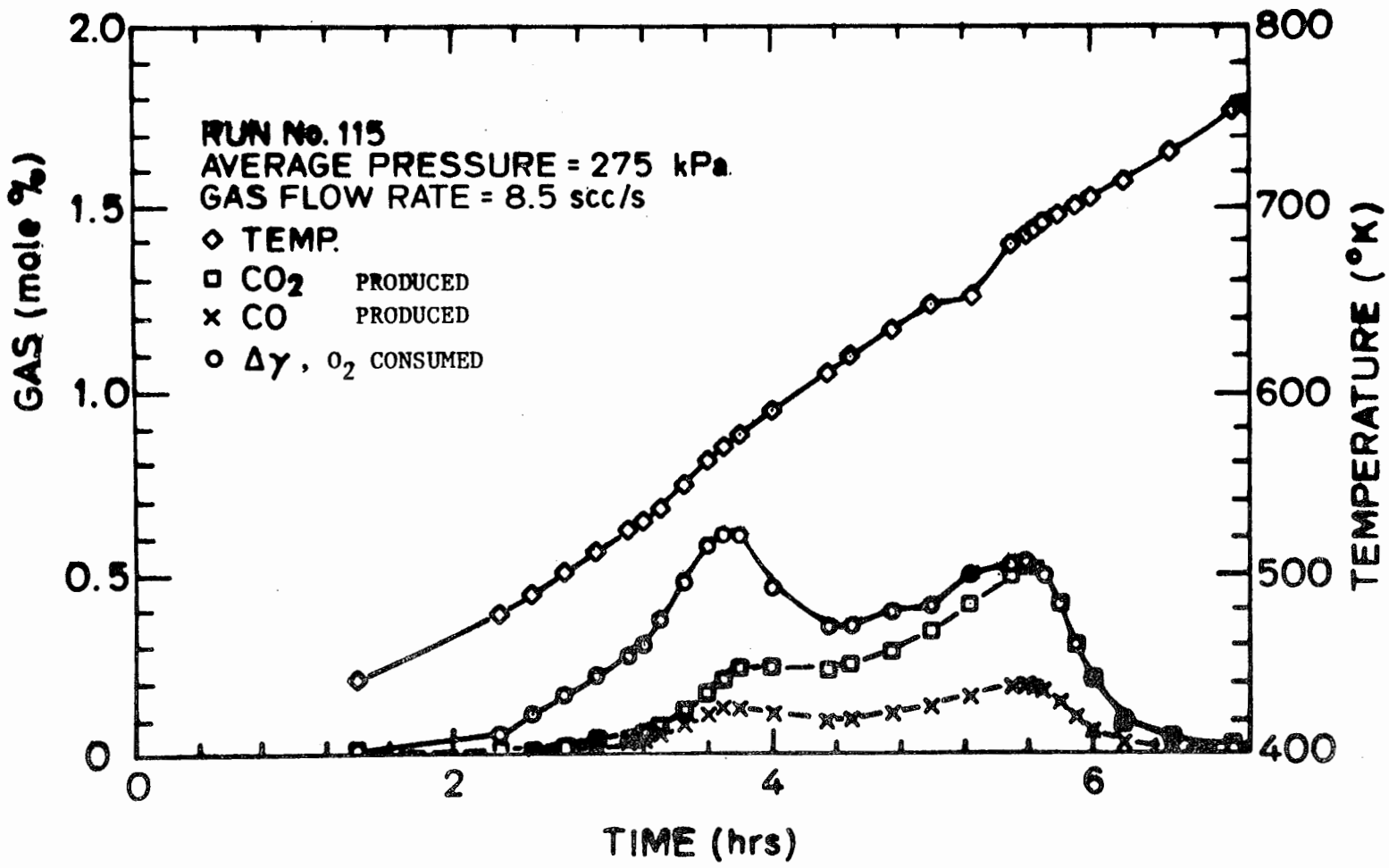

Fig. 8.43: GAS COMPOSITION AND TEMPERATURE VS TIME FOR SAN ARDO OIL WITH CLAY

Table 8.11

KINETIC DATA FOR COMBUSTION OF SAN ARDO OIL*
(sand with clay)

RUN NO.	p_{O_2}, kPa	Intercept, 1/s	E/R, °K^{-1}	m	n	A_r (kPa)$^{-m}$/s
114	137.2	3.92×10^3	7.514×10^3	0.55	0.4	260
115	31.3	1.75×10^3	7.34×10^3	0.55	0.4	260

* $-R_c = 260 \exp(-61{,}000/RT) p_{O_2}^{0.55} C_f^{0.4}$

8.9-3 Effect of Metallic Additives

As in most heterogeneous reactions, a catalyst can speed up the high-temperature oxidation reaction. In particular, the presence of metallic additives such as Cu, Ni, Va, Fe, etc., create a catalytic effect which lowers the temperature at which the combustion reaction occurs. This is due to a lower activation energy in the presence of additives. The analysis of the data on the oxidation of the French oil (Bardon and Gadelle, 1977) showed that an addition of 2000 ppm Cu to the sand mix (Table 8.9) lowered the activation energy by about 50% (Table 8.10). Figures 8.40 and 8.41 clearly demonstrate this catalytic effect on both fuel combustion and fuel deposition. However, for LTO reactions, a higher Arrhenius constant was obtained without a significant change in the activation energy when copper was added to the sand mix.

Due to this profound dependency of the kinetic parameter on the matrix compounds, the author believes that all combustion studies should be conducted using the parent cores. If this is not possible, the matrix should be analyzed to see whether metallic and clay additives are present. It is also felt that the existence of clay or a very fine matrix may lead to a successful combustion project in a field.

9. SUMMARY AND CONCLUSIONS

In this section, the results of the experiments are summarized and conclusions are listed along with suggestions for future work.

9.1 Summary

Table 9.1 summarizes the results of kinetic runs for three different kinds of crude oil using Ottawa sand of the same mesh size.

As is shown, although the energies of activation for both LTO and fuel deposition reactions are similar, they are almost twice as high for fuel combustion reactions. This indicates that the fuel combustion reaction is the slowest reaction and, therefore, is the rate-determining step. It should also be noted that the calculated activation energies are similar to the reported ones (Table 2.2) and are almost independent of the type of oil used. However, clay and metallic additives act as catalysts and lower both activation energies and the temperature of combustion reactions. This can cause the rate-determining step to be shifted toward fuel deposition.

Although the reaction order with respect to fuel concentration, n, does not change, the reaction order with respect to oxygen partial pressure, m, varies and is always less than one.

The Arrhenius constants, A_r, are different for different oils. In addition, the A_r for combustion reaction is directly related to the available surface area of the matrix. Knowledge of this relationship and of the quality of crude oils may lead to determination of the amount of fuel available for combustion.

Table 9.1

SUMMARY OF KINETIC DATA

$$R = A_r \exp(-E/RT) p_{O_2}{}^m C_f{}^n$$

CRUDE TYPE	LTO REACTION				FUEL DEPOSITION				FUEL COMBUSTION			
	A_r	E	m	n	A_r	E	m	n	A_r	E	m	n
Huntington Beach	1.9×10^2	6.7×10^4	0.57	1	1.2×10^3	8.0×10^4	0.46	1	6×10^5	1.35×10^5	0.66	1
San Ardo	1.9×10^2	6.4×10^4	0.4	1	4.5×10^2	7.4×10^4	0.4	1	4×10^4	1.20×10^5	0.58	1
Venezuela	1.0×10^3	7.0×10^4	0.42	1	8.8	5.1×10^4	0.18	1	2×10^6	1.33×10^5	0.23	1

NOTE: The data was obtained using Ottawa Sand.

Also, for more reactive oil, the A_r for LTO reactions is higher. Thus, A_r is also a good indicator of whether spontaneous ignition will occur in a rock.

Pressure is an important factor of the frontal behavior because of a combination of the effect of partial pressure of oxygen, p_{O_2}, on these reactions and the effect of total pressure on distillation.

9.2 Conclusions

1. An apparatus was designed to study the reactions kinetics of oil oxidation in porous media.
2. A kinetic model was developed to evaluate the experimental data.
3. The overall oxidation mechanism of crude oil in porous medium at different temperatures is an overlap of several consecutive reactions from which three can be distinguished:
   (a) LTO reactions are heterogeneous (gas-liquid) without any carbon oxides produced. Spontaneous ignition occurs due to LTO reactions.
   (b) Middle-temperature reactions are mainly homogeneous (gas phase) and result from the oxidation of the products of distillation and pyrolysis. These in turn, leave a heavy oil residue on the solid matrix.
   (c) High-temperature reactions are heterogeneous (gas and solid phase) and are a result of the combustion of the deposited residue.
4. The superimposed reactions can be easily differentiated by using the proposed model in this report.

5. These reactions are kinetically controlled and diffusion effects were found to be minimal.
6. The combustion reaction is slower than fuel deposition in a clean sand matrix.
7. Metallic additives and clays have catalytic effects on the reactions. Clays and fine sands enhance deposition of more fuel due to the adsorption characteristics on a higher surface area. These additives shift the rate-determining step from fuel combustion toward fuel deposition.
8. It is possible to formulate any frontal behavior in the field by using this model in conjuction with the temperature profile ahead of the front.
9. The correlations obtained for the Apparent H/C ratio and the molar carbon dioxide-carbon monoxide ratio can be used along with the model to estimate combustion heat.
10. Omission of any of these reactions in a combustion simulator may lead to erroneous results in the prediction of overall frontal behavior.

9.3 Suggestions for Future Work

1. Some correlations should be obtained between the burning front velocity and its thickness in the combustion tube and the rate of fuel combustion. This would facilitate calculation of the air requirement in the field by evaluating the kinetic data for the oil and the matrix.
2. The effects of heat loss on the frontal temperature and frontal velocity should be investigated.

3. A model should be developed to analyze the gases produced at different sections of a combustion tube and to directly measure the kinetic rates.
4. Although both sandstones and reservoir cores were used in this work, future work should focus on natural cores. The whole suite of kinetic data should be obtained.
5. Experiments should be run to measure directly the quantity and quality of fuel deposited at different temperatures in the presence of air. The results should determine the amount of distillation in porous media. A possible relationship between the Arrhenius constant for fuel combustion and the quantity of fuel deposited should also be investigated.
6. A simpler method for decomposition of the different reaction rates in non-isothermal runs should be developed. Use of a fully automatic computer program is suggested.

REFERENCES

1. Abramowitz, M., and Stegun, I. A.: Handbook of Mathematical Functions, Dover Publications Inc., New York (1972), pp. 228-231.

2. Alexander, J. D., Martin, W. L., and Dew, J. N.: "Factors Affecting Fuel Availability and Composition During In-Situ Combustion," J. of Pet. Tech. (October, 1962), pp. 1154-1164.

3. Bae, J. H.: "Characterization of Crude Oil for Fireflooding Using Thermal Analysis Methods," Soc. Pet. Eng. J. (June, 1977), pp. 211-217.

4. Bailey, H. R., and Larkin, B. K.: "Conduction-Convection in Underground Combustions," Trans. AIME (1960) Vol. 219, p. 321.

5. Bardon, C., and Gadelle, C.: "Essai de Laboratoire Pour L'Etude de la Combustion In-Situ," Institute Francais du Petrole, Paris (May, 1977).

6. Berry, H. J.: "An Experimental Investigation of Forward Combustion Oil Recovery," Ph.D. Dissertation, Texas A & M University (May, 1968).

7. Berry, V. J., Jr., and Parrish, D. R.: "A Theoretical Analysis of Heat Flow in Reverse Combustion," Trans. AIME (1960) Vol. 219, pp. 124-131.

8. Bousaid, I. S.: "Oxidation of Crude Oil in Porous Media," Ph.D. Dissertation, Texas A & M University (May, 1967).

9. Bousaid, I.S., and Ramey, H. J., Jr.: "Oxidation of Crude Oil in Porous Media," Soc. Pet. Eng. J. (June, 1968), pp. 137-148; Trans. AIME, Vol. 243.

10. Brigham, W. E., Satman, A., Soliman, M. Y.: "Recovery Correlations for In-Situ Combustion Field Projects and Application to Combustion Pilots," J. Pet. Tech. (December, 1980), pp. 2132-2214.

11. Burger, J. G.: "Spontaneous Ignition in Oil Reservoirs," Soc. Pet. Eng. J. (April, 1976), pp. 73-80.

12. Burger, J. G., and Sahuquet, B. C.: "Chemical Aspects of In-Situ Combustion Heat of Combustion and Kinetics," Soc. Pet. Eng. J. (October, 1972), pp. 410-422.

13. Burger, J. G., and Sahuquet, B. C.: "Les Methods Thermiques De Production Des Hydrocarbures--Combustion In-Situ, Principles Et Etudes De Laboratoire," Revue de L'Institute Francais du Petrole (March-April, 1977), No. 2, pp. 141-188.

14. Burger, J. G., and Sahuquet, B. C.: "La Production du Petrole--VII.1. Principles et Description des Methods Classiques D'exploitation par Combustion," Petrolieri International (June, 1977), pp. 45-90.

15. Carberry, J. J.: Chemical and Catalytic Reaction Engineering, McGraw-Hill Book Company, Inc., New York, N.Y. (1976), p. 495.

16. Carslaw, H. S., and Jaeger, J. C.: Conduction of Heat in Solids, Oxford University Press, 2nd edition (1978), pp. 201, 208.

17. Chieh, C.: "Two-Dimensional Analysis of a Radial Heat Wave," J. Pet. Tech. (October, 1963), pp. 1137-1144.

18. Coats, K. H.: "In-Situ Combustion Model," Soc. Pet. Eng. J. (December, 1980), pp. 533-555.

19. Crawford, P. B., and Cunningham, W. A.: "Carbon Formation in Cat Cracking," Pet. Refiner (January, 1956), Vol. 35, No. 1, pp. 169-173.

20. Crawford, P. B.: "Water Technology--Underground Combustion of Hydrocarbons," Producers' Monthly (June, 1968), p. 15.

21. Crookston, R. B., Culham, W. E., and Chen, W. H.: "Numerical Simulation Model for Thermal Recovery Processes," Soc. Pet. Eng. J. (February, 1979), pp. 37-58.

22. Dabbous, M. K.: "In-Situ Oxidation of Crude Oils in Porous Media," Ph.D. Dissertation, University of Pittsburgh (1971).

23. Dabbous, M. K., and Fulton, P. F.: "Low-Temperature Oxidation Reaction Kinetics and Effects on the In-Situ Combustion Process," Soc. Pet. Eng. J. (June, 1974), pp. 253-262.

24. Farouq, Ali, S. M.: "A Current Appraisal of In-Situ Combustion Field Tests," J. Pet. Tech. (April, 1972), pp. 477-486.

25. Fassihi, M. R., Brigham, W. E., and Ramey, H. J., Jr.: "Laboratory Combustion Tube Studies--Final Report," Stanford University Petroleum Research Institute, Stanford, CA., SUPRI TR-22, Report submitted to DOE (September, 1980).

26. Gates, C. F., and Ramey, H. J., Jr.: "Field Results of South Belridge Thermal Recovery Experiment," Trans. AIME (1958), Vol. 213, pp. 236-244.

27. Gates, C. G., and Ramey, H. J., Jr.: "A Method for Engineering In-Situ Combustion Oil Recovery Projects," J. Pet. Tech. (February, 1980), pp. 285-294.

28. Gottfried, B. S.: "Some Theoretical Aspects of Underground Combustion in Segregated Oil Reservoirs," Soc. of Pet. Eng. J. (September, 1966), pp. 281-290.

29. Grant, B. F., and Szasz, S. E.: "Development of an Underground Heat Wave for Oil Recovery," Trans. AIME (1954) Vol. 201, pp. 108-118.

30. Johnson, H. R., and Burwell, E. L.: "Carbon Deposition for Thermal Recovery of Petroleum--A Statistical Approach to Research," Producers' Monthly (July, 1968), pp. 8-15.

31. Kanury, A. M.: Introduction to Combustion Phenomena, Gordon and Breach Science Publishers (1977), pp. 366-368.

32. Kuhn, C. S., and Koch, R. L.: "In-Situ Combustion--Newest Method of Increasing Oil Recovery," Oil and Gas J. (August 10, 1953), Vol. 52, No. 14, pp. 92-96.

33. Lewis, W. K., Gilliland, E. R., and Paxton, R. R.: "Low-Temperature Oxidation of Carbon," Ind. & Eng. Chem. (June, 1954), Vol. 46, No. 6, pp. 1327-1331.

34. Madgewick, G. G., Amberg, C. H., and Peterson, W. S.: "The Pyrolysis of a Heavy Crude Oil in a Fluidized Bed," The Can. J. of Chem. Eng. (April, 1959), pp. 65-70.

35. Martin, W. L., Alexander, J. D., and Dew, J. N.: "Process Variables of In-Situ Combustion," Trans. AIME (1958), Vol. 213, pp. 28-35.

36. Moss, J. T., White, P. D., and McNiel, J. S., Jr.: "In-Situ Combustion Process--Results of a Five-Well Field Experiment in Southern Oklahoma," Trans. AIME (1958), Vol. 216, pp. 28-35.

37. Nagorny, L. A.: "Investigation of Coke Formation During In-Situ Combustion Process in Water Saturated Reservoirs with Oil of Average Gravity," Neft Khoz (Russian), (March, 1974) No. 3, pp. 58-61.

38. Nelson, T. W., and McNiel, J. S., Jr.: "How to Engineer an In-Situ Combustion Project," Oil and Gas J. (1961), Vol. 39, No. 23, p. 58.

39. Penberthy, W. L., Ramey, H. J., Jr.: "Design and Operation of Laboratory Combustion Tubes," Soc. of Pet. Eng. J. (June, 1966), pp. 183-198.

40. Penberthy, W. L., Jr.: "An Investigation of the Fundamentals of Combustion Oil Recovery," Ph.D. Dissertation, Texas A & M University (May, 1967).

41. Poettman, F. J., Schilson, R. E., and Surkalo, H.: "Philosophy and Technology of In-Situ Combustion in Light Oil Reservoirs," Proc. of the 7th World Petroleum Congress (1967), Vol. 3, pp. 487-497.

42. Ramey, H. J., Jr.: "Transient Heat Conduction During Radial Movement of a Cylindrical Heat Source--Application to the Thermal Recovery Process," Trans. AIME (1959), Vol. 216, pp. 115-122.

43. Ramey, H. J., Jr.: "In-Situ Combustion," Proceedings of the 8th World Petroleum Congress, Moscow (1971), pp. 253-262.

44. Showalter, W. E.: "Combustion-Drive Tests," Soc. Pet. Eng. J. (March, 1963), pp. 53-58.

45. Smith, J. M.: Chemical Engineering Kinetics, McGraw-Hill Book Company, Inc., New York, N.Y. (1970).

46. Standing, M. B.: Volumetric and Phase Behavior of Oil Field Hydrocarbon Systems, Monograph published by Society of Petroleum Engineers of AIME, Dallas, eighth printing (1977), p. 3.

47. Tadema, H. J.: "Mechanism of Oil Production by Underground Combustion," Proceedings of the 5th World Petroleum Congress (1959), section II, paper 22, pp. 279-287.

48. Tadema, H. J., and Weijdema, J.: "Spontaneous Ignition of Oil Sands," Oil and Gas J. (December 14, 1970), pp. 77-80.

49. Thomas, G. W.: "A Study of Forward Combustion in a Radial System Bounded by Permeable Media," J. Pet. Tech. (October, 1963), pp. 1137-1144.

50. Thomas, G. W., Buthod, A. P., and Allag, O.: "An Experimental Study of the Kinetics of Dry, Forward Combustion--Final Report," Report No. BETC-1820-1, distributed by Department of Energy (February, 1979).

51. Vogel, L. C., and Krueger, R. F.: "An Analog Computer for Studying Heat Transfer During a Thermal Recovery Process," Trans. AIME (1955), Vol. 204, p. 208.

52. Watson, K. M., and Nelson, E. F.: "Characterization of Petroleum Fractions," Ind. and Eng. Chemistry, Vol. 27 (November, 1935), pp. 1460-1464.

53. Weisz, P. B., and Goodwin, R. D.: "Combustion of Carbonaceous Deposits within Forous Catalyst Particles, II, Intrinsic Burning Rate," J. of Catalysis (June, 1966), No. 6, pp. 227-236.

54. Weijdema, J.: "Determination of the Oxidation Kinetics of the In-Situ Combustion Process," Report from Koninklijke/Shell, Exploratie En Produktic Laboratorium, Rijswijk, The Netherlands (1968).

55. Wilson, L. A., Qygal, R. J., Reed, D. W., Gergins, R. L., and Henderson, J. H.: "Fluid Dynamics During an Underground Combustion Process," Trans. AIME (1958), Vol. 213, pp. 146-154.

56. Wilson, L. A., Reed, R. L., Clay, R. R., and Harrison, J. H.: "Some Effects of Pressure on Forward and Reverse Combustion," Soc. Pet. Eng. J. (June, 1963), pp. 127-137.

57. Wu, C. H., and Fulton, P. F.: "Experimental Simulation of the Zones Preceding the Combustion Front of an In-Situ Combustion Process," Soc. of Pet. Eng. J. (March, 1971), pp. 38-46.

58. Yougren, G. K.: "Development and Application of an In-Situ Combustion Reservoir Simulator," Soc. of Pet. Eng. J. (February, 1980), pp. 39-51.

NOMENCLATURE

A = Cross-sectional area, cm^2

A' = Specific rock surface area per unit bulk volume cm^{-1} or per unit weight of sample, cm^2/g

A_r = Arrhenius constant

C_c = Carbon concentration, g C/100g sand

C_f = Fuel concentration, g fuel/100g sand

E = Activation Energy, J/g mole

k = Rate of temperature rise, °C/s

L = Length of the pack, cm

m = Reaction order with respect to oxygen, constant

n = Reaction order with respect to carbon, constant

p = Total pressure, Pa

p_{O_2} = Oxygen partial ressure, Pa

q = Gas flow rate, cc/s

R = Universal gas constant

S_o = Oil saturation, constant

T = Temperature, °C or °K

t = Time, s

V_f = Burning front velocity, cm/hr

ϕ = Porosity

α = Intercept of temperature-time curve, °K or constant of proportionality in Eq. C-8

β = Slope of temperature-time curve, 1/s or a constant in Eq. C-11

β' = Intercept of relative reaction rate curve vs 1/T, 1/s

γ = Oxygen concentration, mole %

δ = Oxygen converted to carbon oxides, mole %

ν = Nitrogen concentration, mole %

η = Apparent hydrogen-carbon ratio

λ = Molar carbon dioxide-carbon monoxide ratio

μ = Viscosity

χ = Thermal diffusivity, cm^2/s

ρc = Thermal capacity, J/cm^3-°C

Appendix A

DISCUSSION OF THE TEMPERATURE DISTRIBUTION IN THE HEATED POROUS MEDIUM

In this appendix, the theoretical radial temperature distribution in porous medium is calculated to find a practical heating rate to be used in the kinetic experiments. Also, the rate of net heat supply to the sand pack by external sources is compared to the heat generated internally by oxidation reactions. This analysis shows the effect of oxidation heat on the temperature distribution of the sand pack. Finally, the effect of injection temperature on the longitudinal temperature distribution within the medium is discussed.

A.1 Calculation of Radial Temperature Distribution in the Heated Sand Pack

For the radial temperature distribution in a circular cylinder, with a constant temperature rise at the cylindrical surface, the boundary values can be described by:

1) Initial temperature T_o
2) The temperature at the surface, r = b, is: $T_o + kt$, where k is constant rate of temperature rise in °C/s. The solution is (Carslaw and Jaeger, 1978):

$$T(r,t) - T_o = k\left(t - \frac{b^2 - r^2}{4\chi}\right) + \frac{2k}{b\chi} \sum_{n=1}^{\infty} e^{-\chi\alpha_n^2 t} \frac{J_o(r\alpha_n)}{\alpha_n^3 J_1(b\alpha_n)} \qquad \text{(A-1)}$$

in which $b\alpha_n$, (n = 1, 2, 3, 4, ...), are the roots for the Bessel function $J_o(b\alpha_n) = 0$ and χ is the thermal diffusivity. Thus the temperature difference between surface and axis of the cylinder is:

$$T(r = b) - T(r = 0) = \frac{kb^2}{4\chi} - \frac{2k}{b\chi} \sum_{n=1}^{\infty} e^{-\chi\alpha_n^2 t} \frac{J_o(0)}{\alpha_n^3 J_1(b\alpha_n)} \qquad \text{(A-2)}$$

If we substitute b = 1.38 cm for the radius of the sand pack and $\chi = 0.015\ cm^2/s$ for the heat diffusivity of the sand pack, we find that within the first 60 seconds the summation term becomes extremely small compared with the first term. Therefore, Eq. A-2 reduces to:

$$T(b) - T(0) = \frac{kb^2}{4\chi} \qquad \text{(A-3)}$$

Equation A-3 is not time dependent; a constant temperature difference develops between surface and axis of the sand pack. Temperature differences for various values of k are given in the following table.

Table A-1

RADIAL TEMPERATURE DIFFERENCES AS A FUNCTION OF THE HEATING RATE

Heating Rate, k °C/Hr	Temperature Difference °C	Net Heat Supply Watts
30	0.26	1.32
60	0.52	2.65
120	1.05	5.30

Note that even at an external heating rate corresponding to a temperature rise of 120°C/hr, the temperature difference between axis and periphery of the sand pack will only be around 1°C.

A.1.1 Effect of the Wall Thickness

In the above calculations, it was assumed that the reactor wall is of infininitesimal thickness. The effect of the metal tube that confines the pack can be taken into account if the actual radius of the pack, b, is replaced to an equivalent radius, b', that accounts for the metal diffusivity. According to Fourier modulus, $\frac{\chi t}{r^2}$, this correction term can be derived as:

$$\Delta r = \left[\frac{\chi(\text{sand})}{\chi(\text{steel})}\right]^{1/2} X(\text{wall thickness}) \qquad \text{(A-4)}$$

where χ, thermal diffusivity, for sand and steel is 0.015 and 0.15 cm^2/s respectively. There were two coil wraps made of 0.01" thick stainless steel tubing. The combustion cell was 0.02" thick. A wall thickness of approximately 0.06" or 0.15 cm can be obtained by neglecting the spacing between the tubes. So,

$$\Delta r = \left[\frac{.015}{0.15}\right]^{1/2} (0.15) \cong 0.05 \text{ cm}$$

Thus, the actual radius of the pack should be increased by only about 3%. This increase does not introduce substantial error into the previous results shown in Table A-1.

A.2 Calculation of the Net Rate of Heat Supply to the Sand Pack

The net rate of heat supply to the sand pack is calculated from:

$$q = A\ell(\rho c)_f \frac{dT}{dt} \qquad \text{(A-5)}$$

Inserting $A = 5.965\ cm^2$; $\ell = 12.7$ cm and $(\rho c)_f = 2.1\ J/cm^3 - °C$, the net rates of heat supply are given in Table A-1.

A.3 Determination of the Effect of Heat of Oxidation on Temperature Distribution

Given an air injection rate of approximately 3 moles/hr (65 sl/hr) and an oxygen consumption of 3 mole percent (these values are higher than the ones used in the experiments), the heat evolved from the oxidation is:

$$\frac{3}{3600}(0.03)\ 419{,}000 = 10.47 \text{ watt} \qquad \text{(Oxidation heat: 419,000 J/mole oxygen)}$$

This heat generation is the same order of magnitude as the rate of heat supply from the external heating source; it is not expected to disturb markedly the even temperature distribution in the sand pack.

A.4 Determination of Effect of Injected Cold Air on the Temperature Distribution

Since injected cold air tends to cool the oil sand, the air has to be preheated to the reactor temperature. This is achieved by wrapping a coil around the reactor. Also, a pack of dry sand is placed before the oil sand and is heated simultaneously with the latter. The heat supply needed to warm up the air is:

$$Q = q_g C_m \Delta T \qquad \text{(A-6)}$$

C_m is the molar specific heat and is equal to 31.0 J/mole-°C for air. At ΔT = 300°C and q_g = 1.5 moles/hr, this heat supply amounts to 3.8 watts. Based on values calculated in Table A-1, in all runs the injected air is expected to be at the same temperature as the pack temperature.

Appendix B

COMBUSTION TUBE RUNS DATA

All the data concerning the effluent gas compositions, fuel consumption rates and air requirements for the combustion tube runs are presented in this Appendix. The following equations have been used in this appendix:

1. Atomic hydrogen-carbon ratio, $\eta = 4\left(\dfrac{\frac{21}{79}\%\ \nu_o - \%CO_2 - \gamma_o - \frac{\%CO}{2}}{\%CO_2 + \%CO}\right)$

where:

ν_o = nitrogen produced, mole %

γ_o = oxygen produced, mole %

2. Lb fuel burned/hour $= q_g\left(\dfrac{\%CO_2 + \%CO}{100\%}\right) \times \left(\dfrac{12 + \eta}{12} \times \dfrac{12}{379}\right)$

where:

q_g = produced gas flow rate, scf/hr

3. Fuel concentration, C_f, lb/cu ft bulk $= \dfrac{\text{lb fuel burned/hr}}{\frac{\pi}{12}\ (r_{tb}^{\ 2} - r_{th}^{\ 2})V_f}$

where: V_f = burning front velocity, in/hr

r = radius, ft. Subscripts tb and th are for tube and thermowell respectively.

4. Lb water formed/lb fuel burned $= \dfrac{9\eta}{12 + \eta}$

5. Injected air-fuel ratio, AFR, scf/lb $= \dfrac{\nu_o \times 100/79 \times 379}{(\%CO_2 + \%CO)\ (12 + \eta)}$

6. Injected air-sand ratio, MMscf/acre-ft = AFR x C_f x 43,560 x 10^{-6}

COMBUSTION TUBE RUN 78- 4

TIME	CO2	O2	N2	CH4	CO
0.4800	1.6372	17.2521	80.1107	0.0000	0.0000
0.6900	3.5162	14.4096	78.9325	0.0000	2.1418
0.9400	7.7995	7.5548	80.4066	0.0000	3.2391
1.2000	6.1964	12.3058	78.8647	0.0000	1.6331
1.4300	6.2748	11.5714	79.3622	0.0000	1.7916
1.7000	9.5475	9.3902	78.1541	0.0000	1.9082
1.9500	10.8862	9.2199	76.6836	0.0000	2.2103
2.2800	8.7616	8.3095	79.6417	0.0000	2.2872
2.7300	12.4090	3.6614	79.2450	0.0000	3.6847
3.1600	16.4144	2.5225	77.4269	0.0000	2.6362
3.4700	15.3264	1.5702	78.8943	0.0000	3.2091
3.7400	15.5088	1.5132	78.6041	0.0000	3.3738
3.9800	18.0532	1.2330	76.2774	0.0000	3.4364
4.4600	15.0157	1.2307	79.0380	0.0000	3.7156
4.8400	14.6365	1.2628	78.1153	0.0000	4.9855
5.2200	12.5240	3.1349	79.7882	0.0000	3.5529
5.7200	13.4682	1.5845	80.6551	0.0000	3.2922
6.0200	13.7630	3.5328	78.6458	0.0000	3.0584
6.5000	12.7799	4.2098	79.4543	0.0000	2.5560
6.8500	14.3175	3.5461	77.5082	0.0000	3.6282
7.2000	15.5154	2.9441	76.6477	0.0000	3.8928
7.5000	15.4912	1.4938	77.7824	0.0000	4.2326
7.8200	14.6268	0.6038	80.0627	0.0000	3.7066
8.2700	12.4420	5.8550	78.4911	0.0000	2.2119
8.6000	16.1466	1.7535	77.7877	0.0000	3.3121
9.0000	14.8230	3.3753	78.1453	0.0000	2.6565
9.3600	12.4259	2.0466	80.6617	0.0000	3.8658
9.6000	9.1337	6.6795	81.8152	0.0000	1.3714
9.7500	12.2441	4.5191	79.5692	0.0000	2.6676
9.9500	9.4760	8.3612	79.0570	0.0000	2.1058

TIME	ATOMIC H/C RATIO	LB WATER FORMED PER LB FUEL BURNED	LB FUEL BURNED PER H O U R	LB FUEL PER CFT BULK VOL.	SCF AIR PER LB FUEL	MMSCF AIR PER AC.FT SAND
0.4800	5.8783	2.9591	0.0030	0.2935	1313.0592	16.7864
0.6900	1.4036	0.9425	0.0078	0.7604	499.3282	16.5395
0.9400	1.5945	1.0556	0.0154	1.5047	257.0568	16.8484
1.2000	0.8406	0.5892	0.0103	1.0081	376.3385	16.5253
1.4300	1.1675	0.7980	0.0109	1.0650	358.4652	16.6295
1.7000	0.3084	0.2255	0.0142	1.3883	265.9135	16.0809
1.9500	-0.2526	-0.1935	0.0155	1.5148	239.1199	15.7774
2.2800	1.0701	0.7369	0.0141	1.3808	264.5811	15.9139
2.7300	0.7835	0.5516	0.0203	1.9884	184.7899	16.0058
3.1600	0.0686	0.0512	0.0257	2.5192	161.5613	17.7293
3.4700	0.5332	0.3829	0.0260	2.5455	162.9266	18.0653
3.7400	0.4630	0.3344	0.0263	2.5786	160.2403	17.9989
3.9800	-0.1355	-0.1028	0.0285	2.7937	143.5268	17.4661
4.4600	0.6206	0.4425	0.0268	2.6269	160.3992	18.3543
4.8400	0.4837	0.3487	0.0274	2.6840	152.9899	17.8870
5.2200	0.9390	0.6532	0.0233	1.1979	184.0122	9.6018
5.7200	1.1315	0.7755	0.0233	1.2016	175.8105	9.2025
6.0200	0.4948	0.3564	0.0211	1.0876	179.5123	8.5045
6.5000	0.7442	0.5255	0.0200	1.0299	195.0342	8.7497
6.8500	0.2063	0.1521	0.0286	1.4697	169.7516	10.8673
7.2000	-0.0064	-0.0048	0.0303	1.5617	157.9711	10.7466
7.5000	0.3194	0.2334	0.0317	1.6302	153.5727	10.9057
7.8200	0.9160	0.6383	0.0309	1.5887	162.2067	11.2254
8.2700	0.3990	0.2896	0.0237	1.2190	207.2492	11.0051
8.6000	0.2306	0.1697	0.0306	1.5741	156.8057	10.7519
9.0000	0.2852	0.2089	0.0270	1.3882	174.5840	10.5574
9.3600	1.2365	0.8408	0.0275	1.4146	179.4480	11.0576
9.6000	1.9988	1.2850	0.0185	0.9507	266.9046	11.0532
9.7500	0.8193	0.5752	0.0222	1.1449	199.6953	9.9593
9.9500	0.7339	0.5187	0.0158	0.8132	257.1664	9.1099

NOTE: Negative numbers are due to an error in integration method.

COMBUSTION TUBE RUN 78- 5

TIME	CO2	O2	N2	CH4	CO
0.1500	6.4767	13.8112	76.7905	0.5609	1.3605
0.3300	6.0548	13.9444	77.8561	0.0000	1.1447
0.6400	7.5393	32.7229	56.7643	0.0000	1.9735
0.9500	3.1416	14.7720	80.4924	0.0000	0.5939
2.0000	6.4819	8.9568	81.2084	0.0000	2.3528
2.8500	13.1741	5.7246	77.2818	0.0000	2.8196
3.1800	12.5601	5.9033	77.6289	0.0000	2.9076
3.8300	14.2522	4.5588	77.1952	0.0000	2.9938
4.3200	16.7917	1.8415	77.3434	0.0000	3.0234
4.6600	14.7491	3.0880	77.8168	0.0000	3.3461
5.0500	12.3244	3.4691	79.7892	0.0000	3.4173
5.4000	15.4899	0.6606	78.9448	0.0000	3.9046
6.0000	16.1260	1.2806	78.4395	0.0000	3.1538
6.5000	15.3963	1.8662	77.4480	0.0000	4.2895
6.8000	15.6529	1.8330	77.9028	0.0000	3.6113
7.1000	15.9968	1.5099	77.0038	0.9199	3.5696
7.5100	13.9457	1.9270	77.4031	0.9783	4.7457
8.1000	12.2913	2.4615	79.0759	0.6248	4.5464
8.5000	14.2685	1.3144	80.1801	0.0000	3.2370
9.0500	12.7621	2.5014	79.7324	0.0000	4.0041
9.3300	6.8829	8.2560	82.5599	0.0000	1.3012
9.5000	8.2146	8.1980	81.0343	0.0000	1.5530
9.8400	8.0663	7.6870	81.3537	0.0000	1.8931

TIME	ATOMIC H/C RATIO	LB WATER FORMED PER LB FUEL BURNED	LB FUEL BURNED PER H O U R	LB FUEL PER CFT BULK VOL.	SCF AIR PER LB FUEL	MMSCF AIR PER AC.FT SAND
0.1500	-0.2836	-0.2178	0.0103	0.5043	401.1990	8.8125
0.3300	0.0691	0.0515	0.0105	0.5165	429.8609	9.6706
0.6400	-10.9998	-98.9766	0.0014	0.0695	2852.0918	8.6602
0.9500	3.4116	1.9923	0.0086	0.4203	670.7510	12.2803
2.0000	2.2511	1.4216	0.0188	0.9192	309.4368	12.3895
2.8500	0.0587	0.0438	0.0270	1.3208	192.2386	11.0601
3.1800	0.1857	0.1372	0.0264	1.2908	197.5862	11.1097
3.8300	0.0493	0.0368	0.0291	1.4231	178.2190	11.0477
4.3200	0.0837	0.0624	0.0379	1.8563	154.9671	12.5308
4.6600	0.2598	0.1907	0.0363	1.7772	168.2824	13.0278
5.0500	0.9421	0.6551	0.0301	1.4742	187.8878	12.0653
5.4000	0.5945	0.4248	0.0342	1.6728	155.0514	11.2981
6.0000	0.3874	0.2815	0.0334	1.6356	157.5658	11.2257
6.5000	0.2398	0.1763	0.0584	2.8581	154.2037	19.1981
6.8000	0.2942	0.2154	0.0342	1.6770	157.8027	11.5276
7.1000	0.2408	0.1770	0.0223	1.0924	154.2424	7.3399
7.5100	0.4986	0.3590	0.0316	1.5455	158.9521	10.7012
8.1000	0.9488	0.6595	0.0317	1.5523	173.9965	11.7652
8.5000	0.9397	0.6536	0.0464	2.2712	169.8172	16.8009
9.0500	0.9374	0.6521	0.0303	1.4855	176.3457	11.4108
9.3300	3.0091	1.8044	0.0172	0.8412	322.4430	11.8154
9.5000	1.7821	1.1637	0.0188	0.9219	288.7871	11.5971
9.8400	1.9784	1.2738	0.0156	0.7645	280.3510	9.3362

COMBUSTION TUBE RUN 78- 6

TIME	CO2	O2	N2	CH4	CO
0.3500	1.0507	19.9642	77.9851	0.0000	0.0000
0.5100	2.0323	14.6467	81.7531	0.0000	0.5679
0.6000	7.6123	5.9848	81.9586	0.6083	2.8359
0.8500	7.1071	9.9780	80.7801	0.0000	1.1348
1.0600	5.9362	15.5569	76.9540	0.0000	0.5529
1.4500	4.6211	18.1655	75.6698	0.0000	0.5437
1.7500	6.3758	13.3671	77.8320	0.0000	1.4252
2.0700	10.3079	7.2729	78.4652	0.0000	2.9540
2.4500	8.2271	9.0959	79.3783	0.0000	2.2987
2.7000	12.2760	7.0778	75.8045	0.0000	3.8417
2.7700	14.4259	5.3558	75.0900	1.4411	2.6872
3.0000	14.5754	4.6100	75.4997	1.5062	2.8086
3.1500	15.8669	2.7267	76.2943	0.6236	3.4886
3.4000	14.5496	1.7332	78.5350	0.6342	3.5479
3.8500	14.5481	1.7021	78.9753	0.0000	3.7746
4.0400	13.7743	1.6712	77.2412	0.6115	5.7018
4.4200	15.3868	1.6802	75.5235	1.5371	4.8725
4.5800	15.4186	2.0900	77.3421	0.2868	3.8625
4.8000	10.4426	5.4734	78.1238	0.0000	4.9602
5.0500	12.4315	2.8959	78.7325	0.0000	4.9401
5.3100	11.9922	3.4468	77.7100	0.0000	5.8509
5.6600	11.0512	3.4718	78.2735	0.0000	6.2035
5.9400	11.8043	1.6107	79.5697	0.0000	6.0152
6.3500	12.0753	2.5790	77.6926	0.0000	6.6532
6.7900	12.0471	1.7203	79.8225	0.0000	5.4101
6.9800	14.1621	1.3378	76.9262	0.0000	6.5739
7.2700	14.0644	1.6933	79.2483	0.0000	3.9939
7.4500	12.7988	2.4450	79.6370	0.0000	4.1192
7.8000	12.7076	4.1616	78.7227	0.0000	3.4082
8.2700	7.1738	8.4953	80.5480	0.0000	2.7829
8.5000	4.9885	10.4506	81.0819	0.0000	2.4791

TIME	ATOMIC H/C RATIO	LB WATER FORMED PER LB FUEL BURNED	LB FUEL BURNED PER H O U R	LB FUEL PER CFT BULK VOL.	SCF AIR PER LB FUEL	MMSCF AIR PER AC.FT SAND
0.3500	-1.0839	-0.8936	0.0017	0.0705	3261.7956	10.0126
0.5100	7.3363	3.4146	0.0075	0.3089	780.0842	10.4964
0.6000	2.5924	1.5989	0.0227	0.9367	257.8928	10.5228
0.8500	1.8543	1.2046	0.0170	0.7015	339.3957	10.3715
1.0600	-0.8096	-0.6511	0.0107	0.4422	508.4122	9.7928
1.4500	-2.2798	-2.1109	0.0078	0.3221	723.1270	10.1453
1.7500	0.1200	0.0891	0.0145	0.5984	394.9305	10.2937
2.0700	0.5429	0.3896	0.0255	1.0527	226.3010	10.3774
2.4500	0.9988	0.6915	0.0210	0.8659	278.3274	10.4982
2.7000	-0.2790	-0.2142	0.0279	1.1504	192.5032	9.6465
2.7700	-0.2722	-0.2089	0.0297	1.2221	179.4941	9.5556
3.0000	-0.1197	-0.0907	0.0272	1.1229	175.3800	8.5784
3.1500	-0.0118	-0.0089	0.0268	1.1026	157.7419	7.5764
3.4000	0.6232	0.4443	0.0259	1.0682	164.9246	7.6740
3.8500	0.6235	0.4445	0.0258	1.0639	163.8083	7.5914
4.0400	0.4593	0.3317	0.0275	1.1346	152.7103	7.5476
4.4200	0.1131	0.0840	0.0297	1.2248	147.6441	7.8774
4.5800	0.2322	0.1709	0.0362	1.4926	157.3228	10.2289
4.8000	0.6157	0.4393	0.0298	1.2298	192.8778	10.3322
5.0500	0.7211	0.5101	0.0339	1.3985	170.9247	10.4128
5.3100	0.5139	0.3696	0.0364	1.5005	166.9641	10.9133
5.6600	0.7377	0.5212	0.0338	1.3909	170.8554	10.3520
5.9400	1.0615	0.7314	0.0368	1.5185	164.0104	10.8490
6.3500	0.5706	0.4085	0.0384	1.5821	158.3194	10.9108
6.7900	1.0875	0.7479	0.0373	1.5354	167.6125	11.2099
6.9800	0.3206	0.2342	0.0361	1.4890	144.4545	9.3697
7.2700	0.7335	0.5184	0.0428	1.7653	165.3399	12.7140
7.4500	0.9140	0.6370	0.0248	1.0216	174.8706	7.7817
7.8000	0.5840	0.4177	0.0230	0.9483	186.2264	7.6923
8.2700	1.7479	1.1443	0.0255	1.0509	282.3008	12.9225
8.5000	2.6112	1.6084	0.0187	0.7712	356.5107	11.9764

COMBUSTION TUBE RUN 78- 7

TIME	CO2	O2	N2	CH4	CO
1.0500	4.5888	9.4347	83.7491	0.0000	1.2274
1.2300	6.4549	5.9247	84.7706	0.0000	1.8498
1.4600	14.2949	1.4975	78.7715	1.0075	3.4286
1.7300	18.3015	0.8819	75.4624	0.9889	3.3653
2.0200	20.3762	0.5776	74.7402	0.0000	3.3060
2.3800	20.6533	0.5687	73.2932	0.6377	3.8471
2.6800	18.7870	1.9803	74.1107	0.0000	4.1220
3.1700	16.0335	2.3324	77.2963	0.0000	3.3377
3.5400	16.0019	3.7127	76.0159	0.0000	3.2694
3.9500	15.4482	0.8933	78.6299	0.0000	4.0286
4.2000	15.7826	2.2959	76.9924	0.6436	3.2854
4.4800	17.4144	0.8991	77.8794	0.0000	2.8071
4.8500	17.0463	0.5974	78.2477	0.0000	3.1086
5.3800	17.3192	0.5756	77.8107	0.0000	3.2945
5.7100	15.7380	2.0033	78.2804	0.0000	2.9783
6.0400	17.8911	0.8480	77.3191	0.0000	2.9418
6.3600	16.7995	1.7990	77.2812	0.0000	3.1203
6.9000	17.2996	2.3400	76.3163	0.0000	3.0441
7.1500	11.1615	5.6615	80.4094	0.0000	1.7676

TIME	ATOMIC H/C RATIO	LB WATER FORMED PER LB FUEL BURNED	LB FUEL BURNED PER H O U R	LB FUEL PER CFT BULK VOL.	SCF AIR PER LB FUEL	MMSCF AIR PER AC.FT SAND
1.0500	5.2441	2.7370	0.0168	0.8274	400.6008	14.4381
1.2300	4.4454	2.4328	0.0225	1.1089	297.7753	14.3841
1.4600	0.7747	0.5458	0.0367	1.8090	166.9094	13.1523
1.7300	-0.1489	-0.1131	0.0417	2.0516	140.9898	12.5998
2.0200	-0.4626	-0.3609	0.0447	2.2008	131.2314	12.5806
2.3800	-0.5980	-0.4720	0.0468	2.3046	125.8691	12.6355
2.6800	-0.5462	-0.4292	0.0402	1.9772	135.4994	11.6699
3.1700	0.1058	0.0786	0.0340	1.6756	158.1325	11.5419
3.5400	-0.2372	-0.1815	0.0374	1.8406	160.8762	12.8986
3.9500	0.5228	0.3758	0.0441	2.1705	154.6604	14.6229
4.2000	0.1563	0.1157	0.0370	1.8219	159.3501	12.6462
4.4800	0.1949	0.1438	0.0403	1.9863	151.5110	13.1090
4.8500	0.3179	0.2323	0.0406	1.9997	151.2045	13.1710
5.3800	0.2216	0.1632	0.0402	1.9801	148.1724	12.7806
5.7100	0.3373	0.2461	0.0366	1.7999	162.6386	12.7515
6.0400	0.0659	0.0491	0.0365	1.7961	147.5672	11.5453
6.3600	0.0772	0.0575	0.0428	2.1097	154.1110	14.1623
6.9000	-0.1720	-0.1309	0.0413	2.0319	152.1564	13.4675
7.1500	1.1348	0.7775	0.0314	1.5443	227.1584	15.2813

COMBUSTION TUBE RUN 79- 1

TIME	CO2	O2	N2	CH4	CO
1.4500	2.6253	10.0864	84.7418	0.0000	1.5465
1.5800	7.5708	8.4837	81.4590	0.0000	1.4865
1.7600	2.5939	14.6373	80.8521	0.0000	0.9168
1.9600	3.0271	14.2350	81.7379	0.0000	0.0000
2.0900	5.4772	12.8533	80.6695	0.0000	0.0000
2.3800	10.9357	5.5437	79.3416	0.3159	2.8630
2.5300	11.6792	4.3820	79.4396	0.6326	2.8666
2.7400	13.3269	4.2859	77.4040	0.6187	3.3644
3.0300	12.2999	7.3838	76.6780	0.3198	2.3185
3.2000	11.6846	7.3195	76.6731	0.3302	2.9926
3.5700	12.8798	1.5464	80.2936	0.3349	3.9453
3.8000	13.8550	2.0429	78.4610	0.6320	4.0091
4.1500	14.5558	1.4325	77.6122	0.6204	4.7791
4.2300	14.8594	1.4624	78.6307	0.3167	3.7308
4.5000	13.3541	2.9152	79.8701	0.0000	2.8605
5.0600	15.0133	1.7167	77.2165	0.0000	5.0536
5.3500	13.5975	2.0778	80.4120	0.0000	2.9127
5.6200	13.1651	1.5199	78.9153	0.3291	5.0706
5.8600	12.6450	1.6151	82.2041	0.0000	2.5357
6.2000	16.1453	1.2308	78.3028	0.0000	3.3212
6.4800	16.5638	0.9179	79.1166	0.0000	2.4018
6.7800	12.5833	1.1849	81.1623	0.0000	4.0695
7.2400	11.8582	1.4831	81.8750	0.0000	3.7837
7.4000	11.5775	1.7375	81.4225	0.0000	4.2624
7.9000	11.3820	1.1883	83.2231	0.0000	3.2066
8.5400	12.2771	2.2678	80.2828	0.0000	4.1723
8.8700	11.1958	2.2880	81.5872	0.0000	3.9290

TIME	ATOMIC H/C RATIO	LB WATER FORMED PER LB FUEL BURNED	LB FUEL BURNED PER H O U R	LB FUEL PER CFT BULK VOL.	SCF AIR PER LB FUEL	MMSCF AIR PER AC.FT SAND
1.4500	8.6691	3.7748	0.0102	0.6016	471.4875	12.3565
1.5800	2.1445	1.3645	0.0155	0.9138	305.0452	12.1418
1.7600	4.3328	2.3875	0.0070	0.4090	676.4769	12.0513
1.9600	5.9009	2.9668	0.0080	0.4705	723.6549	14.8319
2.0900	2.2737	1.4336	0.0103	0.6061	495.0272	13.0697
2.3800	0.9218	0.6420	0.0240	1.4100	213.4768	13.1116
2.5300	0.9961	0.6898	0.0255	1.5007	201.6039	13.1793
2.7400	0.3069	0.2245	0.0278	1.6308	180.7740	12.8416
3.0300	-0.1259	-0.0954	0.0229	1.3457	211.9256	12.4230
3.2000	-0.0324	-0.0244	0.0287	1.6886	209.4135	15.4035
3.5700	1.1756	0.8030	0.0368	2.1655	173.7658	16.3911
3.8000	0.6615	0.4702	0.0384	2.2586	166.4172	16.3729
4.1500	0.4662	0.3365	0.0424	2.4891	154.4783	16.7490
4.2300	0.5841	0.4177	0.0407	2.3941	161.2491	16.8160
4.5000	0.8712	0.6092	0.0320	1.8834	183.5981	15.0624
5.0600	0.2530	0.1858	0.0378	2.2189	150.6613	14.5619
5.3500	1.0281	0.7102	0.0330	1.9377	179.3491	15.1385
5.6200	0.8241	0.5784	0.0358	2.1068	161.8908	14.8567
5.8600	1.6662	1.0973	0.0317	1.8658	190.0916	15.4492
6.2000	0.3653	0.2659	0.0368	2.1647	156.0616	14.7160
6.4800	0.4953	0.3568	0.0363	2.1312	160.1647	14.8690
6.7800	1.3864	0.9321	0.0340	1.9979	174.6691	15.2008
7.2400	1.6702	1.0996	0.0329	1.9363	183.6962	15.4935
7.4000	1.5651	1.0384	0.0349	2.0523	181.7945	16.2521
7.9000	2.1795	1.3834	0.0345	2.0271	193.0105	17.0430
8.5400	1.1453	0.7841	0.0342	2.0117	178.1199	15.6084
8.8700	1.6501	1.0880	0.0327	1.9207	189.5873	15.8620

COMBUSTION TUBE RUN 79- 2

TIME	CO2	O2	N2	CH4	CO
0.1700	12.5792	1.1987	81.9222	0.3553	2.9445
0.2100	14.6484	1.3545	80.1665	0.0000	2.8305
0.3100	13.2302	2.0476	80.7884	0.0000	2.9339
0.3900	12.8547	4.3105	78.9842	0.0000	2.8506
0.4600	11.6868	6.0897	77.7647	0.0000	3.4589
0.5400	10.8468	6.8110	78.3272	0.0000	3.0151
0.6100	9.6407	7.7035	79.2029	0.0000	2.4529
0.6800	9.3039	9.0525	79.0422	0.0000	1.6014
0.7600	7.4125	9.9077	79.1560	0.0000	2.5238
0.8400	7.5477	10.4036	78.9980	0.0000	2.0507
0.9300	7.7872	10.2106	78.9236	0.0000	2.0786
1.0100	7.9263	10.0463	78.9481	0.0000	2.0793
1.1800	9.4281	9.2412	77.8085	0.0000	2.5222
1.3000	10.5525	7.3152	78.2072	0.0000	2.9251
1.4500	11.4634	5.5178	78.3452	0.0000	3.6736
1.6100	10.3991	5.9569	79.4827	0.0000	3.1613
1.6700	10.8351	5.8815	79.2334	0.0000	3.0500
1.7600	10.5750	5.1145	80.2163	0.0000	3.0942
1.8400	12.0451	4.6429	78.5104	0.0000	3.8016
1.9700	13.4659	2.6665	78.2509	0.0000	4.6167
2.0500	13.0568	2.4738	79.0581	0.0000	4.4112
2.1400	13.9813	1.6631	78.9072	0.0000	4.4484
2.2300	14.1241	1.9408	77.5278	0.0000	5.4073
2.3300	13.0222	2.4930	79.8332	0.0000	3.6515
2.4100	13.1285	2.6262	79.3256	0.0000	3.9198
2.5700	12.9620	1.8197	79.9515	0.0000	4.2668
2.7500	12.8066	2.5039	80.1815	0.0000	3.5080
3.0100	13.1401	2.6556	79.3992	0.0000	3.8051
3.2900	11.3096	5.3171	79.2950	0.0000	3.0783
3.3500	8.8598	7.6149	79.8942	0.0000	2.6311
3.4000	7.3393	9.1557	80.9432	0.0000	1.5618
3.4600	7.4865	9.5002	80.4487	0.0000	1.5647
3.5200	7.6340	10.1460	78.7970	0.0000	2.4230
3.5900	8.0248	8.7039	80.1156	0.0000	2.1556
3.6600	7.8775	9.1692	79.9557	0.0000	1.9976
3.7500	7.3795	9.3645	80.2510	0.0000	2.0050
3.8700	6.7027	11.6868	78.4983	0.0000	2.1121

TIME	ATOMIC H/C RATIO	LB WATER FORMED PER LB FUEL BURNED	LB FUEL BURNED PER H O U R	LB FUEL PER CFT BULK VOL.	SCF AIR PER LB FUEL	MMSCF AIR PER AC.FT SAND
0.1700	1.6817	1.1062	0.0308	2.0700	185.0447	16.6856
0.2100	0.8906	0.6218	0.0327	2.1960	170.6933	16.3280
0.3100	1.1707	0.8000	0.0309	2.0749	182.0549	16.4547
0.3900	0.6126	0.4371	0.0287	1.9306	191.2936	16.0872
0.4600	0.3079	0.2251	0.0271	1.8168	200.1352	15.8388
0.5400	0.4778	0.3446	0.0251	1.6858	217.2527	15.9534
0.6100	0.8214	0.5766	0.0225	1.5112	245.0547	16.1317
0.6800	0.6801	0.4827	0.0201	1.3477	274.2279	16.0990
0.7600	0.9901	0.6860	0.0187	1.2580	294.2109	16.1222
0.8400	0.8430	0.5907	0.0179	1.2014	307.4420	16.0900
0.9300	0.7876	0.5543	0.0183	1.2296	300.1210	16.0749
1.0100	0.7892	0.5553	0.0186	1.2472	295.9860	16.0799
1.1800	0.2520	0.1851	0.0212	1.4270	254.9496	15.8477
1.3000	0.4330	0.3135	0.0243	1.6332	223.9079	15.9289
1.4500	0.5306	0.3811	0.0275	1.8486	198.1583	15.9571
1.6100	0.9415	0.6547	0.0255	1.7104	217.2850	16.1887
1.6700	0.8125	0.5707	0.0258	1.7339	213.6675	16.1380
1.7600	1.1959	0.8156	0.0262	1.7580	213.3499	16.3381
1.8400	0.5758	0.4121	0.0289	1.9423	189.0022	15.9907
1.9700	0.5221	0.3752	0.0329	2.2069	165.7920	15.9378
2.0500	0.7509	0.5300	0.0323	2.1708	170.2840	16.1023
2.1400	0.6743	0.4788	0.0339	2.2766	162.0647	16.0715
2.2300	0.3769	0.2740	0.0351	2.3560	153.8602	15.7906
2.3300	0.9309	0.6479	0.0313	2.1014	177.6367	16.2601
2.4100	0.7912	0.5567	0.0316	2.1253	174.5162	16.1567
2.5700	1.0071	0.6968	0.0325	2.1841	171.1607	16.2842
2.7500	1.0419	0.7190	0.0309	2.0738	180.7878	16.3311
3.0100	0.8044	0.5654	0.0315	2.1147	175.5578	16.1717
3.2900	0.8097	0.5689	0.0267	1.7963	206.4057	16.1505
3.3500	1.2000	0.8182	0.0220	1.4783	252.6954	16.2725
3.4000	1.9057	1.2334	0.0180	1.2064	313.7322	16.4862
3.4600	1.5981	1.0577	0.0179	1.1996	313.5818	16.3555
3.5200	0.7774	0.5476	0.0186	1.2524	294.1795	16.0491
3.5900	1.3713	0.9230	0.0193	1.3267	282.3522	16.3176
3.6600	1.2997	0.8795	0.0191	1.2800	292.0638	16.2851
3.7500	1.5285	1.0169	0.0184	1.2374	303.2502	16.3452
3.8700	0.6448	0.4590	0.0162	1.0863	337.8671	15.9882

COMBUSTION TUBE RUN 79- 4

TIME	CO2	O2	N2	CH4	CO
1.1300	5.6094	7.0332	85.1164	0.0000	1.2410
1.2100	10.1597	2.1187	79.1920	0.6451	6.8845
1.2900	14.5738	0.7350	79.6743	0.2238	3.7931
1.3900	13.0854	2.1482	78.1976	0.4361	5.1327
1.6200	13.1937	1.4288	78.0151	0.2175	6.1449
1.7400	15.7043	1.0446	76.0491	0.2120	5.9900
2.2000	14.4343	1.4009	78.5456	0.0000	4.6192
2.3700	11.4635	2.1573	80.6370	0.0000	4.7422
2.5400	11.6914	1.7688	80.4683	0.0000	5.0715
2.6800	11.5054	1.4796	81.7729	0.0000	4.2422
2.8200	12.8054	1.0978	80.8999	0.0000	4.1969
2.9200	9.5513	1.3102	82.8794	0.0000	5.2591
3.1000	10.8235	1.4847	82.6479	0.0000	4.0440
3.2100	11.3879	1.7434	79.8703	0.0000	5.9984
3.3200	11.7786	1.4777	81.0829	0.0000	4.6607
3.5800	11.7222	1.2562	80.8762	0.0000	5.1454
3.8200	10.5989	1.2893	81.8307	0.0000	5.2810
3.9100	10.7897	1.4605	81.3058	0.0000	5.4440
4.1300	11.5308	2.8933	79.1838	0.0000	5.3922
4.4400	8.7368	5.2552	81.4749	0.0000	3.5331
4.5800	8.7821	6.0232	81.8200	0.0000	2.3746
4.7300	6.9407	8.5684	80.8295	0.0000	2.6615
4.8300	5.6362	9.9660	80.6963	0.0000	2.7016
5.0500	6.4962	9.2821	81.0926	0.0000	2.1291
5.1500	5.1913	11.4974	80.6098	0.0000	1.7014
5.4000	2.8416	14.2513	79.8116	0.0000	2.0955
5.6200	2.4495	15.5647	80.3483	0.0000	0.6375
5.9000	3.2722	13.9629	81.1067	0.0000	0.6581
6.3700	1.2040	17.9986	79.7974	0.0000	0.0000

TIME	ATOMIC H/C RATIO	LB WATER FORMED PER LB FUEL BURNED	LB FUEL BURNED PER H O U R	LB FUEL PER CFT BULK VOL.	SCF AIR PER LB FUEL	MMSCF AIR PER AC.FT SAND
1.1300	5.4670	2.8169	0.0173	1.0028	341.2648	14.9070
1.2100	1.2510	0.8496	0.0319	1.8547	168.2164	13.5905
1.2900	0.8654	0.6054	0.0324	1.8790	161.7592	13.2396
1.3900	0.6558	0.4664	0.0311	1.8086	162.7096	12.8190
1.6200	0.6295	0.4486	0.0375	2.1778	153.2429	14.5375
1.7400	0.0870	0.0648	0.0403	2.3382	139.1371	14.1712
2.2000	0.5741	0.4109	0.0346	2.0078	157.2840	13.7562
2.3700	1.3436	0.9062	0.0312	1.8122	178.8994	14.1225
2.5400	1.2872	0.8719	0.0321	1.8666	173.3224	14.0929
2.6800	1.6843	1.1078	0.0311	1.8060	182.0474	14.3214
2.8200	1.2947	0.8765	0.0326	1.8944	171.7012	14.1685
2.9200	2.3065	1.4510	0.0300	1.7400	187.6538	14.2233
3.1000	2.0554	1.3161	0.0299	1.7353	189.7428	14.3424
3.2100	1.1735	0.8017	0.0331	1.9195	167.2966	13.9882
3.3200	1.4519	0.9714	0.0319	1.8533	175.9033	14.2006
3.5800	1.4104	0.9466	0.0326	1.8957	171.5288	14.1644
3.8200	1.8196	1.1850	0.0317	1.8392	178.8894	14.3315
3.9100	1.6363	1.0800	0.0324	1.8789	176.2062	14.4218
4.1300	0.9286	0.6464	0.0320	1.8604	173.6283	14.0708
4.4400	1.9232	1.2432	0.0253	1.4684	228.7998	14.6344
4.5800	2.0640	1.3208	0.0234	1.3583	250.1639	14.8012
4.7300	1.9356	1.2501	0.0199	1.1583	289.7933	14.6220
4.8300	2.1579	1.3717	0.0187	1.0851	327.9570	15.5022
5.0500	2.1859	1.3868	0.0216	1.2560	317.9536	17.3958
5.1500	2.2566	1.4245	0.0174	1.0087	393.5417	17.2923
5.4000	2.4914	1.5473	0.0133	0.7739	535.1789	18.0410
5.6200	3.9202	2.2162	0.0101	0.5843	784.3278	19.9631
5.9000	4.0666	2.2780	0.0123	0.7169	616.1879	19.2426
6.3700	6.6757	3.2171	0.0042	0.2411	1702.5729	17.8845

COMBUSTION TUBE RUN 79- 6

TIME	CO2	O2	N2	CH4	CO
0.5900	1.6792	11.0200	85.2258	0.3116	0.7633
0.7900	5.9474	5.5334	83.6973	0.6271	3.1949
1.0200	9.0982	3.8649	82.6230	0.5276	2.8863
1.2100	9.8405	4.1568	82.1394	0.1327	2.7306
1.3600	9.4819	4.7558	82.2599	0.1320	2.3705
1.5100	9.5299	4.5907	81.9224	0.1747	2.7823
1.7600	9.9738	3.2745	82.7492	0.1800	2.8224
1.9200	10.4272	2.0440	81.3028	0.6157	4.6104
2.1300	9.1610	1.6171	83.0296	0.4446	4.7478
2.3800	7.8243	2.0426	84.8159	0.1797	4.1375
2.5900	9.7903	1.4569	82.9793	0.2704	4.5031
2.9700	10.5297	1.5539	82.4052	0.2126	4.2987
3.1000	8.7526	1.1189	85.0576	0.0923	3.9785
3.4900	9.2742	1.8421	83.9932	0.2735	3.6171
3.7100	10.0912	1.8648	82.6361	0.3061	4.1018
3.8200	10.2895	1.6836	82.4556	0.2252	4.3461
3.9500	11.4299	1.1968	81.8160	0.2278	4.3295
4.1300	7.9366	4.8275	83.6556	0.1753	2.4050
4.2900	2.5235	8.2349	86.0113	0.0000	2.2303
4.4700	2.8554	8.7165	85.9059	0.0000	1.5222
4.6600	6.0187	7.2231	83.8629	0.0000	1.8953
4.9200	6.1884	6.1230	84.5831	0.0000	2.1055
5.2500	5.5398	7.6228	83.7661	0.0000	2.0713
5.4100	7.2346	5.5788	84.0142	0.0000	2.1724
5.7900	7.2321	4.4970	83.3636	0.3852	3.5221
6.0200	12.1627	1.1993	81.1761	0.3469	4.1151
6.2700	11.9560	1.2610	81.9307	0.1387	3.7136
6.7300	11.8687	1.2518	81.6939	0.2294	3.9562
7.3200	9.1670	2.1028	83.7786	0.3167	3.6349
7.7800	12.3682	1.2818	83.9858	1.2686	0.0956

TIME	ATOMIC H/C RATIO	LB WATER FORMED PER LB FUEL BURNED	LB FUEL BURNED PER H O U R	LB FUEL PER CFT BULK VOL.	SCF AIR PER LB FUEL	MMSCF AIR PER AC.FT SAND
0.5900	15.6789	5.0981	0.0128	0.8318	604.7752	21.9123
0.7900	4.0124	2.2552	0.0200	1.2982	274.2943	15.5118
1.0200	2.5222	1.5631	0.0243	1.5762	227.7524	15.6372
1.2100	2.0593	1.3183	0.0247	1.6006	222.9607	15.5457
1.3600	2.1746	1.3808	0.0235	1.5215	234.9002	15.5685
1.5100	2.0354	1.3052	0.0242	1.5650	227.4340	15.5046
1.7600	2.2935	1.4441	0.0256	1.6565	217.0473	15.6611
1.9200	1.8183	1.1843	0.0291	1.8819	187.7093	15.3874
2.1300	2.5651	1.5850	0.0283	1.8347	196.6277	15.7142
2.3800	3.5481	2.0538	0.0242	1.5699	218.7843	14.9619
2.5900	2.3952	1.4975	0.0288	1.8634	193.4760	15.7047
2.9700	2.0696	1.3239	0.0214	1.3832	189.4918	11.4175
3.1000	3.3774	1.9767	0.0292	1.8901	208.4379	17.1611
3.4900	2.9175	1.7602	0.0269	1.7416	209.5387	15.8966
3.7100	2.2433	1.4175	0.0283	1.8308	196.1095	15.6397
3.8200	2.1242	1.3536	0.0289	1.8721	191.3617	15.6056
3.9500	1.7658	1.1545	0.0303	1.9647	180.9287	15.4845
4.1300	3.1991	1.8943	0.0220	1.4235	255.3298	15.8327
4.2900	9.2475	3.9171	0.0141	0.9148	408.5254	16.2785
4.4700	9.5969	3.9993	0.0132	0.8562	435.9224	16.2586
4.6600	4.0956	2.2901	0.0172	1.1144	315.8485	15.3329
4.9200	4.3984	2.4140	0.0202	1.3108	298.3567	17.0352
5.2500	4.2405	2.3500	0.0178	1.1554	325.1126	16.3621
5.4100	3.5860	2.0707	0.0220	1.4230	274.9033	17.0406
5.7900	3.2247	1.9063	0.0230	1.4912	244.2646	15.8667
6.0200	1.5135	1.0080	0.0317	2.0560	177.0435	15.8562
6.2700	1.7117	1.1235	0.0316	2.0486	182.9407	16.3254
6.7300	1.6727	1.1010	0.0292	1.8930	181.1365	14.9353
7.3200	2.8693	1.7367	0.0231	1.4930	211.1458	13.7319
7.7800	2.7688	1.6873	0.0398	2.5793	218.8876	24.5925

COMBUSTION TUBE RUN 79- 7

TIME	CO2	O2	N2	CH4	CO
0.6700	11.7046	1.6749	81.6977	1.0641	2.8688
0.9800	11.9527	2.9623	81.5369	0.4570	2.0910
1.3200	11.3749	4.1319	81.4373	0.1000	1.9559
2.1400	11.2429	3.5762	81.9060	0.2519	2.0229
2.5700	12.2085	2.5933	81.7269	0.3591	2.1122
2.7900	14.0565	1.2760	80.9205	0.3150	2.4319
4.1500	12.4436	1.1778	82.6830	0.5267	2.1688
4.7300	12.3311	1.2224	82.5511	0.5763	2.3190
6.1500	10.3172	1.1464	85.6102	0.1608	1.7655
7.5100	11.5617	2.0151	82.8248	0.5182	2.0803
7.9500	11.7003	1.1726	83.2245	0.4195	2.4831
8.2000	12.0550	0.8243	83.3466	0.2649	2.5092
8.4800	10.8946	1.2105	83.5456	0.5188	2.8305
8.7200	12.0716	1.0318	83.3934	0.3184	2.1849
9.1400	12.2471	0.8730	83.0061	0.2641	2.6098
9.4200	10.6033	1.5357	84.5371	0.3161	2.0068
9.8100	11.0121	1.1216	83.9128	0.5244	2.4291
10.2600	8.5111	2.7375	85.3362	0.3072	2.1080

TIME	ATOMIC H/C RATIO	LB WATER FORMED PER LB FUEL BURNED	LB FUEL BURNED PER H O U R	LB FUEL PER CFT BULK VOL.	SCF AIR PER LB FUEL	MMSCF AIR PER AC.FT SAND
0.6700	1.8940	1.2269	0.0184	2.3396	193.5444	19.7249
0.9800	1.6274	1.0748	0.0205	2.5959	204.3943	23.1126
1.3200	1.5492	1.0291	0.0222	2.8130	216.3042	26.5043
2.1400	1.7916	1.1692	0.0205	2.6042	214.7715	24.3637
2.5700	1.6357	1.0814	0.0219	2.7801	200.7421	24.3105
2.7900	1.2037	0.8205	0.0244	3.0989	178.3171	24.0706
4.1500	1.9910	1.2607	0.0245	3.1155	194.0250	26.3310
4.7300	1.9743	1.2715	0.0264	3.3460	193.4477	28.1957
6.1500	3.4465	2.0081	0.0239	3.0316	220.0609	29.0607
7.5100	2.1697	1.3781	0.0199	1.5781	205.5581	14.1301
7.9500	2.2585	1.4256	0.0221	1.7568	197.4269	15.1084
8.2000	2.2031	1.3960	0.0227	1.7969	193.2999	15.1306
8.4800	2.5320	1.5681	0.0218	1.7326	200.9537	15.1667
8.7200	2.2357	1.4140	0.0222	1.7632	197.1150	15.1391
9.1400	2.0570	1.3170	0.0350	2.7759	190.6793	23.0570
9.4200	2.9599	1.7803	0.0316	2.5074	214.9994	23.4823
9.8100	2.6657	1.6359	0.0338	2.6821	204.2198	23.6595
10.2600	3.9106	2.2121	0.0374	2.9708	242.3100	31.3568

COMBUSTION TUBE RUN 79- 7 (Top)

TIME	CO2	O2	N2	CH4	CO	ATOMIC H/C RATIO	LB WATER FORMED PER LB FUEL BURNED	LB FUEL BURNED PER H O U R	LB FUEL PER CFT BULK VOL.	SCF AIR PER LB FUEL	MMSCF AIR PER AC.FT SAND
0.4600	6.3425	5.6744	83.9306	0.0000	3.0525	3.7329	2.1354	0.0162	2.0544	272.4129	24.3785
0.7400	13.2111	4.0910	80.4747	1.0202	3.2030	1.3375	0.9025	0.0199	2.5296	176.3519	19.4320
1.1000	11.7824	1.4990	82.2388	0.4112	3.0686	1.8976	1.2289	0.0221	2.7996	191.1589	23.3116
1.3900	7.9040	6.7022	82.7801	0.0475	1.5661	2.7943	1.6999	0.0172	2.1819	283.4577	26.9413
1.7800	6.4200	7.1793	84.0850	0.0000	1.3157	4.1656	2.3274	0.0140	1.7822	322.1852	25.0119
2.3300	12.1811	2.6777	80.6977	0.3505	3.0930	1.3214	0.8928	0.0228	2.8962	190.2684	24.0043
3.4000	11.2937	4.1510	81.2121	0.2979	2.0443	1.5354	1.0209	0.0202	2.5699	215.7938	24.1573
3.7200	4.1033	10.9933	83.3620	0.0000	0.5414	5.8494	2.9494	0.0093	1.1801	482.3896	24.7968
3.8400	2.7760	10.9670	84.8941	0.0000	0.3629	11.0133	4.3071	0.0081	1.0282	563.8128	25.2526

COMBUSTION TUBE RUN 79- 7 (MIddle)

TIME	CO2	O2	N2	CH4	CO	ATOMIC H/C RATIO	LB WATER FORMED PER LB FUEL BURNED	LB FUEL BURNED PER H O U R	LB FUEL PER CFT BULK VOL.	SCF AIR PER LB FUEL	MMSCF AIR PER AC.FT SAND
0.5200	14.3998	1.6201	80.2117	0.6249	2.1443	1.0230	0.7070	0.0196	2.4894	178.6152	19.3685
0.8400	12.9663	1.5007	81.1053	0.5145	2.9132	1.4197	0.9521	0.0228	2.8905	182.5925	22.9992
1.1700	9.2701	4.4281	83.1148	0.1485	2.0385	2.6091	1.6074	0.0177	2.2409	241.3561	23.5599
1.4700	10.3825	3.6327	82.8567	0.1010	2.0271	2.2552	1.4238	0.0217	2.7550	224.7023	26.9662
1.8900	10.6136	3.5870	82.6677	0.0505	2.0811	2.1217	1.3522	0.0201	2.5518	221.2256	24.5903
2.4200	11.6279	2.1617	82.6645	0.3103	2.2356	2.0389	1.3071	0.0218	2.7704	203.7618	24.5894
3.4800	13.5933	1.3503	80.4676	0.4115	3.1772	1.1587	0.7925	0.0247	3.1411	174.9338	23.9359
3.7800	12.8358	1.3103	81.5669	0.7257	2.5613	1.6251	1.0735	0.0235	2.9861	186.5288	24.2629
3.8900	11.6034	1.5234	83.1368	0.3656	2.3658	2.2284	1.4095	0.0223	2.8301	200.5972	24.7299
4.5100	12.3001	2.6935	81.6419	0.4104	1.9541	1.6084	1.0637	0.0250	3.1704	201.9180	27.8851
4.9000	11.1301	0.9275	84.2815	0.4240	2.2369	2.7614	1.6836	0.0254	3.2249	204.9194	28.7867
5.3600	11.7782	1.1074	82.5696	0.8801	2.6648	2.1411	1.3627	0.0229	2.9071	193.9514	24.5611
5.6400	10.2959	1.1960	85.5355	0.3209	1.6517	3.4884	2.0271	0.0259	3.2848	221.7536	31.7294
5.9900	10.7041	1.6195	83.8898	0.0000	2.7866	2.5448	1.5747	0.0251	3.1873	205.1064	28.4767
6.7500	8.5323	3.1435	85.4253	0.1026	1.7963	3.9247	2.2181	0.0224	2.8370	249.1659	30.7917
6.8700	8.0044	3.8540	85.5198	0.0000	1.6218	4.1818	2.3259	0.0201	2.5459	263.3877	29.2096
6.9300	9.0867	3.0289	85.3924	0.1558	1.3363	3.8053	2.1668	0.0212	2.6925	248.6787	29.1661
7.0100	2.4353	8.8394	87.2478	0.0000	0.4775	16.0378	5.1481	0.0105	0.8343	512.5109	18.6249
7.1500	1.5748	10.0611	86.9010	0.0000	0.4632	22.0473	5.8279	0.0071	0.5664	600.8429	14.8255
8.0700	11.1311	1.0307	84.2846	0.3710	2.1826	2.7496	1.6778	0.0215	1.7059	205.9130	15.3009

COMBUSTION TUBE RUN 79- 7 (Bottom)

TIME	CO2	O2	N2	CH4	CO	ATOMIC H/C RATIO	LB WATER FORMED PER LB FUEL BURNED	LB FUEL BURNED PER H O U R	LB FUEL PER CFT BULK VOL.	SCF AIR PER LB FUEL	MMSCF AIR PER AC.FT SAND
0.6000	11.9623	1.7294	81.5625	0.7115	3.0344	1.7263	1.1319	0.0187	2.3785	190.0874	19.6947
0.9100	11.5918	2.9382	81.5406	0.8563	2.0740	1.7883	1.1673	0.0201	2.5557	207.6186	23.1136
1.2400	10.3304	3.7610	82.6892	0.1507	2.0687	2.2114	1.4005	0.0191	2.4196	225.1299	23.7286
1.7200	10.3082	4.4461	82.2515	0.0497	1.9445	2.0037	1.2878	0.0192	2.4423	229.9751	24.4655
2.0700	10.8316	3.3404	82.4369	0.0505	2.3406	1.9955	1.2833	0.0207	2.6241	214.5296	24.5217
2.4900	12.1669	2.9216	81.4547	0.2547	2.2021	1.5208	1.0123	0.0218	2.7654	201.1410	24.2295
3.5600	13.9956	1.1650	80.6367	0.5210	2.6817	1.1833	0.8078	0.0247	3.1295	175.9528	23.9862
3.9900	11.5800	1.5137	82.8777	0.5709	2.4576	2.1965	1.3925	0.0223	2.8366	199.5156	24.6528
4.6200	12.2323	1.2585	82.1194	0.7249	2.6650	1.8811	1.2197	0.0266	3.3798	190.5137	28.0482
5.0200	11.0462	1.0228	84.0194	0.4208	2.4908	2.6652	1.6357	0.0197	2.5000	203.0390	22.1109
5.4400	10.5579	1.3594	83.8019	0.8286	2.4522	2.8080	1.7066	0.0216	2.7422	208.6836	24.9277
5.5900	10.7084	1.5189	83.9038	0.8853	1.9035	2.8630	1.7336	0.0264	3.3485	213.3814	31.1241
6.0600	10.1410	1.5355	84.9936	0.1054	2.2234	3.1717	1.8915	0.0240	3.0471	217.3652	28.8514
6.8200	9.7275	0.8750	85.6307	0.4235	2.3433	3.6413	2.0952	0.0243	3.0858	217.5561	29.2475
7.0900	8.0542	0.7804	87.8043	0.2676	2.0934	5.3053	2.7591	0.0226	1.7938	239.8746	18.7437
9.0300	11.6643	1.2706	83.1206	0.5228	2.4217	2.2575	1.4250	0.0336	2.6694	198.5604	23.0888
9.2400	12.9217	0.8353	83.0965	0.3222	1.8242	2.0127	1.2927	0.0346	2.7466	192.9302	23.0821
9.3500	13.3189	0.8308	82.4468	0.5341	1.8693	1.7992	1.1735	0.0373	2.9613	188.7222	24.3443
9.5000	13.5731	0.8467	83.0755	0.2721	1.2326	1.9039	1.2324	0.0353	2.8009	193.6056	23.6214
9.6300	14.9477	1.2975	80.7968	0.6940	1.2640	1.1351	0.7777	0.0365	2.8973	182.0311	22.9735
9.6900	15.3282	1.0481	80.8639	0.5390	1.2207	1.0898	0.7493	0.0372	2.9474	179.0367	22.9926
9.7600	14.1306	0.9048	82.7908	0.3285	0.8453	1.7494	1.1451	0.0353	2.8016	192.8935	23.5405
9.8700	13.0542	0.9495	83.4462	0.5426	1.0054	2.1828	1.3551	0.0342	2.7135	200.7340	23.7268
9.9700	10.9428	2.9280	82.7751	0.3573	1.9968	2.2054	1.3973	0.0407	3.2320	216.0417	30.4157
10.0400	10.3747	4.2601	83.7815	0.0000	0.5837	2.6808	1.6435	0.0357	2.8288	249.8405	30.7855

COMBUSTION TUBE RUN 80- 1

TIME	CO2	O2	N2	CH4	CO
0.7300	13.3391	1.5947	77.0656	0.0000	7.0007
0.9700	12.2265	2.8912	76.3022	0.0000	7.5802
1.3100	9.8182	3.8566	80.1723	0.0000	5.1528
1.4500	9.8182	3.8566	80.1723	0.0000	5.1528
1.6500	6.8277	8.6833	81.9641	0.0000	1.5248
1.7900	4.5859	10.2793	82.4426	0.0000	1.6923
1.9500	4.2897	10.5983	82.6111	0.0000	1.5009
2.1500	3.5599	12.9376	81.5683	0.0000	0.9342
2.3500	4.2787	12.7879	80.9977	0.0000	0.9357
2.6500	4.7517	11.6952	81.0861	0.0000	1.4669
2.9200	6.9744	6.6701	83.1593	0.0000	2.1962
3.1700	7.6346	6.9697	82.7565	0.0000	1.6392
3.4500	7.5438	6.5588	83.4577	0.0000	1.4397
3.7500	6.9042	5.7777	84.8688	0.0000	1.4494
4.0100	7.4141	5.6403	84.1769	0.0000	1.7687
4.9200	6.4947	7.4536	83.3474	0.0000	1.7043
5.5000	5.3809	7.0604	85.1811	0.0000	1.3776
6.1300	5.4417	6.1956	86.0028	0.0000	1.3600
6.4600	5.6802	7.5450	83.7874	0.0000	1.9874
6.7500	5.8830	7.0330	84.3687	0.0000	1.7153
7.4500	5.9980	6.0550	85.1982	0.0000	1.7488
7.9500	5.9980	6.0550	85.1982	0.0000	1.7488
8.5500	6.7326	6.4390	84.4150	0.0000	1.4134
9.0500	5.7215	7.1580	84.7238	0.0000	1.3966
9.5500	6.6219	6.3331	84.6549	0.0000	1.3901
10.2200	5.5057	5.7592	86.2902	0.0000	1.4448
10.6500	5.6121	6.0702	85.7398	0.0000	1.5779

TIME	ATOMIC H/C RATIO	LB WATER FORMED PER LB FUEL BURNED	LB FUEL BURNED PER H O U R	LB FUEL PER CFT BULK VOL.	SCF AIR PER LB FUEL	MMSCF AIR PER AC.FT SAND
0.7300	0.4035	0.2928	0.0353	3.5826	146.5489	22.8700
0.9700	0.2777	0.2036	0.0340	3.4533	150.5290	22.6434
1.3100	1.3520	0.9113	0.0280	2.8386	192.4136	23.7919
1.4500	1.3520	0.9113	0.0280	2.8386	192.4136	23.7919
1.6500	2.6409	1.6234	0.0171	1.7366	321.5526	24.3237
1.7900	3.9527	2.2300	0.0140	1.4222	394.9125	24.4657
1.9500	4.3667	2.4012	0.0133	1.3458	418.1839	24.5157
2.1500	4.1994	2.3331	0.0102	1.0338	537.5197	24.2062
2.3500	3.0658	1.8315	0.0110	1.1156	494.6377	24.0369
2.6500	2.8136	1.7094	0.0129	1.3082	422.2833	24.0631
2.9200	3.2116	1.9002	0.0195	1.9810	285.9915	24.6784
3.1700	2.8358	1.7203	0.0192	1.9538	288.5669	24.5588
3.4500	3.2782	1.9311	0.0192	1.9490	291.7167	24.7669
3.7500	4.3830	2.4078	0.0191	1.9434	297.5042	25.1856
4.0100	3.6753	2.1102	0.0201	2.0441	280.5536	24.9803
4.9200	3.5884	2.0718	0.0179	1.8149	312.8573	24.7342
5.5000	5.6302	2.8742	0.0167	1.6921	342.9623	25.2783
6.1300	6.2010	3.0663	0.0173	1.7580	333.2852	25.5222
6.4600	4.2014	2.3339	0.0174	1.7641	323.5784	24.8647
6.7500	4.5555	2.4765	0.0176	1.7863	321.7623	25.0372
7.4500	5.0190	2.6541	0.0184	1.8722	310.0186	25.2834
7.9500	5.0190	2.6541	0.0184	1.8722	310.0186	25.2834
8.5500	4.2039	2.3349	0.0185	1.8744	306.8097	25.0510
9.0500	5.0259	2.6567	0.0169	1.7210	335.3845	25.1426
9.5500	4.4199	2.4226	0.0184	1.8682	308.7094	25.1222
10.2200	6.3020	3.0990	0.0178	1.8064	325.4304	25.6075
10.6500	5.7415	2.9126	0.0178	1.8114	322.4600	25.4441

COMBUSTION TUBE RUN 80- 1 (Top)

TIME	CO2	O2	N2	CH4	CO	ATOMIC H/C RATIO	LB WATER FORMED PER LB FUEL BURNED	LB FUEL BURNED PER H O U R	LB FUEL PER CFT BULK VOL.	SCF AIR PER LB FUEL	MMSCF AIR PER AC.FT SAND
1.8000	4.2000	11.2500	81.7500	0.0000	1.8000	3.5873	2.0713	0.0131	1.3281	419.3499	24.2601
1.9000	4.2000	11.2500	81.7500	0.0000	1.8000	3.5873	2.0713	0.0131	1.3281	419.3499	24.2601
2.0000	4.0000	13.7500	79.8500	0.0000	1.4000	2.0563	1.3166	0.0196	1.0779	504.6887	23.6963
2.2000	2.2000	16.0000	80.0000	0.0000	0.8000	3.5544	2.0566	0.0065	0.6626	822.4829	23.7408
2.5000	1.0000	18.0000	79.6000	0.0000	0.4000	5.5985	2.8631	0.0034	0.3499	1549.9597	23.6221
4.1000	0.4000	20.0000	78.4000	0.0000	0.2000	2.2700	1.4317	0.0012	0.1216	4392.9169	23.2660

COMBUSTION TUBE RUN 80- 1 (Middle)

TIME	CO2	O2	N2	CH4	CO	ATOMIC H/C RATIO	LB WATER FORMED PER LB FUEL BURNED	LB FUEL BURNED PER H O U R	LB FUEL PER CFT BULK VOL.	SCF AIR PER LB FUEL	MMSCF AIR PER AC.FT SAND
2.3000	4.2000	10.7500	82.9500	0.0000	1.1000	4.9434	2.6258	0.0126	1.2752	443.1515	24.6162
3.1000	8.2000	4.7500	82.9500	0.0000	3.1000	2.6726	1.6393	0.0232	2.3545	240.0181	24.6162
3.3000	8.2000	4.7500	82.9500	0.0000	3.1000	2.6726	1.6393	0.0232	2.3545	240.0181	24.6162
3.5000	7.8000	4.7000	83.5000	0.0000	3.0000	3.0356	1.8171	0.0227	2.3060	246.6909	24.7794
4.9000	6.6000	8.2500	81.6500	0.0000	2.5000	2.4635	1.5329	0.0184	1.8690	297.6144	24.2304
5.0000	6.2000	8.7500	81.6500	0.0000	2.4000	2.5835	1.5943	0.0175	1.7810	312.3269	24.2304
5.1000	6.0000	9.7500	81.0500	0.0000	2.2000	2.2902	1.4424	0.0164	1.6640	331.8277	24.0524
5.2000	5.6000	10.7500	80.6500	0.0000	2.0000	2.1519	1.3685	0.0150	1.5273	359.7396	23.9337
5.3000	4.8000	12.0000	80.4000	0.0000	1.8000	2.2255	1.4080	0.0131	1.3333	410.8235	23.8595
5.7000	3.2000	14.0000	80.7000	0.0000	1.1000	3.4436	2.0068	0.0093	0.9430	582.9992	23.9484
5.8000	2.8000	15.5000	79.7000	0.0000	1.0000	2.5117	1.5577	0.0077	0.7831	693.3776	23.6510
5.9000	2.2000	16.5000	79.5000	0.0000	0.8000	2.7105	1.6583	0.0062	0.6267	864.2299	23.5924
6.0000	2.0000	17.2500	79.0500	0.0000	0.7000	2.0938	1.3370	0.0053	0.5404	996.6057	23.4589
6.9000	1.0000	18.0000	79.6000	0.0000	0.4000	5.5985	2.8631	0.0034	0.3499	1549.9597	23.6221

COMBUSTION TUBE RUN 80- 1 (Bottom)

TIME	CO2	O2	N2	CH4	CO	ATOMIC H/C RATIO	LB WATER FORMED PER LB FUEL BURNED	LB FUEL BURNED PER H O U R	LB FUEL PER CFT BULK VOL.	SCF AIR PER LB FUEL	MMSCF AIR PER AC.FT SAND
2.4000	4.4000	10.5000	82.2000	0.0000	1.9000	3.8099	2.1688	0.0139	1.4144	395.9256	24.3937
3.5000	7.8000	4.8000	83.4000	0.0000	3.0000	2.9887	1.7946	0.0226	2.2988	247.1662	24.7498
4.0000	7.6000	4.6000	83.8000	0.0000	3.0000	3.2362	1.9116	0.0226	2.2934	248.9278	24.8685
5.4000	6.0000	6.2500	84.2500	0.0000	2.5000	4.1861	2.3276	0.0192	1.9537	293.7782	25.0020
5.6000	6.2000	6.2500	84.0500	0.0000	2.5000	3.9735	2.2388	0.0194	1.9734	290.1549	24.9427
6.2000	5.8000	6.5000	84.4000	0.0000	2.3000	4.4373	2.4296	0.0186	1.8907	304.1167	25.0465
6.4000	5.8000	6.2500	84.5500	0.0000	2.4000	4.5002	2.4546	0.0189	1.9214	299.7946	25.0910
6.7000	6.0000	6.0000	84.6000	0.0000	2.4000	4.4231	2.4239	0.0193	1.9590	294.2028	25.1059
7.1000	6.0000	5.7500	84.8500	0.0000	2.4000	4.5738	2.4837	0.0195	1.9770	292.3894	25.1801
7.2000	6.4000	5.2500	84.7500	0.0000	2.6000	4.2571	2.3567	0.0205	2.0777	277.8857	25.1504
7.3000	6.6000	5.2500	84.5500	0.0000	2.6000	4.0545	2.2729	0.0207	2.0974	274.6259	25.0910
7.5000	6.6000	5.0000	84.8000	0.0000	2.6000	4.1921	2.3301	0.0208	2.1154	273.0974	25.1652
7.8000	6.8000	5.0000	84.5000	0.0000	2.7000	3.9209	2.2164	0.0212	2.1478	268.0272	25.0762
8.0000	7.0000	4.7500	84.4500	0.0000	2.8000	3.7954	2.1626	0.0216	2.1902	261.7309	25.0614
8.3000	7.2000	5.0000	84.0000	0.0000	2.8000	3.4916	2.0285	0.0217	2.1999	260.1320	24.9278
8.5000	7.2000	5.2500	83.7500	0.0000	2.8000	3.3651	1.9711	0.0215	2.1819	261.4945	24.8536
8.7000	7.0000	5.7500	83.4500	0.0000	2.8000	3.2787	1.9314	0.0209	2.1263	267.3775	24.7646
9.0000	6.7000	6.7500	82.9500	0.0000	2.6000	3.1398	1.8665	0.0197	1.9994	282.6349	24.6162
9.1000	6.3000	7.7500	82.5000	0.0000	2.4500	3.0425	1.8203	0.0184	1.8691	300.7040	24.4827
9.2000	6.0000	9.0000	81.7000	0.0000	2.3000	2.6832	1.6447	0.0170	1.7306	321.6135	24.2453
9.3000	5.6000	10.0000	81.3000	0.0000	2.1000	2.5773	1.5912	0.0157	1.5939	347.4829	24.1266
9.5000	5.0000	11.5000	80.6500	0.0000	1.8500	2.3437	1.4706	0.0137	1.3953	393.7897	23.9337
9.7000	4.0000	12.7500	80.7500	0.0000	1.5000	2.8838	1.7438	0.0114	1.1625	473.2372	23.9634
10.0000	3.0000	15.1200	79.8300	0.0000	1.0500	2.5438	1.5742	0.0082	0.8364	650.1961	23.6903
10.2500	2.2000	16.5000	79.5000	0.0000	0.8000	2.7105	1.6583	0.0062	0.6267	864.2299	23.5924
10.6000	1.4000	18.1200	78.9300	0.0000	0.5500	2.4336	1.5175	0.0039	0.3997	1345.3773	23.4233

Appendix C

DERIVATION OF EQUATIONS USED IN THE ANALYSIS OF REACTION RATE DATA

This appendix presents the derivation of expressions useful for interpreting reaction kinetic data. These include the relationship between injected and produced gas rates, the interpretative relations for isothermal experiments, and the interpretative relations for non-isothermal experiments. Some of the equations presented in this appendix are generalizations of those originally derived by Weijdema (1968).

C.1 Derivation of the Coefficient for Flow Rate Adjustment

In all runs the injection rate was held constant. Changes in gas composition and volume due to reaction made it necessary to convert the injection rate into the exit flow rate. Designating ν_i and ν_o as the nitrogen concentration and γ_i and γ_o as the oxygen concentration in the inlet and outlet, respectively, and assuming the nitrogen does not react, then:

$$q_i \nu_i = q_o \nu_o \tag{C-1}$$

Also, assuming only oxygen, nitrogen, and carbon oxides exist in the produced gas:

$$\nu_o = 1 - CO_2 - CO - \gamma_o \tag{C-2}$$

where "CO_2", "CO" and "γ_o" are the concentrations in the effluent gas as measured by the analyzers. Thus from Eqs. C-1 and C-2:

$$\nu_i q_i = (1 - CO_2 - CO - \gamma_o)\ q_o \tag{C-3}$$

or,

$$q_o = \nu_i q_i/(1 - CO_2 - CO - \gamma_o) \tag{C-4}$$

If the change in oxygen concentration is desired, then:

$$q_i \Delta\gamma = q_i \gamma_i - q_o \gamma_o = q_i \left[\gamma_i - \nu_i \gamma_o/(1 - CO_2 - CO - \gamma_o)\right] \tag{C-5}$$

Equation C-5 can be divided by q_i to get $\Delta\gamma$. Thus:

$$\Delta\gamma = \gamma_i - \frac{\nu_i \gamma_o}{1 - CO_2 - CO - \gamma_o} = \frac{\left[\gamma_i(1 - CO_2 - CO) - \gamma_o\right]}{1 - CO_2 - CO - \gamma_o} \tag{C-6}$$

Equation C-6 was used throughout the gas analysis to calculate the oxygen consumed.

Assuming a small change in flow rate ($q_i = q_o$), $\Delta\gamma$ is a measure of the oxygen utilization.

C.2 Derivation of Equations for Isothermal Oxidation

The rate of oxygen consumption per unit volume is:

$$\frac{q\Delta\gamma}{AL} = A_r p_{O_2}{}^m C_f{}^n \exp(-E/RT) \tag{C-7}$$

This is also equal to the rate of decrease of oil saturation:

$$\frac{q\Delta\gamma}{AL} = -\alpha \frac{dC_f}{dt} \tag{C-8}$$

in which α is the proportionality factor, equal to the amount of oxygen in moles that reacts with one gram of the oil.

Combining Eqs. C-7 and C-8:

$$- \alpha \frac{dC_f}{dt} = A_r p_{O_2}{}^m \exp(-E/RT)\ C_f{}^n \qquad \text{(C-9)}$$

At constant mass flow rate and at isothermal conditions:

$$- \frac{dC_f}{dt} = \beta C_f{}^n \qquad \text{(C-10)}$$

where:

$$\beta = \frac{1}{\alpha} A_r p_{O_2}{}^m \exp(-E/RT) \qquad \text{(C-11)}$$

Integrating Eq. C-10 between 0 and t and noting that $C_f(0) = S_o$:

$$C_f{}^{1-n} - S_o{}^{1-n} = \beta(n-1)t,\ n \neq 1; \qquad \text{(C-12a)}$$

and:

$$\ell n \frac{S_o}{C_f} = \beta t,\ n = 1 \qquad \text{(C-12b)}$$

From Eq. C-12a:

$$C_f = \left[(n-1)\ \beta t + S_o{}^{1-n} \right]^{\frac{1}{1-n}} \qquad \text{(C-13)}$$

Substituting Eq. C-13 in Eq. C-9, yields:

$$\frac{q\Delta\gamma}{AL} = \alpha\beta \left[(n-1)\ \beta t + S_o{}^{1-n} \right]^{\frac{n}{1-n}} \qquad \text{(C-14)}$$

If n = 1, then from Eq. C-12b:

$$-\frac{dC_f}{C_f} = \beta dt \qquad \text{(C-15)}$$

Combining Eqs. C-8, C-9 and C-15:

$$\frac{q\Delta\gamma}{AL} = A_r p_{O_2}{}^m S_o \exp(-\beta t) \exp(-E/RT) \qquad \text{(C-16)}$$

a graph of $\ell n(\Delta\gamma)$ vs time is a straight line of slope:

$$\beta = \frac{A_r}{\alpha} p_{O_2}{}^m \exp(-E/RT) \qquad \text{(C-17)}$$

If β is evaluated at different temperatures, then the graph of $\ell n(\beta)$ vs (1/T) will have slope and intercept of:

$$\text{slope} = -E/R \qquad \text{(C-18)}$$

$$\text{intercept} = \frac{A_r}{\alpha} p_{O_2}{}^m \qquad \text{(C-19)}$$

Equations C-15 through C-18 were originally derived by Weijdema (1968) and are valid only if n = 1. For $n \neq 1$, the analysis is more complicated.

C.3 Derivation of Equations for Non-Isothermal Oxidation

The rate of oxygen consumption at any time can be obtained by combining Eqs. C-7 and C-8:

$$\frac{q\Delta\gamma}{AL} = A_r p_{O_2}{}^m \exp(-E/RT)\ C_f{}^n = -\alpha \frac{dC_f}{dt} \qquad \text{(C-20)}$$

Integration between t = t and t = ∞ yields:

$$\alpha C_f(t) = \int_t^{\infty} \frac{q\Delta\gamma}{AL}\, dt' \qquad \text{(C-21)}$$

Where $C_f = 0$ at $t = \infty$. From Eq. C-20:

$$C_f^{\,n}(t) = \frac{q\Delta\gamma}{AL} \frac{1}{A_r P_{O_2}^{\,m} \exp(-E/RT)} \qquad \text{(C-22)}$$

If we substitute Eq. C-22 in Eq. C-21 we obtain:

$$\frac{\Delta\gamma}{\left[\int_t^{\infty} \Delta\gamma dt'\right]^n} = \beta' \exp(-E/RT) \qquad \text{(C-23)}$$

where:

$$\beta' = \left(\frac{q}{AL}\right)^{n-1} \frac{A_r P_{O_2}^{\,m}}{\alpha^n} \qquad \text{(C-24)}$$

Values for the left hand side of Eq. C-23 can be found by graphical integration of the curve $\Delta\gamma = f(t)$. Then the logarithm of the left hand side of Eq. C-23 can be graphed vs 1/T to obtain (-E/2.303R) as the slope, and log β' as the intercept.

Appendix D

CALCULATION OF THE TRUE $\Delta\gamma$

In order to extrapolate the relative reaction-rate relationship to low temperatures, and hence permit computation of the true $\Delta\gamma$ corresponding to that rate, the following conversions are useful:

$$\Delta\gamma = -\frac{d}{dt}\int_t^\infty \Delta\gamma dt' \tag{D-1}$$

Substitution of Eq. D-1 in Eq. C-23 yields:

$$\frac{-\frac{d}{dt}\int_t^\infty \Delta\gamma dt'}{\left[\int_t^\infty \Delta\gamma dt'\right]^n} = \beta' \exp(-E/RT) \tag{D-2}$$

For $n \neq 1$, Eq. D-2 can be integrated between t_1 and t_2 to yield:

$$\frac{1}{\left[\int_{t_2}^\infty \Delta\gamma dt'\right]^{n-1}} - \frac{1}{\left[\int_{t_1}^\infty \Delta\gamma dt'\right]^{n-1}} = (n-1)\int_{t_1}^{t_2} \beta' \exp(-E/RT)dt' \tag{D-3}$$

Here t_2 is the upper limit of integration for which no departure from the straight line in Fig. 12 occurs, and $t_1 < t_2$. The first term on the left hand side of Eq. D-3 can be evaluated from the straight line relationship since β' and E are known, i.e.:

$$\frac{1}{\left[\int_{t_2}^{\infty} \Delta\gamma dt'\right]^{n-1}} = \left(\frac{\beta' \exp(-E/RT)}{\Delta\gamma(t_2)}\right)^{\frac{n-1}{n}} \tag{D-4}$$

The term in the right hand side of Eq. D-3 can be calculated using Eq. E-8 in Appendix E. Thus:

$$\int_{t_1}^{\infty} \Delta\gamma dt' = \left[\left(\int_{t_2}^{\infty} \Delta\gamma dt'\right)^{1-n} - (n-1)\int_{t_1}^{t_2} \beta' \exp(-E/RT) dt'\right]^{\frac{n}{1-n}} \tag{D-5}$$

Therefore:

$$\Delta\gamma(\text{true}) = \beta' \exp(-E/RT) \left[\int_{t_1}^{\infty} \Delta\gamma dt'\right]^{n} \tag{D-6}$$

For n = 1, Eqs. D-2 and D-5 can be reduced to:

$$-\frac{d}{dt}\left(\ell n \int_{t}^{\infty} \Delta\gamma dt'\right) = \beta' \exp(-E/RT) \tag{D-7}$$

$$\int_{t_1}^{\infty} \Delta\gamma dt' = \int_{t_2}^{\infty} \Delta\gamma dt' \exp\left[\int_{t_1}^{t_2} \beta' \exp(-E/RT) dt'\right] \tag{D-8}$$

$\Delta\gamma$(true) for n = 1 can be obtained from:

$$\Delta\gamma(\text{true}) = \beta' \exp(-E/RT) \int_{t_1}^{\infty} \Delta\gamma dt' \tag{D-9}$$

Weijdema (1968) proposed graphical integration of the $\Delta\gamma$ curve using Eq. D-7 to calculate $\Delta\gamma$(true). However, in this work, analytical expressions were developed to evaluate the general equations derived above.

Appendix E

CALCULATION OF THE AREA UNDER THE RELATIVE REACTION RATE CURVE VS TIME

In order to evaluate the right hand side of Eq. D-3 we need to perform the integral:

$$X = \int_{t_1}^{t_2} \beta' \exp(-E/RT)dt \qquad \text{(E-1)}$$

where T is a linear function of time as follows:

$$T = \alpha + \beta t \qquad \text{(E-2)}$$

We can change the variable <u>t</u> to <u>U</u> where:

$$U = \frac{(E/R)}{(\alpha + \beta t)} \qquad \text{(E-3)}$$

Hence:

$$dt = -\frac{(E/R)}{\beta U^2} dU \qquad \text{(E-4)}$$

then:

$$X = -\frac{A_r E}{R\beta} \int_{\frac{E/R}{\alpha + \beta t_1}}^{\frac{E/R}{\alpha + \beta t_2}} \left[\exp(-U)/U^2\right] dU \qquad \text{(E-5)}$$

Integrating by parts, Eq. E-5 can be expressed in terms of

$$\exp(-U)/U, \text{ and } \int \exp(-U)/U \, dU.$$

Notice that:

$$\int_{\frac{E}{RT_1}}^{\frac{E}{RT_2}} \exp(-U)/U \, dU = E_1\left(\frac{E}{RT_1}\right) - E_1\left(\frac{E}{RT_2}\right) \tag{E-6}$$

where E_1 is the exponential integral of the first kind and is defined as (Abramowitz and Stegun, 1972):

$$E_1(Z) = \int_Z^{\infty} \exp(-t)/t \, dt \tag{E-7}$$

So:

$$X = \frac{A_r E}{R\beta}\left[\frac{RT_1}{E}\exp(-E/RT_1) - \frac{RT_2}{E}\exp(-E/RT_2) - E_1(E/RT_1) + E_1(E/RT_2)\right] \tag{E-8}$$

The exponential integral can be computed from:

$$Xe^X E_1(X) = \frac{X^2 + a_1X + a_2}{X^2 + b_1X + b_2}, \quad 1 \leq X < \infty$$

Where:

$a_1 = 2.334733$ $\quad b_1 = 3.330657$

$a_2 = 0.250621$ $\quad b_2 = 1.681534$

Appendix F

EVALUATION OF EFFECT OF DIFFUSION

The reaction between air and crude oil is slow, and the assumption that the chemical reaction step controls the overall rate appears reasonable. However, it is possible to check this assumption insofar as diffusion is concerned. The following presents an analysis of the effect of diffusion on oxidation of the crude oils.

In order that steady state conditions prevails, it is necessary that the rate of diffusion of oxygen to the crude oil be equal to the rate of chemical reaction. The rate of diffusion may be expressed as:

$$R_d = K_g A'(p_g - p_i) \qquad \text{(F-1)}$$

Where:

R_d = g mole oxygen diffused/s-g sand

K_g = diffusion rate constant, g mole/s-atm-cm^2

A' = specific area of sand, cm^2/g sand

p_g = partial pressure of oxygen in the main gas stream, atm

p_i = partial pressure of oxygen at oil interface, atm

The diffusion rate constant, K_g, may be computed from (Carberry, 1976):

$$j_D = \frac{K_g \rho}{G} \left(\frac{\mu}{\rho D_{12}} \right)^{2/3} = 1.15 \left(\frac{d_p G}{\mu} \right)^{-1/2} \qquad \text{(F-2)}$$

where D_{12} is the diffusivity of gas 1 in gas 2 and is obtained from (Smith, 1970):

$$D_{12} = 0.0018583 \frac{T^{3/2}}{P_t \sigma_{12}} (1/M_1+1/M_2)^{1/2} \qquad \text{(F-3)}$$

The nomenclature for Eqs. F-2 and F-3 is:

G = mass velocity based on the total (superficial) cross-sectional area, g/s-cm^2

ρ = density of fluid, g/cm^3

d_p = mean diameter of sand grains, cm

T = absolute temperature, ^oK

P_t = total pressure, atm

M_1, M_2 = molecular weights of gases 1 and 2. Here gas 1 is oxygen (M_1 = 32) and gas 2 is nitrogen (M_2 = 28).

σ_{12} = constant in the Lennard-Jones function for the molecular pairs 1 and 2 in Å and can be evaluated from $\sigma_{12} = \frac{1}{2}(\sigma_1+\sigma_2)$

$\sigma_1 = \sigma_{O_2} = 3.433$ Å

$\sigma_2 = \sigma_{N_2} = 3.681$ Å

Diffusion is greatest at the highest temperature and pressure. Corresponding values for pressure and temperature in the experiments were:

T = 900°F = 756°K

P = 160 psig = 11.8 atm

Given these conditions,

ρ (air) = 5.5×10^{-3} g/cc

μ (air) = 3.675×10^{-4} g/cm-s

σ_{12} = 3.55 Å

D_{12} = 0.238 cm^2/s (from Eq. F-3)

To evaluate kg, the diffusion rate constant, Reynolds number, R_e, and Schmidt number, S_c, must be determined using the following equations:

$$R_e = \frac{d\rho G}{\mu} \tag{F-4}$$

$$S_c = \frac{\mu}{\rho D_{12}} \tag{F-5}$$

In Eq. F-4, G is the mass velocity and can be obtained using this equation:

$$G = \frac{\rho q}{A\phi} \tag{F-6}$$

where:

q = 10 cc/s (typical injection rate)

A = 5.945 cm^2 (reactor cross-sectional area)

ϕ = 0.4 (assumed)

d_p = 0.04 cm (average grain size diameter of the sand mix)

Therefore:

G = 0.0231 $g/s\text{-}cm^2$

R_e = 2.517

S_c = 0.281

kg = 7.1 g mole/s-atm-cm^2 (from Eq. F-2)

Assuming that the sand grains are spherical, the area per unit mass, A', can be found from:

$$A' = \frac{6}{\rho_s d_p} \tag{F-7}$$

where $_s$ is the density of sand. Therefore,

$$A' = \frac{6}{2.65 \times 0.04} = 56.6 \text{ cm}^2/\text{g}$$

The combustion reaction rate for Huntington Beach oil was found to be:

$$R_c = 6 \times 10^5 \exp(-1.62 \times 10^4/T)\ p_{O_2}^{0.66}\ C_f$$

where:

$$p_{O_2} = 0.21 \times 1205 = 253 \text{ kPa}$$

$$c_f = 3 \text{ g/100 g sand}$$

Therefore,

$$R_c = 3.428 \times 10^{-4} \text{ g mole } O_2/\text{s-g sand}$$

The rate of diffusion must be equal to the rate of reaction. So,

$$7.11 \times 56.6\ (P_g - P_i) = 3.428 \times 10^{-4}$$

or

$$P_g - P_i = 8.518 \times 10^{-7} \text{ atm.}$$

As is shown, $(P_g - P_i)$ is very small, i.e., the interfacial partial pressure of oxygen is nearly equal to the partial pressure of oxygen in the bulk gas stream. Thus, diffusion of oxygen from the bulk gas stream to the fuel interface is not an important consideration in the subject study.

Appendix G

EXPERIMENTAL DATA

All the data obtained during the kinetic experiments and the results therefrom are presented in this appendix. The computer programs are also included.

G-1 Computer Programs

The folowing program was used to analyze the laboratory data, to calculate the relative reaction rates, and to store the results in files. These files were used in conjunction with a computer program which plotted the data (TOPDRAW). The inputs are:

I = serial No. (interger)

TIME = time (hours)

TEMP = temperature (°F)

CO_2 = chart for CO_2 analyzer

CO = chart for CO analyzer

O_2 = chart for O_2 analyzer

NO = Run No.

Q = gas flow rate (slpm)

The program also calculates the amount of carbon and hydrogen burned. However, the results are not reported here.

```
 1.      // JOB
 2.      /*JOBPARM FORMS=9511,CHARS=TN15,FCB=8
 3.      // EXEC WATFIV
 4.      //GO.FT01F001 DD UNIT=DISK,DISP=(OLD,KEEP),DSN=WYL.JE.MRF.FILE1,
 5.      // VOL=SER=PUB002,SPACE=(TRK,(20,5),RLSE),DCB=(RECFM=FB,LRECL=40,
 6.      // BLKSIZE=6200)
 7.      //GO.FT02F001 DD UNIT=DISK,DISP=(OLD,KEEP),DSN=WYL.JE.MRF.FILE2,
 8.      // VOL=SER=PUB002,SPACE=(TRK,(20,5),RLSE),DCB=(RECFM=FB,LRECL=40,
 9.      // BLKSIZE=6200)
10.      //GO.FT03F001 DD UNIT=DISK,DISP=(OLD,KEEP),DSN=WYL.JE.MRF.FILE3,
11.      // VOL=SER=PUB002,SPACE=(TRK,(20,5),RLSE),DCB=(RECFM=FB,LRECL=40,
12.      // BLKSIZE=6200)
13.      //GO.FT04F001 DD UNIT=DISK,DISP=(OLD,KEEP),DSN=WYL.JE.MRF.FILE4,
14.      // VOL=SER=PUB002,SPACE=(TRK,(20,5),RLSE),DCB=(RECFM=FB,LRECL=40,
15.      // BLKSIZE=6200)
16.      //GO.FT08F001 DD UNIT=DISK,DISP=(OLD,KEEP),DSN=WYL.JE.MRF.FILE8,
17.      // VOL=SER=PUB002,SPACE=(TRK,(20,5),RLSE),DCB=(RECFM=FB,LRECL=40,
18.      // BLKSIZE=6200)
18.2     //GO.FT09F001 DD UNIT=DISK,DISP=(OLD,KEEP),DSN=WYL.JE.MRF.FILE9,
18.4     // VOL=SER=PUB002,SPACE=(TRK,(20,5),RLSE),DCB=(RECFM=FB,LRECL=40,
18.6     // BLKSIZE=6200)
18.7     //GO.FT10F001 DD UNIT=DISK,DISP=(OLD,KEEP),DSN=WYL.JE.MRF.FILE10,
18.8     // VOL=SER=PUB002,SPACE=(TRK,(20,5),RLSE),DCB=(RECFM=FB,LRECL=40,
18.85    // BLKSIZE=6200)
19.      //SYSIN DD *
20.      $WATFIV LINES=0
21.              REAL T(200),TT(200),G(200),GG(200),GGG(200)
22.              REAL GAMA(200),INT(200),X(200),Y(200),HB(200),HC(200)
23.              REAL DC(200),CB(200),IC(200),DCI(200)
24.              REAL YY(200),YYY(200),YYYY(200)
25.       10     READ,I,TIME,TEMP,CO2,CO,O2
26.              IF(I.EQ.0)GOTO 15
27.              T(I)=TIME
28.              TT(I)=(TEMP+460.)/1.8
29.              PCNT=21.
30.              NO=131
31.               O2=21.-O2/50.
32.              Q=.60
33.      C ***********************************
34.      C FOR CO & CO2 ANALYZERS BOTH ON RANGE 3
35.         5     CO=.71446E-3+1.66965E-2*CO+3.3035E-5*CO**2
36.               CO2=.674287E-2+3.12535E-2*CO2+1.866075E-4*CO2**2
37.              GOTO 11
38.                O2=(100.*O2+.265*CO2-.004*CO+35.8)/100.358
39.       11       G(I)=CO
40.                GG(I)=CO2
41.                GGG(I)=O2
42.                GAMA(I)=100.*(PCNT/100.*(100.-G(I)-GG(I))-GGG(I))/(100.-
43.            &  G(I)-GG(I)-GGG(I))
44.              IF(GAMA(I).LT.0.)GAMA(I)=0.
45.               IF(G(I).EQ.0.)G(I)=.0001
46.              HC(I)=4./(G(I)+GG(I))*(PCNT/(100.-PCNT)*(100.-G(I)-GG(I)-GGG(I))
47.            & -GGG(I)-GG(I)-.5*G(I))
48.              CB(I)=GG(I)/G(I)
49.              K=I
50.              GOTO 10
51.       15      WRITE(6,30)NO
52.         30 FORMAT('1',////60X,'RUN   NO. ',I4,//)
53.              WRITE(6,20)
54.       20     FORMAT(23X,'TIME',2X,'TEMPERATURE',2X,'CO',5X,'CO2',6X,'O2',6X,
```

```
55.          &'GAMA',3X,'CO2/CO',3X,'H/C',5X,'INV.TEMP.',5X,'RELATIVE',/23X,'HRS
56.          &',8X,'K',4(7X,'%'),6X,2('RATIO',4X),3X,'1/K',7X,'RATE,1/S',/
57.          &23X,'----',2X,11('-'),2X,'--',5X,'---',6X,'--',6X,'----',3X,6('-')
58.          &,3X,5('-'),3X,9('-'),5X,8('-'),//)
59.     C  ***************************************
60.     C   CALCULATION OF RELATIVE REACTION RATE
61.            I=1
62.            INT(1)=0.
63.      50    I=I+1
64.            INT(I)=INT(I-1)+.5*(GAMA(I)+GAMA(I-1))*(T(I)-T(I-1))*3600.
65.            IF(I.LT.K)GOTO 50
66.            J=K-1
67.            ICT=0
68.            DO 60 I=1,J
69.              IF(GAMA(I).EQ.0.)GOTO 60
70.            Y(I)=GAMA(I)/(INT(K)-INT(I))
71.            X(I)=1./TT(I)
72.           WRITE(6,40)T(I),TT(I),G(I),GG(I),GGG(I),GAMA(I),CB(I),HC(I),X(I),
73.          &Y(I)
74.      40    FORMAT(22X,F6.3,3X,F6.2,3X,5(F5.2,3X),F6.2,2(3X,E10.4),/)
75.            ICT=ICT+1
76.            IF(ICT.LT.33)GOTO 60
77.            WRITE(6,41)NO
78.      41    FORMAT('1',////60X,'RUN NO.',I4,' (CONT.)',//)
79.            WRITE(6,20)
80.            ICT=0
81.      60     CONTINUE
82.             DO 90 I=1,K
83.             WRITE(1,100)T(I),GG(I)
84.             WRITE(2,100)T(I),G(I)
85.             WRITE(3,100)T(I),GAMA(I)
86.             WRITE(4,100)T(I),TT(I)
86.1           WRITE(9,100)TT(I),HC(I)
86.2           WRITE(10,100)TT(I),CB(I)
87.              IF(GAMA(I).EQ.0.)GOTO 90
88.             IF(I.EQ.K)GOTO 90
89.             XXX=X(I)*1000.
90.             WRITE(8,80)XXX,Y(I)
91.      80       FORMAT(/5X,2(E10.3,5X))
92.     100     FORMAT(2X,2F9.4)
93.      90     CONTINUE
94.     C     ***************************************
95.     C   CALCULATION OF THE AMOUNT OF CARBON AND HYDROGEN BURNED
96.     C**CB=CARBON BURNED, HB=HYDROGEN BURNED, DC=DCB/DT, IC=INSTANTANEOUS C
97.      85        CB(1)=0.
98.               HB(1)=0.
99.               XX=0.
100.             DO 150 I=2,K
101.             CB(I)=CB(I-1)+Q*18./112.*(G(I)+GG(I)+G(I-1)+GG(I-1))*
102.          $ (T(I)-T(I-1))
103.             XY=XX
104.             XX=Q*12./112.*(GAMA(I)-(100.-PCNT)*(GG(I)+.5*G(I))/(100.-
105.          & G(I)-GG(I)-GGG(I)))
106.            HB(I)=(XY+XX)*(T(I)-T(I-1))/2.+HB(I-1)
107.            IF(T(I).NE.T(I-1))GOTO 49
108.            DC(I)=0.
109.            GOTO 150
110.     49     DC(I)=(CB(I)-CB(I-1))/(T(I)-T(I-1))/3600.
111.     150    CONTINUE
112.            DO 51 I=1,K
```

```
113.        51     IC(I)=CB(K)-CB(I)
114.               J=K-1
115.               DO 52 I=2,J
116.                IF(T(I).NE.T(I-1).AND.T(I).NE.T(I+1))GOTO 511
117.                DC(I)=0.
118.                DCI(I)=0.
119.                GOTO 52
120.        511     DC(I)=DC(I)+(DC(I+1)-DC(I))/(T(I+1)-T(I))*(T(I)-T(I-1))/2.
121.                DCI(I)=DC(I)/IC(I)/(PCNT+GGG(I))*2.
122.        52       CONTINUE
123.                WRITE(6,30)NO
124.                 WRITE(6,130)
125.        130     FORMAT(25X,'TEMP.',3X,'CARBON BURNED',2X,'BURN RATE',4X,
126.            & 'INST. C',5X, 'DC/CDT',6X,'1/T',2X,'HYDROGEN BURNED',/
127.            $ 27X,'K',10X,'G',11X,'G/S',10X,'G',9X,'1/S',9X,'1/K',10X,'G',//)
128.                ICT=0
129.                DCI(1)=0.
130.                DO 53 I=1,J
131.                WRITE(6,54)TT(I),CB(I),DC(I),IC(I),DCI(I),X(I),HB(I)
132.        54     FORMAT(21X,7(E10.3,2X),/)
133.               ICT=ICT+1
134.               IF(ICT.LT.33)GOTO 53
135.               WRITE(6,41)NO
136.               WRITE(6,130)
137.               ICT=0
138.         53     CONTINUE
139.                WRITE(6,55)
140.        55      FORMAT('1')
141.               STOP
142.               END
143.       $DATA
144.       1,1.6,255.,0.,0.,0.
145.       2,2.,290.,0.,0.,1.5
146.       3,2.1,300.,0.,0.,2.5
147.       4,2.2,310.,0.,0.,4.
148.       5,2.3,321.,.1,.3,6.
149.       6,2.4,331.,.2,.3,8.5
150.       7,2.5,343.,.5,.8,11.5
151.       8,2.6,355.,.9,1.1,15.5
152.       9,2.7,367.,1.,1.8,21.5
153.       10,2.8,379.,2.,2.8,28.
154.       11,2.9,391.,3.,4.5,40.
155.       12,2.95,397.,4.2,6.,49.
156.       13,3.,402.,5.1,7.,57.5
157.       14,3.05,408.,7.,9.1,68.
158.       15,3.1,414.,9.,11.5,71.5
159.       16,3.2,430.,13.4,16.8,107.5
160.       17,3.25,437.,17.,20.,122.5
161.       18,3.3,445.,19.,22.5,132.5
162.       19,3.35,453.,22.,25.,140.
163.       20,3.4,461.,24.,26.5,143.
164.       21,3.45,467.,26.5,28.,145.
165.       22,3.5,474.,27.5,28.5,142.2
166.       23,3.55,479.,28.5,28.5,138.8
167.       24,3.6,485.,28.5,27.5,130.
168.       25,3.65,490.,27.5,26.,117.5
169.       26,3.7,494.,26.,24.,107.5
170.       27,3.75,498.,24.5,22.,95.
171.       28,3.8,502.,23.,20.5,86.
172.       29,3.85,505.,21.5,18.5,76.
```

G-2 Pocket Calculator Program

The following programs were run through a programmable calculator to decompose the curves of the reaction rates. For the program details, see Appendix C.

TITLE Decomposition of $\Delta\gamma$ (n = 1) PAGE 1 OF 2

PROGRAMMER M. R. Fassihi DATE Dec. 1979

TI Programmable **Program Record**

Partitioning (Op 17) Library Module Printer Cards

PROGRAM DESCRIPTION

This program extrapolates the consumed oxygen by a reaction (with n = 1) to lower temperatures (see Appendix C). The intercept and the slope, E, of the Arrhenius plot for the reaction should be known. Also, the rate of temperature rise, β, and the point at which the reaction rate deviates from the straight line, x_1, should be available. Note:

$$x_1 = \frac{\Delta\gamma(\text{at the deviation point})}{\text{Relative Reaction Rate(at this point)}}$$

USER INSTRUCTIONS

STEP	PROCEDURE	ENTER	PRESS	DISPLAY
1	Run the program			
2	Initialize		A'	0
3	Input data	Intercept	B'	Intercept
		Slope	C'	Slope, E
		β (°K/s)	D'	β
		x_1	E	---
4	Enter 1/T, °K^{-1}	1/T	A	Relative Reaction Rate
5	Find $\Delta\gamma$		B	$\Delta\gamma$
6	Repeat Step 4 as necessary			

USER DEFINED KEYS		DATA REGISTERS (INV Adr)			LABELS (Op 08)
A	1/T	0	β	10	
B	RRR	1	x_1	11	E/T
C		2		12	
D		3		13	$E_1(E/T)$
E		4		14	exp(-E/T)/(E/T)
A'	Initialize	5	Intercept	15	i exp(-E/T)
B'	Intercept	6	E	16	
C'	Slope	7	1/T	17	
D'	β	8	A exp(-E/RT)	18	
E'	x_1	9		19	

FLAGS 0 124 1 2 3 4 5 6 7 8 9

© 1977 Texas Instruments Incorporated 1014966-1

TITLE _____ PAGE 2 OF 2

PROGRAMMER _____ DATE _____

TI Programmable Coding Form

LOC	CODE	KEY	COMMENTS
000	76	LBL	
001	16	A'	
002	22	INV	
003	86	STF	
004	01	01	
005	00	0	
006	42	STO	
007	50	50	
008	91	R/S	
009	76	LBL	
010	17	B'	
011	42	STO	
012	05	05	
013	91	R/S	
014	76	LBL	
015	18	C'	
016	42	STO	
017	06	06	
018	91	R/S	
019	76	LBL	
020	19	D'	
021	42	STO	
022	00	00	
023	91	R/S	
024	76	LBL	
025	11	A	
026	42	STO	
027	07	07	
028	65	×	
029	43	RCL	
030	06	06	
031	95	=	
032	42	STO	
033	11	11	
034	94	+/-	
035	22	INV	
036	23	LNX	
037	65	×	
038	43	RCL	
039	05	05	
040	95	=	
041	42	STO	
042	08	08	
043	91	R/S	
044	76	LBL	
045	10	E'	
046	42	STO	
047	01	01	
048	91	R/S	
049	76	LBL	
050	12	B	
051	43	RCL	
052	11	11	
053	33	X^2	
054	85	+	
055	43	RCL	
056	11	11	
057	65	×	
058	02	2	
059	93	.	
060	03	3	
061	03	3	
062	04	4	
063	07	7	
064	03	3	
065	03	3	
066	85	+	
067	93	.	
068	02	2	
069	05	5	
070	00	0	
071	06	6	
072	02	2	
073	01	1	
074	95	=	
075	55	÷	
076	53	(	
077	43	RCL	
078	11	11	
079	33	X^2	
080	85	+	
081	43	RCL	
082	11	11	
083	65	×	
084	03	3	
085	93	.	
086	03	3	
087	03	3	
088	00	0	
089	06	6	
090	05	5	
091	07	7	
092	85	+	
093	01	1	
094	93	.	
095	06	6	
096	08	8	
097	01	1	
098	05	5	
099	03	3	
100	04	4	
101	54	)	
102	55	÷	
103	43	RCL	
104	11	11	
105	55	÷	
106	43	RCL	
107	11	11	
108	22	INV	
109	23	LNX	
110	95	=	
111	42	STO	
112	13	13	
113	43	RCL	
114	11	11	
115	94	+/-	
116	22	INV	
117	23	LNX	
118	55	÷	
119	43	RCL	
120	11	11	
121	95	=	
122	42	STO	
123	14	14	
124	87	IFF	
125	01	01	
126	01	01	
127	38	38	
128	43	RCL	
129	13	13	
130	75	-	
131	43	RCL	
132	14	14	
133	95	=	
134	42	STO	
135	50	50	
136	86	STF	
137	01	01	
138	43	RCL	
139	14	14	
140	75	-	
141	43	RCL	
142	13	13	
143	85	+	
144	43	RCL	
145	50	50	
146	95	=	
147	65	×	
148	43	RCL	
149	05	05	
150	65	×	
151	43	RCL	
152	06	06	
153	55	÷	
154	43	RCL	
155	00	00	
156	95	=	
157	94	+/-	
158	22	INV	
159	23	LNX	
160	65	×	
161	43	RCL	
162	08	08	
163	65	×	
164	43	RCL	
165	01	01	
166	95	=	
167	91	R/S	

© 1977 Texas Instruments Incorporated

TITLE Decomposition of $\Delta\gamma$ ($n \neq 1$) PAGE 1 OF 3

PROGRAMMER M. R. Fassihi DATE Dec. 79

TI Programmable Program Record

Partitioning (Op 17) Library Module _____ Printer _____ Cards 1

PROGRAM DESCRIPTION

This program extrapolates the consumed oxygen by a reaction (with $n \neq 1$) to lower temperatures (see Appendix C). The intercept and the slope, E, of the Arrhenius plot for the reaction should be known. Also, the rate of temperature rise, β, and the point at which deviation from the straight line, x_1, occurs should be available. Note:

$$x_1 = \frac{\Delta\gamma(\text{at the deviation point})}{\text{Relative Reaction Rate (at this point)}}$$

USER INSTRUCTIONS

STEP	PROCEDURE	ENTER	PRESS	DISPLAY
1	Run the program			
2	Initialize		A'	0
3	Input data	Intercept	B'	Intercept
		Slope	C'	E
		β(°K/s)	D'	β
		x_1	E'	
		n	E	n
4	Enter 1/T, °K^{-1}	1/T	A	Relative Reaction Rate
5	Find $\Delta\gamma$		B	$\Delta\gamma$
6	Repeat Step 4 as necessary			

USER DEFINED KEYS		DATA REGISTERS (INV LNX)				LABELS (Op 08)
A	1/T	1 0	β	2 0	n	
B	RRR	1 1	x_1	2 1	n-1	
C		1 2		2 2		
D		1 3		2 3		
E	n	1 4		2 4		
A'	Initialize	1 5	Intercept	2 5		
B'	Intercept	1 6	E	2 6		
C'	Slope	1 7	1/T	2 7		
D'	β	1 8	A exp(-E/RT)	2 8		
E'	x_1	1 9		2 9		

FLAGS 0	124 1	2	3	4	5	6	7	8	9

© 1977 Texas Instruments Incorporated

1014966-1

TITLE Δγ (n ≠ 1) PAGE 2 OF 3

PROGRAMMER DATE

TI Programmable **Coding Form**

LOC	CODE	KEY	COMMENTS
		000	76 LBL
		001	16 A'
		002	22 INV
		003	86 STF
		004	01 01
		005	00 0
		006	42 STO
		007	50 50
		008	91 R/S
		009	76 LBL
		010	17 B'
		011	42 STO
		012	05 05
		013	91 R/S
		014	76 LBL
		015	18 C'
		016	42 STO
		017	06 06
		018	91 R/S
		019	76 LBL
		020	19 D'
		021	42 STO
		022	00 00
		023	91 R/S
		024	76 LBL
		025	11 A
		026	42 STO
		027	07 07
		028	65 ×
		029	43 RCL
		030	06 06
		031	95 =
		032	42 STO
		033	11 11
		034	94 +/-
		035	22 INV
		036	23 LNX
		037	65 ×
		038	43 RCL
		039	05 05
		040	95 =
		041	42 STO
		042	08 08
		043	91 R/S
		044	76 LBL
		045	10 E'
		046	42 STO
		047	01 01
		048	91 R/S
		049	76 LBL
		050	12 B
		051	43 RCL
		052	11 11
		053	33 X²
		054	85 +

LOC	CODE	KEY	COMMENTS
		055	43 RCL
		056	11 11
		057	65 ×
		058	02 2
		059	93 .
		060	03 3
		061	03 3
		062	04 4
		063	07 7
		064	03 3
		065	03 3
		066	85 +
		067	93 .
		068	02 2
		069	05 5
		070	00 0
		071	06 6
		072	02 2
		073	01 1
		074	95 =
		075	55 ÷
		076	53 (
		077	43 RCL
		078	11 11
		079	33 X²
		080	85 +
		081	43 RCL
		082	11 11
		083	65 ×
		084	03 3
		085	93 .
		086	03 3
		087	03 3
		088	00 0
		089	06 6
		090	05 5
		091	07 7
		092	85 +
		093	01 1
		094	93 .
		095	06 6
		096	08 8
		097	01 1
		098	05 5
		099	03 3
		100	04 4
		101	54)
		102	55 ÷
		103	43 RCL
		104	11 11
		105	55 ÷
		106	43 RCL
		107	11 11
		108	22 INV
		109	23 LNX

LOC	CODE	KEY	COMMENTS
		110	95 =
		111	42 STO
		112	13 13
		113	43 RCL
		114	11 11
		115	94 +/-
		116	22 INV
		117	23 LNX
		118	55 ÷
		119	43 RCL
		120	11 11
		121	95 =
		122	42 STO
		123	14 14
		124	87 IFF
		125	01 01
		126	01 01
		127	38 38
		128	43 RCL
		129	13 13
		130	75 -
		131	43 RCL
		132	14 14
		133	95 =
		134	42 STO
		135	50 50
		136	86 STF
		137	01 01
		138	43 RCL
		139	14 14
		140	75 -
		141	43 RCL
		142	13 13
		143	85 +
		144	43 RCL
		145	50 50
		146	95 =
		147	65 ×
		148	43 RCL
		149	05 05
		150	65 ×
		151	43 RCL
		152	06 06
		153	55 ÷
		154	43 RCL
		155	00 00
		156	95 =
		157	65 ×
		158	43 RCL
		159	21 21
		160	94 +/-
		161	85 +
		162	43 RCL
		163	22 22
		164	95 =

© 1977 Texas Instruments Incorporated

TI 24181

TITLE Δy (n ≠ 1) PAGE 3 OF 3

PROGRAMMER DATE

TI Programmable **Coding Form**

LOC	CODE	KEY	COMMENTS
165		45	Y^X
166		53	(
167		43	RCL
168		20	20
169		55	÷
170		43	RCL
171		21	21
172		94	+/-
173		54	)
174		65	×
175		43	RCL
176		08	08
177		95	=
178		91	R/S
179		76	LBL
180		15	E
181		42	STO
182		20	20
183		75	-
184		01	1
185		95	=
186		42	STO
187		21	21
188		43	RCL
189		01	01
190		45	Y^X
191		53	(
192		43	RCL
193		21	21
194		94	+/-
195		55	÷
196		43	RCL
197		20	20
198		54	)
199		95	=
200		42	STO
201		22	22
202		91	R/S

MERGED CODES

62 [A] [▼]	72 [STO] [▼]	83 [GTO] [▼]
63 [B] [▼]	73 [RCL] [▼]	84 [X] [▼]
64 [C] [▼]	74 [SUM] [▼]	92 [INV] [SBR]

TEXAS INSTRUMENTS INCORPORATED

© 1977 Texas Instruments Incorporated

TI-24181

G-2 Data

All the experimental data for the kinetic data are reported in the following tables. The tables are arranged in the serial order the runs were conducted in. In addition, the results of the data of Bardon and Gadelle (1977) are included.

RUN NO. 105

TIME HRS	TEMPERATURE K	CO %	CO2 %	O2 %	GAMA %	CO2/CO RATIO	H/C RATIO	INV.TEMP. 1/K	RELATIVE RATE,1/S
5.000	483.33	0.00	0.02	20.92	0.10	*****	15.10	0.2069E-02	0.8292E-05
5.500	517.78	0.03	0.10	20.75	0.28	3.33	5.14	0.1931E-02	0.2508E-04
5.700	529.44	0.05	0.13	20.65	0.39	2.60	5.34	0.1889E-02	0.3592E-04
5.900	541.67	0.08	0.20	20.60	0.43	2.50	2.74	0.1846E-02	0.4037E-04
6.000	547.22	0.08	0.20	20.57	0.47	2.50	3.28	0.1827E-02	0.4458E-04
6.150	558.33	0.08	0.22	20.54	0.50	2.75	3.23	0.1791E-02	0.4889E-04
6.300	565.00	0.08	0.22	20.60	0.43	2.75	2.22	0.1770E-02	0.4257E-04
6.500	577.78	0.08	0.25	20.57	0.46	3.13	2.02	0.1731E-02	0.4706E-04
6.600	583.33	0.08	0.27	20.54	0.49	3.38	2.05	0.1714E-02	0.5132E-04
6.800	597.22	0.09	0.30	20.51	0.52	3.33	1.76	0.1674E-02	0.5634E-04
7.000	611.11	0.10	0.40	20.49	0.51	4.00	0.50	0.1636E-02	0.5833E-04
7.100	617.78	0.11	0.45	20.42	0.59	4.09	0.57	0.1619E-02	0.6812E-04
7.200	625.00	0.12	0.50	20.30	0.72	4.17	1.04	0.1600E-02	0.8624E-04
7.300	630.56	0.13	0.60	20.17	0.86	4.62	1.05	0.1586E-02	0.1060E-03
7.500	641.67	0.18	0.70	19.92	1.13	3.89	1.56	0.1558E-02	0.1537E-03
7.600	648.33	0.20	0.80	19.75	1.31	4.00	1.67	0.1542E-02	0.1897E-03
7.700	654.44	0.20	0.90	19.62	1.45	4.50	1.65	0.1528E-02	0.2258E-03
7.800	661.11	0.20	0.93	19.50	1.59	4.65	2.01	0.1513E-02	0.2709E-03
7.900	666.67	0.22	0.96	19.47	1.62	4.36	1.87	0.1500E-02	0.3052E-03
8.000	673.33	0.20	0.92	19.40	1.72	4.60	2.53	0.1485E-02	0.3657E-03
8.100	677.78	0.17	0.75	19.37	1.80	4.41	4.28	0.1475E-02	0.4438E-03
8.200	681.67	0.12	0.55	19.45	1.76	4.58	7.01	0.1467E-02	0.5159E-03
8.500	701.11	0.04	0.20	19.62	1.66	5.00	24.38	0.1426E-02	0.1056E-02

RUN NO. 109

TIME HRS	TEMPERATURE K	CO %	CO2 %	O2 %	GAMA %	CO2/CO RATIO	H/C RATIO	INV.TEMP. 1/K	RELATIVE RATE,1/S
0.250	463.89	0.00	0.00	8.25	0.05	0.00	******	0.2156E-02	0.4477E-05
0.800	477.78	0.00	0.00	8.25	0.05	0.00	******	0.2093E-02	0.4517E-05
1.200	488.89	0.00	0.01	8.20	0.11	*****	38.84	0.2045E-02	0.9044E-05
1.500	501.67	0.01	0.02	8.13	0.18	2.00	21.02	0.1993E-02	0.1547E-04
1.700	516.67	0.03	0.05	8.05	0.26	1.67	10.02	0.1935E-02	0.2278E-04
1.900	527.78	0.04	0.05	7.97	0.35	1.25	12.52	0.1895E-02	0.3075E-04
2.100	540.00	0.08	0.15	7.75	0.58	1.88	6.76	0.1852E-02	0.5211E-04
2.300	552.78	0.12	0.20	7.62	0.71	1.67	5.66	0.1809E-02	0.6690E-04
2.500	563.33	0.14	0.25	7.58	0.75	1.79	4.41	0.1775E-02	0.7409E-04
2.600	567.78	0.14	0.27	7.59	0.73	1.93	3.87	0.1761E-02	0.7404E-04
2.700	572.22	0.14	0.29	7.60	0.72	2.07	3.39	0.1748E-02	0.7559E-04
2.800	575.56	0.14	0.30	7.63	0.69	2.14	2.92	0.1737E-02	0.7402E-04
3.000	585.00	0.12	0.28	7.70	0.62	2.33	2.78	0.1709E-02	0.6904E-04
3.600	611.11	0.11	0.27	7.80	0.51	2.45	1.96	0.1636E-02	0.6700E-04
4.000	627.78	0.13	0.33	7.75	0.56	2.54	1.42	0.1593E-02	0.8145E-04
4.100	633.33	0.14	0.36	7.70	0.61	2.57	1.43	0.1579E-02	0.9165E-04
4.500	652.22	0.19	0.45	7.62	0.68	2.37	0.87	0.1533E-02	0.1196E-03
4.700	663.33	0.22	0.50	7.55	0.75	2.27	0.79	0.1508E-02	0.1450E-03
5.000	682.22	0.30	0.65	7.37	0.93	2.17	0.54	0.1466E-02	0.2169E-03
5.200	692.22	0.36	0.80	7.22	1.07	2.22	0.32	0.1445E-02	0.3016E-03
5.300	697.22	0.38	0.85	7.19	1.10	2.24	0.19	0.1434E-02	0.3473E-03
5.400	702.78	0.40	0.90	7.12	1.17	2.25	0.21	0.1423E-02	0.4241E-03
5.500	707.78	0.40	0.90	7.10	1.19	2.25	0.28	0.1413E-02	0.5106E-03
5.600	711.67	0.39	0.88	7.13	1.16	2.26	0.27	0.1405E-02	0.6001E-03
5.700	715.00	0.36	0.83	7.20	1.09	2.31	0.28	0.1399E-02	0.7261E-03
5.800	717.78	0.30	0.75	7.28	1.02	2.50	0.45	0.1393E-02	0.9043E-03
5.900	720.56	0.22	0.60	7.45	0.85	2.73	0.70	0.1388E-02	0.1081E-02
6.000	723.33	0.14	0.35	7.66	0.65	2.50	1.91	0.1382E-02	0.1260E-02
6.100	725.00	0.04	0.17	7.85	0.47	4.25	5.37	0.1379E-02	0.1490E-02
6.150	725.56	0.02	0.10	7.90	0.42	5.00	10.51	0.1378E-02	0.1803E-02
6.200	726.67	0.01	0.07	7.95	0.37	7.00	14.97	0.1376E-02	0.2285E-02
6.300	728.89	0.00	0.05	8.10	0.21	10.00	11.68	0.1372E-02	0.3675E-02

RUN NO. 110

TIME HRS	TEMPERATURE K	CO %	CO2 %	O2 %	GAMA %	CO2/CO RATIO	H/C RATIO	INV.TEMP. 1/K	RELATIVE RATE,1/S
5.300	441.67	0.00	0.00	8.24	0.07	0.00	******	0.2264E-02	0.3139E-05
5.700	453.89	0.00	0.00	8.20	0.11	0.00	******	0.2203E-02	0.5261E-05
6.200	472.22	0.00	0.02	8.10	0.22	*****	39.05	0.2118E-02	0.1057E-04
6.700	491.67	0.04	0.05	7.90	0.43	1.25	15.91	0.2034E-02	0.2151E-04
7.300	511.11	0.08	0.10	7.70	0.64	1.25	11.07	0.1957E-02	0.3398E-04
7.600	521.67	0.09	0.15	7.67	0.66	1.67	7.84	0.1917E-02	0.3683E-04
7.900	533.33	0.09	0.20	7.63	0.70	2.22	6.34	0.1875E-02	0.4066E-04
8.200	545.56	0.12	0.27	7.60	0.73	2.25	4.08	0.1833E-02	0.4403E-04
8.600	561.11	0.14	0.27	7.70	0.62	1.93	2.70	0.1782E-02	0.3970E-04
9.100	578.89	0.12	0.20	7.84	0.47	1.67	2.66	0.1727E-02	0.3247E-04
9.300	585.56	0.12	0.20	7.88	0.43	1.67	2.11	0.1708E-02	0.3016E-04
9.500	593.89	0.13	0.20	7.88	0.43	1.54	1.98	0.1684E-02	0.3076E-04
9.700	598.89	0.15	0.25	7.86	0.44	1.67	1.19	0.1670E-02	0.3263E-04
10.000	610.56	0.13	0.27	7.73	0.58	2.08	2.50	0.1638E-02	0.4483E-04
10.300	620.56	0.18	0.42	7.60	0.71	2.33	1.33	0.1611E-02	0.5741E-04
10.500	627.78	0.24	0.55	7.38	0.93	2.29	1.33	0.1593E-02	0.7921E-04
10.800	639.44	0.37	0.80	7.03	1.28	2.16	1.01	0.1564E-02	0.1210E-03
11.200	651.11	0.44	1.05	6.75	1.55	2.39	0.77	0.1536E-02	0.1805E-03
11.400	657.22	0.50	1.15	6.65	1.65	2.30	0.61	0.1522E-02	0.2241E-03
11.700	666.67	0.54	1.30	6.60	1.69	2.41	0.26	0.1500E-02	0.3040E-03
11.800	668.89	0.52	1.25	6.65	1.64	2.40	0.29	0.1495E-02	0.3310E-03
12.000	674.44	0.50	1.22	6.73	1.56	2.44	0.20	0.1483E-02	0.4095E-03
12.100	676.67	0.47	1.15	6.80	1.49	2.45	0.26	0.1478E-02	0.4577E-03
12.400	680.00	0.36	0.95	7.20	1.08	2.64	-0.15	0.1471E-02	0.5801E-03
12.600	690.56	0.26	0.72	7.40	0.89	2.77	0.17	0.1448E-02	0.7730E-03
12.800	697.78	0.14	0.45	7.70	0.60	3.21	0.55	0.1433E-02	0.9724E-03
13.000	707.78	0.08	0.25	7.90	0.41	3.13	1.41	0.1413E-02	0.1590E-02
13.200	717.78	0.03	0.10	8.15	0.15	3.33	1.13	0.1393E-02	0.2778E-02

RUN NO. 111

TIME HRS	TEMPERATURE K	CO %	CO2 %	O2 %	GAMA %	CO2/CO RATIO	H/C RATIO	INV.TEMP. 1/K	RELATIVE RATE,1/S
12.000	469.44	0.00	0.00	8.30	0.00	0.00	-2.53		
12.020	469.44	0.00	0.00	8.09	0.23	1.00	454.64		
12.500	469.44	0.00	0.00	8.10	0.22	1.00	432.83		
12.500	496.67	0.04	0.05	7.80	0.53	1.25	20.76		
13.100	496.67	0.04	0.05	7.80	0.53	1.25	20.76		
13.100	523.89	0.12	0.17	7.15	1.22	1.42	13.76		
13.300	523.89	0.12	0.17	7.20	1.16	1.42	13.01		
13.400	524.44	0.12	0.17	7.40	0.95	1.42	10.00		
13.500	525.00	0.11	0.16	7.50	0.84	1.45	9.38		
13.600	525.56	0.10	0.15	7.60	0.74	1.50	8.65		
13.700	526.11	0.10	0.15	7.65	0.68	1.50	7.78		
13.800	527.22	0.09	0.15	7.70	0.63	1.67	7.29		
14.000	527.78	0.09	0.14	7.80	0.52	1.56	5.90		
14.400	527.22	0.08	0.12	7.90	0.42	1.50	5.16		
14.800	526.11	0.05	0.10	7.95	0.37	2.00	6.48		
14.800	550.56	0.11	0.18	7.80	0.52	1.64	3.92		
14.950	550.56	0.11	0.18	7.80	0.52	1.64	3.92		
15.250	551.67	0.09	0.17	7.95	0.36	1.89	2.20		
15.550	552.78	0.06	0.15	8.05	0.25	2.50	1.40		
16.050	548.89	0.04	0.10	8.13	0.17	2.50	1.51		
16.050	575.00	0.09	0.20	7.95	0.36	2.22	1.52		
16.350	575.00	0.09	0.20	7.95	0.36	2.22	1.52		
16.850	578.33	0.08	0.17	8.00	0.30	2.13	1.51		
16.850	602.22	0.12	0.35	7.80	0.50	2.92	0.79		
17.250	602.22	0.12	0.35	7.80	0.50	2.92	0.79		
17.350	605.56	0.12	0.32	7.80	0.51	2.67	1.14		
17.350	634.44	0.34	0.88	7.15	1.14	2.59	0.31		
17.650	634.44	0.34	0.88	7.15	1.14	2.59	0.31		
17.950	637.78	0.32	0.80	7.10	1.21	2.50	0.88		
17.950	655.56	0.48	1.25	6.70	1.59	2.60	0.23		
18.000	655.56	0.48	1.25	6.70	1.59	2.60	0.23		
18.050	656.67	0.56	1.50	6.50	1.78	2.68	-0.01		
18.250	659.44	0.66	1.75	6.00	2.29	2.65	0.35		

RUN NO. 111 (CONT.)

TIME HRS	TEMPERATURE K	CO %	CO2 %	O2 %	GAMA %	CO2/CO RATIO	H/C RATIO	INV.TEMP. 1/K	RELATIVE RATE,1/S
18.350	661.67	0.68	1.80	5.85	2.45	2.65	0.50		
18.650	664.44	0.68	1.70	5.80	2.51	2.50	0.79		
18.850	666.11	0.78	1.90	5.40	2.91	2.44	0.94		
18.880	661.11	0.90	2.00	6.00	2.26	2.22	-0.28		
18.950	663.33	1.00	2.45	5.00	3.29	2.45	0.39		
19.050	665.56	1.02	2.55	4.90	3.39	2.50	0.36		
19.150	666.11	0.94	2.50	5.30	2.97	2.66	-0.01		
19.250	670.56	0.92	2.45	5.50	2.77	2.66	-0.19		
19.350	675.00	0.80	2.20	5.80	2.47	2.75	-0.19		
19.550	675.56	0.39	1.15	6.75	1.55	2.95	0.53		
19.650	676.11	0.24	0.75	7.20	1.11	3.12	0.97		
19.750	675.56	0.16	0.45	7.50	0.82	2.81	1.88		
19.850	675.00	0.09	0.28	7.85	0.46	3.11	1.43		
19.950	674.44	0.06	0.18	7.90	0.41	3.00	3.41		

RUN NO. 112

TIME HRS	TEMPERATURE K	CO %	CO2 %	O2 %	GAMA %	CO2/CO RATIO	H/C RATIO	INV.TEMP. 1/K	RELATIVE RATE,1/S
2.050	333.33	0.00	0.01	8.22	0.09	9.44	42.62	0.3000E-02	0.4526E-05
4.000	383.33	0.00	0.01	8.22	0.09	9.44	42.62	0.2609E-02	0.4739E-05
4.500	411.11	0.00	0.01	8.20	0.11	9.44	54.32	0.2432E-02	0.5989E-05
5.000	438.89	0.00	0.01	8.17	0.14	1.66	48.90	0.2278E-02	0.7876E-05
5.300	457.22	0.01	0.01	8.11	0.21	0.74	49.19	0.2187E-02	0.1163E-04
5.600	472.22	0.02	0.01	8.07	0.25	0.75	29.74	0.2118E-02	0.1421E-04
6.000	497.22	0.03	0.04	7.85	0.48	1.12	23.69	0.2011E-02	0.2854E-04
6.200	508.33	0.06	0.07	7.67	0.67	1.18	17.77	0.1967E-02	0.4076E-04
6.400	519.44	0.08	0.10	7.57	0.77	1.25	13.85	0.1925E-02	0.4955E-04
6.500	523.33	0.09	0.12	7.54	0.81	1.37	12.64	0.1911E-02	0.5138E-04
6.700	536.11	0.11	0.15	7.57	0.77	1.37	8.65	0.1865E-02	0.5007E-04
6.900	547.22	0.12	0.20	7.59	0.74	1.62	5.92	0.1827E-02	0.5033E-04
7.000	555.56	0.13	0.22	7.61	0.72	1.70	5.09	0.1800E-02	0.5024E-04
7.100	561.11	0.13	0.23	7.64	0.68	1.79	4.22	0.1782E-02	0.4872E-04
7.200	566.67	0.13	0.23	7.70	0.62	1.84	3.56	0.1765E-02	0.4487E-04
7.400	577.78	0.11	0.23	7.80	0.51	2.12	2.60	0.1731E-02	0.3808E-04
7.600	588.89	0.11	0.23	7.85	0.46	2.19	2.01	0.1698E-02	0.3517E-04
7.700	594.44	0.11	0.24	7.85	0.46	2.25	1.88	0.1682E-02	0.3550E-04
7.800	600.00	0.11	0.27	7.85	0.46	2.39	1.38	0.1667E-02	0.3582E-04
8.000	611.11	0.13	0.30	7.80	0.51	2.40	1.31	0.1636E-02	0.4037E-04
8.200	623.33	0.15	0.37	7.70	0.61	2.43	1.19	0.1604E-02	0.5060E-04
8.400	634.44	0.19	0.48	7.57	0.73	2.48	0.93	0.1576E-02	0.6389E-04
8.500	639.44	0.22	0.52	7.49	0.82	2.35	0.99	0.1564E-02	0.7270E-04
8.600	645.56	0.26	0.60	7.40	0.90	2.33	0.82	0.1549E-02	0.8283E-04
8.700	651.11	0.32	0.71	7.27	1.03	2.24	0.65	0.1536E-02	0.9760E-04
8.800	655.56	0.34	0.82	7.14	1.16	2.42	0.57	0.1525E-02	0.1141E-03
8.900	661.11	0.41	0.99	6.89	1.41	2.40	0.63	0.1513E-02	0.1454E-03
9.000	665.56	0.50	1.24	6.54	1.76	2.47	0.62	0.1503E-02	0.1928E-03
9.100	675.00	0.62	1.58	6.04	2.26	2.56	0.69	0.1481E-02	0.2693E-03
9.200	683.33	0.67	1.73	5.73	2.58	2.57	0.87	0.1463E-02	0.3424E-03
9.300	688.89	0.78	1.94	5.24	3.08	2.48	1.13	0.1452E-02	0.4726E-03
9.350	693.33	1.06	2.45	4.33	3.99	2.31	1.18	0.1442E-02	0.6788E-03
9.400	700.00	2.00	4.46	2.02	6.28	2.23	0.50	0.1429E-02	0.1266E-02

RUN NO. 112 (CONT.)

TIME HRS	TEMPERATURE K	CO %	CO2 %	O2 %	GAMA %	CO2/CO RATIO	H/C RATIO	INV.TEMP. 1/K	RELATIVE RATE,1/S
9.450	703.89	2.12	5.56	1.57	6.71	2.62	0.01	0.1421E-02	0.1773E-02
9.500	708.33	2.00	4.73	2.12	6.17	2.36	0.24	0.1412E-02	0.2347E-02
9.600	713.33	1.12	2.99	4.73	3.54	2.67	-0.03	0.1402E-02	0.4023E-02
9.650	715.56	0.72	2.04	6.34	1.90	2.82	-0.74	0.1398E-02	0.4800E-02
9.700	718.33	0.22	0.71	7.54	0.75	3.16	-0.32	0.1392E-02	0.4917E-02
9.750	720.00	0.09	0.23	8.00	0.30	2.76	0.26	0.1389E-02	0.5166E-02
9.800	721.67	0.03	0.07	8.22	0.08	2.71	-0.18	0.1386E-02	0.3297E-02

RUN NO. 113

TIME HRS	TEMPERATURE K	CO %	CO2 %	O2 %	GAMA %	CO2/CO RATIO	H/C RATIO	INV.TEMP. 1/K	RELATIVE RATE,1/S
1.800	497.22	0.02	0.02	8.20	0.11	1.29	7.46	0.2011E-02	0.1214E-04
2.100	513.89	0.03	0.04	8.12	0.19	1.48	8.71	0.1946E-02	0.2233E-04
2.200	519.44	0.03	0.04	8.07	0.24	1.30	9.25	0.1925E-02	0.2882E-04
2.400	530.56	0.05	0.07	7.97	0.35	1.37	8.37	0.1885E-02	0.4230E-04
2.600	542.78	0.08	0.12	7.85	0.47	1.55	6.49	0.1842E-02	0.5946E-04
2.700	548.33	0.10	0.16	7.77	0.55	1.66	5.35	0.1824E-02	0.7135E-04
2.800	552.78	0.11	0.19	7.67	0.66	1.64	5.50	0.1809E-02	0.8727E-04
2.850	554.44	0.12	0.20	7.72	0.60	1.74	4.36	0.1804E-02	0.9116E-04
2.900	556.67	0.11	0.20	7.75	0.57	1.82	4.05	0.1796E-02	0.7795E-04
3.000	558.33	0.10	0.18	7.79	0.53	1.81	4.12	0.1791E-02	0.7434E-04
3.250	568.89	0.10	0.20	7.83	0.48	1.97	3.08	0.1758E-02	0.7271E-04
3.650	588.33	0.10	0.23	7.89	0.42	2.31	1.72	0.1700E-02	0.6941E-04
3.800	595.00	0.10	0.23	7.93	0.37	2.30	1.04	0.1681E-02	0.6430E-04
4.200	615.00	0.12	0.24	7.91	0.39	2.09	1.05	0.1626E-02	0.7400E-04
4.700	644.44	0.17	0.39	7.79	0.51	2.29	0.21	0.1552E-02	0.1134E-03
4.800	649.44	0.19	0.41	7.75	0.55	2.17	0.29	0.1540E-02	0.1201E-03
4.900	655.56	0.21	0.44	7.73	0.56	2.16	0.09	0.1525E-02	0.1391E-03
5.000	661.11	0.22	0.48	7.69	0.60	2.15	0.05	0.1513E-02	0.1568E-03
5.100	666.67	0.24	0.52	7.65	0.64	2.15	0.01	0.1500E-02	0.1773E-03
5.200	672.78	0.27	0.57	7.60	0.69	2.14	-0.09	0.1486E-02	0.2039E-03
5.300	678.89	0.29	0.63	7.55	0.74	2.14	-0.18	0.1473E-02	0.2350E-03
5.700	703.89	0.45	0.88	7.24	1.04	1.97	-0.22	0.1421E-02	0.5637E-03
5.800	709.44	0.47	0.92	7.24	1.03	1.97	-0.35	0.1410E-02	0.7042E-03
5.850	712.22	0.47	0.93	7.24	1.03	1.99	-0.40	0.1404E-02	0.8051E-03
5.900	715.00	0.47	0.94	7.24	1.03	2.01	-0.40	0.1399E-02	0.9415E-03
5.950	717.78	0.45	0.91	7.29	0.98	2.04	-0.47	0.1393E-02	0.1072E-02
6.000	720.56	0.42	0.86	7.34	0.93	2.06	-0.45	0.1388E-02	0.1257E-02
6.050	722.22	0.38	0.82	7.43	0.84	2.15	-0.59	0.1385E-02	0.1444E-02
6.100	723.89	0.31	0.71	7.54	0.74	2.26	-0.49	0.1381E-02	0.1675E-02
6.150	726.11	0.27	0.61	7.65	0.63	2.30	-0.54	0.1377E-02	0.1904E-02
6.200	727.78	0.18	0.44	7.81	0.48	2.47	-0.36	0.1374E-02	0.2135E-02
6.250	729.44	0.13	0.32	7.95	0.34	2.51	-0.39	0.1371E-02	0.2368E-02
6.300	731.67	0.09	0.22	8.06	0.23	2.56	-0.34	0.1367E-02	0.2539E-02
6.350	733.33	0.06	0.15	8.15	0.14	2.54	-0.69	0.1364E-02	0.2483E-02
6.400	735.00	0.03	0.10	8.20	0.10	2.80	-0.48	0.1361E-02	0.2669E-02
6.460	737.78	0.02	0.05	8.25	0.05	3.10	-0.82	0.1355E-02	0.2315E-02

RUN NO. 114

TIME HRS	TEMPERATURE K	CO %	CO2 %	O2 %	GAMA %	CO2/CO RATIO	H/C RATIO	INV.TEMP. 1/K	RELATIVE RATE,1/S
1.550	436.11	0.01	0.04	20.97	0.02	4.21	-2.00	0.2293E-02	0.2217E-05
2.000	453.33	0.01	0.04	20.92	0.08	2.71	2.74	0.2206E-02	0.9501E-05
2.200	463.89	0.02	0.04	20.90	0.11	2.19	4.67	0.2156E-02	0.1321E-04
2.500	480.00	0.03	0.04	20.82	0.20	1.30	7.06	0.2083E-02	0.2417E-04
2.700	491.67	0.04	0.07	20.63	0.44	1.64	12.55	0.2034E-02	0.5501E-04
2.900	503.89	0.07	0.10	20.50	0.59	1.50	10.61	0.1985E-02	0.7613E-04
3.100	515.00	0.09	0.13	20.40	0.70	1.58	9.53	0.1942E-02	0.9656E-04
3.300	526.67	0.12	0.18	20.27	0.83	1.49	8.11	0.1899E-02	0.1250E-03
3.500	539.44	0.15	0.25	20.22	0.87	1.64	5.39	0.1854E-02	0.1434E-03
3.600	545.56	0.17	0.30	20.15	0.95	1.77	4.94	0.1833E-02	0.1653E-03
3.650	548.33	0.17	0.30	20.16	0.93	1.77	4.63	0.1824E-02	0.1677E-03
3.700	551.67	0.17	0.32	20.17	0.91	1.87	4.13	0.1813E-02	0.1695E-03
3.800	557.78	0.16	0.32	20.22	0.85	1.97	3.74	0.1793E-02	0.1672E-03
3.900	563.89	0.15	0.30	20.30	0.76	1.97	3.37	0.1773E-02	0.1591E-03
4.000	568.89	0.15	0.30	20.38	0.67	2.09	2.65	0.1758E-02	0.1479E-03
4.100	573.89	0.14	0.29	20.47	0.55	2.10	1.88	0.1742E-02	0.1279E-03
4.200	578.89	0.13	0.27	20.52	0.50	2.10	1.65	0.1727E-02	0.1201E-03
4.300	584.44	0.12	0.27	20.55	0.46	2.25	1.36	0.1711E-02	0.1163E-03
4.400	588.89	0.12	0.26	20.58	0.42	2.20	1.08	0.1698E-02	0.1117E-03
4.500	593.33	0.12	0.27	20.60	0.40	2.25	0.77	0.1685E-02	0.1106E-03
4.600	598.89	0.12	0.28	20.59	0.41	2.31	0.80	0.1670E-02	0.1183E-03
4.700	605.56	0.12	0.29	20.56	0.44	2.30	0.91	0.1651E-02	0.1320E-03
4.800	610.56	0.14	0.31	20.55	0.45	2.27	0.65	0.1638E-02	0.1416E-03
4.900	616.67	0.14	0.37	20.50	0.50	2.68	0.52	0.1622E-02	0.1657E-03
5.200	633.33	0.18	0.43	20.39	0.61	2.37	0.62	0.1579E-02	0.2532E-03
5.400	644.44	0.21	0.53	20.32	0.66	2.59	0.12	0.1552E-02	0.3367E-03
5.500	650.00	0.22	0.57	20.27	0.71	2.57	0.11	0.1538E-02	0.4131E-03
5.600	655.56	0.26	0.63	20.22	0.75	2.44	-0.06	0.1525E-02	0.5149E-03
5.700	663.89	0.26	0.69	20.16	0.81	2.66	-0.02	0.1506E-02	0.6457E-03
5.750	666.67	0.26	0.71	20.13	0.85	2.68	0.05	0.1500E-02	0.6[illegible]E-03
5.800	669.44	0.26	0.73	20.12	0.85	2.77	-0.02	0.1494E-02	0.9849E-03
5.850	671.67	0.26	0.71	20.14	0.83	2.80	-0.04	0.1489E-02	0.1164E-02
5.900	673.89	0.24	0.69	20.17	0.80	2.89	-0.03	0.1484E-02	0.1410E-02

RUN NO. 114 (CONT.)

TIME HRS	TEMPERATURE K	CO %	CO2 %	O2 %	GAMA %	CO2/CO RATIO	H/C RATIO	INV.TEMP. 1/K	RELATIVE RATE,1/S
5.950	676.67	0.21	0.62	20.26	0.72	3.02	-0.04	0.1478E-02	0.1664E-02
6.000	678.89	0.17	0.52	20.40	0.58	3.09	-0.14	0.1473E-02	0.1941E-02
6.050	680.56	0.12	0.41	20.55	0.43	3.43	-0.30	0.1469E-02	0.1925E-02
6.100	682.22	0.08	0.29	20.67	0.31	3.50	-0.14	0.1466E-02	0.2000E-02
6.150	684.44	0.05	0.20	20.77	0.22	3.81	-0.16	0.1461E-02	0.2004E-02
6.200	686.67	0.03	0.13	20.85	0.14	3.94	-0.16	0.1456E-02	0.1911E-02
6.250	688.89	0.02	0.10	20.90	0.09	4.55	-0.64	0.1452E-02	0.1710E-02
6.300	691.11	0.02	0.07	20.92	0.07	4.01	-0.32	0.1447E-02	0.1813E-02
6.500	701.11	0.01	0.04	20.97	0.02	4.21	-2.00	0.1426E-02	0.2778E-02

RUN NO. 115

TIME HRS	TEMPERATURE K	CO %	CO2 %	O2 %	GAMA %	CO2/CO RATIO	H/C RATIO	INV.TEMP. 1/K	RELATIVE RATE,1/S
2.300	477.78	0.00	0.01	8.25	0.05	9.44	25.07	0.2093E-02	0.1032E-04
2.500	487.78	0.01	0.01	8.20	0.11	0.74	24.37	0.2050E-02	0.2097E-04
2.700	500.00	0.01	0.02	8.15	0.16	1.81	15.13	0.2000E-02	0.3180E-04
2.900	511.11	0.02	0.04	8.10	0.21	1.84	11.13	0.1957E-02	0.4330E-04
3.100	522.22	0.03	0.04	8.05	0.27	1.48	13.48	0.1915E-02	0.5436E-04
3.200	527.78	0.03	0.05	8.02	0.30	1.58	10.25	0.1895E-02	0.6417E-04
3.300	535.00	0.05	0.07	7.95	0.37	1.47	9.42	0.1869E-02	0.8217E-04
3.450	547.22	0.08	0.12	7.85	0.47	1.55	6.49	0.1827E-02	0.1103E-03
3.600	561.11	0.10	0.17	7.75	0.57	1.64	5.29	0.1782E-02	0.1434E-03
3.700	568.33	0.12	0.20	7.72	0.60	1.69	4.28	0.1760E-02	0.1591E-03
3.800	575.56	0.12	0.23	7.72	0.60	1.97	3.46	0.1737E-02	0.1679E-03
4.000	587.78	0.11	0.23	7.85	0.46	2.12	1.96	0.1701E-02	0.1641E-03
4.200	600.00	0.09	0.22	7.92	0.39	2.44	1.46	0.1667E-02	0.1330E-03
4.350	608.33	0.09	0.23	7.95	0.35	2.68	1.04	0.1644E-02	0.1317E-03
4.500	617.22	0.09	0.24	7.95	0.35	2.58	0.75	0.1620E-02	0.1410E-03
4.600	622.22	0.10	0.26	7.95	0.35	2.57	0.39	0.1607E-02	0.1474E-03
4.750	632.22	0.11	0.28	7.91	0.39	2.60	0.60	0.1582E-02	0.1860E-03
4.900	640.56	0.12	0.31	7.90	0.40	2.60	0.26	0.1561E-02	0.2034E-03
5.000	646.11	0.13	0.34	7.89	0.41	2.64	0.03	0.1548E-02	0.2240E-03
5.100	652.78	0.14	0.37	7.85	0.44	2.74	0.03	0.1532E-02	0.2609E-03
5.250	662.22	0.15	0.41	7.80	0.49	2.66	0.06	0.1510E-02	0.3227E-03
5.400	672.22	0.17	0.46	7.79	0.50	2.71	-0.31	0.1488E-02	0.442[illegible]E-03
5.500	678.33	0.18	0.49	7.77	0.52	2.72	-0.36	0.1474E-02	0.5450E-03
5.600	684.44	0.18	0.51	7.76	0.53	2.84	-0.43	0.1461E-02	0.6213E-03
5.650	687.22	0.18	0.51	7.78	0.51	2.85	-0.53	0.1455E-02	0.7556E-03
5.700	690.00	0.17	0.50	7.80	0.49	2.90	-0.58	0.1449E-02	0.8369E-03
5.800	695.56	0.14	0.42	7.88	0.41	3.05	-0.55	0.1438E-02	0.9741E-03
5.900	700.00	0.09	0.30	8.00	0.29	3.24	-0.59	0.1429E-02	0.9973E-03
6.000	704.44	0.06	0.20	8.10	0.19	3.37	-0.56	0.1420E-02	0.9450E-03
6.200	713.33	0.03	0.08	8.21	0.09	2.96	-0.02	0.1402E-02	0.8540E-03
6.500	729.44	0.02	0.04	8.26	0.04	2.19	-0.60	0.1371E-02	0.1102E-02
6.900	751.67	0.01	0.02	8.29	0.01	2.47	-2.40	0.1330E-02	0.5564E-02

RUN NO. 116

TIME HRS	TEMPERATURE K	CO %	CO2 %	O2 %	GAMA %	CO2/CO RATIO	H/C RATIO	INV.TEMP. 1/K	RELATIVE RATE,1/S
4.500	451.67	0.02	0.06	20.67	0.39	3.65	15.67		
5.450	453.89	0.01	0.05	20.70	0.36	5.96	19.29		
5.450	478.89	0.03	0.10	20.20	0.97	2.80	26.63		
6.450	483.89	0.03	0.09	20.27	0.88	3.33	28.21		
6.850	483.89	0.03	0.09	20.38	0.76	3.33	23.68		
6.850	511.11	0.09	0.17	20.63	0.40	1.79	2.92		
7.450	513.89	0.06	0.10	20.82	0.18	1.72	1.15		
7.850	513.33	0.05	0.10	20.95	0.02	2.00	-2.75		
8.250	512.78	0.04	0.09	21.00	0.00	2.02	-4.40		
8.250	538.33	0.12	0.23	20.70	0.29	1.97	-0.10		
8.550	542.78	0.08	0.15	20.70	0.32	1.98	2.28		
8.850	542.22	0.06	0.12	20.82	0.17	1.99	0.58		
9.050	541.67	0.05	0.10	20.85	0.15	2.00	0.56		
9.650	541.11	0.04	0.09	20.88	0.12	2.02	0.52		
9.650	556.11	0.08	0.20	20.75	0.24	2.63	0.05		
9.850	558.89	0.07	0.20	20.85	0.12	2.95	-1.73		
10.050	561.67	0.07	0.19	20.85	0.12	2.86	-1.65		
10.450	561.67	0.06	0.18	20.88	0.09	2.85	-2.00		
10.850	562.22	0.06	0.17	20.92	0.03	2.82	-2.87		
11.050	561.67	0.05	0.17	20.97	0.00	3.28	-4.02		
11.050	579.44	0.12	0.32	20.50	0.52	2.69	1.24		
11.150	582.22	0.10	0.30	20.67	0.31	2.90	-0.42		
11.350	583.33	0.09	0.26	20.75	0.22	3.08	-0.92		
11.450	583.89	0.08	0.21	20.77	0.21	2.59	-0.61		
11.650	585.00	0.07	0.22	20.82	0.15	3.20	-1.49		
11.850	584.44	0.06	0.20	20.88	0.09	3.11	-2.19		
12.050	584.44	0.05	0.18	20.88	0.09	3.38	-1.96		
12.250	583.89	0.05	0.17	20.92	0.04	3.28	-2.86		
12.450	583.89	0.05	0.16	20.92	0.04	3.15	-2.79		
12.550	583.89	0.05	0.15	20.95	0.01	3.06	-3.31		
12.550	610.00	0.17	0.52	20.50	0.45	3.03	-0.89		
12.750	614.44	0.14	0.39	20.50	0.49	2.87	0.26		
12.850	613.89	0.12	0.34	20.65	0.32	2.83	-0.67		

RUN NO. 116 (CONT.)

TIME HRS	TEMPERATURE K	CO %	CO2 %	O2 %	GAMA %	CO2/CO RATIO	H/C RATIO	INV.TEMP. 1/K	RELATIVE RATE,1/S
13.050	613.33	0.10	0.30	20.72	0.24	2.90	-1.05		
13.250	612.78	0.09	0.24	20.77	0.20	2.88	-1.09		
13.350	612.78	0.08	0.23	20.80	0.17	2.88	-1.35		
13.550	612.22	0.07	0.20	20.85	0.12	2.95	-1.73		
13.750	612.22	0.06	0.19	20.90	0.06	3.01	-2.61		
13.950	611.67	0.06	0.18	20.92	0.03	3.16	-2.96		
14.050	611.67	0.05	0.17	20.92	0.04	3.28	-2.86		
14.050	633.89	0.17	0.48	20.47	0.49	2.81	-0.46		
14.150	633.89	0.14	0.39	20.57	0.40	2.87	-0.46		
14.350	636.67	0.12	0.34	20.67	0.29	2.92	-0.93		
14.550	636.11	0.10	0.30	20.70	0.27	2.90	-0.74		
14.750	635.56	0.09	0.27	20.75	0.22	3.16	-1.00		
14.950	635.56	0.08	0.23	20.77	0.20	3.07	-0.91		
15.150	635.56	0.07	0.22	20.82	0.15	3.20	-1.49		
15.450	635.56	0.06	0.20	20.88	0.09	3.37	-2.18		
15.450	658.89	0.18	0.52	20.47	0.48	2.88	-0.74		
15.550	660.00	0.16	0.48	20.52	0.43	2.96	-0.82		
15.750	661.11	0.14	0.41	20.57	0.39	3.00	-0.61		
15.950	661.67	0.10	0.34	20.67	0.29	3.31	-0.86		
16.150	661.11	0.07	0.27	20.72	0.26	3.95	-0.52		
16.250	660.56	0.06	0.23	20.75	0.24	3.94	-0.36		
16.450	660.00	0.03	0.17	20.82	0.17	4.90	-0.34		
16.550	659.44	0.03	0.14	20.85	0.15	5.47	-0.21		

RUN NO. 117

TIME HRS	TEMPERATURE K	CO %	CO2 %	O2 %	GAMA %	CO2/CO RATIO	H/C RATIO	INV.TEMP. 1/K	RELATIVE RATE,1/S
2.600	405.56	0.00	0.01	20.95	0.06	9.44	29.08	0.2466E-02	0.3903E-05
3.200	430.00	0.00	0.01	20.90	0.12	9.44	63.03	0.2326E-02	0.7996E-05
3.400	442.22	0.00	0.01	20.85	0.19	9.44	96.98	0.2261E-02	0.1214E-04
3.600	453.33	0.01	0.02	20.77	0.28	2.47	31.69	0.2206E-02	0.1804E-04
3.700	458.89	0.02	0.04	20.72	0.33	2.19	20.59	0.2179E-02	0.2190E-04
3.800	464.44	0.02	0.04	20.64	0.44	1.84	26.55	0.2153E-02	0.2915E-04
3.900	471.67	0.03	0.05	20.54	0.56	1.58	22.09	0.2120E-02	0.3743E-04
4.100	486.67	0.06	0.10	20.30	0.84	1.72	17.59	0.2055E-02	0.5833E-04
4.300	498.33	0.10	0.16	20.10	1.06	1.63	13.24	0.2007E-02	0.7765E-04
4.400	507.22	0.12	0.19	20.00	1.17	1.68	12.01	0.1972E-02	0.8840E-04
4.500	514.44	0.14	0.23	19.94	1.23	1.72	10.14	0.1944E-02	0.9600E-04
4.600	520.56	0.15	0.26	19.89	1.28	1.70	9.20	0.1921E-02	0.1036E-03
4.700	526.11	0.17	0.30	19.85	1.32	1.74	7.86	0.1901E-02	0.1106E-03
4.800	531.67	0.20	0.36	19.82	1.33	1.80	6.42	0.1881E-02	0.1163E-03
4.850	534.44	0.21	0.37	19.83	1.32	1.81	5.88	0.1871E-02	0.1176E-03
4.900	537.22	0.21	0.39	19.85	1.29	1.92	5.32	0.1861E-02	0.1174E-03
4.950	540.00	0.21	0.41	19.88	1.25	1.99	4.88	0.1852E-02	0.1166E-03
5.000	542.78	0.21	0.42	19.91	1.21	2.04	4.42	0.1842E-02	0.1147E-03
5.100	548.89	0.20	0.43	20.01	1.07	2.13	3.46	0.1822E-02	0.1063E-03
5.200	554.44	0.19	0.41	20.11	0.96	2.19	3.09	0.1804E-02	0.9840E-04
5.300	558.89	0.17	0.39	20.20	0.86	2.29	2.76	0.1789E-02	0.9143E-04
5.400	563.89	0.16	0.37	20.27	0.77	2.37	2.45	0.1773E-02	0.8497E-04
5.500	568.89	0.15	0.37	20.31	0.73	2.46	2.19	0.1758E-02	0.8221E-04
5.600	573.89	0.14	0.36	20.35	0.69	2.59	2.04	0.1742E-02	0.8005E-04
5.700	578.89	0.14	0.36	20.38	0.65	2.61	1.87	0.1727E-02	0.7818E-04
5.800	583.33	0.14	0.37	20.38	0.65	2.74	1.63	0.1714E-02	0.7988E-04
5.900	589.44	0.14	0.39	20.37	0.66	2.76	1.46	0.1697E-02	0.8310E-04
6.000	594.44	0.15	0.42	20.33	0.69	2.73	1.35	0.1682E-02	0.9011E-04
6.100	599.44	0.16	0.45	20.30	0.72	2.78	1.24	0.1668E-02	0.9773E-04
6.200	605.00	0.18	0.51	20.25	0.77	2.82	0.99	0.1653E-02	0.1076E-03
6.300	610.56	0.21	0.57	20.16	0.85	2.78	0.89	0.1638E-02	0.1244E-03
6.400	617.22	0.24	0.66	20.07	0.93	2.78	0.68	0.1620E-02	0.1432E-03
6.500	625.00	0.28	0.76	19.95	1.05	2.77	0.57	0.1600E-02	0.1711E-03

RUN NO. 117 (CONT.)

TIME HRS	TEMPERATURE K	CO %	CO2 %	O2 %	GAMA %	CO2/CO RATIO	H/C RATIO	INV.TEMP. 1/K	RELATIVE RATE,1/S
6.600	630.56	0.33	0.90	19.79	1.21	2.72	0.47	0.1586E-02	0.2099E-03
6.700	638.89	0.41	1.08	19.59	1.39	2.62	0.28	0.1565E-02	0.2634E-03
6.750	642.22	0.46	1.20	19.45	1.52	2.62	0.23	0.1557E-02	0.3039E-03
6.800	645.56	0.52	1.34	19.25	1.72	2.56	0.26	0.1549E-02	0.3648E-03
6.850	652.22	0.61	1.56	18.95	2.02	2.58	0.28	0.1533E-02	0.4607E-03
6.875	655.56	0.64	1.65	18.85	2.12	2.56	0.25	0.1525E-02	0.5038E-03
6.900	658.89	0.66	1.71	18.80	2.16	2.57	0.20	0.1518E-02	0.5389E-03
6.950	662.22	0.67	1.74	18.84	2.10	2.60	0.02	0.1510E-02	0.5793E-03
7.000	666.11	0.64	1.67	18.97	1.95	2.59	-0.08	0.1501E-02	0.5997E-03
7.050	668.33	0.62	1.60	19.10	1.82	2.58	-0.18	0.1496E-02	0.6239E-03
7.100	671.11	0.60	1.55	19.22	1.68	2.59	-0.31	0.1490E-02	0.6471E-03
7.200	676.11	0.55	1.44	19.36	1.55	2.62	-0.35	0.1479E-02	0.7652E-03
7.300	680.56	0.50	1.33	19.51	1.41	2.65	-0.39	0.1469E-02	0.9429E-03
7.400	684.44	0.42	1.19	19.71	1.21	2.80	-0.49	0.1461E-02	0.1185E-02
7.450	686.11	0.38	1.11	19.80	1.12	2.90	-0.51	0.1457E-02	0.1381E-02
7.500	688.33	0.33	0.99	19.94	1.00	2.99	-0.49	0.1453E-02	0.1604E-02
7.550	690.00	0.27	0.86	20.08	0.86	3.14	-0.48	0.1449E-02	0.1899E-02
7.600	692.22	0.21	0.67	20.27	0.69	3.25	-0.39	0.1445E-02	0.2187E-02
7.700	694.44	0.08	0.30	20.65	0.34	3.71	-0.03	0.1440E-02	0.2643E-02
7.750	696.11	0.05	0.20	20.77	0.22	3.93	-0.14	0.1437E-02	0.2768E-02
7.800	697.78	0.03	0.11	20.85	0.15	4.21	0.97	0.1433E-02	0.3407E-02
7.900	700.56	0.01	0.04	20.95	0.05	4.14	-0.09	0.1427E-02	0.5557E-02

RUN NO. 118

TIME HRS	TEMPERATURE K	CO %	CO2 %	O2 %	GAMA %	CO2/CO RATIO	H/C RATIO	INV.TEMP. 1/K	RELATIVE RATE,1/S
2.800	433.33	0.00	0.01	20.99	0.02	9.44	5.31	0.2308E-02	0.2700E-05
3.300	462.22	0.00	0.01	20.95	0.06	9.44	29.08	0.2163E-02	0.9846E-05
3.600	480.56	0.00	0.01	20.90	0.12	2.83	50.93	0.2081E-02	0.2025E-04
3.800	491.67	0.01	0.01	20.85	0.18	1.33	39.78	0.2034E-02	0.3077E-04
4.000	503.33	0.02	0.03	20.81	0.23	1.62	18.98	0.1987E-02	0.3907E-04
4.200	514.44	0.02	0.03	20.77	0.27	1.67	18.03	0.1944E-02	0.4762E-04
4.400	526.11	0.03	0.04	20.75	0.30	1.50	14.12	0.1901E-02	0.5429E-04
4.600	538.33	0.04	0.07	20.70	0.34	1.57	9.36	0.1858E-02	0.6546E-04
4.700	544.44	0.05	0.08	20.69	0.36	1.50	8.05	0.1837E-02	0.6904E-04
4.800	550.56	0.06	0.10	20.67	0.37	1.72	5.85	0.1816E-02	0.7366E-04
4.900	556.67	0.06	0.12	20.65	0.39	1.78	5.37	0.1796E-02	0.7994E-04
4.950	560.00	0.07	0.12	20.66	0.38	1.79	4.97	0.1786E-02	0.7951E-04
5.000	562.78	0.07	0.12	20.66	0.37	1.83	4.66	0.1777E-02	0.7914E-04
5.100	568.33	0.06	0.13	20.70	0.33	1.98	3.48	0.1760E-02	0.7144E-04
5.200	573.33	0.06	0.12	20.72	0.31	2.04	3.42	0.1744E-02	0.6831E-04
5.300	578.89	0.05	0.12	20.75	0.27	2.25	3.16	0.1727E-02	0.6218E-04
5.400	583.89	0.05	0.12	20.77	0.25	2.25	2.56	0.1713E-02	0.5765E-04
5.500	589.44	0.05	0.11	20.79	0.22	2.20	2.29	0.1697E-02	0.5331E-04
5.600	595.00	0.05	0.11	20.81	0.20	2.28	1.70	0.1681E-02	0.4827E-04
5.800	605.56	0.05	0.11	20.80	0.20	2.34	1.72	0.1651E-02	0.5141E-04
6.000	616.11	0.05	0.13	20.79	0.21	2.64	1.07	0.1623E-02	0.5491E-04
6.200	626.67	0.06	0.16	20.75	0.26	2.49	1.12	0.1596E-02	0.7010E-04
6.300	632.78	0.07	0.17	20.72	0.28	2.50	1.21	0.1580E-02	0.7953E-04
6.400	638.89	0.08	0.20	20.69	0.31	2.41	0.95	0.1565E-02	0.8989E-04
6.500	645.56	0.10	0.23	20.64	0.37	2.34	0.98	0.1549E-02	0.1100E-03
6.600	651.67	0.12	0.28	20.55	0.46	2.34	1.26	0.1535E-02	0.1457E-03
6.700	658.33	0.15	0.34	20.46	0.55	2.22	1.14	0.1519E-02	0.1844E-03
6.800	664.44	0.18	0.41	20.39	0.62	2.27	0.80	0.1505E-02	0.2207E-03
6.900	671.11	0.21	0.47	20.29	0.71	2.26	0.78	0.1490E-02	0.2787E-03
7.000	677.78	0.25	0.55	20.20	0.80	2.22	0.59	0.1475E-02	0.3506E-03
7.100	683.89	0.29	0.64	20.07	0.92	2.21	0.59	0.1462E-02	0.4691E-03
7.200	690.00	0.33	0.75	19.97	1.01	2.24	0.37	0.1449E-02	0.6243E-03
7.300	696.11	0.37	0.84	19.87	1.11	2.25	0.24	0.1437E-02	0.8941E-03

RUN NO. 118 (CONT.)

TIME HRS	TEMPERATURE K	CO %	CO2 %	O2 %	GAMA %	CO2/CO RATIO	H/C RATIO	INV.TEMP. 1/K	RELATIVE RATE,1/S
7.325	697.78	0.40	0.86	19.86	1.11	2.15	0.17	0.1433E-02	0.9756E-03
7.350	699.44	0.38	0.85	19.89	1.07	2.26	0.10	0.1430E-02	0.1032E-02
7.400	701.67	0.36	0.82	19.96	1.00	2.30	-0.01	0.1425E-02	0.1176E-02
7.450	703.89	0.33	0.77	20.06	0.89	2.33	-0.15	0.1421E-02	0.1308E-02
7.500	705.56	0.29	0.68	20.20	0.76	2.35	-0.26	0.1417E-02	0.1420E-02
7.550	707.22	0.24	0.59	20.32	0.63	2.44	-0.39	0.1414E-02	0.1550E-02
7.600	708.33	0.20	0.48	20.45	0.51	2.39	-0.42	0.1412E-02	0.1684E-02
7.700	711.67	0.15	0.37	20.65	0.30	2.46	-1.11	0.1405E-02	0.1923E-02
7.750	713.33	0.09	0.24	20.72	0.26	2.58	-0.35	0.1402E-02	0.2412E-02
7.800	715.56	0.07	0.17	20.80	0.19	2.58	-0.24	0.1398E-02	0.2838E-02
7.850	717.78	0.04	0.12	20.87	0.12	3.01	-0.39	0.1393E-02	0.3157E-02
7.900	719.44	0.02	0.07	20.92	0.08	3.66	-0.09	0.1390E-02	0.3722E-02
8.000	723.33	0.00	0.02	20.97	0.03	31.38	0.47	0.1382E-02	0.1112E-01

RUN NO. 119

TIME HRS	TEMPERATURE K	CO %	CO2 %	O2 %	GAMA %	CO2/CO RATIO	H/C RATIO	INV.TEMP. 1/K	RELATIVE RATE,1/S
1.500	375.00	0.00	0.01	20.99	0.01	9.44	1.92	0.2667E-02	0.1322E-05
2.000	403.33	0.00	0.01	20.96	0.04	9.44	18.89	0.2479E-02	0.5267E-05
2.150	411.67	0.00	0.01	20.95	0.06	9.44	29.08	0.2429E-02	0.7656E-05
2.400	426.11	0.00	0.01	20.92	0.09	13.81	30.95	0.2347E-02	0.1160E-04
3.000	460.00	0.00	0.01	20.90	0.12	5.45	28.15	0.2174E-02	0.1588E-04
3.300	477.78	0.01	0.03	20.85	0.18	2.31	14.01	0.2093E-02	0.2370E-04
3.550	491.67	0.02	0.05	20.75	0.30	2.12	13.62	0.2034E-02	0.4056E-04
3.800	505.56	0.04	0.10	20.65	0.41	2.66	8.94	0.1978E-02	0.5805E-04
4.100	522.78	0.06	0.13	20.57	0.49	2.40	6.80	0.1913E-02	0.7442E-04
4.350	537.78	0.08	0.19	20.54	0.50	2.34	3.99	0.1860E-02	0.8258E-04
4.450	543.89	0.09	0.20	20.54	0.50	2.32	3.63	0.1839E-02	0.8552E-04
4.500	547.22	0.09	0.20	20.55	0.49	2.36	3.36	0.1827E-02	0.8453E-04
4.600	552.78	0.09	0.22	20.59	0.44	2.46	2.29	0.1809E-02	0.7742E-04
4.700	557.78	0.09	0.22	20.63	0.39	2.56	1.77	0.1793E-02	0.7167E-04
5.000	573.33	0.07	0.20	20.74	0.26	2.91	0.50	0.1744E-02	0.5152E-04
5.200	584.44	0.06	0.19	20.74	0.26	3.17	0.57	0.1711E-02	0.5276E-04
5.300	589.44	0.06	0.20	20.73	0.27	3.37	0.64	0.1697E-02	0.5613E-04
5.550	602.22	0.07	0.22	20.70	0.30	3.20	0.73	0.1661E-02	0.6610E-04
5.800	616.11	0.08	0.25	20.65	0.35	3.08	0.74	0.1623E-02	0.8244E-04
6.000	627.22	0.10	0.30	20.57	0.43	2.97	0.75	0.1594E-02	0.1071E-03
6.100	633.33	0.12	0.34	20.55	0.45	2.83	0.44	0.1579E-02	0.1162E-03
6.200	638.89	0.14	0.38	20.49	0.52	2.76	0.55	0.1565E-02	0.1399E-03
6.300	645.00	0.16	0.44	20.40	0.60	2.74	0.48	0.1550E-02	0.1717E-03
6.400	651.67	0.20	0.52	20.27	0.73	2.63	0.63	0.1535E-02	0.2242E-03
6.500	658.33	0.24	0.61	20.15	0.85	2.54	0.56	0.1519E-02	0.2868E-03
6.600	664.44	0.28	0.71	20.05	0.94	2.56	0.39	0.1505E-02	0.3568E-03
6.700	670.56	0.31	0.77	19.96	1.02	2.48	0.34	0.1491E-02	0.4473E-03
6.750	673.89	0.33	0.82	19.92	1.06	2.50	0.25	0.1484E-02	0.5058E-03
6.800	676.67	0.35	0.86	19.89	1.08	2.48	0.13	0.1478E-02	0.5656E-03
6.850	679.44	0.35	0.88	19.88	1.08	2.52	0.07	0.1472E-02	0.6338E-03
6.900	682.22	0.36	0.90	19.90	1.06	2.54	-0.08	0.1466E-02	0.6976E-03
6.950	685.00	0.36	0.90	19.90	1.05	2.54	-0.10	0.1460E-02	0.7928E-03
7.000	687.78	0.35	0.90	19.94	1.01	2.58	-0.23	0.1454E-02	0.8798E-03

RUN NO. 119 (CONT.)

TIME HRS	TEMPERATURE K	CO %	CO2 %	O2 %	GAMA %	CO2/CO RATIO	H/C RATIO	INV.TEMP. 1/K	RELATIVE RATE,1/S
7.050	690.56	0.34	0.88	19.98	0.97	2.59	-0.26	0.1448E-02	0.1006E-02
7.100	693.33	0.32	0.84	20.05	0.90	2.63	-0.38	0.1442E-02	0.1123E-02
7.200	697.78	0.26	0.71	20.22	0.72	2.76	-0.50	0.1433E-02	0.1432E-02
7.300	702.22	0.17	0.52	20.46	0.50	2.97	-0.61	0.1424E-02	0.1755E-02
7.400	706.11	0.11	0.36	20.66	0.31	3.21	-0.90	0.1416E-02	0.2195E-02
7.500	711.11	0.05	0.20	20.82	0.15	3.93	-1.14	0.1406E-02	0.2726E-02
7.600	716.11	0.02	0.10	20.92	0.06	5.86	-1.60	0.1396E-02	0.3605E-02
7.700	721.11	0.00	0.05	20.97	0.02	75.64	-2.73	0.1387E-02	0.5562E-02

RUN NO. 120

TIME HRS	TEMPERATURE K	CO %	CO2 %	O2 %	GAMA %	CO2/CO RATIO	H/C RATIO	INV.TEMP. 1/K	RELATIVE RATE,1/S
1.600	417.22	0.00	0.01	20.97	0.03	9.44	12.10	0.2397E-02	0.3342E-05
1.900	434.44	0.00	0.01	20.95	0.06	9.44	29.08	0.2302E-02	0.6943E-05
2.200	451.67	0.00	0.01	20.90	0.12	4.14	36.64	0.2214E-02	0.1412E-04
2.400	463.33	0.01	0.02	20.85	0.18	1.30	22.40	0.2158E-02	0.2112E-04
2.600	475.56	0.02	0.04	20.75	0.30	2.01	19.73	0.2103E-02	0.3574E-04
2.800	487.78	0.03	0.06	20.64	0.43	1.86	14.27	0.2050E-02	0.5236E-04
3.000	500.00	0.05	0.10	20.52	0.56	1.87	12.01	0.2000E-02	0.7157E-04
3.100	506.11	0.07	0.11	20.48	0.61	1.64	10.74	0.1976E-02	0.8000E-04
3.200	512.22	0.07	0.13	20.43	0.66	1.80	9.63	0.1952E-02	0.8908E-04
3.300	518.33	0.09	0.14	20.40	0.69	1.67	8.82	0.1929E-02	0.9729E-04
3.400	524.44	0.10	0.17	20.38	0.72	1.64	7.42	0.1907E-02	0.1040E-03
3.500	530.56	0.11	0.19	20.39	0.69	1.70	6.03	0.1885E-02	0.1040E-03
3.600	536.67	0.12	0.22	20.41	0.65	1.86	4.41	0.1863E-02	0.1024E-03
3.800	547.78	0.12	0.26	20.49	0.55	2.05	2.47	0.1826E-02	0.9232E-04
4.000	558.89	0.12	0.25	20.56	0.45	2.17	1.56	0.1789E-02	0.8085E-04
4.200	570.00	0.10	0.24	20.61	0.40	2.33	1.27	0.1754E-02	0.7496E-04
4.400	581.11	0.09	0.23	20.63	0.37	2.51	1.14	0.1721E-02	0.7471E-04
4.500	586.67	0.10	0.24	20.63	0.38	2.49	1.05	0.1705E-02	0.7753E-04
4.600	592.22	0.10	0.26	20.63	0.38	2.58	0.86	0.1689E-02	0.8025E-04
4.700	598.33	0.10	0.27	20.60	0.40	2.63	0.88	0.1671E-02	0.8721E-04
4.800	604.44	0.11	0.30	20.59	0.41	2.76	0.61	0.1654E-02	0.9241E-04
4.900	610.00	0.12	0.32	20.55	0.45	2.69	0.66	0.1639E-02	0.1053E-03
5.000	616.11	0.14	0.37	20.45	0.56	2.71	0.93	0.1623E-02	0.1348E-03
5.100	621.11	0.15	0.42	20.45	0.54	2.71	0.37	0.1610E-02	0.1390E-03
5.200	625.56	0.18	0.48	20.38	0.62	2.68	0.27	0.1599E-02	0.1659E-03
5.300	633.33	0.21	0.57	20.29	0.69	2.70	0.08	0.1579E-02	0.1990E-03
5.400	642.22	0.26	0.69	20.15	0.83	2.66	0.03	0.1557E-02	0.2578E-03
5.500	651.11	0.33	0.88	19.95	1.00	2.68	-0.16	0.1536E-02	0.3487E-03
5.550	655.56	0.37	0.95	19.83	1.13	2.57	0.01	0.1525E-02	0.4229E-03
5.600	660.00	0.41	1.05	19.78	1.16	2.55	-0.27	0.1515E-02	0.4685E-03
5.650	663.89	0.45	1.15	19.65	1.29	2.56	-0.25	0.1506E-02	0.5703E-03
5.700	667.22	0.46	1.15	19.67	1.26	2.53	-0.32	0.1499E-02	0.6217E-03
5.750	670.56	0.45	1.13	19.72	1.20	2.53	-0.41	0.1491E-02	0.6640E-03

RUN NO. 120 (CONT.)

TIME HRS	TEMPERATURE K	CO %	CO2 %	O2 %	GAMA %	CO2/CO RATIO	H/C RATIO	INV.TEMP. 1/K	RELATIVE RATE,1/S
5.800	673.33	0.44	1.10	19.80	1.11	2.53	-0.57	0.1485E-02	0.6937E-03
5.850	676.11	0.41	1.05	19.86	1.05	2.55	-0.56	0.1479E-02	0.7507E-03
5.900	678.89	0.40	1.03	19.91	1.00	2.56	-0.66	0.1473E-02	0.8190E-03
6.000	683.33	0.37	0.95	20.00	0.92	2.61	-0.67	0.1463E-02	0.1052E-02
6.100	688.89	0.33	0.88	20.10	0.82	2.71	-0.76	0.1452E-02	0.1465E-02
6.200	692.22	0.24	0.71	20.32	0.60	2.93	-0.95	0.1445E-02	0.1992E-02
6.300	694.44	0.14	0.43	20.60	0.36	3.13	-0.98	0.1440E-02	0.2743E-02
6.350	695.56	0.09	0.28	20.74	0.24	3.24	-0.87	0.1438E-02	0.3134E-02
6.400	696.67	0.06	0.20	20.83	0.15	3.37	-1.30	0.1435E-02	0.3494E-02
6.500	698.89	0.02	0.06	20.95	0.04	3.65	-1.51	0.1431E-02	0.5222E-02

RUN NO. 121

TIME HRS	TEMPERATURE K	CO %	CO2 %	O2 %	GAMA %	CO2/CO RATIO	H/C RATIO	INV.TEMP. 1/K	RELATIVE RATE,1/S
3.000	407.22	0.00	0.01	20.99	0.02	9.44	5.31	0.2456E-02	0.1680E-05
3.100	412.78	0.00	0.01	20.97	0.03	9.44	12.10	0.2423E-02	0.2934E-05
3.400	430.56	0.00	0.01	20.95	0.06	9.44	29.08	0.2323E-02	0.6091E-05
3.600	443.33	0.00	0.01	20.92	0.09	9.44	46.05	0.2256E-02	0.9285E-05
3.700	450.00	0.00	0.01	20.90	0.12	9.44	63.03	0.2222E-02	0.1249E-04
3.900	462.78	0.00	0.01	20.85	0.19	4.14	57.30	0.2161E-02	0.1891E-04
4.000	468.89	0.01	0.02	20.82	0.22	2.82	35.99	0.2133E-02	0.2201E-04
4.200	481.67	0.02	0.04	20.71	0.34	2.00	20.79	0.2076E-02	0.3597E-04
4.400	494.44	0.03	0.06	20.59	0.49	1.76	17.33	0.2022E-02	0.5233E-04
4.600	506.67	0.05	0.09	20.49	0.60	1.75	13.26	0.1974E-02	0.6726E-04
4.700	512.78	0.06	0.10	20.45	0.65	1.62	12.56	0.1950E-02	0.7491E-04
4.800	518.89	0.07	0.12	20.42	0.67	1.70	10.75	0.1927E-02	0.7989E-04
4.900	525.00	0.09	0.13	20.40	0.69	1.58	9.42	0.1905E-02	0.8451E-04
5.000	531.11	0.10	0.16	20.40	0.69	1.67	7.24	0.1883E-02	0.8655E-04
5.100	537.22	0.10	0.18	20.39	0.69	1.81	6.35	0.1861E-02	0.8937E-04
5.200	542.78	0.11	0.20	20.40	0.67	1.82	5.40	0.1842E-02	0.9060E-04
5.300	548.89	0.12	0.23	20.42	0.63	1.97	4.08	0.1822E-02	0.8807E-04
5.400	554.44	0.11	0.23	20.47	0.57	2.12	3.28	0.1804E-02	0.8177E-04
5.500	560.00	0.10	0.23	20.52	0.51	2.23	2.84	0.1786E-02	0.7546E-04
5.600	565.00	0.09	0.22	20.57	0.45	2.33	2.45	0.1770E-02	0.6867E-04
5.700	570.56	0.09	0.20	20.63	0.40	2.40	2.09	0.1753E-02	0.6145E-04
5.800	575.56	0.08	0.20	20.65	0.37	2.41	1.76	0.1737E-02	0.5801E-04
5.900	580.56	0.08	0.20	20.67	0.34	2.58	1.50	0.1722E-02	0.5455E-04
6.000	586.11	0.07	0.20	20.67	0.34	2.64	1.53	0.1706E-02	0.5572E-04
6.100	591.11	0.08	0.20	20.68	0.33	2.63	1.33	0.1692E-02	0.5556E-04
6.200	596.11	0.08	0.22	20.67	0.34	2.67	1.06	0.1678E-02	0.5789E-04
6.300	601.67	0.09	0.23	20.65	0.36	2.76	1.01	0.1662E-02	0.6265E-04
6.400	607.22	0.09	0.25	20.63	0.38	2.74	1.00	0.1647E-02	0.6868E-04
6.500	612.78	0.10	0.28	20.59	0.41	2.77	0.80	0.1632E-02	0.7547E-04
6.600	618.33	0.12	0.32	20.55	0.45	2.69	0.66	0.1617E-02	0.8571E-04
6.700	624.44	0.13	0.36	20.49	0.51	2.67	0.72	0.1601E-02	0.9969E-04
6.800	630.56	0.15	0.41	20.41	0.60	2.68	0.76	0.1586E-02	0.1214E-03
6.900	637.22	0.19	0.48	20.32	0.68	2.57	0.61	0.1569E-02	0.1457E-03

RUN NO. 121 (CONT.)

TIME HRS	TEMPERATURE K	CO %	CO2 %	O2 %	GAMA %	CO2/CO RATIO	H/C RATIO	INV.TEMP. 1/K	RELATIVE RATE,1/S
7.000	644.44	0.23	0.60	20.17	0.82	2.60	0.49	0.1552E-02	0.1865E-03
7.050	648.89	0.26	0.66	20.06	0.95	2.54	0.70	0.1541E-02	0.2227E-03
7.100	653.33	0.30	0.75	19.90	1.11	2.46	0.83	0.1531E-02	0.2738E-03
7.150	656.67	0.37	0.90	19.70	1.31	2.47	0.69	0.1523E-02	0.3399E-03
7.200	661.67	0.40	0.99	19.61	1.38	2.46	0.57	0.1511E-02	0.3841E-03
7.300	670.00	0.45	1.11	19.51	1.47	2.47	0.33	0.1493E-02	0.4742E-03
7.400	677.78	0.50	1.24	19.41	1.55	2.48	0.13	0.1475E-02	0.6095E-03
7.450	681.11	0.51	1.29	19.38	1.58	2.52	0.07	0.1468E-02	0.6980E-03
7.500	684.44	0.53	1.32	19.38	1.57	2.49	-0.04	0.1461E-02	0.7919E-03
7.550	687.22	0.53	1.33	19.39	1.55	2.52	-0.10	0.1455E-02	0.9106E-03
7.600	690.00	0.51	1.31	19.45	1.48	2.54	-0.19	0.1449E-02	0.1038E-02
7.650	692.22	0.49	1.24	19.55	1.38	2.55	-0.25	0.1445E-02	0.1180E-02
7.700	694.44	0.45	1.15	19.70	1.22	2.59	-0.39	0.1440E-02	0.1308E-02
7.800	697.78	0.32	0.86	20.05	0.89	2.72	-0.46	0.1433E-02	0.1604E-02
7.900	700.00	0.19	0.54	20.41	0.56	2.85	-0.42	0.1429E-02	0.1881E-02
7.950	701.11	0.14	0.39	20.56	0.42	2.87	-0.32	0.1426E-02	0.2010E-02
8.000	702.22	0.10	0.29	20.68	0.30	3.00	-0.31	0.1424E-02	0.2130E-02
8.050	703.33	0.06	0.20	20.77	0.21	3.19	-0.27	0.1422E-02	0.2237E-02
8.100	705.56	0.04	0.14	20.84	0.16	3.51	-0.05	0.1417E-02	0.2479E-02
8.200	715.00	0.02	0.06	20.92	0.07	3.65	0.05	0.1399E-02	0.3414E-02
8.300	724.44	0.00	0.02	20.97	0.03	9.40	0.23	0.1380E-02	0.6625E-02

RUN NO. 122

TIME HRS	TEMPERATURE K	CO %	CO2 %	O2 %	GAMA %	CO2/CO RATIO	H/C RATIO	INV.TEMP. 1/K	RELATIVE RATE,1/S
2.300	440.56	0.00	0.01	8.28	0.02	9.44	7.53	0.2270E-02	0.2646E-05
2.500	452.22	0.00	0.01	8.26	0.04	9.44	19.22	0.2211E-02	0.5391E-05
2.700	463.89	0.00	0.01	8.25	0.05	9.44	25.07	0.2156E-02	0.6789E-05
3.100	487.22	0.00	0.01	8.20	0.11	9.44	54.32	0.2052E-02	0.1386E-04
3.300	498.89	0.00	0.01	8.15	0.16	2.43	43.21	0.2004E-02	0.2101E-04
3.500	510.56	0.01	0.02	8.10	0.22	1.78	30.97	0.1959E-02	0.2843E-04
3.700	522.22	0.02	0.03	8.05	0.27	1.83	18.46	0.1915E-02	0.3614E-04
3.900	533.89	0.03	0.04	8.01	0.32	1.48	16.55	0.1873E-02	0.4380E-04
4.200	552.22	0.05	0.07	7.98	0.34	1.47	8.31	0.1811E-02	0.4934E-04
4.300	557.78	0.05	0.09	7.95	0.37	1.63	7.40	0.1793E-02	0.5485E-04
4.400	563.89	0.06	0.10	7.93	0.39	1.62	6.17	0.1773E-02	0.5893E-04
4.500	569.44	0.07	0.12	7.91	0.41	1.74	5.49	0.1756E-02	0.6333E-04
4.600	575.56	0.08	0.13	7.92	0.39	1.76	4.21	0.1737E-02	0.6272E-04
4.700	581.11	0.07	0.14	7.94	0.37	1.89	3.60	0.1721E-02	0.6053E-04
4.800	586.67	0.07	0.14	7.96	0.35	1.98	3.28	0.1705E-02	0.5829E-04
4.900	591.67	0.07	0.14	7.99	0.32	2.03	2.86	0.1690E-02	0.5406E-04
5.000	596.67	0.06	0.14	8.03	0.28	2.14	2.09	0.1676E-02	0.4761E-04
5.200	607.22	0.06	0.13	8.06	0.24	2.26	1.64	0.1647E-02	0.4351E-04
5.400	617.22	0.06	0.14	8.06	0.24	2.36	1.32	0.1620E-02	0.4473E-04
5.600	627.78	0.07	0.17	8.04	0.26	2.46	1.03	0.1593E-02	0.4993E-04
5.800	640.56	0.09	0.20	8.00	0.30	2.36	0.81	0.1561E-02	0.5968E-04
6.000	652.22	0.10	0.23	7.96	0.34	2.30	0.65	0.1533E-02	0.7065E-04
6.150	660.56	0.12	0.27	7.90	0.40	2.25	0.75	0.1514E-02	0.8687E-04
6.300	670.56	0.15	0.34	7.80	0.50	2.20	0.70	0.1491E-02	0.1145E-03
6.500	683.33	0.21	0.44	7.63	0.67	2.07	0.72	0.1463E-02	0.1698E-03
6.600	690.00	0.25	0.52	7.53	0.77	2.06	0.66	0.1449E-02	0.2086E-03
6.700	696.67	0.30	0.62	7.40	0.90	2.04	0.56	0.1435E-02	0.2649E-03
6.750	700.00	0.34	0.69	7.26	1.04	2.03	0.72	0.1429E-02	0.3236E-03
6.800	703.33	0.40	0.82	7.05	1.25	2.07	0.75	0.1422E-02	0.4159E-03
6.850	707.22	0.50	1.01	6.70	1.61	2.03	0.94	0.1414E-02	0.5037E-03
6.900	711.11	0.59	1.20	6.47	1.83	2.03	0.76	0.1406E-02	0.7500E-03
6.950	713.89	0.64	1.26	6.47	1.83	1.99	0.51	0.1401E-02	0.8632E-03
7.000	716.67	0.62	1.24	6.65	1.63	2.00	0.17	0.1395E-02	0.9065E-03

RUN NO. 122 (CONT.)

TIME HRS	TEMPERATURE K	CO %	CO2 %	O2 %	GAMA %	CO2/CO RATIO	H/C RATIO	INV.TEMP. 1/K	RELATIVE RATE,1/S
7.050	718.89	0.57	1.14	6.87	1.41	2.00	-0.04	0.1391E-02	0.9215E-03
7.100	720.00	0.51	1.03	7.05	1.23	2.01	-0.16	0.1389E-02	0.9502E-03
7.200	722.78	0.42	0.86	7.33	0.94	2.06	-0.41	0.1384E-02	0.1049E-02
7.300	726.11	0.33	0.69	7.55	0.73	2.09	-0.51	0.1377E-02	0.1213E-02
7.400	729.44	0.24	0.52	7.73	0.55	2.18	-0.49	0.1371E-02	0.1499E-02
7.500	732.78	0.15	0.36	7.92	0.37	2.31	-0.50	0.1365E-02	0.1815E-02
7.600	738.33	0.10	0.23	8.05	0.24	2.30	-0.52	0.1354E-02	0.2600E-02
7.700	743.89	0.04	0.12	8.18	0.12	2.78	-0.58	0.1344E-02	0.4059E-02
7.800	748.89	0.01	0.04	8.28	0.02	4.21	-2.13	0.1335E-02	0.3842E-02
7.900	753.33	0.00	0.02	8.29	0.00	22.58	-2.98	0.1327E-02	0.5577E-02

RUN NO. 123

TIME HRS	TEMPERATURE K	CO %	CO2 %	O2 %	GAMA %	CO2/CO RATIO	H/C RATIO	INV.TEMP. 1/K	RELATIVE RATE,1/S
4.100	403.33	0.00	0.01	20.99	0.01	9.44	1.92	0.2479E-02	0.1391E-05
4.500	425.00	0.00	0.01	20.98	0.02	9.44	8.71	0.2353E-02	0.3047E-05
4.700	436.11	0.00	0.01	20.97	0.04	9.44	15.50	0.2293E-02	0.4714E-05
4.900	447.22	0.00	0.01	20.96	0.05	9.44	22.28	0.2236E-02	0.6395E-05
5.100	457.78	0.00	0.01	20.94	0.07	9.44	35.87	0.2184E-02	0.9778E-05
5.400	474.44	0.00	0.01	20.92	0.10	3.21	20.35	0.2108E-02	0.1362E-04
5.700	490.56	0.01	0.02	20.87	0.15	2.47	15.77	0.2039E-02	0.2059E-04
5.900	501.11	0.01	0.03	20.84	0.19	2.26	13.18	0.1996E-02	0.2637E-04
6.100	512.22	0.02	0.04	20.79	0.25	2.19	14.68	0.1952E-02	0.3555E-04
6.300	523.89	0.03	0.04	20.76	0.28	1.72	12.94	0.1909E-02	0.4150E-04
6.500	522.22	0.03	0.06	20.71	0.34	1.76	11.79	0.1915E-02	0.5087E-04
6.600	528.33	0.03	0.06	20.71	0.34	1.76	11.17	0.1893E-02	0.5240E-04
6.700	535.00	0.05	0.07	20.68	0.37	1.47	9.51	0.1869E-02	0.5842E-04
6.800	542.22	0.06	0.09	20.64	0.42	1.50	7.98	0.1844E-02	0.6652E-04
6.900	548.89	0.07	0.12	20.60	0.45	1.62	6.27	0.1822E-02	0.7467E-04
7.000	555.56	0.09	0.13	20.56	0.50	1.58	5.85	0.1800E-02	0.8410E-04
7.100	561.67	0.09	0.17	20.53	0.52	1.79	4.69	0.1780E-02	0.9061E-04
7.150	563.89	0.10	0.17	20.53	0.52	1.77	4.38	0.1773E-02	0.9247E-04
7.200	566.67	0.10	0.18	20.53	0.52	1.81	3.96	0.1765E-02	0.9340E-04
7.250	569.44	0.10	0.19	20.54	0.51	1.84	3.72	0.1756E-02	0.9298E-04
7.300	572.78	0.10	0.19	20.55	0.49	1.90	3.31	0.1746E-02	0.9140E-04
7.400	578.89	0.10	0.20	20.60	0.43	2.07	2.50	0.1727E-02	0.8237E-04
7.500	584.44	0.10	0.20	20.60	0.43	2.07	2.50	0.1711E-02	0.8469E-04
7.600	590.56	0.09	0.20	20.61	0.42	2.19	2.42	0.1693E-02	0.8523E-04
7.700	597.22	0.09	0.20	20.62	0.40	2.23	2.17	0.1674E-02	0.8504E-04
7.800	603.33	0.09	0.21	20.63	0.39	2.26	1.77	0.1657E-02	0.8528E-04
7.900	609.44	0.10	0.23	20.63	0.39	2.31	1.34	0.1641E-02	0.8668E-04
8.000	616.11	0.10	0.23	20.62	0.40	2.30	1.32	0.1623E-02	0.9181E-04
8.100	622.22	0.10	0.25	20.61	0.40	2.42	1.10	0.1607E-02	0.9622E-04
8.200	628.89	0.12	0.27	20.59	0.41	2.32	0.89	0.1590E-02	0.1022E-03
8.300	635.56	0.12	0.29	20.57	0.44	2.40	0.90	0.1573E-02	0.1127E-03
8.400	642.22	0.13	0.30	20.55	0.45	2.28	0.77	0.1557E-02	0.1221E-03
8.500	648.89	0.15	0.34	20.52	0.48	2.33	0.57	0.1541E-02	0.1351E-03

RUN NO. 123 (CONT.)

TIME HRS	TEMPERATURE K	CO %	CO2 %	O2 %	GAMA %	CO2/CO RATIO	H/C RATIO	INV.TEMP. 1/K	RELATIVE RATE,1/S
8.600	655.56	0.16	0.37	20.50	0.49	2.30	0.27	0.1525E-02	0.1456E-03
8.700	662.22	0.18	0.41	20.46	0.53	2.27	0.19	0.1510E-02	0.1654E-03
8.800	668.89	0.21	0.44	20.39	0.60	2.16	0.32	0.1495E-02	0.2008E-03
8.900	675.56	0.24	0.52	20.32	0.66	2.15	0.11	0.1480E-02	0.2392E-03
9.000	682.22	0.27	0.56	20.25	0.73	2.09	0.15	0.1466E-02	0.2907E-03
9.100	688.33	0.31	0.64	20.17	0.80	2.07	0.03	0.1453E-02	0.3584E-03
9.200	694.44	0.34	0.71	20.11	0.85	2.08	-0.10	0.1440E-02	0.4392E-03
9.250	697.22	0.35	0.75	20.07	0.89	2.14	-0.12	0.1434E-02	0.4992E-03
9.300	700.00	0.37	0.78	20.00	0.96	2.14	-0.03	0.1429E-02	0.5962E-03
9.350	702.78	0.39	0.84	19.92	1.04	2.15	-0.01	0.1423E-02	0.7260E-03
9.400	705.56	0.42	0.90	19.83	1.13	2.15	0.04	0.1417E-02	0.9139E-03
9.425	707.22	0.43	0.95	19.81	1.14	2.20	-0.06	0.1414E-02	0.1007E-02
9.450	708.33	0.44	0.95	19.82	1.13	2.17	-0.11	0.1412E-02	0.1094E-02
9.500	711.67	0.40	0.88	19.96	0.98	2.20	-0.35	0.1405E-02	0.1159E-02
9.550	713.89	0.35	0.80	20.10	0.84	2.31	-0.50	0.1401E-02	0.1229E-02
9.600	716.11	0.31	0.71	20.22	0.72	2.26	-0.57	0.1396E-02	0.1331E-02
9.700	720.56	0.21	0.50	20.45	0.51	2.33	-0.56	0.1388E-02	0.1589E-02
9.800	725.00	0.12	0.30	20.64	0.34	2.54	-0.18	0.1379E-02	0.2068E-02
9.850	727.78	0.09	0.23	20.75	0.23	2.76	-0.57	0.1374E-02	0.2024E-02
9.900	730.56	0.06	0.18	20.82	0.16	2.93	-0.87	0.1369E-02	0.2054E-02
10.000	735.00	0.02	0.10	20.92	0.07	5.86	-1.39	0.1361E-02	0.1864E-02
10.100	738.89	0.01	0.04	20.96	0.04	5.16	-0.30	0.1353E-02	0.2159E-02
10.200	743.89	0.01	0.01	20.98	0.02	1.72	2.16	0.1344E-02	0.2982E-02

RUN NO. 124

TIME HRS	TEMPERATURE K	CO %	CO2 %	O2 %	GAMA %	CO2/CO RATIO	H/C RATIO	INV.TEMP. 1/K	RELATIVE RATE,1/S
1.200	428.89	0.00	0.01	20.98	0.02	9.44	8.71	0.2332E-02	0.1881E-05
1.400	440.00	0.00	0.01	20.96	0.05	9.44	22.28	0.2273E-02	0.3930E-05
1.600	451.11	0.00	0.01	20.92	0.10	9.44	49.44	0.2217E-02	0.8051E-05
1.800	462.78	0.00	0.01	20.89	0.14	2.43	35.51	0.2161E-02	0.1106E-04
1.900	469.44	0.01	0.01	20.86	0.17	1.43	27.87	0.2130E-02	0.1404E-04
2.000	475.56	0.01	0.02	20.82	0.22	1.14	26.02	0.2103E-02	0.1812E-04
2.100	481.67	0.02	0.02	20.77	0.28	1.29	25.03	0.2076E-02	0.2328E-04
2.200	487.78	0.02	0.03	20.70	0.37	1.34	29.79	0.2050E-02	0.3080E-04
2.300	493.89	0.03	0.04	20.64	0.44	1.24	22.23	0.2025E-02	0.3705E-04
2.400	500.00	0.04	0.04	20.58	0.51	1.15	23.39	0.2000E-02	0.4391E-04
2.500	506.11	0.05	0.06	20.52	0.58	1.31	18.63	0.1976E-02	0.5060E-04
2.600	512.22	0.05	0.07	20.50	0.60	1.37	16.69	0.1952E-02	0.5346E-04
2.700	518.33	0.06	0.09	20.47	0.63	1.33	13.60	0.1929E-02	0.5727E-04
2.800	524.44	0.07	0.10	20.44	0.66	1.43	12.09	0.1907E-02	0.6146E-04
2.900	531.11	0.09	0.12	20.42	0.68	1.39	10.21	0.1883E-02	0.6452E-04
3.000	537.22	0.10	0.13	20.39	0.71	1.32	8.84	0.1861E-02	0.6892E-04
3.100	543.33	0.12	0.17	20.36	0.73	1.41	7.06	0.1840E-02	0.7318E-04
3.200	548.89	0.13	0.20	20.35	0.74	1.51	5.65	0.1822E-02	0.7574E-04
3.300	555.00	0.14	0.23	20.34	0.73	1.66	4.57	0.1802E-02	0.7751E-04
3.400	561.11	0.15	0.25	20.35	0.71	1.64	3.82	0.1782E-02	0.7753E-04
3.600	577.22	0.13	0.23	20.46	0.59	1.81	3.16	0.1732E-02	0.6708E-04
3.700	580.00	0.11	0.22	20.56	0.47	1.97	2.39	0.1724E-02	0.5493E-04
3.800	583.33	0.10	0.20	20.62	0.40	1.97	1.96	0.1714E-02	0.4773E-04
3.900	587.78	0.10	0.19	20.64	0.37	1.97	1.76	0.1701E-02	0.4519E-04
4.000	591.67	0.10	0.20	20.65	0.36	2.00	1.42	0.1690E-02	0.4410E-04
4.100	596.11	0.10	0.20	20.66	0.35	2.07	1.27	0.1678E-02	0.4380E-04
4.300	606.11	0.10	0.23	20.64	0.37	2.23	1.08	0.1650E-02	0.4762E-04
4.400	611.67	0.11	0.24	20.62	0.39	2.22	1.13	0.1635E-02	0.5127E-04
4.500	617.22	0.12	0.27	20.58	0.43	2.25	1.03	0.1620E-02	0.5756E-04
4.600	622.22	0.13	0.30	20.53	0.48	2.28	1.00	0.1607E-02	0.6579E-04
4.700	627.78	0.15	0.34	20.49	0.51	2.20	0.81	0.1593E-02	0.7251E-04
4.800	633.89	0.17	0.39	20.43	0.57	2.29	0.68	0.1578E-02	0.8287E-04
4.900	640.00	0.20	0.46	20.33	0.67	2.31	0.74	0.1563E-02	0.1010E-03

RUN NO. 124 (CONT.)

TIME HRS	TEMPERATURE K	CO %	CO2 %	O2 %	GAMA %	CO2/CO RATIO	H/C RATIO	INV.TEMP. 1/K	RELATIVE RATE,1/S
5.000	646.67	0.23	0.54	20.21	0.80	2.31	0.75	0.1546E-02	0.1240E-03
5.100	652.78	0.28	0.64	20.04	0.97	2.29	0.85	0.1532E-02	0.1593E-03
5.200	660.00	0.35	0.78	19.83	1.18	2.26	0.78	0.1515E-02	0.2066E-03
5.300	668.33	0.42	0.95	19.60	1.41	2.27	0.71	0.1496E-02	0.2682E-03
5.400	676.11	0.51	1.18	19.30	1.70	2.29	0.64	0.1479E-02	0.3635E-03
5.500	684.44	0.64	1.46	19.00	1.97	2.27	0.35	0.1461E-02	0.4907E-03
5.600	692.22	0.75	1.71	18.73	2.22	2.29	0.22	0.1445E-02	0.6796E-03
5.650	696.11	0.78	1.79	18.66	2.29	2.30	0.15	0.1437E-02	0.7985E-03
5.700	699.44	0.81	1.88	18.64	2.28	2.32	-0.01	0.1430E-02	0.9313E-03
5.750	702.78	0.80	1.88	18.71	2.20	2.34	-0.14	0.1423E-02	0.1073E-02
5.800	705.00	0.75	1.77	18.90	2.00	2.35	-0.24	0.1418E-02	0.1197E-02
5.900	707.78	0.59	1.44	19.38	1.52	2.45	-0.44	0.1413E-02	0.1466E-02
6.000	710.56	0.40	0.99	19.92	1.00	2.45	-0.55	0.1407E-02	0.1719E-02
6.100	711.67	0.24	0.59	20.36	0.59	2.46	-0.59	0.1405E-02	0.1992E-02
6.150	712.22	0.19	0.46	20.52	0.44	2.46	-0.75	0.1404E-02	0.2135E-02
6.200	713.33	0.13	0.34	20.63	0.34	2.54	-0.52	0.1402E-02	0.2567E-02
6.300	718.89	0.07	0.17	20.81	0.18	2.46	-0.40	0.1391E-02	0.4449E-02

RUN NO. 125

TIME HRS	TEMPERATURE K	CO %	CO2 %	O2 %	GAMA %	CO2/CO RATIO	H/C RATIO	INV.TEMP. 1/K	RELATIVE RATE,1/S
0.700	430.56	0.00	0.01	20.99	0.01	9.44	3.28	0.2323E-02	0.1133E-05
0.900	442.22	0.00	0.01	20.96	0.04	9.44	19.57	0.2261E-02	0.3743E-05
1.100	453.89	0.01	0.01	20.92	0.10	1.72	21.64	0.2203E-02	0.8370E-05
1.200	460.56	0.01	0.01	20.88	0.14	1.76	24.46	0.2171E-02	0.1223E-04
1.300	467.22	0.01	0.02	20.84	0.19	1.37	20.06	0.2140E-02	0.1683E-04
1.400	474.44	0.02	0.03	20.77	0.28	1.65	20.92	0.2108E-02	0.2439E-04
1.500	481.67	0.03	0.04	20.68	0.39	1.31	19.85	0.2076E-02	0.3419E-04
1.600	489.44	0.04	0.05	20.57	0.52	1.32	18.71	0.2043E-02	0.4646E-04
1.700	496.67	0.06	0.08	20.45	0.66	1.38	16.03	0.2013E-02	0.6014E-04
1.800	503.33	0.07	0.10	20.36	0.75	1.40	14.14	0.1987E-02	0.7075E-04
1.850	506.67	0.08	0.12	20.34	0.78	1.45	12.46	0.1974E-02	0.7393E-04
1.900	509.44	0.09	0.13	20.34	0.77	1.51	11.41	0.1963E-02	0.7460E-04
1.950	512.22	0.09	0.13	20.35	0.76	1.58	10.69	0.1952E-02	0.7422E-04
2.000	515.00	0.09	0.13	20.37	0.73	1.55	10.12	0.1942E-02	0.7269E-04
2.100	520.56	0.09	0.13	20.42	0.67	1.55	8.98	0.1921E-02	0.6821E-04
2.200	526.67	0.09	0.14	20.46	0.62	1.60	7.35	0.1899E-02	0.6430E-04
2.300	532.78	0.10	0.16	20.49	0.57	1.67	5.50	0.1877E-02	0.6100E-04
2.500	545.00	0.10	0.19	20.52	0.53	1.90	3.83	0.1835E-02	0.5855E-04
2.700	556.67	0.10	0.19	20.57	0.46	1.90	2.90	0.1796E-02	0.5311E-04
2.900	567.78	0.09	0.19	20.64	0.38	2.29	2.07	0.1761E-02	0.4562E-04
3.100	578.33	0.08	0.19	20.69	0.32	2.34	1.29	0.1729E-02	0.3948E-04
3.200	583.89	0.08	0.19	20.70	0.31	2.38	1.03	0.1713E-02	0.3834E-04
3.300	589.44	0.08	0.20	20.70	0.30	2.46	0.89	0.1697E-02	0.3866E-04
3.400	595.00	0.09	0.21	20.69	0.31	2.48	0.81	0.1681E-02	0.4038E-04
3.500	600.56	0.09	0.23	20.67	0.33	2.65	0.66	0.1665E-02	0.4337E-04
3.600	606.11	0.09	0.24	20.64	0.36	2.62	0.82	0.1650E-02	0.4791E-04
3.700	611.67	0.10	0.27	20.62	0.38	2.63	0.68	0.1635E-02	0.5173E-04
3.800	617.78	0.12	0.30	20.57	0.43	2.62	0.69	0.1619E-02	0.5974E-04
3.900	623.89	0.13	0.34	20.52	0.49	2.59	0.62	0.1603E-02	0.6858E-04
4.000	630.00	0.15	0.40	20.46	0.53	2.61	0.38	0.1587E-02	0.7699E-04
4.100	636.11	0.18	0.47	20.38	0.61	2.64	0.29	0.1572E-02	0.9137E-04
4.200	643.33	0.21	0.55	20.27	0.72	2.58	0.33	0.1554E-02	0.1124E-03
4.300	651.67	0.26	0.67	20.10	0.89	2.58	0.41	0.1535E-02	0.1450E-03

RUN NO. 125 (CONT.)

TIME HRS	TEMPERATURE K	CO %	CO2 %	O2 %	GAMA %	CO2/CO RATIO	H/C RATIO	INV.TEMP. 1/K	RELATIVE RATE,1/S
4.350	655.56	0.29	0.76	20.00	0.99	2.60	0.27	0.1525E-02	0.1644E-03
4.400	660.00	0.33	0.86	19.88	1.10	2.60	0.27	0.1515E-02	0.1901E-03
4.450	665.00	0.37	0.99	19.72	1.26	2.63	0.25	0.1504E-02	0.2253E-03
4.500	669.44	0.43	1.11	19.54	1.44	2.61	0.30	0.1494E-02	0.2694E-03
4.550	674.44	0.48	1.31	19.30	1.68	2.70	0.28	0.1483E-02	0.3311E-03
4.600	680.00	0.55	1.51	19.03	1.95	2.74	0.32	0.1471E-02	0.4121E-03
4.650	685.56	0.64	1.74	18.72	2.26	2.74	0.33	0.1459E-02	0.5187E-03
4.700	691.11	0.70	1.90	18.45	2.54	2.73	0.44	0.1447E-02	0.6462E-03
4.750	696.67	0.74	2.04	18.25	2.74	2.75	0.48	0.1435E-02	0.7946E-03
4.800	702.22	0.81	2.15	18.03	2.98	2.66	0.57	0.1424E-02	0.1013E-02
4.850	706.67	0.88	2.34	17.79	3.21	2.67	0.53	0.1415E-02	0.1347E-02
4.875	708.89	0.90	2.39	17.72	3.28	2.65	0.53	0.1411E-02	0.1570E-02
4.900	710.00	0.91	2.42	17.71	3.28	2.65	0.47	0.1408E-02	0.1825E-02
4.950	706.67	0.83	2.19	18.13	2.84	2.64	0.31	0.1415E-02	0.2284E-02
5.000	704.44	0.61	1.67	18.75	2.24	2.76	0.47	0.1420E-02	0.2852E-02
5.050	702.22	0.40	1.11	19.55	1.43	2.77	0.32	0.1424E-02	0.3148E-02
5.100	701.67	0.25	0.73	20.13	0.85	2.91	-0.02	0.1425E-02	0.3391E-02
5.150	701.11	0.15	0.41	20.50	0.49	2.82	0.03	0.1426E-02	0.3738E-02
5.200	700.56	0.08	0.23	20.72	0.27	3.07	-0.02	0.1427E-02	0.4398E-02
5.250	702.22	0.03	0.12	20.87	0.12	3.46	-0.30	0.1424E-02	0.4736E-02
5.300	703.89	0.02	0.07	20.94	0.05	4.01	-1.19	0.1421E-02	0.5129E-02
5.350	705.56	0.01	0.04	20.97	0.03	4.21	-1.46	0.1417E-02	0.7823E-02

RUN NO. 126

TIME HRS	TEMPERATURE K	CO %	CO2 %	O2 %	GAMA %	CO2/CO RATIO	H/C RATIO	INV.TEMP. 1/K	RELATIVE RATE,1/S
2.500	375.56	0.00	0.01	20.98	0.02	9.44	8.71	0.2663E-02	0.3389E-06
2.800	390.00	0.00	0.01	20.98	0.02	9.44	8.71	0.2564E-02	0.3390E-06
3.000	400.00	0.00	0.01	20.96	0.05	9.44	22.28	0.2500E-02	0.7070E-06
3.200	410.56	0.00	0.01	20.94	0.07	9.44	35.87	0.2436E-02	0.1075E-05
3.400	421.67	0.00	0.01	20.89	0.14	4.14	40.77	0.2372E-02	0.1978E-05
3.500	427.78	0.00	0.01	20.86	0.17	4.14	53.17	0.2338E-02	0.2531E-05
3.600	433.89	0.00	0.01	20.81	0.24	2.43	64.60	0.2305E-02	0.3447E-05
3.700	440.00	0.01	0.02	20.74	0.32	1.78	47.88	0.2273E-02	0.4697E-05
3.800	446.67	0.02	0.03	20.63	0.45	1.83	33.64	0.2239E-02	0.6638E-05
3.900	453.33	0.03	0.04	20.50	0.61	1.60	33.39	0.2206E-02	0.8981E-05
4.000	460.00	0.04	0.07	20.34	0.80	1.64	25.36	0.2174E-02	0.1179E-04
4.050	463.33	0.05	0.07	20.25	0.91	1.43	26.31	0.2158E-02	0.1343E-04
4.100	466.67	0.06	0.10	20.10	1.09	1.61	25.05	0.2143E-02	0.1611E-04
4.200	475.56	0.10	0.17	19.72	1.53	1.76	20.31	0.2103E-02	0.2283E-04
4.250	480.56	0.12	0.20	19.52	1.76	1.64	18.85	0.2081E-02	0.2639E-04
4.300	485.56	0.15	0.27	19.22	2.10	1.75	16.94	0.2059E-02	0.3160E-04
4.400	496.67	0.23	0.41	18.63	2.78	1.76	14.43	0.2013E-02	0.4235E-04
4.500	507.78	0.31	0.59	17.92	3.55	1.90	12.85	0.1969E-02	0.5520E-04
4.600	519.44	0.43	0.82	17.35	4.16	1.92	10.36	0.1925E-02	0.6604E-04
4.700	531.67	0.53	1.07	16.80	4.74	2.01	8.88	0.1881E-02	0.7712E-04
4.750	537.22	0.58	1.20	16.64	4.88	2.06	7.98	0.1861E-02	0.8062E-04
4.800	542.22	0.62	1.31	16.50	5.02	2.12	7.42	0.1844E-02	0.8419E-04
4.900	550.56	0.66	1.52	16.40	5.09	2.29	6.22	0.1816E-02	0.8797E-04
5.000	557.78	0.71	1.74	16.38	5.06	2.45	5.06	0.1793E-02	0.9041E-04
5.100	563.33	0.72	1.88	16.45	4.95	2.60	4.35	0.1775E-02	0.9127E-04
5.200	568.33	0.70	1.95	16.67	4.67	2.77	3.73	0.1760E-02	0.8904E-04
5.300	572.78	0.68	1.97	16.90	4.41	2.91	3.31	0.1746E-02	0.8669E-04
5.400	576.67	0.64	1.97	17.15	4.12	3.09	2.90	0.1734E-02	0.8348E-04
5.500	580.56	0.61	1.98	17.35	3.88	3.27	2.55	0.1722E-02	0.8108E-04
5.600	585.00	0.59	2.01	17.50	3.70	3.42	2.21	0.1709E-02	0.7953E-04
5.700	589.44	0.59	2.09	17.57	3.60	3.57	1.86	0.1697E-02	0.7959E-04
5.800	595.00	0.59	2.21	17.59	3.55	3.76	1.53	0.1681E-02	0.8078E-04
5.900	600.56	0.61	2.39	17.50	3.61	3.91	1.24	0.1665E-02	0.8469E-04

RUN NO. 126 (CONT.)

TIME HRS	TEMPERATURE K	CO %	CO2 %	O2 %	GAMA %	CO2/CO RATIO	H/C RATIO	INV.TEMP. 1/K	RELATIVE RATE,1/S
5.950	603.33	0.63	2.51	17.45	3.64	4.01	1.07	0.1657E-02	0.8678E-04
6.000	606.67	0.65	2.66	17.36	3.70	4.07	0.88	0.1648E-02	0.8972E-04
6.050	610.00	0.68	2.83	17.25	3.80	4.14	0.74	0.1639E-02	0.9361E-04
6.100	613.33	0.72	3.05	17.10	3.93	4.23	0.55	0.1630E-02	0.9838E-04
6.150	617.78	0.78	3.31	16.90	4.10	4.25	0.39	0.1619E-02	0.1046E-03
6.200	622.22	0.84	3.58	16.65	4.34	4.27	0.30	0.1607E-02	0.1128E-03
6.250	627.22	0.92	3.95	16.33	4.63	4.30	0.17	0.1594E-02	0.1230E-03
6.300	633.33	1.03	4.40	15.85	5.09	4.27	0.12	0.1579E-02	0.1386E-03
6.350	638.89	1.14	4.90	15.40	5.51	4.29	0.01	0.1565E-02	0.1540E-03
6.400	646.11	1.28	5.45	14.73	6.18	4.26	0.04	0.1548E-02	0.1780E-03
6.450	653.89	1.42	6.04	14.10	6.80	4.26	0.00	0.1529E-02	0.2025E-03
6.500	661.67	1.51	6.40	13.55	7.37	4.22	0.09	0.1511E-02	0.2281E-03
6.550	664.44	1.53	6.50	13.48	7.43	4.26	0.06	0.1505E-02	0.2400E-03
6.600	667.22	1.53	6.30	13.50	7.44	4.13	0.18	0.1499E-02	0.2512E-03
6.700	672.22	1.44	5.90	13.80	7.18	4.10	0.30	0.1488E-02	0.2657E-03
6.800	678.89	1.37	5.45	14.08	6.94	3.97	0.47	0.1473E-02	0.2836E-03
6.900	683.89	1.29	5.02	14.45	6.59	3.90	0.60	0.1462E-02	0.2993E-03
7.000	688.33	1.23	4.67	14.78	6.28	3.81	0.69	0.1453E-02	0.3186E-03
7.100	692.78	1.17	4.45	15.04	6.02	3.80	0.72	0.1443E-02	0.3444E-03
7.200	696.67	1.12	4.25	15.26	5.81	3.79	0.77	0.1435E-02	0.3782E-03
7.300	699.44	1.06	4.03	15.54	5.53	3.80	0.78	0.1430E-02	0.4152E-03
7.400	702.22	0.98	3.76	15.90	5.17	3.85	0.80	0.1424E-02	0.4539E-03
7.500	704.44	0.90	3.52	16.30	4.76	3.92	0.73	0.1420E-02	0.4952E-03
7.600	706.67	0.82	3.27	16.70	4.34	3.99	0.66	0.1415E-02	0.5450E-03
7.700	708.33	0.74	2.99	17.10	3.94	4.04	0.62	0.1412E-02	0.6073E-03
7.800	708.89	0.66	2.72	17.53	3.48	4.09	0.52	0.1411E-02	0.6772E-03
7.900	709.44	0.57	2.39	17.95	3.07	4.21	0.53	0.1410E-02	0.7742E-03
8.000	710.56	0.49	2.11	18.35	2.66	4.27	0.47	0.1407E-02	0.9068E-03
8.100	711.67	0.43	1.84	18.70	2.31	4.28	0.45	0.1405E-02	0.1131E-02
8.200	712.78	0.34	1.46	19.20	1.80	4.32	0.37	0.1403E-02	0.1384E-02
8.300	713.89	0.24	1.05	19.72	1.27	4.35	0.31	0.1401E-02	0.1700E-02
8.400	715.56	0.16	0.70	20.15	0.85	4.30	0.31	0.1398E-02	0.2312E-02
8.500	718.33	0.08	0.32	20.63	0.37	3.93	0.06	0.1392E-02	0.2491E-02
8.550	719.44	0.03	0.17	20.81	0.18	4.90	-0.08	0.1390E-02	0.1835E-02
8.600	721.11	0.02	0.09	20.90	0.10	5.12	0.01	0.1387E-02	0.1340E-02

RUN NO. 127

TIME HRS	TEMPERATURE K	CO %	CO2 %	O2 %	GAMA %	CO2/CO RATIO	H/C RATIO	INV.TEMP. 1/K	RELATIVE RATE,1/S
0.600	416.11	0.00	0.01	20.96	0.05	9.44	22.28	0.2403E-02	0.3965E-05
1.000	441.67	0.00	0.01	20.93	0.09	9.44	42.66	0.2264E-02	0.7113E-05
1.200	453.33	0.01	0.02	20.90	0.12	2.82	18.62	0.2206E-02	0.9974E-05
1.500	473.33	0.02	0.04	20.77	0.28	2.19	16.50	0.2113E-02	0.2321E-04
1.700	486.67	0.03	0.06	20.60	0.48	1.67	17.83	0.2055E-02	0.4136E-04
1.900	501.11	0.06	0.10	20.44	0.66	1.72	13.20	0.1996E-02	0.5917E-04
2.000	507.78	0.07	0.12	20.38	0.73	1.66	12.23	0.1969E-02	0.6672E-04
2.100	513.33	0.09	0.14	20.34	0.77	1.62	10.68	0.1948E-02	0.7230E-04
2.200	518.89	0.09	0.17	20.32	0.79	1.79	8.83	0.1927E-02	0.7572E-04
2.300	525.00	0.10	0.18	20.30	0.81	1.81	8.03	0.1905E-02	0.7970E-04
2.400	530.56	0.12	0.22	20.30	0.79	1.83	6.16	0.1885E-02	0.8072E-04
2.500	536.11	0.13	0.25	20.31	0.77	1.97	4.82	0.1865E-02	0.8066E-04
2.600	541.67	0.14	0.28	20.33	0.74	2.05	3.76	0.1846E-02	0.7933E-04
2.700	547.78	0.13	0.28	20.35	0.71	2.18	3.55	0.1826E-02	0.7894E-04
2.800	553.33	0.12	0.29	20.38	0.67	2.30	3.20	0.1807E-02	0.7694E-04
2.900	558.89	0.12	0.28	20.43	0.61	2.37	2.72	0.1789E-02	0.7193E-04
3.000	564.44	0.11	0.28	20.50	0.53	2.56	2.02	0.1772E-02	0.6357E-04
3.100	569.44	0.11	0.27	20.54	0.48	2.58	1.66	0.1756E-02	0.5913E-04
3.200	575.00	0.10	0.27	20.58	0.43	2.63	1.22	0.1739E-02	0.5426E-04
3.300	580.56	0.10	0.26	20.60	0.41	2.63	1.24	0.1722E-02	0.5272E-04
3.400	586.11	0.09	0.25	20.62	0.39	2.69	1.05	0.1706E-02	0.5066E-04
3.500	591.67	0.09	0.25	20.62	0.39	2.69	1.05	0.1690E-02	0.5161E-04
3.600	597.22	0.09	0.27	20.61	0.40	2.87	0.90	0.1674E-02	0.5369E-04
3.700	602.78	0.10	0.29	20.59	0.42	2.80	0.87	0.1659E-02	0.5803E-04
3.800	608.33	0.12	0.32	20.56	0.44	2.77	0.57	0.1644E-02	0.6215E-04
3.900	614.44	0.13	0.36	20.48	0.53	2.78	0.91	0.1627E-02	0.7651E-04
4.000	620.56	0.14	0.39	20.41	0.60	2.76	1.08	0.1611E-02	0.9005E-04
4.100	626.67	0.17	0.44	20.33	0.68	2.65	1.03	0.1596E-02	0.1056E-03
4.200	632.78	0.20	0.52	20.23	0.78	2.63	0.94	0.1580E-02	0.1261E-03
4.300	639.44	0.23	0.61	20.09	0.93	2.63	0.95	0.1564E-02	0.1568E-03
4.400	646.67	0.29	0.73	19.92	1.10	2.57	0.86	0.1546E-02	0.1974E-03
4.500	655.00	0.36	0.90	19.69	1.32	2.54	0.76	0.1527E-02	0.2586E-03
4.600	663.33	0.44	1.09	19.43	1.58	2.49	0.71	0.1508E-02	0.3441E-03

RUN NO. 127 (CONT.)

TIME HRS	TEMPERATURE K	CO %	CO2 %	O2 %	GAMA %	CO2/CO RATIO	H/C RATIO	INV.TEMP. 1/K	RELATIVE RATE,1/S
4.700	672.22	0.52	1.33	19.17	1.82	2.55	0.51	0.1488E-02	0.4588E-03
4.800	681.11	0.61	1.56	18.93	2.05	2.58	0.33	0.1468E-02	0.6252E-03
4.900	689.44	0.67	1.77	18.75	2.20	2.62	0.16	0.1450E-02	0.8769E-03
4.950	698.89	0.68	1.81	18.75	2.19	2.65	0.05	0.1431E-02	0.1035E-02
5.000	696.11	0.66	1.79	18.80	2.14	2.70	0.02	0.1437E-02	0.1237E-02
5.100	700.00	0.51	1.46	19.24	1.71	2.86	-0.04	0.1429E-02	0.1647E-02
5.200	700.56	0.32	0.95	19.92	1.03	2.95	-0.24	0.1427E-02	0.1901E-02
5.300	700.56	0.17	0.48	20.43	0.55	2.81	-0.11	0.1427E-02	0.2123E-02
5.400	703.89	0.08	0.23	20.70	0.30	3.07	0.31	0.1421E-02	0.2796E-02
5.500	708.33	0.02	0.09	20.88	0.12	4.93	1.15	0.1412E-02	0.4093E-02

RUN NO. 128

TIME HRS	TEMPERATURE K	CO %	CO2 %	O2 %	GAMA %	CO2/CO RATIO	H/C RATIO	INV.TEMP. 1/K	RELATIVE RATE,1/S
0.600	391.67	0.00	0.01	21.00	0.00	9.44	-3.51	0.2553E-02	0.7936E-07
1.000	414.44	0.00	0.01	20.99	0.01	2.83	1.01	0.2413E-02	0.1452E-05
1.400	437.78	0.00	0.01	20.98	0.02	1.66	3.19	0.2284E-02	0.2472E-05
1.700	455.00	0.01	0.01	20.97	0.04	1.33	5.18	0.2198E-02	0.5130E-05
2.000	472.22	0.01	0.01	20.94	0.07	1.43	9.52	0.2118E-02	0.1009E-04
2.200	483.89	0.01	0.02	20.91	0.11	1.55	10.10	0.2067E-02	0.1532E-04
2.400	495.56	0.02	0.02	20.87	0.15	1.29	11.82	0.2018E-02	0.2190E-04
2.600	507.22	0.02	0.03	20.83	0.20	1.65	13.90	0.1972E-02	0.2964E-04
2.800	518.89	0.02	0.04	20.79	0.24	1.58	12.44	0.1927E-02	0.3746E-04
3.000	530.00	0.03	0.05	20.76	0.28	1.39	10.60	0.1887E-02	0.4455E-04
3.200	541.67	0.05	0.07	20.72	0.32	1.47	7.70	0.1846E-02	0.5244E-04
3.300	547.78	0.05	0.08	20.70	0.34	1.62	6.97	0.1826E-02	0.5698E-04
3.400	554.44	0.06	0.10	20.68	0.37	1.58	5.55	0.1804E-02	0.6234E-04
3.500	560.56	0.07	0.12	20.65	0.39	1.66	4.92	0.1784E-02	0.6762E-04
3.600	566.67	0.08	0.13	20.64	0.40	1.65	4.12	0.1765E-02	0.7124E-04
3.700	573.33	0.09	0.15	20.64	0.39	1.78	3.29	0.1744E-02	0.7122E-04
3.800	578.89	0.09	0.15	20.67	0.36	1.78	2.82	0.1727E-02	0.6780E-04
3.900	583.89	0.08	0.15	20.70	0.32	1.93	2.24	0.1713E-02	0.6147E-04
4.000	589.44	0.07	0.14	20.73	0.29	1.98	2.19	0.1697E-02	0.5645E-04
4.100	593.89	0.07	0.13	20.76	0.25	1.98	1.60	0.1684E-02	0.5020E-04
4.300	605.00	0.06	0.14	20.78	0.22	2.14	0.97	0.1653E-02	0.4566E-04
4.500	615.00	0.07	0.15	20.78	0.22	2.22	0.64	0.1626E-02	0.4737E-04
4.700	626.11	0.07	0.17	20.76	0.24	2.40	0.64	0.1597E-02	0.5369E-04
4.800	631.67	0.08	0.18	20.74	0.26	2.26	0.60	0.1583E-02	0.5914E-04
4.900	637.22	0.09	0.19	20.72	0.28	2.29	0.62	0.1569E-02	0.6523E-04
5.000	642.78	0.09	0.21	20.69	0.31	2.26	0.70	0.1556E-02	0.7434E-04
5.100	648.89	0.11	0.23	20.64	0.37	2.22	0.92	0.1541E-02	0.8979E-04
5.200	655.56	0.13	0.28	20.58	0.42	2.18	0.79	0.1525E-02	0.1079E-03
5.300	662.22	0.15	0.33	20.51	0.49	2.15	0.69	0.1510E-02	0.1307E-03
5.400	668.89	0.19	0.39	20.43	0.57	2.07	0.57	0.1495E-02	0.1590E-03
5.500	676.11	0.22	0.46	20.34	0.65	2.06	0.51	0.1479E-02	0.1950E-03
5.600	683.33	0.26	0.53	20.24	0.75	2.04	0.48	0.1463E-02	0.2432E-03
5.700	690.56	0.30	0.63	20.12	0.87	2.08	0.36	0.1448E-02	0.3089E-03

RUN NO. 128 (CONT.)

TIME HRS	TEMPERATURE K	CO %	CO2 %	O2 %	GAMA %	CO2/CO RATIO	H/C RATIO	INV.TEMP. 1/K	RELATIVE RATE,1/S
5.750	693.89	0.34	0.69	20.03	0.95	2.04	0.36	0.1441E-02	0.3615E-03
5.800	697.78	0.37	0.76	19.93	1.05	2.05	0.38	0.1433E-02	0.4284E-03
5.850	701.67	0.42	0.86	19.80	1.18	2.06	0.32	0.1425E-02	0.5216E-03
5.900	705.56	0.47	0.98	19.62	1.36	2.07	0.41	0.1417E-02	0.6709E-03
5.950	709.44	0.53	1.11	19.46	1.51	2.09	0.33	0.1410E-02	0.8546E-03
6.000	712.22	0.55	1.15	19.44	1.52	2.10	0.21	0.1404E-02	0.1017E-02
6.050	714.44	0.53	1.10	19.56	1.39	2.08	0.05	0.1400E-02	0.1126E-02
6.100	716.11	0.48	1.01	19.76	1.18	2.08	-0.21	0.1396E-02	0.1171E-02
6.150	718.33	0.42	0.88	19.94	1.00	2.10	-0.31	0.1392E-02	0.1233E-02
6.200	720.00	0.37	0.78	20.10	0.83	2.10	-0.48	0.1389E-02	0.1295E-02
6.250	721.11	0.31	0.69	20.24	0.70	2.19	-0.59	0.1387E-02	0.1378E-02
6.300	722.22	0.28	0.59	20.36	0.58	2.14	-0.69	0.1385E-02	0.1484E-02
6.400	723.89	0.19	0.43	20.56	0.39	2.26	-0.83	0.1381E-02	0.1827E-02
6.500	726.67	0.12	0.27	20.73	0.24	2.25	-0.92	0.1376E-02	0.2347E-02
6.600	730.56	0.06	0.14	20.87	0.11	2.37	-1.19	0.1369E-02	0.2869E-02
6.650	732.78	0.03	0.09	20.92	0.07	2.70	-1.33	0.1365E-02	0.2979E-02
6.700	735.00	0.02	0.06	20.95	0.04	3.06	-1.45	0.1361E-02	0.3416E-02
6.800	740.00	0.01	0.02	20.98	0.01	3.37	-1.37	0.1351E-02	0.5561E-02

RUN NO. 129

TIME HRS	TEMPERATURE K	CO %	CO2 %	O2 %	GAMA %	CO2/CO RATIO	H/C RATIO	INV.TEMP. 1/K	RELATIVE RATE,1/S
1.000	417.78	0.00	0.01	20.99	0.01	9.44	1.92	0.2394E-02	0.1196E-05
1.300	435.56	0.00	0.01	20.98	0.02	9.44	8.71	0.2296E-02	0.2617E-05
1.500	448.33	0.00	0.01	20.96	0.05	9.44	22.28	0.2230E-02	0.5472E-05
1.700	460.56	0.00	0.01	20.94	0.07	9.44	35.87	0.2171E-02	0.8359E-05
1.850	470.00	0.00	0.01	20.92	0.10	3.21	19.16	0.2128E-02	0.1099E-04
2.000	479.44	0.01	0.02	20.86	0.17	2.82	26.96	0.2086E-02	0.1903E-04
2.100	485.56	0.01	0.02	20.84	0.19	2.47	21.24	0.2059E-02	0.2238E-04
2.300	497.78	0.02	0.03	20.80	0.24	1.83	16.59	0.2009E-02	0.2876E-04
2.500	510.00	0.03	0.04	20.73	0.32	1.60	16.06	0.1961E-02	0.3892E-04
2.700	522.22	0.03	0.07	20.69	0.37	2.40	11.45	0.1915E-02	0.4565E-04
2.900	534.44	0.05	0.08	20.64	0.42	1.56	9.66	0.1871E-02	0.5403E-04
3.000	540.56	0.06	0.10	20.61	0.45	1.58	7.55	0.1850E-02	0.5886E-04
3.100	546.67	0.08	0.12	20.58	0.48	1.55	6.63	0.1829E-02	0.6426E-04
3.200	552.78	0.09	0.14	20.54	0.51	1.70	5.73	0.1809E-02	0.7083E-04
3.300	558.89	0.09	0.17	20.54	0.52	1.79	4.65	0.1789E-02	0.7295E-04
3.400	564.44	0.10	0.18	20.54	0.51	1.83	3.97	0.1772E-02	0.7348E-04
3.500	570.56	0.09	0.18	20.57	0.47	1.97	3.45	0.1753E-02	0.6986E-04
3.600	576.11	0.09	0.18	20.62	0.41	1.97	2.80	0.1736E-02	0.6236E-04
3.800	587.22	0.08	0.17	20.68	0.34	2.19	2.20	0.1703E-02	0.5400E-04
4.000	592.78	0.07	0.17	20.72	0.29	2.46	1.53	0.1687E-02	0.4807E-04
4.100	603.89	0.07	0.17	20.72	0.29	2.51	1.44	0.1656E-02	0.4877E-04
4.200	609.44	0.07	0.18	20.70	0.31	2.53	1.52	0.1641E-02	0.5339E-04
4.500	626.11	0.09	0.21	20.67	0.34	2.48	1.22	0.1597E-02	0.6255E-04
4.600	632.22	0.09	0.23	20.64	0.37	2.51	1.06	0.1582E-02	0.6858E-04
4.700	638.33	0.10	0.26	20.60	0.41	2.57	1.06	0.1567E-02	0.7828E-04
4.800	644.44	0.12	0.29	20.55	0.46	2.40	1.15	0.1552E-02	0.9100E-04
4.900	650.00	0.14	0.34	20.50	0.51	2.42	0.82	0.1538E-02	0.1032E-03
5.000	656.11	0.17	0.41	20.38	0.63	2.39	0.94	0.1524E-02	0.1343E-03
5.100	662.22	0.22	0.51	20.23	0.78	2.27	0.89	0.1510E-02	0.1757E-03
5.200	673.89	0.28	0.63	20.06	0.95	2.28	0.80	0.1484E-02	0.2297E-03
5.300	680.56	0.34	0.77	19.87	1.13	2.28	0.69	0.1469E-02	0.3022E-03
5.400	687.22	0.40	0.93	19.68	1.32	2.30	0.58	0.1455E-02	0.3979E-03
5.500	695.00	0.48	1.09	19.47	1.52	2.29	0.49	0.1439E-02	0.5428E-03

RUN NO. 129 (CONT.)

TIME HRS	TEMPERATURE K	CO %	CO2 %	O2 %	GAMA %	CO2/CO RATIO	H/C RATIO	INV.TEMP. 1/K	RELATIVE RATE,1/S
5.600	702.78	0.54	1.26	19.30	1.67	2.34	0.31	0.1423E-02	0.7521E-03
5.700	710.56	0.60	1.42	19.09	1.88	2.38	0.33	0.1407E-02	0.1188E-02
5.725	712.22	0.61	1.44	19.05	1.92	2.38	0.34	0.1404E-02	0.1358E-02
5.750	713.33	0.61	1.44	19.08	1.89	2.38	0.28	0.1402E-02	0.1519E-02
5.775	714.44	0.59	1.40	19.16	1.81	2.38	0.23	0.1400E-02	0.1676E-02
5.800	715.00	0.55	1.31	19.30	1.66	2.38	0.16	0.1399E-02	0.1804E-02
5.850	716.11	0.47	1.11	19.62	1.33	2.39	-0.05	0.1396E-02	0.2041E-02
5.900	716.67	0.37	0.90	19.93	1.02	2.41	-0.24	0.1395E-02	0.2308E-02
5.950	718.33	0.29	0.71	20.19	0.76	2.48	-0.35	0.1392E-02	0.2723E-02
6.000	720.56	0.20	0.50	20.44	0.52	2.53	-0.42	0.1388E-02	0.3191E-02
6.050	721.67	0.12	0.34	20.64	0.33	2.83	-0.55	0.1386E-02	0.3842E-02
6.100	722.78	0.05	0.17	20.81	0.18	3.28	-0.20	0.1384E-02	0.4498E-02
6.150	723.33	0.02	0.09	20.91	0.09	4.14	-0.41	0.1382E-02	0.5205E-02
6.200	725.00	0.01	0.04	20.96	0.04	6.67	-0.19	0.1379E-02	0.7449E-02

RUN NO. 130

TIME HRS	TEMPERATURE K	CO %	CO2 %	O2 %	GAMA %	CO2/CO RATIO	H/C RATIO	INV.TEMP. 1/K	RELATIVE RATE,1/S
0.900	348.89	0.00	0.01	20.98	0.02	9.44	8.71	0.2866E-02	0.8756E-05
1.300	367.78	0.00	0.01	20.94	0.07	9.44	35.87	0.2719E-02	0.2849E-04
1.600	386.67	0.00	0.01	20.94	0.07	9.44	35.87	0.2586E-02	0.2940E-04
1.900	406.11	0.00	0.01	20.90	0.12	9.44	63.03	0.2462E-02	0.5170E-04
2.200	425.00	0.00	0.01	20.80	0.25	2.83	106.41	0.2353E-02	0.1134E-03
2.400	439.44	0.00	0.01	20.68	0.40	2.43	111.88	0.2276E-02	0.2028E-03
2.600	453.33	0.02	0.04	20.46	0.66	1.70	40.75	0.2206E-02	0.4176E-03
2.700	461.11	0.04	0.05	20.24	0.93	1.50	38.51	0.2169E-02	0.7147E-03
2.800	471.11	0.07	0.10	19.92	1.31	1.50	27.86	0.2123E-02	0.1454E-02
2.900	483.33	0.10	0.15	19.56	1.73	1.48	24.53	0.2069E-02	0.4908E-02

RUN NO. 131

TIME HRS	TEMPERATURE K	CO %	CO2 %	O2 %	GAMA %	CO2/CO RATIO	H/C RATIO	INV.TEMP. 1/K	RELATIVE RATE,1/S
2.000	416.67	0.00	0.01	20.97	0.04	9.44	15.50	0.2400E-02	0.1907E-05
2.100	422.22	0.00	0.01	20.95	0.06	9.44	29.08	0.2368E-02	0.3249E-05
2.200	427.78	0.00	0.01	20.92	0.10	9.44	49.44	0.2338E-02	0.5267E-05
2.300	433.89	0.01	0.01	20.88	0.15	1.72	34.63	0.2305E-02	0.7854E-05
2.400	439.44	0.01	0.01	20.83	0.21	2.27	41.51	0.2276E-02	0.1121E-04
2.500	446.11	0.01	0.02	20.77	0.28	1.59	27.61	0.2242E-02	0.1507E-04
2.600	452.78	0.02	0.04	20.69	0.38	1.83	24.63	0.2209E-02	0.2035E-04
2.700	459.44	0.03	0.04	20.57	0.52	1.24	27.36	0.2177E-02	0.2852E-04
2.800	466.11	0.05	0.07	20.44	0.67	1.47	19.83	0.2145E-02	0.3715E-04
2.900	472.78	0.08	0.10	20.20	0.96	1.34	18.46	0.2115E-02	0.5366E-04
2.950	476.11	0.10	0.14	20.02	1.16	1.38	16.16	0.2100E-02	0.6598E-04
3.000	478.89	0.12	0.17	19.85	1.36	1.43	15.82	0.2088E-02	0.7825E-04
3.050	482.22	0.16	0.23	19.64	1.60	1.51	13.39	0.2074E-02	0.9313E-04
3.100	485.56	0.20	0.30	19.57	1.66	1.54	10.20	0.2059E-02	0.9828E-04
3.200	494.44	0.29	0.46	18.85	2.48	1.58	10.23	0.2022E-02	0.1537E-03
3.250	498.33	0.35	0.59	18.55	2.80	1.70	8.88	0.2007E-02	0.1788E-03
3.300	502.78	0.39	0.67	18.35	3.01	1.70	8.32	0.1989E-02	0.1991E-03
3.350	507.22	0.44	0.78	18.20	3.16	1.79	7.24	0.1972E-02	0.2166E-03
3.400	511.67	0.47	0.86	18.14	3.20	1.85	6.52	0.1954E-02	0.2289E-03
3.450	515.00	0.49	0.97	18.10	3.22	1.96	5.67	0.1942E-02	0.2403E-03
3.500	518.89	0.50	1.01	18.16	3.15	2.00	5.13	0.1927E-02	0.2449E-03
3.550	521.67	0.50	1.05	18.22	3.05	2.08	4.64	0.1917E-02	0.2485E-03
3.600	525.00	0.48	1.05	18.40	2.84	2.16	4.15	0.1905E-02	0.2420E-03
3.650	527.78	0.46	1.01	18.65	2.56	2.20	3.69	0.1895E-02	0.2268E-03
3.700	530.00	0.42	0.95	18.85	2.34	2.25	3.52	0.1887E-02	0.2156E-03
3.750	532.22	0.38	0.88	19.10	2.05	2.30	3.13	0.1879E-02	0.1966E-03
3.800	534.44	0.36	0.82	19.28	1.85	2.31	2.91	0.1871E-02	0.1835E-03
3.850	536.11	0.32	0.76	19.48	1.63	2.38	2.62	0.1865E-02	0.1664E-03
3.900	538.33	0.29	0.73	19.60	1.49	2.47	2.46	0.1858E-02	0.1574E-03
4.000	542.22	0.26	0.63	19.86	1.20	2.44	2.02	0.1844E-02	0.1336E-03
4.100	547.22	0.23	0.59	20.00	1.05	2.59	1.66	0.1827E-02	0.1215E-03
4.200	550.56	0.21	0.57	20.09	0.94	2.68	1.41	0.1816E-02	0.1145E-03
4.300	556.67	0.20	0.55	20.16	0.86	2.81	1.12	0.1796E-02	0.1089E-03

RUN NO. 131 (CONT.)

TIME HRS	TEMPERATURE K	CO %	CO2 %	O2 %	GAMA %	CO2/CO RATIO	H/C RATIO	INV.TEMP. 1/K	RELATIVE RATE,1/S
4.400	562.22	0.19	0.55	20.19	0.83	2.89	0.95	0.1779E-02	0.1085E-03
4.500	567.78	0.19	0.57	20.20	0.81	2.99	0.73	0.1761E-02	0.1105E-03
4.600	573.33	0.20	0.61	20.19	0.81	3.10	0.50	0.1744E-02	0.1153E-03
4.700	578.33	0.21	0.65	20.16	0.84	3.15	0.39	0.1729E-02	0.1242E-03
4.850	586.67	0.24	0.78	20.10	0.87	3.26	-0.15	0.1705E-02	0.1384E-03
4.950	593.33	0.28	0.90	20.00	0.95	3.27	-0.31	0.1685E-02	0.1605E-03
5.000	595.56	0.29	0.97	19.93	1.02	3.28	-0.30	0.1679E-02	0.1773E-03
5.100	601.11	0.35	1.18	19.72	1.22	3.38	-0.35	0.1664E-02	0.2273E-03
5.200	607.78	0.42	1.46	19.44	1.48	3.48	-0.43	0.1645E-02	0.3035E-03
5.250	610.56	0.46	1.60	19.29	1.62	3.50	-0.41	0.1638E-02	0.3534E-03
5.300	613.33	0.50	1.74	19.15	1.75	3.46	-0.45	0.1630E-02	0.4084E-03
5.350	616.67	0.52	1.84	19.05	1.85	3.52	-0.44	0.1622E-02	0.4662E-03
5.400	620.00	0.54	1.88	19.00	1.90	3.49	-0.43	0.1613E-02	0.5230E-03
5.450	622.78	0.54	1.89	18.94	1.97	3.52	-0.32	0.1606E-02	0.6008E-03
5.500	626.11	0.53	1.86	18.98	1.93	3.51	-0.35	0.1597E-02	0.6582E-03
5.550	628.89	0.52	1.82	19.06	1.84	3.48	-0.41	0.1590E-02	0.7113E-03
5.600	631.67	0.50	1.74	19.12	1.79	3.46	-0.39	0.1583E-02	0.7884E-03
5.650	633.89	0.48	1.67	19.24	1.67	3.52	-0.47	0.1578E-02	0.8519E-03
5.700	636.67	0.44	1.56	19.35	1.57	3.55	-0.43	0.1571E-02	0.9407E-03
5.800	641.11	0.35	1.24	19.70	1.23	3.57	-0.48	0.1560E-02	0.1057E-02
5.900	646.11	0.26	0.90	20.02	0.93	3.50	-0.35	0.1548E-02	0.1209E-02
5.950	648.33	0.21	0.76	20.18	0.78	3.56	-0.39	0.1542E-02	0.1261E-02
6.000	650.56	0.18	0.66	20.29	0.68	3.65	-0.33	0.1537E-02	0.1391E-02
6.100	655.56	0.12	0.46	20.49	0.49	3.77	-0.23	0.1525E-02	0.1772E-02
6.150	658.33	0.10	0.37	20.56	0.43	3.65	0.05	0.1519E-02	0.2223E-02
6.200	660.56	0.09	0.32	20.62	0.37	3.77	0.10	0.1514E-02	0.3073E-02

ANALYSIS OF DATA OF BARDON AND GADELLE, RUN NO. 1(SAND MIX)

TIME HRS	TEMPERATURE K	CO %	CO2 %	O2 %	GAMA %	CO2/CO RATIO	H/C RATIO	INV.TEMP. 1/K	RELATIVE RATE,1/S
1.800	473.00	0.00	0.00	20.95	0.06	0.00	******	0.2114E-02	0.3443E-05
1.900	483.00	0.00	0.00	20.90	0.13	0.00	******	0.2070E-02	0.6896E-05
2.000	493.00	0.02	0.00	20.76	0.30	0.00	57.70	0.2028E-02	0.1630E-04
2.100	505.00	0.07	0.03	20.47	0.64	0.43	23.17	0.1980E-02	0.3543E-04
2.150	511.00	0.10	0.06	20.20	0.96	0.60	21.50	0.1957E-02	0.5363E-04
2.200	516.00	0.13	0.09	19.90	1.32	0.69	21.43	0.1938E-02	0.7438E-04
2.250	523.00	0.19	0.12	19.50	1.79	0.63	20.66	0.1912E-02	0.1025E-03
2.300	528.00	0.25	0.18	19.10	2.25	0.72	18.47	0.1894E-02	0.1316E-03
2.350	535.00	0.33	0.26	18.30	3.18	0.79	19.23	0.1869E-02	0.1913E-03
2.400	543.00	0.45	0.35	17.50	4.08	0.78	18.21	0.1842E-02	0.2556E-03
2.450	549.00	0.58	0.45	16.90	4.73	0.78	16.22	0.1821E-02	0.3122E-03
2.500	557.00	0.66	0.55	16.88	4.72	0.83	13.27	0.1795E-02	0.3298E-03
2.550	563.00	0.70	0.60	17.12	4.42	0.86	11.13	0.1776E-02	0.3278E-03
2.600	568.00	0.68	0.61	17.40	4.09	0.90	10.12	0.1761E-02	0.3219E-03
2.700	578.00	0.62	0.62	18.00	3.39	1.00	8.19	0.1730E-02	0.2983E-03
2.750	583.00	0.57	0.62	18.20	3.16	1.09	7.81	0.1715E-02	0.2934E-03
2.800	586.00	0.55	0.61	18.50	2.81	1.11	6.80	0.1706E-02	0.2741E-03
2.900	593.00	0.50	0.60	18.90	2.34	1.20	5.51	0.1686E-02	0.2507E-03
3.000	600.00	0.45	0.60	19.20	1.98	1.33	4.47	0.1667E-02	0.2319E-03
3.100	608.00	0.40	0.61	19.45	1.68	1.52	3.50	0.1645E-02	0.2134E-03
3.200	618.00	0.38	0.63	19.60	1.50	1.66	2.71	0.1618E-02	0.2047E-03
3.300	628.00	0.36	0.64	19.75	1.31	1.78	1.99	0.1592E-02	0.1928E-03
3.400	639.00	0.35	0.66	19.80	1.25	1.89	1.65	0.1565E-02	0.1966E-03
3.500	651.00	0.36	0.70	19.82	1.21	1.94	1.25	0.1536E-02	0.2050E-03
3.600	663.00	0.40	0.76	19.78	1.24	1.90	0.95	0.1508E-02	0.2261E-03
3.700	673.00	0.43	0.83	19.70	1.31	1.93	0.84	0.1486E-02	0.2618E-03
3.800	683.00	0.49	0.95	19.55	1.45	1.94	0.72	0.1464E-02	0.3223E-03
3.900	693.00	0.56	1.10	19.40	1.59	1.96	0.49	0.1443E-02	0.4004E-03
4.000	703.00	0.63	1.20	19.22	1.77	1.90	0.55	0.1422E-02	0.5268E-03
4.050	708.00	0.64	1.20	19.20	1.79	1.87	0.59	0.1412E-02	0.5897E-03
4.100	713.00	0.62	1.15	19.24	1.76	1.85	0.67	0.1403E-02	0.6470E-03
4.200	721.00	0.55	1.00	19.50	1.49	1.82	0.55	0.1387E-02	0.6976E-03
4.300	728.00	0.45	0.80	19.75	1.25	1.78	0.72	0.1374E-02	0.7624E-03

RUN NO. 1 (CONT.)

TIME HRS	TEMPERATURE K	CO %	CO2 %	O2 %	GAMA %	CO2/CO RATIO	H/C RATIO	INV.TEMP. 1/K	RELATIVE RATE,1/S
4.400	735.00	0.35	0.60	19.98	1.04	1.71	1.11	0.1361E-02	0.8451E-03
4.500	743.00	0.25	0.48	20.20	0.82	1.92	1.17	0.1346E-02	0.9150E-03
4.600	751.00	0.20	0.38	20.35	0.67	1.90	1.30	0.1332E-02	0.1066E-02
4.700	760.00	0.12	0.30	20.52	0.50	2.50	1.29	0.1316E-02	0.1189E-02
4.800	768.00	0.08	0.20	20.65	0.37	2.50	1.84	0.1302E-02	0.1409E-02
4.900	776.00	0.04	0.13	20.78	0.23	3.25	1.96	0.1289E-02	0.1522E-02
5.000	783.00	0.02	0.09	20.85	0.16	4.50	2.20	0.1277E-02	0.1949E-02
5.100	790.00	0.00	0.05	20.90	0.11	*****	5.05	0.1266E-02	0.3422E-02

ANALYSIS OF DATA OF BARDON AND GADELLE, RUN NO. 2(SILICA SAND)

TIME HRS	TEMPERATURE K	CO %	CO2 %	O2 %	GAMA %	CO2/CO RATIO	H/C RATIO	INV.TEMP. 1/K	RELATIVE RATE,1/S
1.650	463.00	0.00	0.00	20.93	0.09	0.00	******	0.2160E-02	0.6140E-05
1.750	475.00	0.02	0.02	20.85	0.18	1.00	14.92	0.2105E-02	0.1246E-04
1.800	480.00	0.02	0.06	20.80	0.23	3.00	8.10	0.2083E-02	0.1616E-04
1.900	490.00	0.07	0.17	20.63	0.40	2.43	3.33	0.2041E-02	0.2841E-04
2.000	503.00	0.12	0.27	20.30	0.78	2.25	4.64	0.1988E-02	0.5565E-04
2.100	513.00	0.20	0.42	19.95	1.16	2.10	4.16	0.1949E-02	0.8480E-04
2.200	528.00	0.30	0.57	19.55	1.59	1.90	4.07	0.1894E-02	0.1210E-03
2.250	535.00	0.33	0.65	19.28	1.90	1.97	4.50	0.1869E-02	0.1478E-03
2.300	543.00	0.37	0.75	18.98	2.23	2.03	4.73	0.1842E-02	0.1791E-03
2.350	550.00	0.45	0.82	18.50	2.78	1.82	5.61	0.1818E-02	0.2315E-03
2.375	553.00	0.47	0.87	18.13	3.21	1.85	6.48	0.1808E-02	0.2735E-03
2.400	558.00	0.50	0.92	17.75	3.65	1.84	7.23	0.1792E-02	0.3191E-03
2.450	567.00	0.57	1.02	17.50	3.91	1.79	6.80	0.1764E-02	0.3636E-03
2.500	572.00	0.60	1.07	17.45	3.96	1.78	6.42	0.1748E-02	0.3934E-03
2.550	577.00	0.55	1.10	17.63	3.75	2.00	5.94	0.1733E-02	0.4001E-03
2.600	579.00	0.52	1.07	18.08	3.22	2.06	4.89	0.1727E-02	0.3686E-03
2.650	581.00	0.47	1.05	18.73	2.45	2.23	3.12	0.1721E-02	0.2974E-03
2.700	584.00	0.42	1.02	19.10	2.01	2.43	2.20	0.1712E-02	0.2570E-03
2.750	586.00	0.37	0.97	19.35	1.73	2.62	1.72	0.1706E-02	0.2305E-03
2.800	588.00	0.33	0.92	19.55	1.50	2.79	1.34	0.1701E-02	0.2083E-03
2.850	592.00	0.30	0.87	19.70	1.33	2.90	1.08	0.1689E-02	0.1919E-03
2.900	596.00	0.27	0.80	19.85	1.17	2.96	0.88	0.1678E-02	0.1742E-03
3.000	603.00	0.25	0.70	20.07	0.92	2.80	0.42	0.1658E-02	0.1459E-03
3.100	610.00	0.22	0.70	20.23	0.73	3.18	-0.35	0.1639E-02	0.1211E-03
3.200	620.00	0.22	0.72	20.25	0.70	3.27	-0.56	0.1613E-02	0.1212E-03
3.300	630.00	0.25	0.78	20.18	0.77	3.12	-0.55	0.1587E-02	0.1388E-03
3.400	640.00	0.30	0.87	20.08	0.86	2.90	-0.57	0.1562E-02	0.1638E-03
3.500	652.00	0.35	0.97	19.97	0.96	2.77	-0.58	0.1534E-02	0.1951E-03
3.600	663.00	0.41	1.10	19.80	1.12	2.68	-0.50	0.1508E-02	0.2478E-03
3.700	678.00	0.47	1.25	19.63	1.28	2.66	-0.48	0.1475E-02	0.3132E-03
3.750	685.00	0.52	1.35	19.50	1.41	2.60	-0.45	0.1460E-02	0.3655E-03
3.800	690.00	0.57	1.50	19.35	1.55	2.63	-0.48	0.1449E-02	0.4312E-03
3.850	695.00	0.60	1.65	19.15	1.75	2.75	-0.37	0.1439E-02	0.5327E-03

RUN NO. 2 (CONT.)

TIME HRS	TEMPERATURE K	CO %	CO2 %	O2 %	GAMA %	CO2/CO RATIO	H/C RATIO	INV.TEMP. 1/K	RELATIVE RATE,1/S
3.900	700.00	0.65	1.92	18.93	1.95	2.95	-0.48	0.1429E-02	0.6593E-03
3.950	706.00	0.67	2.05	18.83	2.04	3.06	-0.53	0.1416E-02	0.7845E-03
4.000	710.00	0.62	2.06	18.82	2.06	3.32	-0.48	0.1408E-02	0.9243E-03
4.050	715.00	0.55	1.87	18.95	1.96	3.40	-0.32	0.1399E-02	0.1050E-02
4.100	720.00	0.47	1.65	19.18	1.75	3.51	-0.27	0.1389E-02	0.1139E-02
4.200	728.00	0.30	1.05	19.75	1.22	3.50	0.07	0.1374E-02	0.1227E-02
4.300	735.00	0.20	0.70	20.18	0.80	3.50	-0.01	0.1361E-02	0.1261E-02
4.400	743.00	0.15	0.45	20.45	0.54	3.00	0.08	0.1346E-02	0.1365E-02
4.500	749.00	0.10	0.30	20.65	0.34	3.00	-0.13	0.1335E-02	0.1427E-02
4.600	758.00	0.05	0.20	20.78	0.21	4.00	-0.21	0.1319E-02	0.1545E-02
4.700	768.00	0.05	0.07	20.78	0.25	1.40	5.05	0.1302E-02	0.4498E-02

ANALYSIS OF DATA OF BARDON AND GADELLE, RUN NO. 3(SAND MIX • CU)

TIME HRS	TEMPERATURE K	CO %	CO2 %	O2 %	GAMA %	CO2/CO RATIO	H/C RATIO	INV.TEMP. 1/K	RELATIVE RATE,1/S
1.500	438.00	0.02	0.02	20.90	0.12	1.00	8.60	0.2283E-02	0.5013E-05
1.650	455.00	0.06	0.06	20.73	0.31	1.00	7.33	0.2198E-02	0.1345E-04
1.750	468.00	0.10	0.10	20.60	0.45	1.00	6.06	0.2137E-02	0.1977E-04
1.850	480.00	0.15	0.13	20.35	0.74	0.87	7.76	0.2083E-02	0.3289E-04
1.900	484.00	0.20	0.17	20.15	0.97	0.85	7.65	0.2066E-02	0.4320E-04
1.950	493.00	0.25	0.18	20.00	1.14	0.72	7.87	0.2028E-02	0.5126E-04
2.000	498.00	0.30	0.20	19.70	1.50	0.67	9.30	0.2008E-02	0.6787E-04
2.100	513.00	0.40	0.32	18.80	2.55	0.80	11.52	0.1949E-02	0.1193E-03
2.150	520.00	0.51	0.44	18.33	3.06	0.86	10.24	0.1923E-02	0.1469E-03
2.200	530.00	0.62	0.57	17.80	3.64	0.92	9.59	0.1887E-02	0.1800E-03
2.250	538.00	0.77	0.70	17.00	4.53	0.91	9.76	0.1859E-02	0.2323E-03
2.300	548.00	0.92	1.00	16.35	5.20	1.09	8.16	0.1825E-02	0.2791E-03
2.350	559.00	1.04	1.40	15.40	6.19	1.35	7.41	0.1789E-02	0.3520E-03
2.400	567.00	1.07	1.77	15.16	6.39	1.65	6.10	0.1764E-02	0.3885E-03
2.450	570.00	1.03	1.80	15.45	6.06	1.75	5.59	0.1754E-02	0.3954E-03
2.500	571.00	0.93	1.67	16.03	5.44	1.80	5.33	0.1751E-02	0.3801E-03
2.550	572.00	0.83	1.60	16.53	4.89	1.93	4.93	0.1748E-02	0.3653E-03
2.600	575.00	0.75	1.55	16.97	4.39	2.07	4.46	0.1739E-02	0.3504E-03
2.650	580.00	0.70	1.60	17.20	4.12	2.29	3.91	0.1724E-02	0.3500E-03
2.700	583.00	0.67	1.70	17.23	4.07	2.54	3.56	0.1715E-02	0.3688E-03
2.750	588.00	0.67	1.93	17.20	4.06	2.88	2.85	0.1701E-02	0.3938E-03
2.800	593.00	0.70	2.20	17.13	4.08	3.14	2.18	0.1686E-02	0.4260E-03
2.850	601.00	0.71	2.53	17.00	4.16	3.56	1.63	0.1664E-02	0.4713E-03
2.900	606.00	0.70	2.63	17.05	4.08	3.76	1.36	0.1650E-02	0.5048E-03
2.950	611.00	0.67	2.57	17.37	3.72	3.84	1.02	0.1637E-02	0.5030E-03
3.000	613.00	0.60	2.40	17.70	3.37	4.00	0.91	0.1631E-02	0.4989E-03
3.100	618.00	0.50	2.03	18.20	2.86	4.06	0.94	0.1618E-02	0.5085E-03
3.200	623.00	0.40	1.73	18.67	2.38	4.32	0.85	0.1605E-02	0.5074E-03
3.300	630.00	0.33	1.47	19.00	2.05	4.45	0.93	0.1587E-02	0.5267E-03
3.400	635.00	0.30	1.20	19.27	1.79	4.00	1.18	0.1575E-02	0.5584E-03
3.500	646.00	0.23	1.00	19.50	1.57	4.35	1.49	0.1548E-02	0.6036E-03
3.600	650.00	0.20	0.83	19.73	1.33	4.15	1.57	0.1538E-02	0.6413E-03
3.700	665.00	0.17	0.67	19.93	1.13	3.94	1.79	0.1504E-02	0.6914E-03
3.800	670.00	0.13	0.50	20.13	0.93	3.85	2.34	0.1493E-02	0.7385E-03
3.900	680.00	0.10	0.40	20.30	0.75	4.00	2.43	0.1471E-02	0.7843E-03
4.000	690.00	0.08	0.30	20.47	0.57	3.75	2.42	0.1449E-02	0.7897E-03
4.200	708.00	0.04	0.20	20.67	0.35	5.00	2.23	0.1412E-02	0.9106E-03
4.500	738.00	0.00	0.10	20.80	0.23	*****	5.06	0.1355E-02	0.3012E-02

ANALYSIS OF DATA OF BARDON AND GADELLE, RUN NO. 4(ORIGINAL MATRIX)

TIME HRS	TEMPERATURE K	CO %	CO2 %	O2 %	GAMA %	CO2/CO RATIO	H/C RATIO	INV.TEMP. 1/K	RELATIVE RATE,1/S
1.500	433.00	0.00	0.00	20.93	0.09	0.00	******	0.2309E-02	0.3835E-05
1.650	448.00	0.00	0.00	20.83	0.21	0.00	******	0.2232E-02	0.9336E-05
1.750	458.00	0.00	0.00	20.73	0.34	0.00	******	0.2183E-02	0.1487E-04
1.850	470.00	0.02	0.00	20.63	0.46	0.00	90.61	0.2128E-02	0.2026E-04
1.950	483.00	0.07	0.00	20.43	0.70	0.00	38.17	0.2070E-02	0.3098E-04
2.000	493.00	0.10	0.02	20.27	0.89	0.20	27.41	0.2028E-02	0.3951E-04
2.050	498.00	0.20	0.10	19.90	1.30	0.50	14.84	0.2008E-02	0.5851E-04
2.100	508.00	0.37	0.20	19.37	1.89	0.54	10.71	0.1969E-02	0.8605E-04
2.150	518.00	0.50	0.33	18.40	3.00	0.66	12.00	0.1931E-02	0.1398E-03
2.200	530.00	0.67	0.50	16.90	4.70	0.75	13.83	0.1887E-02	0.2263E-03
2.250	538.00	0.80	0.67	15.63	6.11	0.84	14.52	0.1859E-02	0.3081E-03
2.300	543.00	0.83	0.87	15.40	6.32	1.05	12.59	0.1842E-02	0.3383E-03
2.350	548.00	0.77	0.87	15.83	5.85	1.13	11.84	0.1825E-02	0.3322E-03
2.400	550.00	0.67	0.83	16.67	4.91	1.24	10.45	0.1818E-02	0.2950E-03
2.450	553.00	0.57	0.70	17.50	3.93	1.23	9.79	0.1808E-02	0.2514E-03
2.500	555.00	0.55	0.64	18.07	3.32	1.16	8.33	0.1802E-02	0.2187E-03
2.550	558.00	0.54	0.63	18.27	3.08	1.17	7.67	0.1792E-02	0.2112E-03
2.600	560.00	0.53	0.63	18.40	2.93	1.19	7.20	0.1786E-02	0.2084E-03
2.650	563.00	0.52	0.65	18.50	2.81	1.25	6.64	0.1776E-02	0.2072E-03
2.700	568.00	0.51	0.67	18.62	2.66	1.31	6.01	0.1761E-02	0.2037E-03
2.750	573.00	0.50	0.70	18.70	2.56	1.40	5.47	0.1745E-02	0.2032E-03
2.850	580.00	0.49	0.73	18.90	2.31	1.49	4.46	0.1724E-02	0.1972E-03
3.000	595.00	0.47	0.80	19.10	2.05	1.70	3.25	0.1681E-02	0.1948E-03
3.100	605.00	0.43	0.83	19.23	1.89	1.93	2.73	0.1653E-02	0.1928E-03
3.250	620.00	0.40	0.87	19.34	1.76	2.17	2.18	0.1613E-02	0.1987E-03
3.350	630.00	0.43	0.97	19.30	1.77	2.26	1.70	0.1587E-02	0.2162E-03
3.500	643.00	0.50	1.27	19.13	1.89	2.54	0.85	0.1555E-02	0.2628E-03
3.600	658.00	0.60	1.50	18.93	2.06	2.50	0.50	0.1520E-02	0.3175E-03
3.700	670.00	0.63	1.62	18.77	2.23	2.57	0.51	0.1493E-02	0.3887E-03
3.750	673.00	0.64	1.66	18.67	2.34	2.59	0.62	0.1486E-02	0.4398E-03
3.800	678.00	0.64	1.62	18.63	2.40	2.53	0.81	0.1475E-02	0.4901E-03
3.850	683.00	0.63	1.47	18.67	2.38	2.33	1.15	0.1464E-02	0.5348E-03
3.900	685.00	0.60	1.57	18.70	2.33	2.62	0.86	0.1460E-02	0.5778E-03

RUN NO. 4 (CONT.)

TIME HRS	TEMPERATURE K	CO %	CO2 %	O2 %	GAMA %	CO2/CO RATIO	H/C RATIO	INV.TEMP. 1/K	RELATIVE RATE,1/S
4.000	693.00	0.50	1.33	19.00	2.04	2.66	1.02	0.1443E-02	0.6286E-03
4.150	705.00	0.40	1.00	19.47	1.56	2.50	1.04	0.1418E-02	0.6869E-03
4.250	715.00	0.33	0.77	19.73	1.31	2.33	1.38	0.1399E-02	0.7471E-03
4.400	728.00	0.23	0.50	20.10	0.94	2.17	1.81	0.1374E-02	0.8218E-03
4.500	738.00	0.20	0.37	20.30	0.73	1.85	1.86	0.1355E-02	0.8669E-03
4.750	761.00	0.10	0.17	20.60	0.43	1.70	3.18	0.1314E-02	0.1353E-02

☆U.S. GOVERNMENT PRINTING OFFICE: 1982-546-085/47